



**D 3.4**

**DELIVERABLE**

**PROJECT INFORMATION**

Project Title: **Harmonized approach to stress tests for critical infrastructures against natural hazards**

Acronym: **STREST**

Project N°: 603389

Call N°: FP7-ENV-2013-two-stage

Project start: 01 October 2013

Duration: 36 months

**DELIVERABLE INFORMATION**

Deliverable Title: **Guidelines and case studies of site monitoring to reduce the uncertainties affecting site-specific earthquake hazard assessment**

Date of issue: 7 March 2016

Work Package: WP3 – Integrated low probability-high consequence hazard assessment for critical infrastructures

Editor/Author: C. Aristizábal - P.-Y. Bard - C. Beauval (Institut des Sciences de la Terre)

S. Lorito – J. Selva (Istituto Nazionale di Geofisica e Vulcanologia)

Reviewer: Fabrice Cotton (GFZ)

REVISION: Version 1

---

 <p>SEVENTH FRAMEWORK PROGRAMME</p>	Project Coordinator: Prof. Domenico Giardini Institution: ETH Zürich e-mail: <a href="mailto:giardini@sed.ethz.ch">giardini@sed.ethz.ch</a> fax: + 41 446331065 telephone: + 41 446332610	Prof. Domenico Giardini ETH Zürich <a href="mailto:giardini@sed.ethz.ch">giardini@sed.ethz.ch</a> + 41 446331065 + 41 446332610
--------------------------------------------------------------------------------------------------------------------------	-------------------------------------------------------------------------------------------------------------------------------------------------------------------------------------------------------	---------------------------------------------------------------------------------------------------------------------------------------------

---

# Abstract

This report presents an overview of the available approaches for site-specific probabilistic seismic hazard assessment in terms of ground motion estimates, together with some example applications on one particular site, and a similar section for tsunami hazard methods.

Concerning ground motion estimates, a general framework is first presented with various options from the simplest to the most sophisticated approach. The various techniques are then presented and discussed, especially regarding their pros and cons, and the corresponding requirements in terms of site characterization. They can be classified in generic methods making use of simple site proxies (such as  $V_{S30}$ ) and ergodic sigma, and site-specific methods where the use of single-site sigma is authorized, together with a specific estimate of the site amplification: the latter may be estimated from instrumental recordings (with different options) or numerical simulation, and in the linear or non-linear domains. Such site-specific approaches are thus associated with an additional level of epistemic uncertainty which must be accounted for. The variability of the results from these various approaches are illustrated on one example application for the Euroseistest site in North-Eastern Greece, which allows to estimate the amount of efforts that is required in each option. Recommendations are thus given as a conclusion for an "optimal" approach depending on the available information. Even though the long term objective is to reduce uncertainties with site monitoring, one must admit that this reduction is not yet reached, as there still exist remaining knowledge and site investigation gaps, which result in relatively high levels of epistemic uncertainties, especially regarding the non-linear site response.

The second part presents site-specific approach for tsunami, as run-up heights and destructive effects are also very sensitive to local topography characteristics (on-shore and also off-shore shallow bathymetry).

This document benefitted from a parallel ongoing project sponsored by the French nuclear industry (SIGMA)

*Keywords: instrumental recordings – probabilistic assessment – non-linear – aleatory variability – single site - tsunami*



---

## Acknowledgments

The research leading to these results has received funding from the European Community's Seventh Framework Programme [FP7/2007-2013] under grant agreement n° 603389

This work also benefitted a lot from an on-going R&D research programme launched by the French nuclear engineering (projects CASHIMA by CEA-ILL and SIGMA by EDF-CEA-AREVA-ENEL, within which is scheduled the writing of a set of operational guidelines to account for site effects. These guidelines thus benefit from a large number of side investigations (much broader than what could be accomplished within the limited funding of the STREST project), involving a large number of institutions and individuals.



---

## Deliverable Contributors

[ISTerre] [ISTerre]

Claudia Aristizábal

Pierre-Yves Bard

Céline Beauval

Fabrice Hollender

Vincent Perron

[GFZ] Fabrice Cotton  
Olga-Joan Ktenidou

INGV Stefano Lorito

Jacopo Selva

Beatriz Brizuela

Roberto Basili

Fabrizio Romano

[Outside the STREST consortium] Gabriele AMERI (Fugro - GEOTER)

Fabrice Hollender (CEA Cadarache)

Vincent Perron (CEA Cadarache)

---

# Table of Contents

<b>1</b>	<b>Introduction : Objectives and organization of the document .....</b>	<b>1</b>
<b>2</b>	<b>General methodological framework: Inventory of available approaches and associated issues .....</b>	<b>2</b>
<b>2.1</b>	<b>Overview .....</b>	<b>2</b>
<b>2.2</b>	<b>Generic (not fully site-specific approaches) .....</b>	<b>4</b>
2.2.1	Direct use of GMPEs.....	4
2.2.2	A-posteriori modifications of the site term : use of "SAPes" .....	7
2.2.2.1	Site Amplification models accounting for other site proxies .....	7
2.2.2.2	Accounting for subsurface geometry effects with "Aggravation Factors" .....	8
2.2.2.3	Other types of "SAPE" .....	8
<b>2.3</b>	<b>Site-specific approaches .....</b>	<b>9</b>
2.3.1	Overview .....	9
2.3.2	Host-to-target adjustment: what, when and how.....	9
2.3.2.1	Background.....	9
2.3.2.2	Application of Vs- $\kappa$ adjustment.....	10
2.3.2.3	Uncertainties .....	11
2.3.3	Site response estimates: instrumental approach .....	12
2.3.3.1	Usefulness of seismological instrumentation, with a special focus on moderate seismicity countries.....	13
2.3.3.2	Implementation recommendations.....	14
2.3.3.3	Site-specific residuals: $\delta S_{2S,s}$ and $\Delta\delta S_{2S,s}$ : .....	17
2.3.3.3.1	Method of ground motion residual analysis.....	18
2.3.3.3.2	Use of $\delta S_{2S}$ to modify GMPEs in hazard analyses.....	19
2.3.4	Site response estimates: numerical approach / linear case.....	20
2.3.4.1	Introductory remark about the role of empirical methods to account for site effects .....	20
2.3.4.2	Numerical modeling and consideration of complex geometries (1D, 2D and 3D) .....	20
2.3.5	Site response estimates: numerical approach / non-linear case.....	23
2.3.6	Uncertainties .....	25
2.3.6.1	Sources of uncertainties in site response estimation .....	26
2.3.6.2	Different "levels" of uncertainty .....	28
2.3.7	Surface hazard .....	28
<b>3</b>	<b>Example application to Euroseistest .....</b>	<b>31</b>
<b>3.1</b>	<b>Overview .....</b>	<b>31</b>
<b>3.2</b>	<b>Euroseistest : The site .....</b>	<b>32</b>
3.2.1	Soil Site Characterization .....	33
3.2.2	Probabilistic Seismic Hazard Analysis.....	34
<b>3.3</b>	<b>Site PSHA1 : Generic or partially Site-Specific Approaches.....</b>	<b>35</b>
3.3.1	Level 0: Site effect by proxy in GMPEs ( $V_{s30}$ ) .....	35
3.3.2	Level 0.5: Site effect by proxy in GMPEs + Amplification factors ( $V_{s,i} + f_0$ ) .....	39
<b>3.4</b>	<b>PSHA2 : Site-Specific Approaches.....</b>	<b>42</b>
3.4.1	Host to target adjustments .....	42

---

3.4.1.1	Correction 1: Shear Wave Velocity Correction Factor (Amplification term $A(f)$ ) .....	43
3.4.1.2	Correction 2: High Attenuation factor “kappa” correction (Diminution function $Df$ ) .....	45
3.4.1.3	Host to target application .....	46
3.4.1.3.1	Step 1: From Disaggregation Select the Mw that contributes more to the hazard....	46
3.4.1.3.2	Step 2: Calculate the host GMPE response spectra for the selected Mw, D scenario.	48
3.4.1.3.3	Step 3: Calculate the FAS via IRVT .....	48
3.4.1.3.4	Step 4: Apply the Vs correction factors .....	48
3.4.1.3.5	Step 5: Calculate kappa host ( $kh$ ) and kappa target ( $kt$ ) .....	49
3.4.1.3.6	Step 6: Correct kappa host ( $kh$ ) to kappa target ( $kt$ ) .....	50
3.4.1.3.7	Step 7: Apply IRV to obtain Vs-kappa corrected Response Spectra.....	50
3.4.1.3.8	Step 8: Vs-k scaling factors.....	51
3.4.2	Level 1a) Linear Site specific residual ( $\delta S2s, s$ from GMPEs) .....	52
3.4.3	Level 1b) Linear Site response analysis, Instrumental. ....	58
3.4.3.1	Case 1: Standard Spectral Ratios (SSR) .....	59
3.4.3.2	Case 2: $\delta S2S$ Approach Amplification Function .....	60
3.4.4	Levels 1c and 2a: Linear and Nonlinear Site response analysis, Numerical. ....	62
3.4.4.1	Sensitivity to acceleration level .....	64
3.4.4.2	Overall methodology.....	68
3.4.4.3	Application to Euroseistest.....	69
3.4.4.3.1	Selection of input accelerograms .....	69
3.4.4.3.2	Non-lienar 1D simulations .....	70
3.4.4.3.3	Fourier Transfer functions.....	73
<b>3.5</b>	<b>Comparison of all approaches, conclusions and recommendations .....</b>	<b>77</b>
3.5.1	Overall comparison.....	77
3.5.2	Conclusions and recommendations.....	83
3.5.2.1	Euroseistest results : limitations and missing analysis .....	83
3.5.2.2	Conclusions for Euroseistest.....	85
3.5.2.3	Tentative recommendations .....	87
<b>4</b>	<b>REGIONAL AND SITE-SPECIFIC TSUNAMI HAZARD ASSESSMENT FOR STREST TEST SITES.....</b>	<b>90</b>
<b>4.1</b>	<b>A METHODOLOGY FOR A FEASIBLE SITE-SPECIFIC SPTHA, from lorito et al., 2015</b>	<b>91</b>
4.1.1	The simplified Event Tree for seismic source aleatory variability analysis .....	91
4.1.2	Definition of the optimal subset of sources for site-specific PTHA (probabilistic inundation maps).....	92
4.1.3	preparation of site-specific analysis for strest test sites .....	95
<b>5</b>	<b>References .....</b>	<b>98</b>
<b>6</b>	<b>Appendix A - Overview of in-situ site characteri-zation surveys (from Ameri et al., 2015).....</b>	<b>110</b>
<b>6.1</b>	<b>Geological, geophysical and geotechnical characterization.....</b>	<b>111</b>
6.1.1	Basic preliminary studies.....	111
6.1.2	H/V method.....	111
6.1.3	Soil class, Vs30 and velocity profile determination.....	112
6.1.3.1	Invasive methods .....	113
6.1.3.2	Non-invasive methods .....	114
6.1.3.3	Invasive vs. non-invasive methods .....	114
<b>7</b>	<b>Appendix B: Ground motion records, Amplitude Fourier Spectra and Transfer Functions used on numerical approaches.....</b>	<b>116</b>

---

---

<b>7.1 Linear case (Level 1C)</b> .....	<b>116</b>
7.1.1 Acceleration records .....	116
7.1.2 Amplitude Fourier Spectra .....	118
7.1.3 Transfer Functions .....	120
<b>7.2 Non-Linear case (Level 2A)</b> .....	<b>124</b>
7.2.1 Acceleration records .....	124
7.2.2 Amplitude Fourier Spectra .....	125
7.2.3 Transfer Functions .....	128

---

## List of Figures

- Figure 1 :  $V_{S30}$ -scaling of a few selected GMPEs for a reference rock peak acceleration of  $PGAr = 0.1g$ . Amplification has been computed relative to a consistent reference velocity of  $V_{ref} = 1000$  m/s, regardless of the reference condition used in the GMPE. Stepped relationships (e.g., AB10) describe site response relative to discrete categories whereas continuous relations use  $V_{S30}$  directly as the site parameter. From Stewart et al., (2014). .....6
- Figure 2 : Example of VS- and K-correction functions evaluated for Abrahamson & Silva (2008). From Biro and Renault (2012) ..... 11
- Figure 3: Evaluation of the signal to noise ratio of the 101 events recorded on a cumulated duration of 231 days of continuous recording at a rock station of our test-site (south-east of France) with an accelerometer. Each sub-figure shows the analysis at a given frequency, from 0.25 to 32 Hz, within a magnitude to distance plot. Each point corresponds to 1 earthquake. The color gives an indication about the corresponding signal-to-noise ratio (computed with a time windows centered on signal and another one on noise before the earthquake arrival). For example, we see that at 1 Hz, 1 event was recorded with a  $S/N > 10$  (green point). ..... 16
- Figure 4: This figure is the same as the previous one, but realized with data coming from a velocimeter at the same place and on the rigorously same period of time. We see that the “usable” events are much more numerous than with the accelerometer. This amount of signals allows SRR analysis and  $\kappa$  determination. The recording duration is less than one year. .... 17
- Figure 5: Example of site term  $\delta S2S_s$  (left) and amplification factor (right) for selected stations in New Zealand. From Chen and Faccioli (2013). .....20
- Figure 6. Location of the Euroseistest and the Mygdonian basin in the NE Greece. ....32
- Figure 7. 2D N-S (Profitis - Stivos) soil model (Raptakis et al., 2000). Line F1 coincides with the seismogenic fault of the 1978, M6.5 earthquake.....33
- Figure 8. **a)** Euroseistest shear-wave velocity soil profile in the middle of the basin (TST\_0 station) (Maufroy et al., 2015a, b; Ameri et al., 2015). **b)** Instrumental Standard Spectral Ratios at the Euroseistests, where a fundamental frequency at about 0.6 - 0.7 Hz was identified (from Maufroy et al., 2016).....34
- Figure 9. Hazard Curves at the Euroseistest a) for standard rock ( $V_{S30}=800$  m/s) with full sigma for the eight different selected ground-motion prediction equations. b) on soil ( $V_{S30}=186$  m/s) with full sigma for the eight different selected ground-motion prediction equations. ....36
- Figure 10. Hazard curves at the Euroseistest for PGA on rock (black) and soil (blue) conditions, derived for 8 ground-motion prediction equations. a) AB10, b) AA14, c) CF08, d) CA14, e) CY08, f) CY14, g) ZA06 and h) BA14. ....37

---

Figure 11. . 5000 years Uniform Hazard Spectra at the Euroseistest on rock ( <b>black</b> ) and soil ( <b>blue</b> ) conditions, derived for the 8 selected ground-motion prediction equations. a) AB10, b) AA14, c) CF08, d) CA14, e) CY08, f) CY14, g) ZA06 and h) BA14. ....	39
Figure 12. a) Uniform hazard Spectrum at the Euroseistest, for 5000 years return periods on standard rock (800 m/s). b) Response Spectra ratios for couple-parameters ( $V_{S,Z}$ , fo) from Cadet et al. (2011a; 2011b) .....	40
Figure 13. Euroseistest site amplification prediction equations (SAPE) for various proxies based on Cadet et al. (2011b).....	41
Figure 14. Uniform hazard spectrum at the Euroseistest, for a 5000 years return period, using Akkar et al. 2014 (AA14) GMPE : <b>Level 0</b> - standard rock (black dotted line), <b>Level 0 - Soil</b> $V_{S30}=186$ m/s (black dash-dotted line), <b>Level 0.5 – Soil</b> (fo) ( <b>red</b> ), <b>Level 0.5 – Soil</b> ( $f_o, V_{S5}$ ) ( <b>light green</b> ), <b>Level 0.5 – Soil</b> ( $f_o, V_{S10}$ ) ( <b>green</b> ), <b>Level 0.5 – Soil</b> ( $f_o, V_{S20}$ ) ( <b>blue</b> ), ( $f_o, V_{S30}$ ) ( <b>magenta</b> ).....	41
Figure 15. S-wave velocity versus depth used by Boore and Joyner (1997) for computing amplifications on generic “soft” rock sites (adapted from Boore and Joyner, 1997.) .....	44
Figure 16. Impedance amplification term for various rock $V_{S30}$ values (Boore et al 2003a). .	44
Figure 17. a) Site amplification functions for a standard rock with a $V_S=800$ m/s and for a hard rock with a $V_S=2600$ m/s. b) $V_S$ (impedance) correction factor.....	45
Figure 18. Combined effect of generic rock amplification and diminution terms for a rock with $V_S=600$ m/s. (Boore 2003a). .....	46
Figure 19. . . Disaggregation in magnitude and distance (GMPE AA14) – $T_r=5000$ years, for different oscillator periods : a) $S_a(0\text{ s})=PGA$ , b) $S_a(0.2\text{ s})$ , c) $S_a(1.0\text{ s})$ .....	47
Figure 20. a) Response spectra on standard rock for AA14, $M_w=6.5$ , $D=10$ km and $V_{S30}=800$ m/s. b) Fourier Amplitude spectra obtained via IRVT (Strata) for AA14 standard rock, $M_w=6.5$ , $D=10$ km and $V_{S30}=800$ m/s.....	48
Figure 21. a) Fourier Amplitude spectra for AA14 standard rock, $M_w=6.5$ , $D=10$ km and $V_{S30}=800$ m/s, b) $V_S$ correction factors, to move from a standard rock (800m/s) to a very hard rock (2600 m/s). .....	49
Figure 22. Fourier Amplitude spectra for AA14 standard rock, $M_w=6.5$ , $D=10$ km and $V_{S30}=800$ m/s (black) and Fourier Amplitude spectra for AA14 standard rock, $M_w=6.5$ , $D=10$ km and $V_{S30}=2600$ m/s (black).....	49
Figure 23. AA14 Fourier Amplitude Spectra for $M_w=6.5$ , $D=10$ and $V_S=2600$ m/s: a) Kappa host ( $kh$ ). b) Kappa target ( $kt$ ). .....	50
Figure 24. a) Original AA14 response spectra (blue) and $V_S$ -kappa corrected AA14 response spectra (red). .....	51
Figure 25. Step 8: $V_S$ – kappa scaling factors for AA14 response spectra. ....	51
Figure 26. Steps for deriving vs-kappa scaling factors using the IRVT approach. (Modified Flux diagram from Al Atik et al. 2014). .....	52
Figure 27. a) hazard curves for PGA spectral ordinate. b) hazard curves for $S_a=0.2$ s. c) hazard curves for a $S_a=1.0$ s. d) uniform hazard spectra for a $T_r=5000$ years.	

---

---

Calculations are performed with GMPE AA14. Total sigma (black), $\phi$ term replaced by single station sigma $\phi_{ss,s} T = 0.45$ following Rodriguez-Marek et al (blue) and $\phi$ term replaced by single station sigma $\phi_{ss,s}(T)$ derived by Ktenidou et al. 2015 (red).....	55
Figure 28. a) AA14 systematic deviation of the observed amplification ( $\delta S2S$ residual) without including the site term as a function of the period, for station TST_0 (black) at the surface and TST_196 (red) at depth. b) Corresponding Amplification Factors (AA14) as a function of the period. ....	57
Figure 29. Application of site-specific residual $\delta S2Ss$ to the AA14 Uniform Hazard Spectrum for 5000 years return period on rock. <b>a)</b> Soil Hazard : Level 1a: single station sigma $\phi_{ss,s}(T)$ on soil with $\delta S2SsTST0 - WIST$ (green), and single station sigma $\phi_{ss,s}(T)$ on soil with $\delta S2SsTST0 - WOST$ (red), to be compared with the "Level0" full sigma $\phi(T)$ on soil (blue) <b>b)</b> Rock hazard with various assumptions: Full sigma $\phi(T)$ on standard rock (black), Level 1a: single station sigma $\phi_{ss,s}(T)$ on standard rock (sahed black), and the single station sigma $\phi_{ss,s}(T)$ on very hard rock corected with the site residual $\delta S2Ss_{TST196}$ (red), thus corresponding to within motion at depth.....	57
Figure 30. Standard spectral ratios (SSR) derived using information from stations TST_0 at the surface on soft soil, and PRO station also at surface but on weathered rock with shear wave velocity around 800 m/s Raptakis et al. 1998.....	59
Figure 31. AA14 uniform hazard spectrum for 5000 years return period: <b>a) Level 1a - Rock:</b> Single station sigma (blue), <b>Level 1b - Soil Raptakis:</b> Single-station sigma, Raptakis et al. 1998 transfer function, (dark green). b) Ratio (UHS Soil / UHS Rock).....	60
Figure 32. Linear transfer function obtained via $\delta S2S$ approach by Ktenidou et al. 2015 between station TST_0 at the surface (soft soil) and station TST_196 at the bottom of the basin (very hard rock).....	61
Figure 33. Depth correction factors according to Cadet et al. 2012a (Borehole/Surface), Fourier domain. ....	61
Figure 34. AA14 uniform hazard spectrum for 5000 years return period: <b>Level 1a - Rock:</b> Single-station sigma (blue), <b>Level 1a - Rock:</b> Single-station sigma, host-to-target adjustments (red), <b>Level 1a - Rock:</b> Single station sigma, host-to-target adjustments, depth correction (black), <b>Level 1b - Soil:</b> Single-station sigma, host-to-target adjustments, depth correction and Ktenidou et al. 2015 transfer function, (dark green). b) Ratio UHS Soil ( $\phi_{ss}$ -htt-DCF-Ktenidou (dark green) / UHS Rock ( $\phi_{ss}$ -htt-DCF (black)).....	62
Figure 35. Euroseistest Degradations Curves proposed within the framework of the SIGMA project for the nonlinear site specific model. ....	63
Figure 36. a) RSN809_LOMAP_UC2000 Accelerogram scaled to a PGA values on rock: a) 0.001 g, b) 0.01 g, c) 0.1 g, d) 0.2 g, e) 0.5 g, f) 1.0 g, for rock at TST_196 (blue) and soil (red) cases at station TST_0 at the surface.....	64
Figure 37. <b>a) RSN809_LOMAP_UC2000 Fourier amplitude spectra scaled to a PGA values on rock: a) 0.001 g, b) 0.01 g, c) 0.1 g, d) 0.2 g, e) 0.5 g, f) 1.0 g, for rock at</b>	

---

	<i>depth at station TST_196 (blue) and on soil at station TST_0 at the surface (red)</i> .....	66
Figure 38.	a) Raw Transfer Functions at the Fourier domain, for each of the 6 scaled acceleration records to different acceleration levels b) Smoothed Transfer Functions at the Fourier domain, for each of the 6 scaled acceleration records to different acceleration levels.....	67
Figure 39.	Selected Records fitting the 5000 years return period, uniform hazard spectra using single station sigma and host to target adjustments at the Euroseistest. .	70
Figure 40.	Linear case: Acceleration records on rock from the PEER database (blue) and on soil at the surface obtained after performing wave propagation with NOAH (red). The other accelerograms are displayed in Appendix B.....	71
Figure 41.	Nonlinear case: Acceleration records on rock from the PEER database (blue) and at the surface obtained after performing wave propagation with NOAH (red). The other accelerograms are displayed in Appendix B. ....	71
Figure 42.	Linear case: Amplitude Fourier Spectras on rock (blue) and at soil (red) for each one of the considered acceleration records. The additional Fourier Amplitude Spectra's corresponding to the ten selected accelerograms and both horizontal components are provided in Appendix B.....	72
Figure 43.	Nonlinear case: Amplitude Fourier Spectras on rock (blue) and at soil (red) for each one of the considered acceleration records. The additional Fourier Amplitude Spectra's corresponding to the ten selected accelerograms and both horizontal components are provided in Appendix B. ....	73
Figure 44.	Linear case: Fourier domain transfer functions soil/outcropping rock for the considered acceleration records. Blue lines correspond to raw transfer function, black lines to smoothed one. The other transfer functions are displayed in Appendix B. ....	73
Figure 45.	Nonlinear case Fourier domain transfer functions soil/outcropping rock for the considered acceleration records. Blue lines correspond to raw transfer function, black lines to smoothed one. The other transfer functions are displayed in Appendix B. ....	74
Figure 46.	Linear Case: Transfer Functions in the Fourier domain for the 10 selected acceleration records and both horizontal components.....	74
Figure 47.	Nonlinear Transfer Functions in the Fourier domain for the 10 selected acceleration records and both horizontal components.....	75
Figure 48.	Smoothed Linear Transfer Functions in the Fourier domain for the 10 selected acceleration records and both horizontal components.....	75
Figure 49.	Smoothed Nonlinear Transfer Functions in the Fourier domain for the 10 selected acceleration records and both horizontal components.....	76
Figure 50.	AA14 uniform hazard spectrum for 5000 years return period: <b>a) Level 1a - Rock:</b> Single-station sigma (blue), <b>Level 1b - Rock:</b> Single-station sigma, host-to-target adjustments, (red), <b>Level 1c - Soil Linear-htt:</b> Single-station sigma, host-to-target adjustments, linear transfer function $\pm$ stdv (dark green), <b>Level 2a - Soil Nonlinear-htt:</b> Single-station sigma, host-to-target adjustments,	

nonlinear transfer function  $\pm$  stdv (magenta). **b)** Ratio between soil and rock UHS spectra in the linear (solid black line, = green PSA / red PSA), and nonlinear (dashed line, = magenta PSA / red PSA). .....76

Figure 51. AA14 uniform hazard spectrum for 5000 years return period. Generic or partially site specific Approaches: Level 0 – Standard Rock ( $\phi$ ): Full sigma and  $VS30 = 800\text{ m/s}$  (black), Level 0 – Soil ( $\phi$ ): Full sigma,  $VS30 = 186\text{ m/s}$  (red), Level 0.5 - Soil ( $\phi, SAPE$ ): Full sigma, SAPE ( $VS30, f_o$ ) (blue). .....77

Figure 52. AA14 uniform hazard spectrum for 5000 years return period. Site specific Approaches: Level 0 – Standard Rock ( $\phi$ ): Full sigma and  $VS30 = 800\text{ m/s}$  (black), Level 1a – Rock ( $\phi_{ss}$ ): Single station sigma and  $VS30 = 800\text{ m/s}$  (red), Level 1a – Hard Rock ( $\phi_{ss, htt}$ ): Single station sigma,  $VS30 = 800\text{ m/s}$ , host to target adjustments (blue), Level 1a – Hard Rock ( $\phi_{ss, \delta S2S\ TST_{196}}$ ): Single station sigma,  $VS30 = 800\text{ m/s}$ ,  $\delta S2S\ TST_{196}\ WOST$  (dark green), Level 1a – Hard Rock ( $\phi_{ss, htt, DCF}$ ): Single station sigma,  $VS30 = 800\text{ m/s}$ , host to target adjustments, depth correction factors (magenta). .....78

Figure 53. AA14 uniform hazard spectrum for 5000 years return period. Site specific Approaches – Level 1: Level 1a – Standard Rock ( $\phi_{ss}$ ): Single station sigma and  $VS30 = 800\text{ m/s}$  (dark green dashed), Level 1a – Soil ( $\phi_{ss, \delta S2S\ TST_0}$ ): Single station sigma,  $VS30 = 186\text{ m/s}$ ,  $\delta S2S\ TST_0\ WIST$  (dark green continuous), Level 1a – Standard Rock ( $\phi_{ss}$ ): Single station sigma and  $VS30 = 800\text{ m/s}$  (blue dashed), Level 1b – Soil ( $\phi_{ss, Raptakis}$ ): Single station sigma,  $VS30 = 800\text{ m/s}$ , Raptakis et al. 1998 transfer function (blue continuous), Level 1a – Hard Rock ( $\phi_{ss, htt, DCF}$ ): Single station sigma,  $VS30 = 800\text{ m/s}$ , host to target adjustments, depth correction factors (DCF), (magenta dashed), Level 1b – Soil ( $\phi_{ss, htt, DCF, Ktenidou}$ ): Single station sigma,  $VS30 = 800\text{ m/s}$ , host to target adjustments, depth correction factors (DCF), Ktenidou et al. 2015 transfer function (magenta continuous), Level 1a – Hard Rock ( $\phi_{ss, htt}$ ): Single station sigma,  $VS30 = 800\text{ m/s}$ , host to target adjustments (red dashed), Level 1c – Soil ( $\phi_{ss, htt, Linear}$ ): Single station sigma,  $VS30 = 800\text{ m/s}$ , host to target adjustments, linear transfer function NOAH (red continuous). .....79

Figure 54. AA14 uniform hazard spectrum for 5000 years return period. Site specific Approaches – Level 2: Level 1a – Rock ( $\phi_{ss, htt}$ ): Single station sigma, host to target adjustments,  $VS30 = 2600\text{ m/s}$  (blue dashed), Level 2a – Soil ( $\phi_{ss, htt, Nonlinear}$ ): Single station sigma, host to target adjustments, nonlinear transfer function NOAH,  $VS30 = 186\text{ m/s}$  (blue continuous). .....80

Figure 55. AA14 uniform hazard spectrum for 5000 years return period. All approaches on Soil: Level 0 – Soil ( $\phi$ ): Full sigma,  $VS30 = 186\text{ m/s}$  (blue), Level 0.5 - Soil ( $\phi, SAPE$ ): Full sigma, SAPE ( $VS30, f_o$ ) (blue dashed), Level 1a – Soil ( $\phi_{ss, \delta S2S\ TST_0}$ ): Single station sigma,  $VS30 = 186\text{ m/s}$ ,  $\delta S2S\ TST_0\ WIST$ , (red), Level 1b – Soil ( $\phi_{ss, Raptakis}$ ): Single station sigma,  $VS30 = 800\text{ m/s}$ , Raptakis et al. 1998 transfer function (red dashed), Level 1b – Soil ( $\phi_{ss, htt, DCF, Ktenidou}$ ): Single station sigma,  $VS30 = 800\text{ m/s}$ , host to target adjustments, depth correction factors (DCF), Ktenidou et al. 2015 transfer function (yellow), Level 1c – Soil ( $\phi_{ss, htt, Linear}$ ): Single station sigma,  $VS30 = 800\text{ m/s}$ , host to target adjustments, NOAH Linear transfer function (yellow dashed), Level 2a – Soil ( $\phi_{ss, htt, Nonlinear}$ ): Single station sigma,

---

$VS30 = 800 \text{ m/s}$ , host to target adjustments, NOAH Nonlinear transfer function (dark green).....	81
Figure 56. Overall comparison of soil and rock spectra obtained with the various approaches from Level 0 to Level 2a, for the AA14 GMPE and 5000 years return period: Level 0 – Rock ( $\phi$ ): Full sigma and $VS30 = 800 \text{ m/s}$ (black), Level 1a – Rock ( $\phi_{ss}$ ): Single station sigma and $VS30 = 800 \text{ m/s}$ (dark grey), Level 1a – Rock ( $\phi_{ss,htt}$ ): Single station sigma, host to target adjustments, $VS30 = 2600 \text{ m/s}$ (grey), Level 1b – Rock ( $\phi_{ss,htt,DCF}$ ): Single station sigma, htt, DCF, $VS30 = 2600 \text{ m/s}$ (light grey), Level 1b – Rock ( $\phi_{ss,Raptakis}$ ): Single station sigma, $VS30 = 186 \text{ m/s}$ (magenta), Level 0 – Soil ( $\phi$ ): Full sigma, $VS30 = 186 \text{ m/s}$ (red), Level 0.5 - Soil ( $\phi, SAPE$ ): Full sigma, SAPE ( $VS30, fo$ ), (dark green), Level 1a – Soil ( $\phi_{ss, \delta S2S TST\_0}$ ): Single station sigma, $VS30, \delta S2S TST\_0$ (magenta), Level 1b – Soil ( $\phi_{ss, Raptakis}$ ): Single station sigma, Raptakis et al.1998 transfer function, (dark blue), Level 1b – Soil ( $\phi_{ss, htt, DCF, Ktenidou}$ ): Single station sigma, host to target adjustments, depth correction factors, Ktenidou et al. 2015 transfer function (light blue), Level 1c – Soil ( $\phi_{ss, htt, Linear TF}$ ): Single station sigma, host to target adjustments, linear transfer function NOAH (orange), Level 2a – Soil ( $\phi_{ss, htt, Nonlinear TF}$ ): Single station sigma, host to target adjustments, nonlinear transfer function NOAH (light green). .....	82
Figure 57 : Example of annual probability of exceedance of 1m tsunami wave height at the 50 m isobaths around the Mediterranean Sea due to subduction earthquakes on the Hellenic Arc .....	92
Figure 58. Examples of target sites used in L15 and control profiles (red dots) used for the filtering (selection of the sources relevant for inundation calculations) .....	93
Figure 59 : Illustration of the two-step filtering procedure. Filter 1 selects only those seismic sources that generate a tsunami over the ‘noise threshold’; Filter 2 finds clusters of sources producing comparable effects. To the right, the hazard curves obtained only with selected sources are compared to those obtained with the full set.....	94
Figure 60 : Comparison of inundation maps obtained with the selected sources to those obtained with the full set.....	95
Figure 61 : Snapshot of the high resolution grid (10 m) of the Thessaloniki bay area. This grid will be used to perform simulations of inundation.....	96
Figure 62 :Example of tsunami inundation modelling results on a high resolution grid .....	96
Figure 63: Main results of InterPacific project (Garofalo et al., 2016a,b): Comparison among the $V_s$ profiles obtained with invasive methods (in green) and non-invasive methods, distinguishing between those profiles related to the analysis of active and passive seismic data (in red) and only passive seismic data (in blue). The comparison is performed for each site: Mirandola (MIR, in the left panel), Grenoble (GRE, in the central panel) and Cadarache (CAD, in the right panel). .....	115
Figure 64. Linear case: Acceleration records on rock from the PEER database (blue) and at the surface obtained after performing wave propagation with NOAH (red).....	117

---

Figure 65. Linear case: Amplitude Fourier Spectra on rock (blue) and at soil (red) for each one of the considered acceleration records. ....	120
Figure 66. Linear case: Transfer Function on rock (blue) and at soil (red) at the Fourier domain for each one of the considered acceleration records.....	123
Figure 67. Nonlinear case: Acceleration records on rock from the PEER database (blue) and at the surface obtained after performing wave propagation with NOAH (red)..	125
Figure 68. Nonlinear case: Amplitude Fourier Spectras on rock (blue) and at soil (red) for each one of the considered acceleration records.....	127
Figure 69. Nonlinear case: Transfer Function on rock (blue) and at soil (red) at the Fourier domain for each one of the considered acceleration records.....	130



---

## List of Tables

Table 1 : Main characteristics of the two approaches for consideration of site effects in SHA presented in this document.....	3
Table 2 :Example of site effect proxies used in GMPEs.....	5
Table 3: Contributions to total variability in ground-response estimates (modified from Roblee et al., 1996).....	26
Table 4. Euroseistest Soil Profile Characterization.....	33
Table 5. Ground Motion Prediction Equations used on this study.....	35
Table 6: Euroseistest average shear wave velocity up to top z meters and its fundamental frequency.....	40
Table 7 High frequency attenuation factor ( $kh$ ) for the selected ground motion models, where ( $\phi$ ) and ( $\tau$ ) were separated terms.....	50
Table 8. High frequency attenuation factor ( $kh$ ) at the Euroseistest derived from the analysis of ground motion records at station TST_196.....	50
Table 9: Euroseistest single station sigma (ln scale) calculated at station TST_196 at depth. (Ktenidou et al. 2015).....	54
Table 10: Euroseistest systematic deviation of the observed amplification, $\delta S2Ss$ , as estimated by Ktenidou et al. 2015 for the AA14 GMPE (second and third columns), and corrected using Akkar et al. 2014 site term (fourth and fifth columns), and converted into amplification factors (sixth and seventh columns). .....	56
Table 11. Euroseistest material properties model with water table below at 1m depth. ....	63
Table 12. Euroseistest material resistance model.....	63
Table 13. Summary of Metadata of Selected Records fitting the 5000 years return period uniform hazard spectra at the Euroseistest (PEEER database). ....	70



# 1 Introduction : Objectives and organization of the document

This report presents an overview of the available approaches for site-specific probabilistic seismic hazard assessment in terms of ground motion estimates, together with some example applications on one particular site, and a similar section for tsunami hazard methods.

The seismic hazard at a given site integrates several components : the local and regional level of seismic activity and the way the ground motion evolves with respect to magnitude, distance and site characteristics. The probabilistic hazard assessment may be done either in one single step using a "generic" approach for sites with poor information on site characteristics, or separated in two steps for "site-specific" studies. In the latter case, the first step deals with the assessment of hazard at a virtual "reference" rock site with the same coordinates, while the second step focuses on the hazard modulation linked with local, specific, site conditions. The latter modulation should imply detailed local investigations which may be based either on in-situ instrumentation, or specific geotechnical and geophysical measurements feeding models for numerical simulation (or both). The two-steps approach, which obviously implies an additional cost, should in principle be more precise and reliable. It does indeed allow to replace the classical, ergodic, full- sigma value used in the one-step approach by a reduced, "single-site" sigma value, which intrinsically leads to reduced hazard values, especially at long return periods. However, having a more sophisticated approach introduces new sources of epistemic uncertainty, linked with the in-situ measurements and/or the subsequent numerical simulation (including some inherent assumptions on the underlying models), which may *in fine* balance the hazard reduction effects of the decreased aleatory variability. The present report is intended to present an overview of the possible approaches, outlining their respective advantages and drawbacks, the corresponding requirements in terms of site characterization, and illustrating their respective results on one example at a real site.

Tsunami effects are also very sensitive to the local characteristics of the on-shore topography and off-shore shallow bathymetry, and the probabilistic tsunami hazard assessment thus faces similar issues as ground motion hazard: the last section presents recent developments allowing to limit the numerical cost of site-specific tsunami hazard assessment.

## 2 General methodological framework: Inventory of available approaches and associated issues

### 2.1 OVERVIEW

This section describes the different methods that can be applied to take into account local geotechnical conditions in the assessment of seismic hazard. Most of the proposed approaches can, in general, be applied to either deterministic (“D”) or probabilistic (“P”) seismic hazard assessment (DSHA or PSHA). However, because probabilistic seismic hazard assessment (PSHA) has become the dominant practice at the international level, the example applications and discussions along this text will refer only to PSHA.

This section will present different approaches for the consideration of site effects with an increasing level of detail and complexity. We split the different approaches in two main categories.

- (1) **Generic (Level 0) or “partially site-specific” approaches (level 0.5).** Here, the site effect is taken into account in an average, approximate way through one or several site proxies, and based on simplified approaches. The basic site proxy used in GMPEs is the travel-time average of the shear wave velocity over the topmost 30 m (parameter  $V_{S30}$ , level 0 approach), but some other may be used to somehow refine the site correction factors (level 0.5). As these correction factors are derived from average, non site-specific correlations, the aleatory uncertainty to be used in the selected GMPEs must be the full, ergodic sigma, and cannot be reduced.
- (2) **Site-specific approaches.** Here, the actual site amplification is considered on the basis of more refined, instrumental or numerical, analysis, which allows using a single-site value for the aleatory uncertainty. Two main sub categories are introduced, depending on whether the site response is considered linear (i.e., independent of the rock hazard level: Level 1), or non-linear (Level 2). These approaches (Levels 1 and 2) need a detailed site characterization and, most often, also need host-to-target adjustments, since the actual reference rock with respect to which the site amplification is estimated, is most often different from the “standard rock” that is used for standard PSHA estimates because of the existing limitations in GMPEs. An alternative approach, fully empirical, linear approach, labelled Level 1a is also mentioned, which however requires careful site monitoring and data analysis.

The main elements of the two categories of approaches that will be detailed in this section are summarized in Table 1. This table lists a total of 7 various approaches (one per column, labeled as detailed in the first rows), and indicates, for each of them, the method to be used for the estimation of site amplification, the gross characteristics of the associated rock hazard estimate (is it needed or not, with or without host-to-target adjustment, full or single-site sigma), and the kind of uncertainties (aleatory ad/or epistemic) that should be taken into account in the estimation of site amplification. It also indicates (last row) a rough correspondence to the US nuclear regulatory practice as mentioned in NUREG6728.

Methodological framework

Table 1 : Main characteristics of the two approaches for consideration of site effects in SHA presented in this document.

	Generic or partially site-specific		Site-specific					
	Level 0	Level 0.5	Level 1 (linear)			Level 2 (NL site response)		
<b>Method for site-effects estimation</b>	Site effect by proxy in GMPEs ( $v_{vs30}$ , measured or inferred, L or NL)	Site effect by proxy in GMPEs + amplification factor based on simplified approaches ( $V_{s,i} + f_0$ , + other possible proxies)	1a Site specific residual ( $\delta S2S,s$ from GMPEs)	Site response analysis		Nonlinear site response analysis (Nonlinear amplification function)		
				1b Instrumental (spectral ratio wrt local reference)	1c Numerical (any kind: nD, linear)	2a NL site response analysis after disaggregation for the considered return period	2b Full convolution PSHARock *AF(pga)	
<b>Prerequisite : rock hazard</b>	Not necessary	"standard rock" (e.g., $V_{s30} = 800$ M/S)	"Standard rock"	Site specific bedrock		Site specific bedrock :	Site specific bedrock	
<b>GMPEs host-to-target adjustment</b>	No	No	No	Yes		Yes	Yes	
<b>Uncertainty in GMPEs for rock hazard</b>	Total Sigma (measured or inferred site proxies)		Single-station sigma					
<b>Site response uncertainties</b>	Aleatory	No additional uncertainty	No uncertainties (Level 0)	$\Phi_{ss,s}$ , no additional variability	$\Phi_{ss,s}$ or $\Phi_{ss}$ , no additional variability		$\Phi_{ss,s}$ or $\Phi_{ss}$ , no additional variability	$\Phi_{ss,s}$ or $\Phi_{ss}$ , no additional variability
	Epistemic	No additional branch	Various SAPE	Uncertainty on $\delta S2S,s$	None unless clear evidence	Various profiles or models	Various profiles or models (possibility of...)	
<b>Calculation of soil hazard</b>	n/a	n/a	Approach 1 or Approach 2 NUREG 6728			Approach 2 NUREG 6728		

## 2.2 GENERIC (NOT FULLY SITE-SPECIFIC APPROACHES)

Generic simplified approaches to account for local site amplification can be used if they are expected to provide reliable and realistic results. These “Level 0” approaches make use of the site amplification as defined within the considered GMPEs, so the main condition that shall be fulfilled is that the site parameters (e.g., most often,  $V_{S30}$ ) estimated (and preferably of course measured) at the site are included in the validity domain of considered GMPEs.

It is also possible to somewhat refine the estimate of the site amplification term considering some additional site information. Even though there are not many possibilities right now for the “Level 0.5” approach, they are expected to become more numerous in the near future (i.e., next 3-5 years), and to enlarge and enrich the panel of available, simple techniques which do not require a prominent expertise in the field of SHA.

### 2.2.1 Direct use of GMPEs

A simple and widely used approach assumes that the soil conditions at the site resemble those at the stations in the database considered for the development of the GMPEs used for the hazard estimation. In this approach, the site response is assumed to be correctly captured by the site model included in the adopted GMPEs, and therefore the hazard spectra (deterministic or probabilistic) estimated with these GMPEs and the value of the required site proxy, already accounts, in a simplified and generic way, for site effects through an “averaged” site factor. It should be noted that this approach ignores virtually almost all the site-specific information (except for the value of the considered site-proxy) and, therefore, produces only an imprecise, generic assessment of the hazard corresponding to a global average over many sites with similar values of the site proxy.

Depending on the selected GMPEs several parameterization of the site response can be used. In general, the site amplification is described by one or more variables that act as proxies of the site amplification. Several proxies are proposed in the literature. A non-exhaustive list of the most commonly used proxies is presented in Table 2, including a brief description and reference to recent GMPEs employing them. Some GMPEs use a combination of two proxies (e.g.,  $V_{S30}$  and  $Z_{1.0}$ ) aiming to capture different characteristics of the site amplification.  $Z_{1.0}$ ,  $Z_{2.5}$  alone are usually not considered as a site proxy but they are used complementary with  $V_{S30}$  in order to account for the site amplification due to basin effects and deep sediments in general. One must keep in mind however that these terms are very poorly constrained, even in the most extensively studied areas of the planet such as California, as different models conclude on quite different values, and as the associated so-called “basin effects” are indeed related to very specific basins such as those of the LA area, which cannot necessarily be extrapolated to other areas of the world.

Most of the presently existing site models are based on  $V_{S30}$  as a principal proxy, and can be divided into two categories, depending on the consideration or not of soil nonlinearity. Nonlinear site amplification as a function of  $V_{S30}$  and of the ground motion at a reference “rock” condition has been examined in depth by recent studies (Sandikkaya et al., 2013; Seyhan and Stewart, 2014). These studies developed empirical (or semi-empirical) models for prediction of linear and nonlinear amplification factors for 5%-damped acceleration response spectra. Such results are then used in the development of nonlinear site models in GMPEs (e.g., Akkar et al., 2014; Boore et al., 2014). However, although not disputing the existence of soil nonlinearity for strong shaking at soil sites, several parallel studies also

pointed out that such effects are not so obvious in their database and thus did not explicitly modeled it in GMPEs (e.g., Akkar and Bommer 2007; Cauzzi and Faccioli 2008; Bindi et al., 2014).

Table 2 :Example of site effect proxies used in GMPEs.

Parameter	Description	Use	Example of GMPEs (some of the GMPEs use more than one site proxy)
$V_{S30}$	Sites are classified according to their travel-time average shear-wave velocity over the upper 30 m of the profile.	<p>Site amplification is a continuous function of <math>V_{S30}</math>. Two main models exist.</p> <p><u>Linear model:</u> site amplification is function of <math>V_{S30}</math> and spectral period only.</p> <p><u>Nonlinear model:</u> site amplification at each spectral period is function of <math>V_{S30}</math>, spectral period and ground motion at a reference "rock" site condition (pga or PSA(T))</p>	<p><u>Linear model:</u> Bindi et al. 2014 Bora et al., 2014</p> <p><u>Nonlinear model:</u> Akkar et al., 2014 Boore and Atkinson 2008 Boore et al., 2014 Abrahamson and Silva 2008 Abrahamson et al., 2014 ...</p>
Site classes	Sites are classified according to site categories, usually defined by EC8 or NEHRP. Classification is usually based on surface geology. Site classes are implicitly connected to a range of $V_{S30}$ .	Site amplification is assumed constant within each site class.	Ambraseys et al., 2005 Akkar and Bommer 2010 Bindi et al. 2011 Faccioli et al., 2010 Bindi et al. 2014 Cauzzi and Faccioli, 2008
fundamental frequency (or period)	The fundamental frequency ( $f_0$ ) of a site is usually determined based on the average horizontal-to-vertical (H/V) spectral ratios of ground motion. Classes of $f_0$ are used.	Site amplification is assumed constant within each $f_0$ class.	Zhao et al. 2006 Di Alessandro et al. 2012
$Z_{1.0}$	Depth to the horizon having a $V_s=1.0$ km/s	Continuous function, usually coupled with $V_{S30}$ .	Abrahamson & Silva 2008 Abrahamson et al., 2014 Boore et al., 2014 Chiou & Young 2014
$Z_{2.5}$	Depth to the horizon having a $V_s=2.5$ km/s	Continuous function, usually coupled with $V_{S30}$ .	Campbell & Bozorgnia 2008 Campbell & Bozorgnia 2014

As to GMPEs that use site classes only, it is recommended to use GMPEs that consider site classes representative of Eurocode 8 or NEHRP site categories. The use of site classes simply representative of "rock" or "soil" (e.g., Berge-Thierry et al., 2003) is considered out of date and is thus discouraged.

Table 2 shows that most of the GMPEs use  $V_{S30}$  or  $V_{S30}$  site classes as proxies of site amplification. Only few of them use the site fundamental frequency  $f_0$  as a site proxy. The site parameterization is a relevant source of epistemic uncertainties in the GMPEs as shown

in Figure 1 where the site amplification as a function of  $V_{S30}$  is shown for several GMPEs (Stewart et al. 2014).

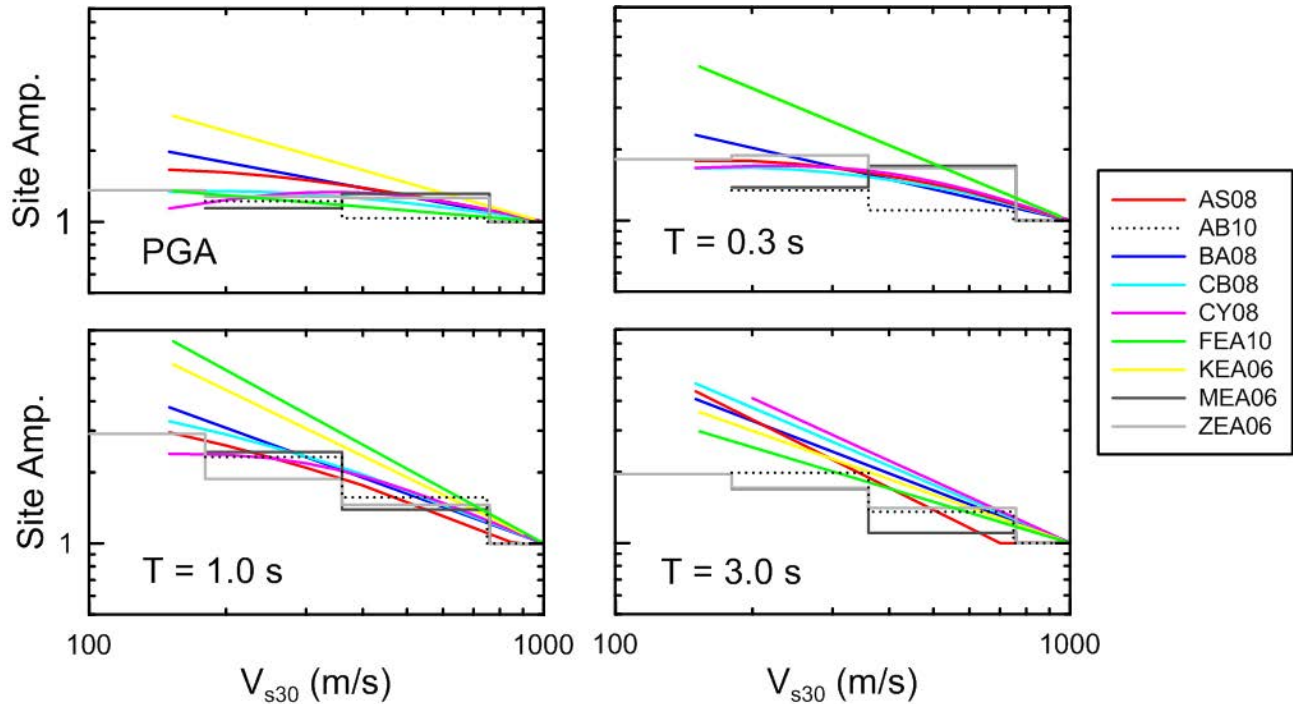


Figure 1 :  $V_{S30}$ -scaling of a few selected GMPEs for a reference rock peak acceleration of  $PGAr = 0.1g$ . Amplification has been computed relative to a consistent reference velocity of  $V_{ref} = 1000$  m/s, regardless of the reference condition used in the GMPE. Stepped relationships (e.g., AB10) describe site response relative to discrete categories whereas continuous relations use  $V_{S30}$  directly as the site parameter. From Stewart et al., (2014).

One important site parameter that has not been included so far in the GMPEs is the factor  $\kappa$  (or  $\kappa_0$ ) introduced by Anderson and Hough (1984) to characterize the high-frequency decay of the acceleration Fourier spectra. This parameter is known to substantially affect the high-frequency ground motion at a site (Ktenidou et al. 2013), and is more and more often attributed to the attenuation (damping) in the shallow-most site layers. It is worth mentioning that Laurendeau et al. 2013 tested the effect of considering  $\kappa_0$  in the development of a GMPE using Japanese recordings. Their conclusions suggest that in the future  $\kappa_0$  may be coupled with  $V_{S30}$  in order to account for high-frequency attenuation. For the time being the limited number of measured  $\kappa_0$  and the huge associated uncertainties prevent the use of such parameter directly in the GMPEs. More discussion on  $\kappa_0$  can be found in Section 2.3.2.

It should also be emphasized at this stage that all the site proxies mentioned in this section and used in the GMPEs should be actually measured and not only guessed from the correlation with other parameters. Indications and recommendations on the way to measure those proxies can be found in Hollender et al., 2015, an extract of which is given in Appendix 1. Some GMPEs change the value of the aleatory variability depending on whether the site proxy (basically  $V_{S30}$ ) is measured or simply "inferred" (Chiou and Youngs, 2008; Derras et al., 2016), with larger values in the latter case.

### **2.2.2 A-posteriori modifications of the site term : use of "SAPEs"**

This approach requires a further methodological step with respect to the previous one. It is assumed that the simple site amplification from the GMPEs is a first-order model for the target site response but that some site-specificity can be included in order to provide a better description of the site response. A correction factor can be developed and applied, as a post-processing, to the hazard spectrum computed as described in sections 2.3.2 and 3.3.2. In other words, the idea is to separate the site term, to be handled through specific "SAPEs" (Site Amplification Prediction Equations), from the GMPEs that are used only to estimate the rock hazard. This allows to take into account some additional site information, and in principle, in the long run, could allow to account for effects of the surface or subsurface geometry (topography or basin effects), or non-linear effects, in a more physical, though still simplified, way than what is proposed even in the most recent, most complex, GMPEs.

#### **2.2.2.1 Site Amplification models accounting for other site proxies**

The term "site amplification prediction equation" (SAPE) was introduced by Cadet et al. (2011a; 2011b) to define empirical prediction of (linear) site amplification as a function of few parameters ( $V_{SZ}$ , with  $z$  equal to 5, 10, 20 and 30m and  $f_0$ ) derived from Japanese strong-motion data (KiK-net). Cadet et al. (2011a; 2011b) estimated the amplification factor from the ratios between the surface and down-hole horizontal response spectra, corrected for the varying depths and impedance of the down-hole sites in order to obtain an amplification factor with respect to "standard, outcropping rock". Several site parameters were selected and tested on the basis of their simplicity and availability at relatively low cost. The amplification factors were then correlated with each of the individual site parameters, also testing twin proxies, i.e. the ( $f_0$ ,  $V_{SZ}$ ) couples, for which the correlation between amplification factors and  $V_{SZ}$  was performed for each dimensionless frequency ( $f / f_0$ ), after a normalization of the frequencies by each site fundamental frequency  $f_0$ . The results showed that the best performances in predicting site amplifications were obtained by the twin parameters  $V_{S30} - f_0$ . The best single parameter proves to be  $f_0$ , in agreement with other studies (Luzi et al., 2011).

The application of this approach requires the knowledge of the  $f_0$  and  $V_{SZ}$  of the site in order to calculate the amplification function. The "standard rock" hazard spectrum is then multiplied by the amplification function. Care must be taken in the combination of hazard spectrum and amplification function in order not to double count the site effect in both GMPEs and SAPE. For example a SAPE based on  $f_0$  can be applied to a hazard spectrum calculated for the selected  $V_{S30}$  value in the adopted GMPEs, assuming that  $V_{S30}$  and  $f_0$  are poorly correlated and thus account for different origins of site amplification. On the contrary if a SAPE based on  $V_{S30}$  and  $f_0$  is used, then the hazard spectrum shall be calculated using a reference rock  $V_{S30}$  (e.g.,  $V_{S30} = 800$  m/s) in the GMPEs.

The advantage of this approach is that it allows considering the fundamental frequency of the site that is usually neglected in the generic approach because only few GMPEs adopt fundamental frequency classes as site effect proxy. The main limitation that is put forward by several authors in the application of such SAPE to account for partially site-specific site amplification in seismic hazard assessment, is that they were derived using Japanese data only, and may thus reflect systematic differences in shallow site amplification in Japan with respect to other regions. However, such an argument will no longer hold when the proxies used in "SAPEs" will capture the main physics of site amplification, and then should not have regional bias (as is the case in any too simple proxy, such as in particular  $V_{S30}$ ). Similar

approaches could be implemented in other regions whenever a sufficient amount of data is available.

### **2.2.2.2 Accounting for subsurface geometry effects with "Aggravation Factors"**

Basically, the notion of aggravation factor (Faccioli et al., 1998; Makra et al. 2001; Kristek et al., 2015a, 2015b; Bard et al., 2014, 2015a, 2015b) is related to the ratio between a multidimensional amplification function and a 1D amplification function. Thus, the aggravation factor aims to evaluate the modulation of site amplification in relation to a complex local geometry with respect to 1D soil response which is due to the soil property log ("soil column") just beneath the studied site.

The aggravation factor could be derived using 1D and 2D/3D computations (if appropriate, investigating different model hypotheses), implementing linear or non-linear rheology and using accelerograms that are consistent with the level of hazard at the site under study. Response spectra are then computed for each type of models and accelerograms, from which ratios between 2D/3D and 1D scenario response spectra are then derived ("single" aggravation factors). A final aggravation factor (and the associated standard deviation) is deduced from this set of "single" aggravation factors, taking into account the variability of the response and/or the lack of knowledge on the actual subsurface geometry of the site. This final aggravation factor is then applied to a pre-established "reference" hazard spectra in which the 1D response of the soil is assumed to be integrated. The aggravation factor does not exclude the use of empirical evaluation of site effects (as SSR approaches) in order to check if the 2D/3D computations are consistent with true amplification at low input motions (usually, strong motions are not addressed by empirical approaches, especially in low to moderate seismicity contexts, but also in more active zones because of the long recurrence intervals of the design motion).

One of the advantages of the aggravation factor approach is related to the use of ratio in the computation: at the first order, a slight to moderate change in the model description (e.g. a velocity change) will act in the same way on both 1D and 2D/3D computations. The overall results are then less sensitive to a change in the model description (Kristek et al., 2015b; Bard et al., 2015b).

One can distinguish two approaches in order to determine the aggravation factor. The first one, the simplest one, consists in determining a set of simplified parameters ( $V_{S30}$ , ratio between height and width of the basin, contrast with bedrock, among others...) and then determining the "Simplified Aggravation Factor" using available results from previous studies (e.g., NERA JRA1 work, Bard et al., 2014, 2015a). This kind of studies involved massive numerical simulations on a wide range of site typologies. The second one consists in computing a "Detailed Aggravation Factor" by 1D, and 2D or 3D simulations using the detailed geotechnical model of the studied site (that needs a higher characterization level). In the former case, "simplified aggravation factors" derived from gross correlation studies, cannot be referred to as "site-specific" and therefore correspond to the 0.5 level, while the latter case is typically site-specific and allows the use of single-site sigma.

### **2.2.2.3 Other types of "SAPE"**

One may also think of other estimates of site amplifications, which may be intermediate between the very crude approach used in most GMPEs, with one single site proxy like  $V_{S30}$ , and site-specific approaches. For instance, some investigations are presently under way to improve the description and accounting of the effects of soil non-linearity through some

"modulation functions" that are function of the site class (defined either through  $V_{S30}$  or  $f_0$ ), and of the rock  $p_{ga}$  value, as proposed for instance in Régnier et al., 2016. Such approaches could for instance be used in addition to classical GMPEs that do not account for soil non-linearity.

## 2.3 SITE-SPECIFIC APPROACHES

### 2.3.1 Overview

The term "site-specific" is here used to indicate that the hazard estimates include the amplification effects induced by the actual local geology: site-specific approaches are based on a detailed consideration of the local site response and the associated uncertainties, which goes much beyond the simple consideration of a "site condition proxy" as used in "generic" approaches (Levels 0 and 0.5). Different methods exist to estimate site amplification, which exhibit different sophistication levels depending on the characteristics of the site (and also, most often, on the available budget...): 1D response accounting for the detailed velocity profile  $V_S(z)$  down to the actual bedrock, accounting for geometrical effects related to the 2D or 3D surface or subsurface topography, non-linear behavior in rather soft soils.

The use of site-specific approaches generally requires the assessment of an input motion at the base of the local soil profile in order to properly account for the soil response. This may require the calculation of the SHA for quite large values of  $V_{S30}$  (hard-rock conditions) that may be outside the validity domain of the adopted GMPEs (i.e.,  $V_{S30}$  larger than 1200-1500 m/s). In this case the rock hazard, and/or the used GMPEs need to be adjusted for such hard-rock conditions in order to correctly represent the input motion for the site response analyses.

This section will thus start with a presentation of the presently existing "host-to-target adjustment" techniques (HTTA), followed by the various techniques which may be used for the estimation of local soil response, either on the basis of in-situ instrumental recordings, or with numerical simulation tools, which may be limited to the linear domain or also consider the non-linear behavior of soft to moderately stiff soils.

### 2.3.2 Host-to-target adjustment: what, when and how

The "host-to-target" adjustment aims at modifying a GMPE, originally valid for a generic host condition, in order to apply it on significantly different, target site conditions. Such adjustments presently consider differences in the  $V_S$  profile and  $\kappa$  values between the host and target conditions, i.e., the host and target regions.

In the context of this document we will discuss only adjustment from generic rock to specific hard-rock conditions. This is generally the required adjustment to compute the seismic hazard that will then be used to specify the input motion for calculation of the site response.

#### 2.3.2.1 *Background*

The adjustment of a GMPE derived for a host region to a target region was first proposed by Campbell (2003) to use GMPEs developed for Western US in applications in the Eastern US. In this case, the GMPEs were adjusted for the generic site characteristics and for the

different regional attenuation. The Campbell (2003) approach is known as hybrid empirical method. In this method, the scaling of response spectra is based on a simple point-source stochastic model (Boore, 2003), using seismological models (source, path, and site) for the host region and for the target region. The point-source model is used to compute the response spectrum for the host and target regions, and the method then scales the response spectral values from the GMPE by the ratio of the point-source response spectral values from the two point-source stochastic models. Examples of application of the Campbell (2003) methodology can be found in several studies (e.g., Cotton et al., 2006; Douglas et al., 2006; Van Houtte et al., 2011).

The Campbell (2003) approach presents two main limitations: 1) the method is applied even if the spectral shape of the GMPE and of the (host) point source model are significantly different; 2) there exists a non-negligible trade-off between the various parameters of the point-source stochastic model ( $\kappa$ , stress drop, and whole-path attenuation), which may bias the scaling factors linked to modifications in only one or two of these parameters. A modified approach has thus been looked for: Al Atik et al., (2014) use the forward and inverse random vibration theory (RVT and IRVT) to move back and forth between Fourier and response spectral domains, in order to translate the  $\kappa$  adjustments, easy to perform in the Fourier domain, into the response spectra domain. Such adjustments are, formally, GMPE and scenario dependent, and may therefore be quite heavy and time consuming.

On the other hand, the " $V_S$ " adjustments associated to the increased rock rigidity, are performed on the basis of the quarter-wavelength impedance term and the "generic rock profiles" proposed by Boore (2003), and in this case is scenario INdependent (and in principle also GMPE independent as soon as the used GMPE may be considered valid for a standard rock with  $V_{S30} = 800$  m/s. They can be conducted as an a priori correction to the host to target adjustments.

Other approaches are presently explored to derive GMPEs directly for rock and hard-rock conditions (Laurendeau et al., 2013, 2015). Such an approach is much simpler. A main issue is that the first results obtained with this approach are very different from the results provided by the previous " $V_S$ - $\kappa$ " HTTA techniques: they lead to significantly reduced estimates in the high-frequency range for very hard rock sites, which demonstrates the large level of epistemic uncertainty in the present adjustment procedures.

### **2.3.2.2 Application of $V_S$ - $\kappa$ adjustment**

In the framework of this document (adjusting GMPEs from rock to hard rock) the general effect of the  $V_S$ - $\kappa$  adjustment, as it is implemented in Campbell (2003) or Al Atik (2014) with the underlying, explicit or implicit, assumptions, is to decrease the ground motion amplitudes at low-to-mid frequencies (say below 10 Hz) and to increase the amplitude at high frequencies. The first effect is caused by the increase of  $V_{S30}$  and the second one by a decrease of  $\kappa$  usually observed for hard-rock sites.

The application of  $V_S$ -  $\kappa$  adjustment can be summarized in the following methodological steps:

1. Estimation of target  $V_S$  and  $\kappa$ . This is done primarily on the basis of data collected at the site of interest. Generally the  $V_S$  profile is available as part of the investigation performed in a site-specific hazard assessment, through direct (e.g., cross-hole) or indirect (e.g., surface-waves inversion) methods. The  $\kappa$  value is usually more difficult to estimate

because it requires a sufficient number of earthquake recordings at the site. Alternatively, correlation of  $\kappa$  with other parameters can be used (Van Houtte et al. 2011; Ktenidou et al. 2014) ; also the estimation of  $\kappa$  at a given site can be derived from the measurements at another site with proven similar characteristics to the target site. These alternatives usually imply large uncertainties in the  $\kappa$  value.

2. Estimation of host  $V_s$  and  $\kappa$ . They are implicitly part of the dataset for which the GMPE was developed and not directly a modifiable variable in the attenuation model. At present, they are most often NOT provided by the authors of the GMPEs. For this reason it is hard to quantify and constrain these parameters, an "equivalent"  $\kappa$  and a representative  $V_s$  profile need to be determined. This can be done using several approaches (see Cotton et al., 2006; Biro and Renault, 2012; Al Atik et al., 2014).
3. Definition of  $V_s$  scaling and  $\kappa$  scaling as a function of spectral period. This step is performed primarily based on results of point-source stochastic model either applied directly to the response spectra or to Fourier spectra, then converted to response spectra via Random Vibration Theory. The definition of the scaling factor should be done for several (magnitude, distance) scenarios (focusing on those contributing the most to seismic hazard at the site, obtained by disaggregating the hazard), and for each GMPE.
4. Modification of GMPEs response spectra to account for host  $V_s$  and  $\kappa$ .

An example of  $V_s$  -  $\kappa$  adjustment for the Abrahamson & Silva (2008) GMPE is presented in Figure 2, considering several values of target  $V_s$  and  $\kappa$ .

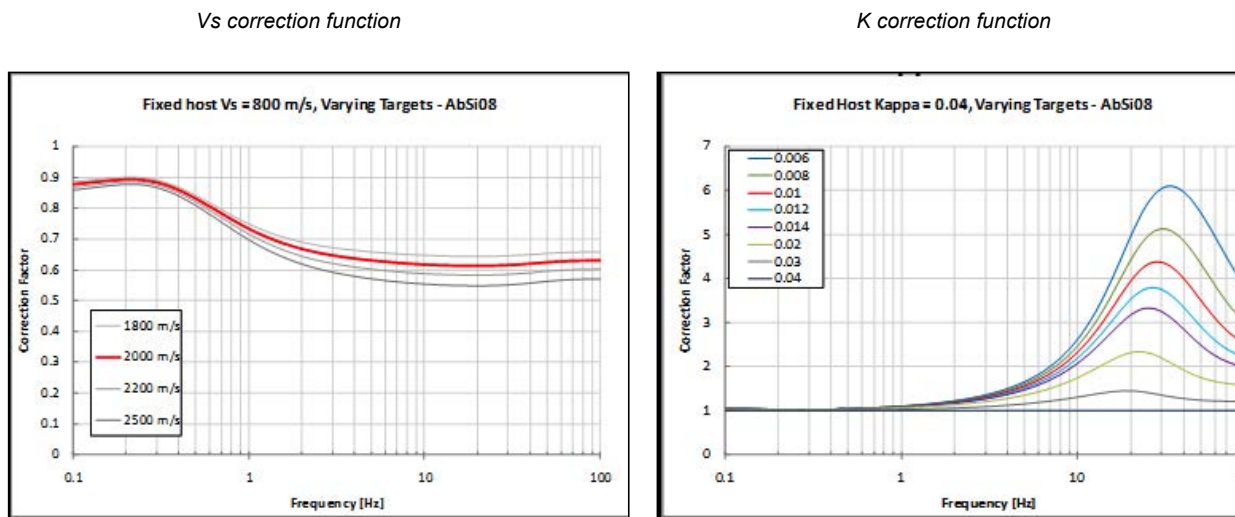


Figure 2 : Example of  $V_s$ - and  $K$ -correction functions evaluated for Abrahamson & Silva (2008). From Biro and Renault (2012)

### 2.3.2.3 Uncertainties

Biro and Renault (2012) clearly showed that in site-specific applications the  $V_s$ -  $\kappa$  adjustment carries several uncertainties that have a significant impact on the hazard results. Such

uncertainties shall be clearly identified in the application of the host-to-target adjustment. The main uncertainties are related to:

- (1) Estimation of the  $\kappa$  values and  $V_s$  profile for the target site. These uncertainties are related to the methodologies used to measure the  $V_s$  and  $\kappa$ .
- (2) Estimation of  $\kappa$  values and  $V_s$  profile for host GMPEs. The estimation of an equivalent  $\kappa$  for a GMPE is still largely method-dependent and there is no consensus on the most appropriate approach. Similarly the definition of a  $V_s$  profile representative of a  $V_{S30}$  is subjected to uncertainties. For this reason, it is recommended to use alternative values of host  $\kappa$  and  $V_s$  profiles in a logic tree to capture such epistemic uncertainty.

A substantial reduction of the uncertainties in the estimation of the host  $\kappa$  would be reached by including in the functional form of the GMPE an explicit dependence on  $\kappa$  values estimated for the dataset used in the GMPE derivation. However, the efforts are still ongoing on this issue, and there are only very few GMPEs with an explicit consideration of  $\kappa$ .

As mentioned above, another direction of improvement is the establishment of new generations of GMPEs which are valid also for very hard-rock, to avoid the required use of poorly constrained rock velocity models, and the use also of the quarter-wavelength impedance approach which may underestimate some resonance effects and bias the  $V_s$  correction factors.

### **2.3.3 Site response estimates: instrumental approach**

The site-specific amplification can be estimated in a purely empirical way on the basis of a dedicated instrumentation, and various approaches, using or not a reference site. By "seismological instrumentation", we designate instruments that allow to record, on the studied site and/or in its vicinity, ground motions induced by real, local or regional or even teleseismic earthquakes. Based, on these recordings, a number of "instrumental" approaches can be implemented that allow:

- 1) To access a direct measurement of the site-specific transfer function or other characteristics of the ground-motion modifications linked with local site conditions, through various techniques (site-to-reference spectral ratio, generalized inversion, deconvolution of coda waves, site-specific residual with respect to existing GMPEs, duration increase, among others...),
- 2) To consider the use of instrumentally based ground-motion prediction methods such as the empirical Green's function technique,
- 3) To evaluate the attenuation of high frequency of seismic signals (measuring the " $\kappa$ " parameter).
- 4) To validate the accuracy of numerical simulation tools

There exists a very abundant literature on the data processing techniques that can be used for deriving the site-specific amplification from instrumental recordings (e.g. Parolai, 2013). The present section will therefore essentially focus on the performance of in-situ seismic instrumentation, and on the resulting recommendations for in-situ monitoring.

### 2.3.3.1 *Usefulness of seismological instrumentation, with a special focus on moderate seismicity countries*

While these approaches seem easy and immediately efficient in high seismicity areas (Japan, Greece ...), where numerous events corresponding to at least moderate magnitudes can be recorded within a rather short lapse-time, they are most generally considered more difficult to implement in low seismicity areas, such as central, northern and western Europe. In those areas, events leading to potential recordings are deemed few and corresponding either to moderate-to-large distant earthquakes (far from the site of interest, and with predominantly low frequency content), or regional and local earthquakes with only low-to-moderate magnitude. In such low-to-moderate seismicity areas, it is therefore often considered useless – especially in the engineering community – to spend money on seismic instrumentation, because of three major factors that are thought to decrease the chances to get a sufficient amount of usable earthquake recordings:

- **The local seismicity:** obviously, the higher the number of earthquakes that may occur at a regional scale, the higher the chances to record valuable time histories. Nevertheless, distant earthquakes can also be used, especially to constrain the low-frequency response.
- **The local level of noise.** Indeed, noise level may exhibit a very high variability from one location to another. For industrial facilities in particular, the existence of heavy machineries is definitely not favorable for getting earthquake recordings from low-to-moderate events with a high enough signal-to-noise ratio.
- **The frequency range of the site effect under study.** This is also important because if we consider a low frequency site effect context, small earthquakes, even close to the site, will be useless because their low frequency content is too weak, and may not exceed the noise level. Conversely, even distant earthquakes (but with quite large magnitude) could produce valuable records.

Actually, this feeling, or belief about the limited usefulness of *in situ* seismic instrumentation has been recently proved inappropriate through dedicated experiments in sites of industrial facilities located in low-seismicity areas (Perron et al., 2015). The following lines describe what are the main findings of these recent investigations, and what the requirements for an economically affordable instrumentation to provide useful recordings within a reasonable, relatively short duration.

**Continuous measurements** performed recently with two types of sensors: **velocimeters** and accelerometers, on several French sites demonstrated that the number of useable events (i.e., those which provide a good signal-to-noise ratio) obtained from a relatively short duration experiment (2 years) is high in comparison with what was expected before implementing the instrumentation, and high enough to get valuable information on site characteristics and site response. On one French site with low seismicity in a rather low noise context, it was possible to obtain very robust estimates of the amplification function, based on SSR analysis, with more than one hundred of usable events in the intermediate frequency range [1 – 15 Hz]. On this site, it was also possible to evaluate the  $\kappa_0$  parameter (i.e., the site component of the high-frequency spectral decay), which is an even more encouraging result on the usefulness of site monitoring because it needs a high frequency analysis, where S/N is usually lower, and also needs numerous events for the extrapolation of single events  $\kappa_T$  values, mixing the site-specific component and the regional contributions, to the sole site-component  $\kappa_0$ .

These results, obtained at sites with relatively low-noise level within a large industrial / research area, have been extrapolated to other sites with relatively higher ambient noise level and/or a lower seismicity, to evaluate the number of recordings which would still have an acceptable signal-to-noise ratio to allow a useful analysis, as a function of the noise level. This extrapolation procedure may be discussed, but can provide useful though rough estimates. The conclusion (Perron et al., 2015) is that a velocimetric instrumentation is likely to produce within a couple of years of continuous monitoring a sufficient number of recordings to obtain a robust estimate of the site amplification, while the estimation of  $\kappa_0$  parameter, with the current classical methods, may be more difficult in case of a high level of noise at high frequency and / or a too low local seismicity.

It must be stressed however that site instrumentation, even if it can and does provide important and very useful information about site effects, cannot solve alone the whole site amplification issues. Indeed, the events that one can expect to record in low-to-moderate seismicity areas within a reasonable duration (i.e., a few years), are most often regional or teleseismic events, with only a few local, weak events than can be assimilated to “point source” events. Numerical simulations thus remain unavoidable to assess the effect of sensitivity of the site response to path and source characteristics (incidence and back-azimuth angles, extended sources), and above all to the loading level: reasonably expectable events produce (very) weak motions with very low strain levels, which cannot provide information on the actual non-linear response of the shallow, softer soils. Meanwhile, as repeatedly shown in all benchmarking exercises over recent years (for a recent overview see Chaljub et al., 2015 and Maufroy et al., 2015a, 2015b, 2016), site instrumentation appears a key element to allow the validation of numerical simulation tools for a given range of incidence angles, source sizes and motion levels. Once the simulation codes and models are validated by a successful comparison to instrumental measurements, they can be used to explore other scenarios involving extended sources, non-linearity, etc.

### **2.3.3.2 Implementation recommendations**

This section presents the main recommendations derived from the dedicated investigations conducted within the framework and the French Cashima and SIGMA R&D projects.

In order to implement an instrumental setup that aims to provide information about site effects, it is strongly recommended to use (at least) **velocimeters** (Figure 3 and Figure 4). Of course, a few accelerometers can be used as a complement and safety in case of strong events, for example one at the reference station and another one as close as possible to the location to study.

The **position** of velocimeters on soil conditions should be a compromise between noise level (as low as possible) and distance from the site of interest (as close as possible); it is recommended to install **several** velocimeters (not only one) around the area of interest in order to avoid possible bias due to spatial variability. Very often in “old, developed” countries such as in Europe, site-specific seismic hazard assessment studies are performed for already existing facilities or for new facilities on already existing, industrialized sites. This is of course a drawback for instrumentation as it raises the anthropogenic noise level. It is thus recommended to prepare the instrumentation by performing a quick analysis of noise on several locations around the site before implementing longer recordings. In order to choose a “rather low noise” location, we may consider the overall geometry of the basin /

sedimentary cover that is expected to produce site effects, in order to prefer station location that are in similar context (eg. depth of the basin beneath the station, distance from the border of the basin...) with respect to the exact location of the actual target site. In addition to one or a few “**rather low noise**” stations equipped with velocimeters, it is recommended to **install a station located closer to the target site, and equipped with both a velocimeter and an accelerometer**:

- The basic aim of such “rather low noise stations” is to record as much events as possible.
- This purpose of the “closest” station is two-fold: 1/ comparing response with other stations on the “strongest” events (the one that will exceed the local, higher noise level), 2/ obtaining unclipped recordings of (rare but possible) events that may induce a saturation of the velocimeter recordings, thanks to the accelerometer (local environmental noise or instrumental noise are no more an issue for such strong local events).

The **choice of good reference station(s)** (which allow a direct measurement of the site amplification) is also an important issue. The noise level issue is generally less problematical for such sites, but there exist other important requirements, which should be addressed for establishing a good reference station:

1. It should not be too far from the “site” stations (a few kilometers at most)
2. It should not be affected by significant topographic site effects (for instance, rock outcrops outside of an alluvial valley or sedimentary basin are often corresponding to hill slopes or ridges),
3. It should be representative of the rock condition that is present beneath the basin,
4. It should not be affected by any type of “lithological” site effect, even at high frequency (the presence of a thin colluvium deposit layer or a weathered layer may induce a high frequency site effect)

This implies the need for a **careful characterization** of the local conditions **at the reference station(s)** too (including at least geophysical investigations for obtaining the local Vs profile with a reliable  $V_{S30}$  measurement). For topographic site effect estimation, the computation of a quite simple proxy (Maufroy 2010, Maufroy et al. 2014), together with microtremor measurements according to the site-specific procedure proposed within the framework of the NERA project (Bard et al., 2014, 2015; Burjanek et al., 2016) could easily be evaluated.

For very wide basins, finding the “optimal” location of a reference station is not an easy issue. The use of generalized inversion (Drouet et al., 2008), site-specific residual (see below section 2.3.3.3) or specific coda processing techniques (Sèbe et al., 2003, 2005) to evaluate site amplification may allow using “reference” stations that are farther from “site” stations in comparison with standard SSR evaluation. Implementing such approaches requires however not only more sophisticated processing, but also complementing the data from the dedicated, in-situ monitoring instrumentation, with data from regional networks with a good seismological catalogue. Another alternative is of course the use of downhole reference stations that reach the rock beneath the basin; this is relatively affordable when the bedrock is not too deep (i.e., typically less than 100 m), but may become very expensive for very thick deposits.

Finally, another recurrent question about instrumentation has long been the recording mode: continuous or triggered? The mind of engineers dealing with managing the seismic risk at industrial facilities is often oriented towards triggering mode, for mainly historical reasons,

when on-site instrumentation was basically aimed at operational safety purposes in case of strong shaking. It should be clear that the evolution of technology and the changes in the objectives of site monitoring induce a complete reversal in the recording mode selection. On one hand, configuring an acceptable trigger setup takes quite long time during which one may miss a lot of events, as using too high threshold leads to miss a lot of events, whereas using too low threshold leads to get a very high amount of false events that are finally more difficult to manage than a continuous database. On the other hand, both instruments (that have now local storage devices that allow several months of continuous recordings) and transmission capabilities allow today to implement instrumentation in continuous mode, without any problem and any additional cost. **The choice of continuous recording is obvious and should not call for any discussion.**

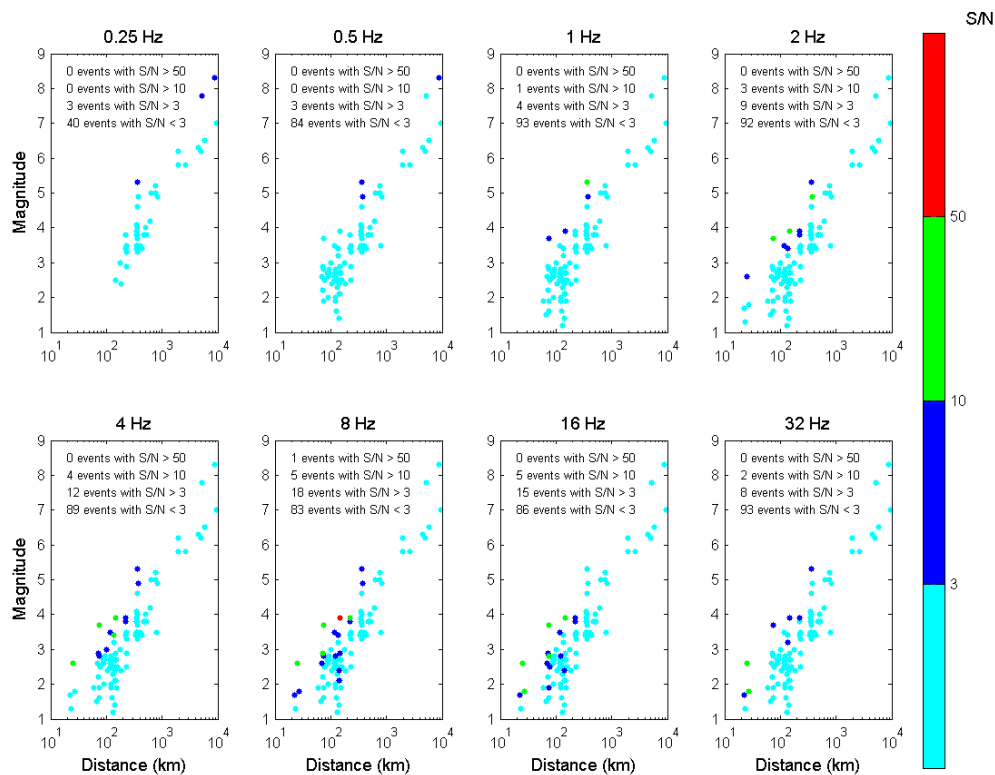


Figure 3: Evaluation of the signal to noise ratio of the 101 events recorded on a cumulated duration of 231 days of continuous recording at a rock station of our test-site (south-east of France) with an accelerometer. Each sub-figure shows the analysis at a given frequency, from 0.25 to 32 Hz, within a magnitude to distance plot. Each point corresponds to 1 earthquake. The color gives an indication about the corresponding signal-to-noise ratio (computed with a time windows centered on signal and another one on noise before the earthquake arrival). For example, we see that at 1 Hz, 1 event was recorded with a S/N > 10 (green point).

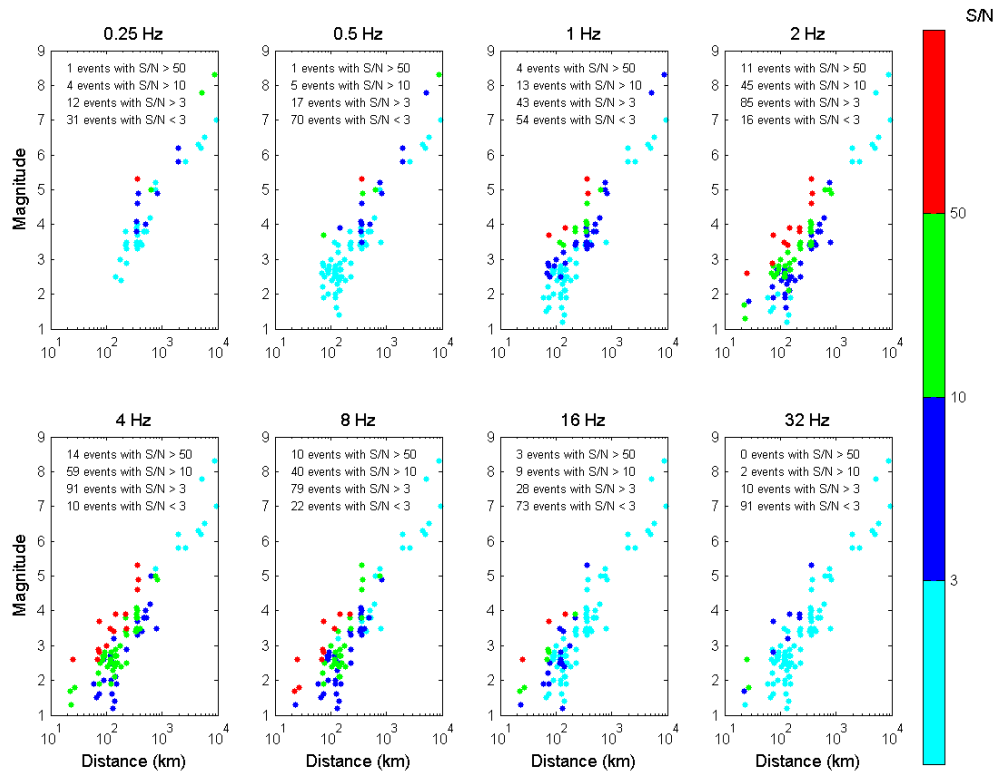


Figure 4: This figure is the same as the previous one, but realized with data coming from a *velocimeter* at the same place and on the rigorously same period of time. We see that the “usable” events are much more numerous than with the accelerometer. This amount of signals allows SRR analysis and  $\kappa$  determination. The recording duration is less than one year.

### 2.3.3.3 Site-specific residuals: $\delta S2S,s$ and $\Delta \delta S2S,s$ :

As mentioned earlier, an alternative site-specific approach consists in applying a purely empirical correction to the GMPEs median values. This approach can be used when a sufficient number of records<sup>1</sup> is available at the target site, and is in essence comparable to the generalized inversion techniques (the main difference is that the latter are applied to Fourier spectra, while the former are applied directly to response spectra, or other kinds of ground-motion parameters). It is in any case desirable, if not mandatory, that the earthquakes recorded at the site span a sufficient range of magnitudes, distances and azimuth angles. An example application within the framework of the SIGMA project can be found in Faccioli et al. (2013) for a site in the Po plain, which greatly “benefitted” from a major earthquake sequence (the Emilia Romagna 2012) which allowed the recording of a large data set.

In this approach GMPE predictions are modified through site-specific correction factors (labeled “ $\delta S2S$ ”) and the GMPE’s aleatory variability (sigma) is replaced - and reduced - with

<sup>1</sup> An exact quantification of the word “sufficient” is not easy and depends on the authors: some (such as Rodriguez-Marek et al., 2011) consider estimations are reliable for 15-20 recordings, other (Maufroy et al., 2016) report mis-estimations (i.e., with bias or underestimation of the scatter) for as many as 50 recordings. The key issue is to have a representative azimuthal and distance coverage.

the single-station sigma ( $\sigma_{ss,s}$ ) [see Rodríguez Marek et al. (2011) for the meaning of the symbols]. It should be kept in mind however that the  $\delta S2S$  residuals are in principle associated to one GMPE, and may vary from one GMPE to another – especially as the "generic site term" (generally linked with  $V_{S30}$ ) does not have the same functional form in all GMPEs - while only the single station variability  $\sigma_{ss,s}$  could in first approximation be considered as an intrinsic characteristic of the site, and, as such, should be roughly independent from the GMPE used to calculate them. However, the comparison of the residuals at two sites, for instance between the site under study and a "reference site", should be approximately GMPE independent, once it is corrected for the site term included in each GMPEs.

### 2.3.3.3.1 Method of ground motion residual analysis

Following Rodríguez Marek et al. (2011), a general form of a ground motion prediction model can be written as:

$$Y_{es} = \mu_{es} + \delta W_{es} + \delta B_e$$

Where  $Y_{es}$  is the logarithm (natural or base10) of the observed ground motion parameter for an event "e" at the site "s", and  $\mu_{es}$  is the median ground motion (log value) predicted by a GMPE.  $\delta B_e$  and  $\delta W_{es}$  are the corresponding ground motion residuals (or *variability*), which represent between-event and within-event residuals, respectively.

The between-event (also called inter-event) residual,  $\delta B_e$ , represents the average shift of the observed ground motion in an individual earthquake, e, from the median predicted by a GMPE.  $\delta B_e$  can be estimated as follows. For an individual earthquake e, let there be  $NS$  stations recording the event. Then, the average misfit between observations and predictions for earthquake e, using a specific GMPE, is:

$$\delta B_e = \frac{1}{NS} \sum_{s=1}^{NS} (Y_{es} - \mu_{es})$$

The within-event (also called intra-event) residual,  $\delta W_{es}$ , is the misfit between an individual observation at station s from the earthquake-specific median prediction, which is defined as the median prediction  $\mu_{es}$  of the model plus the between-event term  $\delta B_e$  for earthquake e. Thus  $\delta W_{es}$  also represents the difference between an individual observation (*i.e.*,  $Y_{es}$ ) and the event-corrected median estimate, *i. e.*

$$\delta W_{es} = Y_{es} - (\mu_{es} + \delta B_e)$$

If  $NE_s$  earthquake events are recorded at station s, the within-event residuals computed from a GMPE for that station are used to define the average site correction term  $\delta S2S_s$ :

$$\delta S2S_s = \frac{1}{NE_s} \sum_{e=1}^{NE_s} \delta W_{es}$$

$\delta S2S_s$  is a random variable that represents the average within-event residual at station s and is referred to as the *site term*. For a given station, it takes a deterministic value. Assuming no bias in the recordings obtained at each station,  $\delta S2S_s$  has zero mean (across all stations used for the derivation of the GMPE) and its variance is  $\phi_{s2s}^2$ . The

latter quantifies the component of site-to-site variability, which is not explained by GMPEs, for instance not captured by the sole consideration of the  $V_{S30}$  parameter. That is why both the  $\delta S2S_s$  and  $\phi_{s2s}^2$  values are GMPE specific and SHOULD NOT be extrapolated from one GMPE to another, at least before having been corrected for the site term included in the GMPE used to compute the site residuals.

At a station  $s$ , the between-event and within-event residuals,  $\delta B_e$  and  $\delta W_{es}$ , are assumed to be normally distributed random variables with respective variances  $\tau^2$  and  $\phi_{ss,s}^2$ . The single-station event-corrected standard deviation (the so-called event-corrected *sigma*) of the within-event residuals is defined as:

$$\phi_{ss,s} = \sqrt{\frac{\sum_{e=1}^{NE_s} (\delta W_{es} - \delta S2S_s)^2}{NE_s - 1}}$$

Then if  $\delta B_e$  and  $\delta W_{es}$  are mutually independent for station  $s$ , the standard deviation of the total residuals at station  $s$  is given by

$$\sigma_{ss,s} = \sqrt{\phi_{ss,s}^2 + \tau^2}$$

#### 2.3.3.3.2 Use of $\delta S2S$ to modify GMPEs in hazard analyses

As said, the main ingredients of this approach are the two coefficients  $\delta S2S_s$  and  $\phi_{ss,s}$ , computed as explained in the previous section. These coefficients may be used to modify the predictions by a GMPE, in a very simple way. The standard error of estimate,  $\sigma_{\log Y}$ , of the GMPE is replaced with the  $\sigma_{ss,s}$  value, while the site correction term modifies the GMPE median prediction ( $\mu_{GMPE}(T)$ ) as follows (if the base 10 logarithm is considered):

$$\mu_{corrected}(T) = \mu_{GMPE}(T) \cdot 10^{\delta S2S_s(T)}$$

Figure 5 shows an example of site terms and relative amplification factors obtained by Chen and Faccioli (2013) from the analysis of strong motions recorded at selected stations during the Canterbury earthquake sequence in New Zealand (another area where the application of this approach greatly "benefitted" from the occurrence of a very active earthquake sequence: applying it before 2010 would have been much more difficult...).

For present applications, there are never enough data to incorporate a non-linear term in such a  $\delta S2S$  approach:  $\delta S2S$  is mainly estimated from weak to moderate events, corresponding to a linear behavior. It should thus be considered as being on the safe side, except if the site frequency is slightly larger than the structural frequencies.

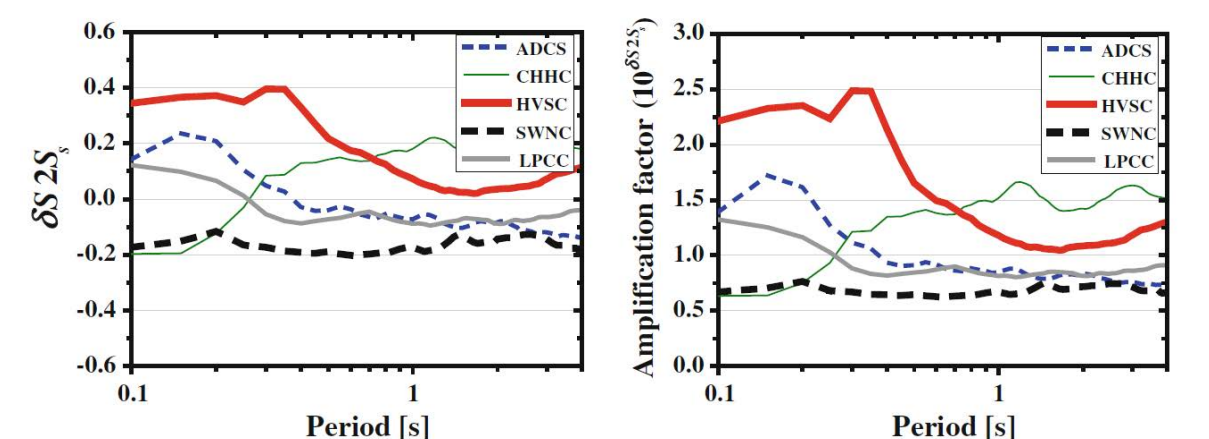


Figure 5: Example of site term  $\Delta S2S_s$  (left) and amplification factor (right) for selected stations in New Zealand. From Chen and Faccioli (2013).

### 2.3.4 Site response estimates: numerical approach / linear case

There exist several possible ways to estimate the site response using simulation tools. For all of them, it is mandatory that the following criteria be fulfilled: proper documentation on the methods used and their implementation in the numerical codes specifically used for the application, with special emphasis if they include new developments, reproducibility of results (in particular, keep track of all hidden parameters), checks on the robustness of the results with respect to the poorly constrained assumptions / parameters, and guarantees on the expertise and experience of the team in order to ensure the reliability of the results.

#### 2.3.4.1 *Introductory remark about the role of empirical methods to account for site effects*

In this section, we fundamentally describe topics related to numerical computations. This does not mean that empirical/ instrumental approaches (that are detailed in section 2.3.3) do not have any role to play in site effect assessment. It is highly recommended that such instrumental approaches be implemented at least in order to control the validity and representativeness of computations: instrumental recordings will definitely help in reducing the epistemic uncertainties (for example to better “tune” the models used for simulation, and to avoid being forced to introduce in hazard computation a too wide range of assumptions on site property description).

However, in low-to-moderate seismicity contexts, these recordings will most often correspond to weak motions, with a limited coverage of back-azimuth and incidence angles. Thus, these records cannot address non-linearity issues or variability due to different incidences. Numerical simulations must therefore be considered as complementary to instrumentation, and indispensable in particular to understand and extrapolate the instrumental observations.

#### 2.3.4.2 *Numerical modeling and consideration of complex geometries (1D, 2D and 3D)*

It consists in estimating the amplification and / or the resulting site-specific ground motion through a numerical simulation of the wave propagation phenomena occurring in the immediate vicinity of the considered site. Many numerical simulation codes have been proposed, using different techniques and numerical schemes (boundary integral methods,

finite differences, finite elements, spectral elements, discrete elements, discontinuous Galerkin,...), which allow to address different configurations:

1. The propagation medium may be 1D (i.e., with horizontally stratified layers) , 2D (i.e., alluvial valley or topographic ridge), or fully 3D;
2. The incident wavefield may be a plane wave with vertical or oblique incidence, a surface wave (typically corresponding to a remote source); when the potential source is close to the site, it is preferable that the model includes the source, which can be either a point source or an extended source, the latter one being more realistic if the source-site distance is smaller or comparable to the fault size, and being thus preferable for earthquakes with magnitude larger than 6;
3. Finally, the rheology of the propagation medium can be viscoelastic (the simplest case, where only elastic and damping characteristics need to be known for P and S waves), or incorporate a constitutive law with non-linear behaviour, at least in a limited area corresponding to the softest soils and/or the largest velocity / mechanical contrasts where the largest strains are expected.

There already exist codes claiming they can deal with 3D geometries and Non-Linear behavior; they have ***never been fully validated, nor even carefully cross-checked*** (this is among other things, one of the objectives of the ongoing SINAPS@ project, <http://www.institut-seism.fr/projets/sinaps/>). It is thus recommended, at this stage, to investigate separately the effects of the underground 2D or 3D geometry, and the effects of soil non-linearities on 1D soil columns. The former are more likely to be related to deeper, larger scale structures, while the latter to be mainly due to shallow soft soils. This distinction may in some cases be incorrect if large enough strains are developed at large depth by a major impedance contrast between a very hard rock and a deep, stiff sedimentary unit; however, the non-linear behavior of such stiff soil under large confining pressure is still poorly known, and the recommended approach is on the safe side.

The use of numerical simulation raises three main issues about the reliability of the results:

1. The first relates to the accuracy and relevance of the numerical method and its implementation. Apart – in principle - from the simple case of a 1D soil column impinged by vertically incident plane waves, such calculations require considerable experience and great caution. Even the simplest 1D case may provide variable results if the problem is not exactly defined, as different communities may interpret differently the same words (see the outcomes of the "Prenolin" project, Régnier et al., 2015a,b, 2016). In particular, the robustness and reliability of the results decrease almost always with the growing sophistication of the models used. Different comparative tests to date (Tsuno et al, 2009; Bielak et al, 2009; Chaljub et al., 2009, 2010, 2015; Maufroy et al., 2016) conclude that at present, it is essential to perform in parallel two independent calculations by two different teams with different simulation codes to ensure a minimum confidence level.
  - It is recommended that the pair (used code, computing team) can prove its expertise by comparing its results to those obtained by a collection of other methods on some "canonical" or "well documented" cases, such a those proposed during the E2VP and available on [www.sismowine.org](http://www.sismowine.org) with on-line, well designed comparison tools
  - A special attention must be devoted to the implementation of attenuation, which may be valid only in a very narrow frequency range, or over a much broader frequency range (to be systematically preferred!)

- The discretization for the medium may also have a significant influence on the computational accuracy: this step must be carefully documented and justified.
2. The second concerns the representativeness of the underground model used for simulation and its relevance to the real site. The results are indeed very sensitive to the exact geometry of the underground structure and to mechanical parameters as well, the most important being the S-wave velocity and damping (and in the nonlinear case their variations with shear strain and confining pressure). When these parameters are not well constrained (see Appendix A for an overview of survey techniques), it is necessary to perform sensitivity studies to assess the variability of the results in relation to the actual uncertainty on input model parameters (see below parametric uncertainty in Table 3 in section 2.3.6.1).
  3. The incorporation of nearby extended fault sources in such simulations adds *de facto* an additional source of epistemic uncertainty, since such sources, whatever the modeling approach (kinematic or dynamic), must be characterized by a series of additional parameters which are very poorly known.
  4. Finally, the decision to consider or not the 2D or 3D character of the structure (topography and/or underground geometry) is not trivial, and is presently a matter of subjectivity. This issue is addressed in the guidelines for the accounting of site effects for the French nuclear facilities, a SIGMA project report that will be issued soon. The propositions included in this report are based on simplified "aggravation factor models" resulting from comprehensive parametric studies performed within the framework of the NERA project, relating the overamplification due to the sole subsurface geometry to simple, relatively easily available geomechanical characteristics of the site (valley width and depth, velocity contrast, position within the valley). The threshold values beyond which such simplified estimates imply the realization of 2D or 3D computations is proposed to be 1.25 (i.e., increase of +25%) for the maximum spectral amplification factor; both the approach and the value would need to be discussed with the engineering community before reaching a consensus.

The main drawbacks of the numerical approach are thus the high sensitivity of the results to the input model parameters, which are affected by large uncertainties in most practical cases. One must in addition be aware that as a general rule, 3D numerical simulations do not presently allow to calculate deterministically beyond a maximum frequency of the order of 2 to 5 Hz, because of limitations both in computer performance, and in the resolution of geophysical survey techniques, which are unable to provide a correct mapping of short wavelength heterogeneities. Finally, this approach is time consuming and requires powerful computers. It is strongly recommended to ask such simulations to expert seismological teams who can demonstrate some experience in the field.

However, the huge advantage of this approach is to help to apprehend the nature of physical phenomena, which may affect the site under consideration, and allow quantifying their potential effects. It can be a very valuable guide to optimize the instrumentation scheme for answering some unsolved issues because of the inaccessibility of some parameters.

It is strongly recommended to always check the results of numerical simulation with any available piece of observation derived from in-situ seismological recording, from simple H/V microtremor measurements to more sophisticated analysis of earthquake recordings (see previous sections 2.3.3): this could help in particular to constrain the variability of input model parameters within limits consistent with the observed variability of fundamental frequency (H/V) or site-to-reference amplification functions.

The latest version of the recommendations from the series of benchmarking exercises for numerical simulation of seismic ground motion in 3D linear media can be found in Maufroy et al., 2015 b and 2016.

### **2.3.5 Site response estimates: numerical approach / non-linear case**

One of the main interests of numerical simulation is to allow the consideration of cases beyond the available recordings (whenever existing...) from in-situ instrumentation. Alike any material, soils do degrade under high mechanical stress and may no longer behave linearly at large loadings. In such cases, the use of NL simulation is the only way to estimate the modifications of site response linked with soil non-linearities.

Such a dependence of the dynamic response to the level of loading, collectively known as "non-linear effects", involves rather complex mechanical processes, which may however be grouped by two main origins. The first is the degradation of the mechanical properties of the material (with is often characterized by a softening: decrease in the shear modulus coupled with an increase of damping as a function of shear strain). The second, which is of particular importance for water saturated granular soils, is related to the changes in pore-water pressure during shear, and the corresponding changes in volume of the soil skeleton, which may produce liquefaction in shallow, soft sandy soils.

Given the complexity of the non-linear behavior of soft soils, many models and codes have been developed and are actually used for such simulations. It is generally accepted that when the deformation remains moderate (i.e., smaller than 0.1 - 0.2 % at most – a level that could also depend on plasticity index and depth), an approximate modeling ("linear equivalent" can be used and yields acceptable results. An equivalent linear analysis is a linear approach which iteratively adjusts the visco-elastic properties – shear modulus and damping – to the local strain level (Schnabel et al., 1972; Seed and Idriss, 1969; Vucetic & Dobry, 1991; Assimaki et al., 2000; Walling et al, 2008; Kaklamanos et al., 2013; Kim et al., 2013; Yee et al., 2013; Bolisetti et al., 2014; Kaklamanos and Bradley, 2015; Zalachoris and Rathje, 2015).

When the strain exceeds these levels (i.e., above 0.2 – 0.5 %, or in other words for very soft soils and / or very severe loads), a complete non-linear modeling is required, with an appropriate constitutive law fed by the correct soil parameters. These models oscillate between two poles: relatively simple constitutive laws with few parameters which can hardly reproduce all possible loading/ unloading paths, and more complex models with many parameters (sometimes exceeding 10), which do succeed in describing all possible behaviors, but the parameters of which remain largely out of reach of direct measurement.

The decision on whether a NL analysis is needed can be either based on information available before a site response analysis is run, or based on information resulting from a site response analysis. The "a priori" (prior to analysis) approach is preferred, as the same care in selection of parameters for an EL analysis is similar to the amount of work required for a NL analysis. The "a priori" approach is discussed in detail in Assimaki and Li (2012) and Kim et al. (2013). Thresholds that can be evaluated prior to site response analyses are provided in this and other literature for deciding when nonlinear site response analyses are preferred to EL analyses. Whenever a NL analysis is performed, an EL analysis needs to be performed as well to confirm the results of the NL analysis.

The validation of these approaches is a major issue, which has not up to now received a fully satisfactory scientific answer for all kinds of conditions. It has thus been the topic of various

projects. It was already one of the targets of the pioneering blind tests initiated in the late 80's/early 90's, on 2 sites of Ashigara Valley (Japan) and Turkey Flat (California); however, those sites lacked strong motion records until the 2004 Parkfield earthquake during which the Turkey Flat site experienced a 0.3 g motion. Since the soils were fairly stiff, the nonlinearity was not very strong. A new benchmarking of 1D non-linear codes was thus carried out in the last decade, based on the Turkey Flat site and a few other sites with vertical array data (La Cienega, California; the KGWH02 KiK-net site in Japan, and Lotung in Taiwan). Its main findings, reported by Kwok et al. (2008), Stewart et al. (2008), Stewart and Kwok (2009), emphasized the key importance of the way these codes are used and of the required in-situ measurements. Significant differences between records and predictions have been postulated as being due to an incorrect velocity profile (although it was derived from redundant borehole measurements), a non-1D soil geometry (non-horizontal layers), and imperfections / deficiencies in the constitutive models, which were unable to represent the actual curves for stiffness reduction and damping increase. It was also the topic of the recent "Prenolin" project carried out within the twin framework of SIGMA and SINAPS@ (ANR-PIA-RSNR) projects, to be completed by 2016 for the former and 2018 for the latter. The main recommendations resulting from benchmarking exercise for 1D soil columns can be summarized as follows.

1. All the general recommendations already indicated for the use of numerical simulation in estimating the site response (see the previous section) should also apply for NL simulations (parallel computations by independent teams with recognized expertise in the field, robustness with respect to poorly constrained model parameters, checks on some "canonical" exercises previously proposed and available online)
2. It is always recommended to start with simple linear computations of site response to check the consistency of non-linear and equivalent linear site response analyses with the available in-situ information including ground motion measurements (fundamental frequency, range of magnitude of the amplification level, ..)
3. The definition of input motion should receive much care: outcropping rock motion or "within" motion at "reference" bedrock depth<sup>2</sup>, frequency and phase contents of the acceleration time series. Rock hazard is most often established for outcropping rock conditions, while a number of simulation codes work easily with prescribed motion at the base of the soil column. Both the ordering person / institution and the contractor should be aware of the differences between "within" and "outcrop" ground motions and the latter should detail the types of motions used in site response analyses.
4. The description of NL soil characteristics and their variations with depth should also be performed very carefully: it should include, in addition to the density and velocity profiles, the strain dependency of  $G/G_{max}$  and damping  $\zeta$ , for each layer, and the shear strength profile. The defined shear modulus and damping curves for each soil layer should be systematically compared with the values and correlations available in literature for similar soils, and thoroughly discussed in case of large deviations. Examples of correlations for nonlinear curves that exist in literature are: Darendeli (2001), Menq (2003), Roblee and Chiou (2004), Andrus (2003), Zhang et al. (2005).

---

<sup>2</sup> From Stewart et al. (2008): "Control Motion Specification: Outcropping control motions should be used as-recorded with an elastic base. Motions recorded at depth should also be used as-recorded but with a rigid base. In both cases, the motions are specified at the base of the site profile. For within motions, the depth at which the recording was made should match the depth of the profile base."

The selected nonlinear soil models should properly replicate the prescribed modulus reduction and damping curves for each soil layer, and any deviations in behavior need to be documented. The implied shear strength of the strain-dependent curves should match the shear strength of the in-situ soil.

5. Merging in-situ, low strain, and laboratory, higher strain measurements. It is a pity that there still does not exist any internationally accepted recommendations on the way to reconcile (large strain) laboratory measurements and in-situ (very low strain) measurements. The practice varies from one continent to another, and sometimes from one country to another. In the US, resonant column/torsional shear (RC/TS) tests are the preferred test for obtaining small-strain modulus reduction and damping behavior, and can be complimented with cyclic triaxial tests with attached bender elements to constrain large-strain soil properties. Bender elements are the best way to obtain  $G_{max}$  from cyclic triaxial tests, but may give slightly different  $G_{max}$  values than those calculated from the field-measured  $V_s$  profile due to sampling disturbance. Cyclic triaxial tests cannot be considered as fully reliable at low strains. In any case, the building of NL model should include a careful comparison of the in-situ measurements of shear modulus (from S-wave and unit mass measurements) and of the corresponding laboratory measurements (cyclic triaxial tests and/or resonant column). When these values are very different (differing by a factor exceeding 2), the way to adapt the degradation curves obtained at large strain in laboratory tests, to the actual in-situ shear modulus, should be detailed, and the associated epistemic uncertainty should be accounted for with various computations.
6. Detailed documentation on the constitutive laws used in NL site response and their implementation in the site response analysis software needs to be provided. Special attention must be paid to the implementation of both low and high strain damping behavior and the way the soil model reproduces prescribed nonlinear soil behavior.
7. Some indications on the associated epistemic uncertainty, with a separation between the one restricted to code-to-code variability, and those also including the additional uncertainties related to the imperfect measurement of the required parameters. Some default values will be proposed for the code-to-code variability on the basis of the (limited) Prenolin benchmarking exercises, but could be replaced by the consideration of different NL simulation codes involving completely different constitutive models.
8. Sensitivity analyses should be performed when conducting nonlinear site response to quantify the variability in surface response due to uncertainty in nonlinear soil properties ( $G/G_{max}$  and damping),  $V_s$ , small-strain damping, soil strength, soil column depth, and water table level by systematically varying the input properties to a nonlinear site response analysis procedure.

### **2.3.6 Uncertainties**

Uncertainties should be considered in evaluating soil response for site-specific studies. The consideration of uncertainties is fundamental because the soil properties are inevitably known with some degree of approximation.

Two main uncertainties are involved in the calculation of site-specific hazard, each one containing aleatory and epistemic components (this nomenclature will be introduced in the next section):

1. Uncertainties in the rock (or hard-rock) hazard. Most of the ground motion uncertainties come from the seismicity model, standard deviation of the GMPE and from host-to-target adjustment, if applied.
2. Uncertainties in the site amplification function. Most of the ground motion uncertainties come from the lack of knowledge on the soil properties.

For an appropriate representation of the seismic hazard it is important that uncertainties in the two above-mentioned parts are not double counted. In a site-specific study, part of the site response variability is already included in the standard deviation of the GMPEs because a large number of different sites is included in the database, and used to represent the variability of ground motion at a single site (ergodic assumption).

For site-specific PSHA, additional information on site response can be used to improve the prediction of the GMPE at the site; in which case, the ergodic standard deviation must also be reduced to reflect this additional information. Such a reduction of the GMPE standard deviation is performed through the use of the single-station sigma, SSS, which drops the “site-to-site variability of the site response, as site-specific hazard is in essence addressing the hazard at a single site (Al-Atik et al., 2010; Rodriguez-Marek et al. 2013, see also the section 2.3.3.3 above). It is important to stress that the SSS can only be used when local site response analysis, including uncertainties, is used to estimate the site-specific hazard at the surface.

### 2.3.6.1 Sources of uncertainties in site response estimation

In the context of quantifying and separating uncertainties, it appears useful to remind that in seismic hazard analysis it has become common practice to distinguish and separately process the uncertainties pertaining to two different types: aleatory and epistemic. Aleatory uncertainties reflect the random, presently unpredictable nature of the process of seismic wave propagation within the sedimentary layers. Epistemic uncertainties reflect the lack of knowledge on the process or on its parameters.

A more detailed nomenclature, particularly useful in the context of ground-response prediction, has been presented by Roblee et al., 1996, and Toro et al., 1994. This nomenclature separates the contribution of modeling variability and parametric variability and each one has aleatory and epistemic components. Table 3 outlines the four components of variability.

Table 3: Contributions to total variability in ground-response estimates (modified from Roblee et al., 1996)

	<b>Modeling</b>	<b>Parametric</b>
<b>Epistemic</b>	Variability in predicted response from a particular model assumptions, simplifications and/or fixed parameter values	Variability in predicted response resulting from incomplete data needed to characterize parameters
<b>Aleatory</b>	Variability in predicted response resulting from discrepancies between model and actual complex physical processes	Variability in predicted response resulting from inherent randomness of parameter values.

The difference between epistemic modeling variability and aleatory modeling variability can be illustrated considering the following example concerning soil nonlinearity. Let suppose that a particular model 'A' considers soil behavior to be linear elastic, and assume that soil behavior is indeed strain-independent. Non-linear soil effects would then contribute to the scatter, or modeling variability, in the residuals between measured ground response and

model 'A' predictions, and this scatter would be considered random (inherently irresolvable). However, if one examines the scatter as a function of ground-motion amplitude, one might find a systematic trend or "bias" to the scatter, with an overprediction of high-amplitude motions and/or underprediction of low-amplitude motions. This bias can be viewed as modeling uncertainty, and one could choose to "calibrate" or correct the linear-soil model (A\*) in some fashion so as to eliminate this consistent trend for the strain levels represented in the data set, thus leaving only the randomness components to the scatter. As an alternative means to remove the amplitude-dependent bias, one might adopt a new model (B), which explicitly accounts for non-linear soil behavior.

Using the same topic, an example of parametric variability is the range in predicted response associated with a range of possible functions describing non-linear material curves for the soil layers. The parametric uncertainty is that portion of response variability that could be reduced by a better definition of the curves, say by using high-quality laboratory testing. However, such curves can never be perfectly defined due to both measurement errors and natural spatial variations within the soil deposit for a particular site. That portion of response variability associated with the "indefinable" range would be considered part of the aleatory parametric variability.

A non-exhaustive list of the aleatory uncertainties includes:

1. Motion-to-motion variability (frequency content and phase) in the set of selected motions representative of the hazard spectrum on rock;
2. The incidence angle of input motion and more generally the variability of the wavefield of the incident motion, which is far from being composed of vertically incident plane S waves...
3. The effect of the input motions on the non-linear behaviour of the soil (e.g., Li and Assimaki, 2010);
4. The small-scale lateral variations of the soil properties. These are commonly taken into account by performing analyses for multiple realizations of e.g., 1D shear-wave velocity profiles assuming some spatial correlation model between the layers (e.g., Toro et al., 1995).

Besides the aleatory uncertainty related to the non-linear soil behaviour dependent on the input motion, the other sources of variability also apply to the rock motion and are to a large extent already included in the aleatory variability of the GMPEs. For this reason, except for cases where the variability of the non-linear behaviour is significant, it is not necessary to increase the sigma of the GMPEs to account for aleatory variability in site response. This would avoid double counting of aleatory uncertainties in the rock hazard and in the site hazard.

Epistemic uncertainties can in principle be reduced with the increase of knowledge on the site properties. A non-exhaustive list includes:

1. Uncertainties (parametric) on the velocity profile and damping ( $V_s(z)$ ,  $\zeta(z)$  in 1D) ;
2. Uncertainties (modeling) on the geometry of the different lithologies (1D, 2D, 3D);
3. Uncertainties (parametric) in the non-linear properties of the soil (degradation curves  $G-\zeta-\gamma$ ,  $\tau-\gamma$ , ...).

These uncertainties are usually considered in the analysis by using logic tree and Monte Carlo random sampling. For example a number of  $V_s$  profiles can be used or alternative hypothesis on the degradation curves of the soil.

### 2.3.6.2 Different "levels" of uncertainty

Epistemic uncertainties can be considered in the calculation of the site-specific hazard with different levels, from a simplified approach to a complete probabilistic consideration of uncertainties. Three levels of consideration of uncertainties are distinguished here:

1. **Level 0:** This is the simplest approach. The site amplification is considered only in terms of a best estimate amplification function. The rock hazard is calculated using GMPEs with a "full sigma" (i.e., ergodic values) because, the site specific response is not accounted for and the SSS ("single-site sigma") cannot be applied.
2. **Level 1:** The epistemic uncertainties in the site response are considered for some of the parameters mentioned in Section 2.3.6.1 (e.g., variations in the Vs profile). The amplification function is defined in terms of distribution (median and standard deviation). In this case the SSS can be used to replace the standard deviation of the considered GMPEs.
3. **Level 2:** Fully probabilistic consideration of uncertainties through detailed logic tree. For each step in the process of the site response calculation, uncertainties are identified and appropriately accounted for in the analyses. The rock hazard is calculated using GMPEs with SSS. Such aleatory sigma could in theory be modified to consider the specificity of the variability of the nonlinear site response in relation with variability of input motions; this requires, however, quite sophisticated analysis and very detailed documentation.

The application of level 2 is in principle preferable. However, such an approach in the consideration of uncertainties is indeed time consuming and rather expensive, and it will therefore be applicable in practice only to very few sites with key importance. It is recommended to apply Level 1 approach in such cases and consider, as a minimum, uncertainties in the Vs profile and in the input time histories.

### 2.3.7 Surface hazard

This section focuses on the way to couple the rock or hard-rock hazard with the results of the site response analysis, within a probabilistic framework as most state-of-the-art seismic hazard assessment studies involve a probabilistic approach.

The U.S. Nuclear Regulatory Commission provides regulatory guidance for developing hazard-consistent ground motions for soil sites (US-NUREG/CR-6728 and US-NUREG/CR-6769). These guides present four approaches for developing site-specific ground motion response spectra. These approaches vary in complexity from simple deterministic amplification of the probabilistically derived rock response spectrum to rigorous treatment of soil amplification within the PSHA. The four approaches are briefly described below.

Approach 1 is the traditional approach consisting in specifying a uniform hazard spectrum for rock conditions, using this spectrum to select input motions for site response analysis, and propagating these motions to the surface to obtain the corresponding soil surface motion. A suite of input motions may be used to incorporate motion-to-motion variability and a few different velocity profiles may be used to consider the uncertainty in the site characteristics, but the approach is essentially deterministic as to the site response, and decoupled from the full PSHA. According to Bazzurro and Cornell (2004) this approach "*does not explicitly account for the amplification function record-to-record variability. It produces surface ground-*

*motion levels whose exceedance rates are unknown, non-uniform, inconsistent across frequency, and generally nonconservative.*" The main shortcoming of Approach 1 is that while one earthquake magnitude may dominate the high-frequency segment of the UHS, another may dominate the low-frequency segment. Consequently, a single motion fitting the entire UHS is unlikely and typically results in excessive nonlinearity in the soil column.

Approach 2 intends to account for one of the shortcomings of Approach 1 by accounting for the fact that the hazard is controlled by different earthquake scenarios depending on the considered oscillator frequency. This approach uses different input motion spectra for the high-frequency (HF) and low-frequency (LF) segments of the input response spectrum, each anchored to the UHS in their corresponding frequency range. Two variants of Approach 2 are described, one considers a single magnitude for each spectrum (Approach 2A) and the other considers multiple magnitudes for each spectrum (Approach 2B).

- Approach 2A defines the HF and LF input response spectra by considering the controlling earthquake scenarios (i.e., magnitude and distance based on the hazard deaggregation) at 10 Hz for the HF spectrum and 1 Hz for the LF spectrum. Each controlling earthquake scenario is used to define a response spectrum and then the spectrum is scaled to the rock UHS at the corresponding frequency (i.e., 10 Hz or 1Hz). These two spectra are used to select input motions for site response analysis and to develop frequency-dependent amplification factors. The mean amplification factors for each input motion **are** applied to the rock UHS and the soil UHS is defined by enveloping the computed soil motions.
- Approach 2B identifies mean, high, and low percentile magnitudes from the deaggregation at 10 Hz and 1 Hz, and uses each of these scenarios to develop input spectra for each frequency (i.e., three input spectra for each frequency). Again, motions are fitted to each input spectrum and propagated through the soil column. The amplification factors for each spectrum are weighted, based on the weights derived from deaggregation, to obtain the mean amplification factors. The mean amplification factors for the HF and LF spectra are applied in the same way as Approach 2A.

While Approach 2 addresses the issues related to excessive nonlinearity from Approach 1, it still does not provide surface ground motions with exactly known hazard levels.

Approach 3 involves the convolution of the entire rock hazard curve at a given frequency with the probability distribution of the soil amplification to generate the hazard curve on soil (see US-NUREG/CR-6728 and Bazzurro and Cornell, 2004, for details of the method).

Approach 4 is the most rigorous way to compute a hazard curve for a soil site. It involves the direct integration of the magnitude and distance distributions with a ground motion prediction equation developed specifically for the site.

Approaches 3 and 4 will not be discussed nor illustrated in the presented document, as they are quite heavy and expensive to implement. The example applications presented in this document will refer only to Approaches 1 and 2.



## **3 Example application to Euroseistest**

### **3.1 OVERVIEW**

Several recent research works have pointed out the importance of further investigations on site-specific probabilistic hazard analysis (McGuire et al. 2001) as the probabilistic approach is the most suited to provide risk estimates for all types of structures. Probabilistic seismic hazard has been traditionally calculated essentially for rock conditions (McGuire and Toro 2008) and site-amplification has been only roughly included by using amplification factors (specified in seismic design codes or the site factors used in GMPEs). Recently, several methods have been proposed to better estimate site-specific effects, which intend to better describe the physical phenomena of wave propagation from rock through a soil media.

The aim here is to show example of application of each one of the methods prented in the previous section, and discuss their pros and cons.

In order to be able to correctly perform a Site Specific Hazard Analysis, a significant amount of data from the site must be required. The ideal site should have:

- Preexisting geological, geophysical and geotechnical characterization in order to produce a realistic model of the soil column;
- Significant amount of seismic event recordings to be able to calculate a partially non-ergodic PSHA.
- A global framework in which these data could be used openly in a large collaborative project.

A pre-existing characterization of the site is essential to provide a soil model, as required in the “Generic or Partially Site Specific” and the “Site Specific” methods. Such data is available at the selected "Euroseistest" site, located several kilometers east of Thessaloniki, in Greece.

### 3.2 EUROSEISTEST : THE SITE

The “Euroseistest” site is located in the Mygdonian basin in North-Eastern Greece, 30 km ENE of Thessaloniki (Figure 6), in the epicentral area of a magnitude 6.5 event that occurred in 1978.



Figure 6. Location of the Euroseistest and the Mygdonian basin in the NE Greece.

The Mygdonian basin is the place of the so-called “Euroseistest”, which has been extensively investigated within the framework of various European projects (Euroseistest, Euroseismod, Euroseisrisk, Ismod) and presently maintained by ITSAK and AUTH (Pitilakis et al., 2009). The basin is currently densely instrumented with surface accelerometers, as well as a vertical array with 6 sensors over 200 m depth at the central TST site.

The velocity model of the site has been published (Jongmans et al., 1998; Raptakis et al., 2000), we use it to define the 1D linear and nonlinear models. Degradation curves are available to characterize each soil layer (communication F. Hollender), as well as amplification functions, among other information that will be mentioned along this study.

The target site considered here is the site "TST\_0" located in the very center of the graben (Figure 7).

### 3.2.1 Soil Site Characterization

To perform a Site Specific Hazard Assessment, all the geological, geophysical and geotechnical data at the site of interest needs to be gathered.

In our case, the Euroseistest has been largely investigated. Previous studies provide a detailed soil profile, the geometry of the basin, the shear-wave velocity at the bedrock and at the surface, which will be useful to properly characterize the soil properties.

The 2D soil profile of the basin in a North-South direction can be observed in Figure 7.

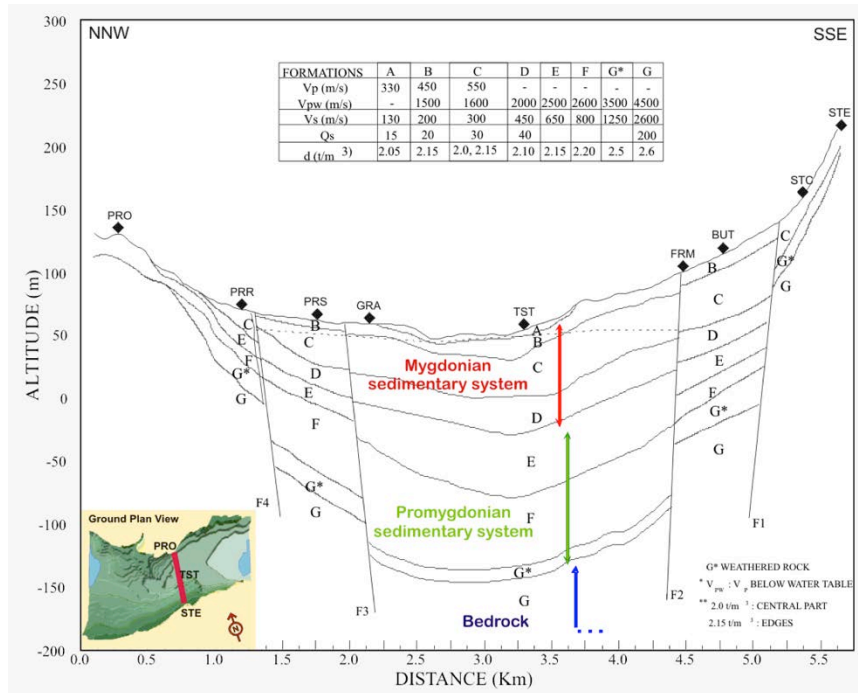


Figure 7. 2D N-S (Profitis - Stivos) soil model (Raptakis et al., 2000). Line F1 coincides with the seismogenic fault of the 1978, M6.5 earthquake.

As shown in the shear-wave velocity profile in Figure 7, the Euroseistest basin is described by a soft soil at the top of the basin, with an average shear wave velocity in the first 30 m of 186 m/s and a shear wave velocity of 2600 m/s at the bedrock (Table 4).

Table 4. Euroseistest Soil Profile Characterization

LAYER	Vp (m/s)	Vpw (m/s)	Vs (m/s)	Qs (adm)	d (t/m <sup>3</sup> )
A	330	-	130	15	2.05
B	450	1500	200	20	2.15
C	550	1600	300	30	2.0-2.15
D	-	2000	450	40	2.10
E	-	2500	650	-	2.15
F	-	2600	800	-	2.20
G*	-	3500	1250	-	2.50
G	-	4500	2600	200	2.60

The high velocity contrast at the bottom of the basin, between the soft soil and the bedrock, makes this particular place a very good example of significant site-specific effects, and one of the reasons why it was selected to be instrumented besides its moderate seismicity.

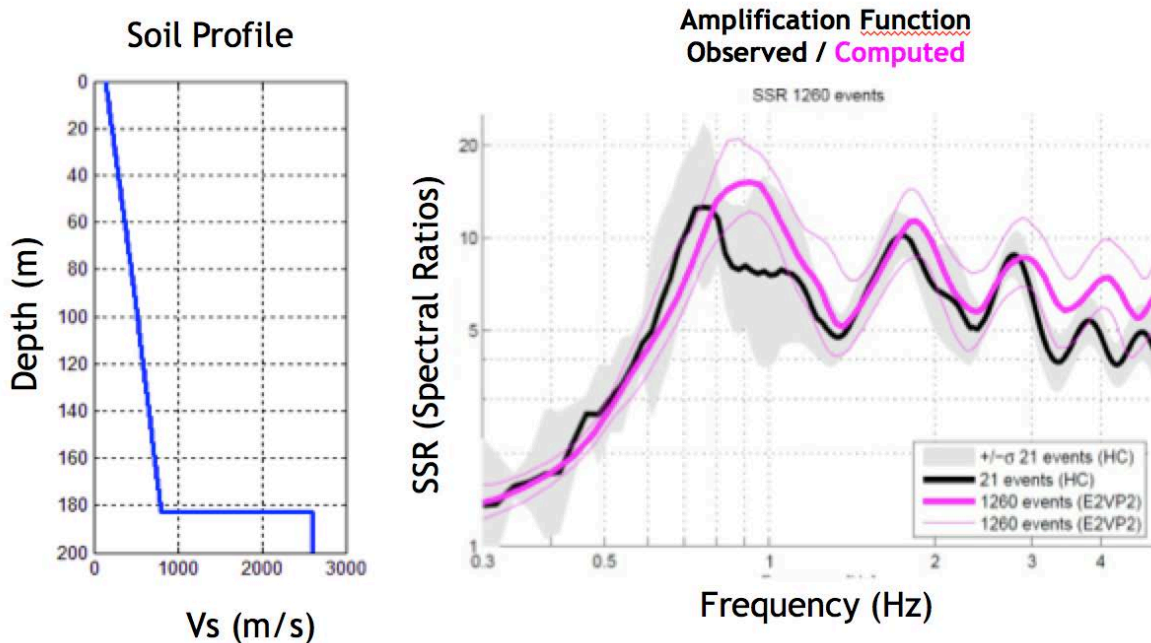


Figure 8. **a)** Euroseistest shear-wave velocity soil profile in the middle of the basin (TST\_0 station) (Maufroy et al., 2015a, b; Ameri et al., 2015). **b)** Instrumental Standard Spectral Ratios at the Euroseistests, where a fundamental frequency at about 0.6 - 0.7 Hz was identified (from Maufroy et al., 2016).

Several studies performed at the Euroseistest, both instrumental and numerical, have shown a fundamental frequency ( $f_0$ ) of the soil column around 0.6 - 0.7 Hz (Figure 8). At this frequency, resonance effects have been both calculated and observed.

### 3.2.2 Probabilistic Seismic Hazard Analysis

The first step to include site-specific effects in a Probabilistic Seismic Hazard Assessment (PSHA) consists in deriving the hazard at the site for “Standard Rock”. A standard rock corresponds to a rock with an average shear-wave velocity in the top 30 m ( $V_{S30}$ ) of 800 m/s.

To calculate PSHA, the seismicity model (the area source model) as well as the GMPE logic tree established in the SHARE project will be used here (Woessner et al. 2015).

Additionally to the ground-motion prediction equations defined by SHARE, four supplementary GMPEs are used in this study. These four GMPEs are updates of the original ones selected in SHARE, moreover they capture the nonlinear effect at high return periods (Table 5).

For the return periods considered, crustal sources are controlling the hazard, thus only crustal GMPEs are considered. A sensitivity analysis was however performed to check this assumption and investigate whether the hazard at long return period (i.e., 5000 years) and long oscillator frequency  $T$  could be affected by very large subduction events in the Aegean sea: the results confirmed that the hazard is controlled by local, crustal events.

Table 5. Ground Motion Prediction Equations used on this study.

<i>Active Shallow Crust (SHARE model)</i>	<i>Active Shallow Crust (Additional models)</i>
<i>Akkar et Bommer 2010 (AB10)</i>	<i>Akkar et al. 2014 (AA14)</i>
<i>Cauzzi et Faccioli 2008 (CF08)</i>	<i>Cauzzi, Faccioli, Vanini and Bianchini 2014 (CA14)</i>
<i>Chiou et Youngs 2008 (CY08)</i>	<i>Chiou and Youngs 2014 (CY14)</i>
<i>Zhao et al. 2006 (ZA06)</i>	<i>Boore, Stewart, Seyhan and Atkinson 2014 (BA14)</i>

The Openquake Engine developed by the Global Earthquake Model (GEM) is used to run calculations. Ground motions for specific scenario earthquakes are predicted with the SMTK modeler toolkit (Weatherhill et al. 2014).

The different site PSHA (generic or and site-specific) approaches listed in Table 1 were applied at the Euroseistest site and the results presented below in sections 3.3 and 3.4 below, before a summary comparison and conclusions from this example in section **Erreur ! Source du renvoi introuvable..**

### 3.3 SITE PSHA1 : GENERIC OR PARTIALLY SITE-SPECIFIC APPROACHES

A generic, or partially site-specific approach includes all the cases in which due to the geological, lithological and morphological characteristics of the site, the generic site amplification provided by the GMPEs can be considered a valid approximation of the actual ground response (e.g., 1D geometry and  $V_{S30}$  within the validity range of the GMPEs considered for the hazard estimate).

#### 3.3.1 Level 0: Site effect by proxy in GMPEs ( $V_{S30}$ )

The first approach consists in introducing site effects by proxies in the ground-motion models.

According to the ground-motion prediction equations selected for this analysis, the only three proxies that are required to calculated probabilistic seismic hazard on soil are:

- The average shear wave velocity in the top 30 m.  $V_{S30} = 186$  m/s
- The reference depth to 2500 m/s = 183 m
- The reference depth to 1000 m/s = 183 m

Probabilistic seismic hazard is calculated using the full standard deviation ( $\sigma$ ) of the ground-motion prediction models (GMPEs), Figure 9.

The hazard curves obtained on rock considering 8 different GMPEs (Figure 9a) show an important discrepancy depending on the GMPE used (factor larger than 2 for a return period of 5000 years). The discrepancy is significantly increased when calculations are performed on soil (Figure 9b), with a factor larger than 3 between the different hazard estimates. This

highlights the importance of correctly including site effects into PSHA, especially for critical facilities (at large return periods).

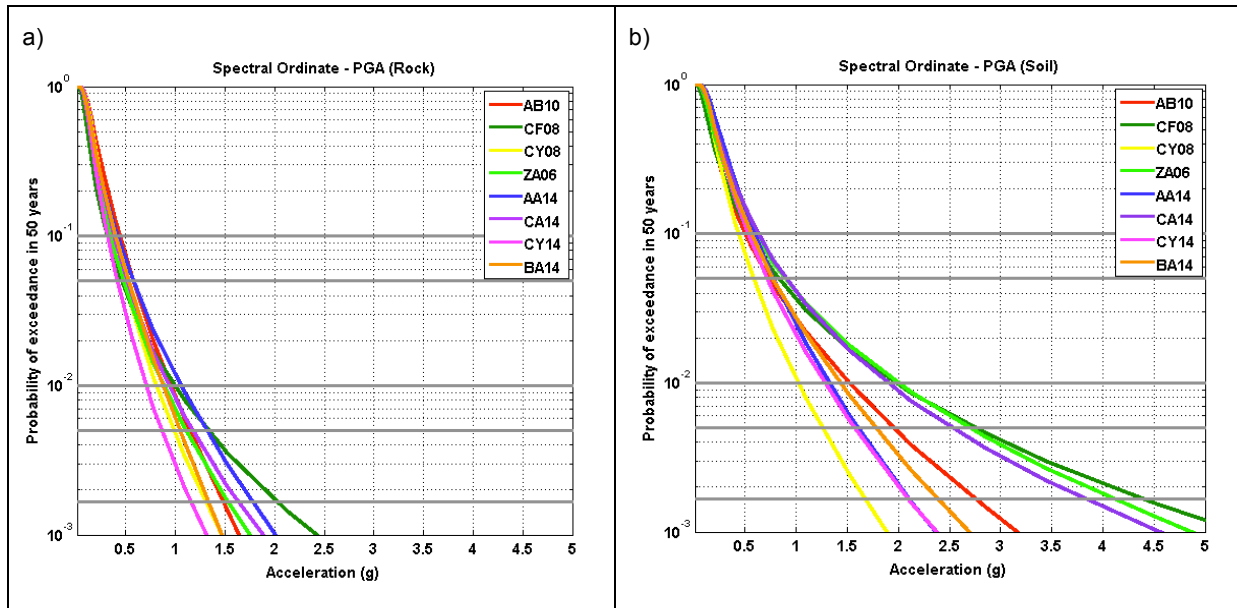
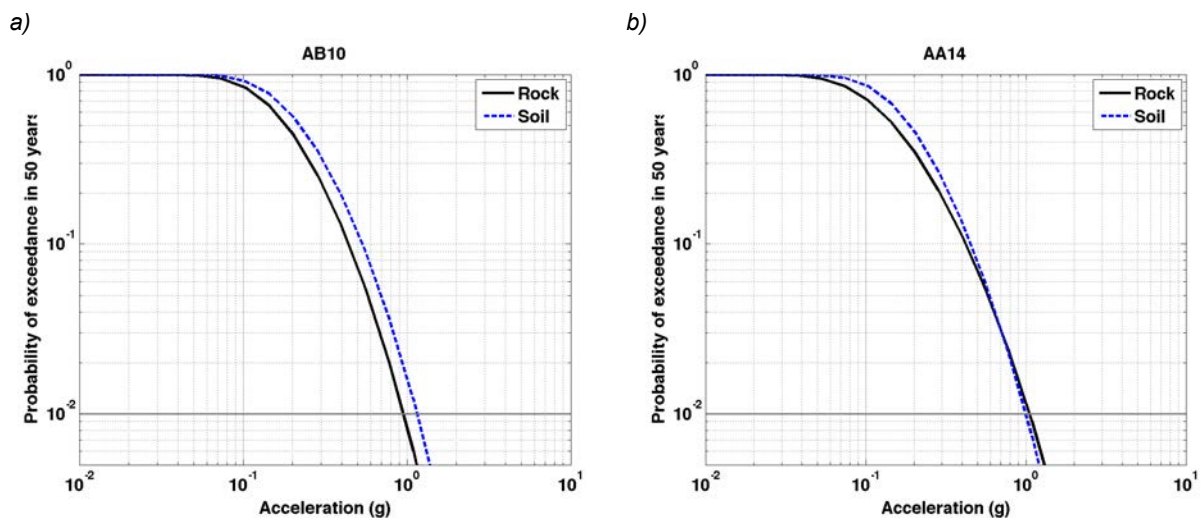


Figure 9. Hazard Curves at the Euroseistest a) for standard rock ( $V_{S30}=800$  m/s) with full sigma for the eight different selected ground-motion prediction equations. b) on soil ( $V_{S30}=186$  m/s) with full sigma for the eight different selected ground-motion prediction equations.

Something to highlight is the impact of nonlinear behaviour of the soil at large return periods, where deamplification due the soil can be observed, for the 4 updated ground-motion models selected AA14, CY08, CY14 and BA14, as illustrated in Figure 10 which compares the hazard curves obtained for a standard rock and on soil (using proxies), for the eight selected ground-motion prediction equations..

The STREST project focuses on low probability - high impact events. Therefore uniform hazard spectra for the return period 5000 years are considered. UHS at 5000 yrs calculated on rock and on soil are displayed in Figure 11 (full  $\sigma$  taken into account).



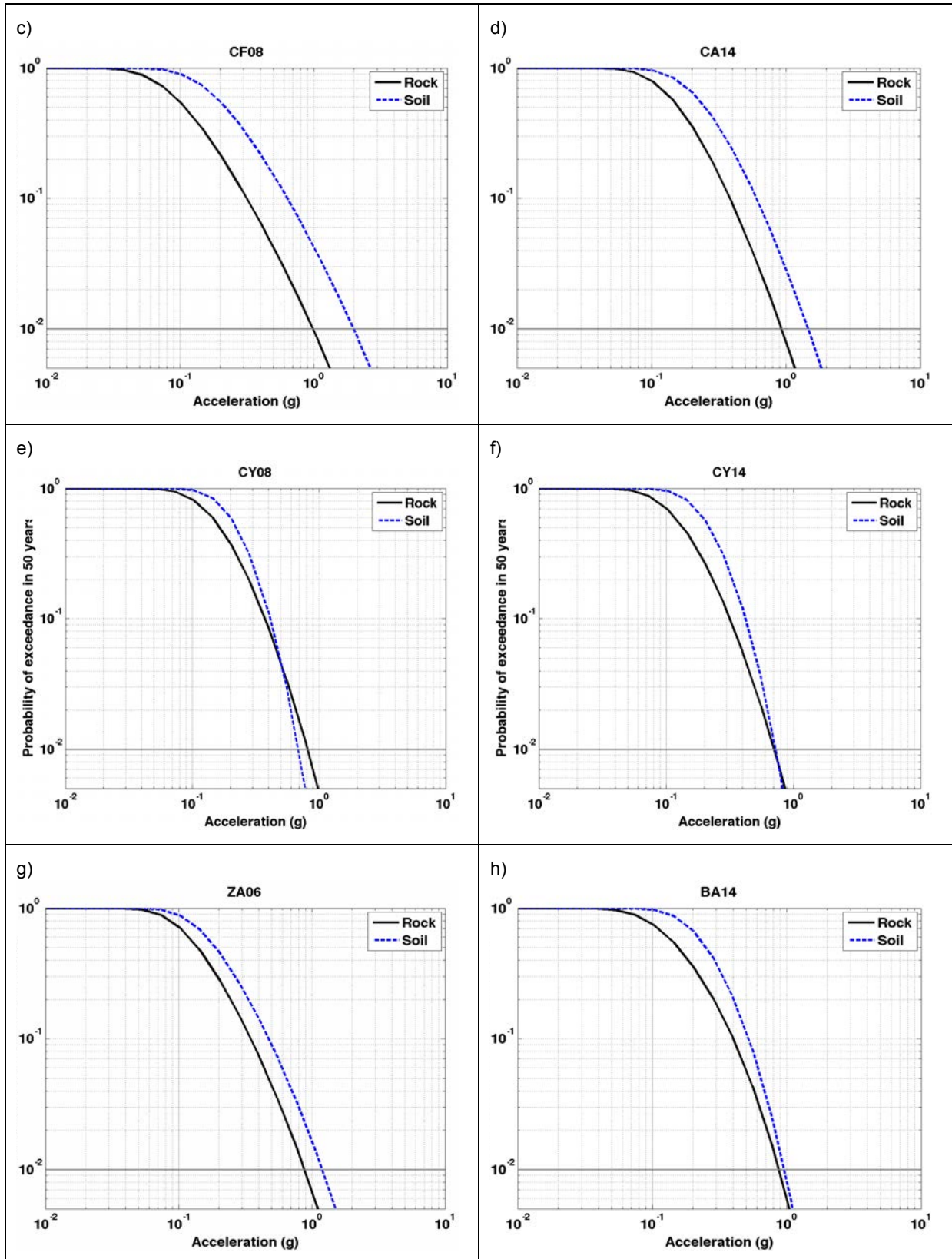
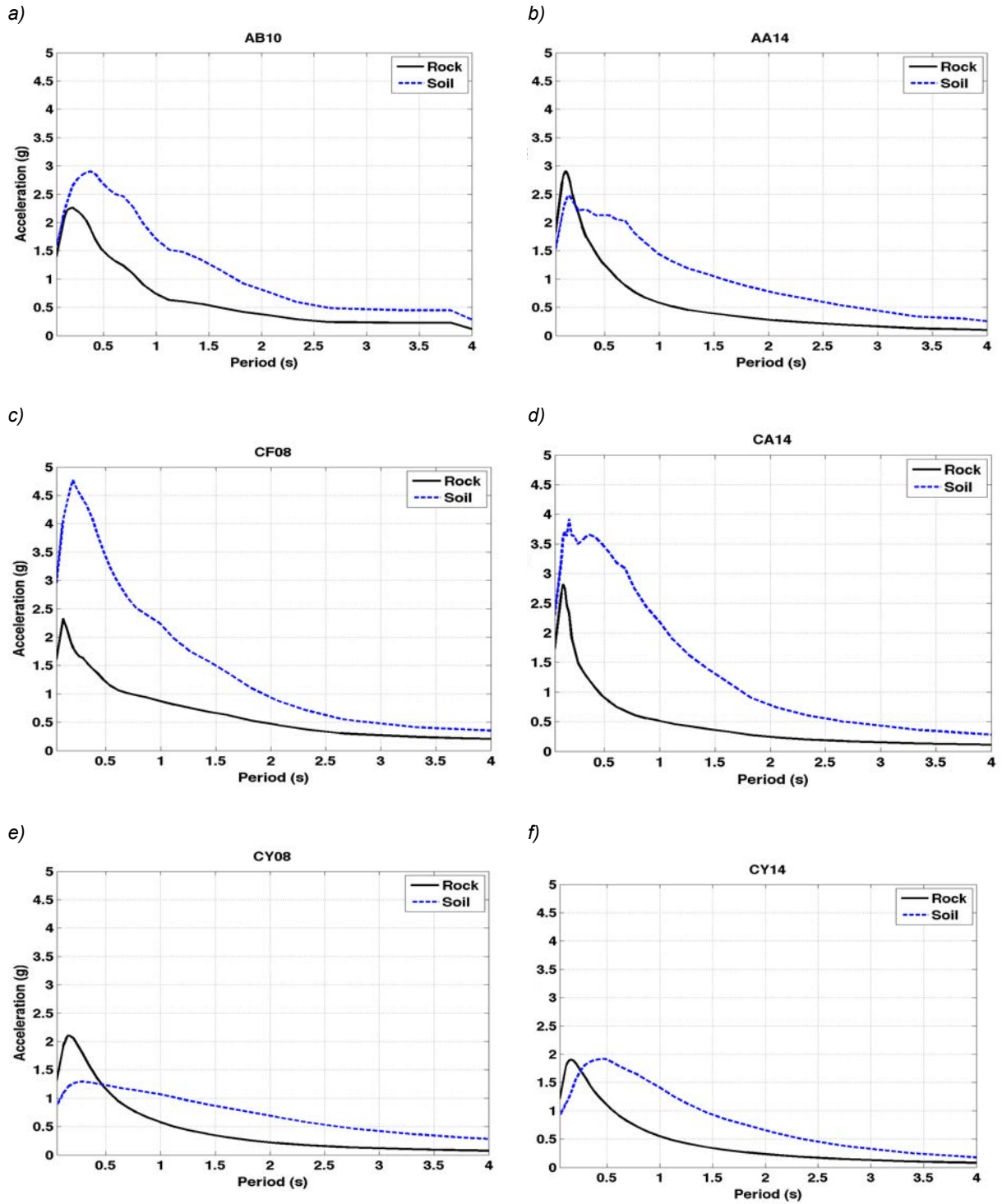


Figure 10. Hazard curves at the Euroseistest for PGA on rock (black) and soil (blue) conditions, derived for 8 ground-motion prediction equations. a) AB10, b) AA14, c) CF08, d) CA14, e) CY08, f) CY14, g) ZA06 and h) BA14.



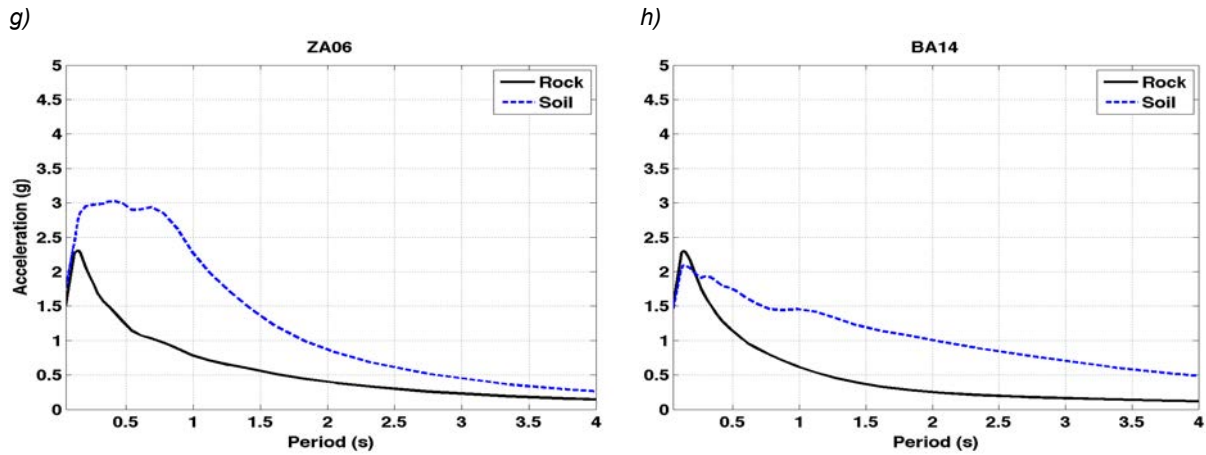


Figure 11. . 5000 years Uniform Hazard Spectra at the Euroseistest on rock (**black**) and soil (**blue**) conditions, derived for the 8 selected ground-motion prediction equations. a) AB10, b) AA14, c) CF08, d) CA14, e) CY08, f) CY14, g) ZA06 and h) BA14.

### 3.3.2 Level 0.5: Site effect by proxy in GMPEs + Amplification factors ( $V_s, i + f_o$ )

In this method, the effect of the soil is taken into account as an amplification function dependent on the fundamental frequency and on the shear-wave velocity of the soil column. The SAPEs (Site Amplification Prediction Equations) proposed by Cadet et al. (2011a; 2011b) are used. These equations implicitly assume a linear behavior of the soil under strong ground motion (strong assumption). For this reason, this amplification functions can be applied in the same way to rock hazard estimates at all return periods.

The uniform hazard spectrum on soil, is obtained simply by multiplying the uniform hazard spectrum (with full  $\sigma$ ) on standard rock (Figure 12a) by the amplification function derived with the SAPE (Figure 12b).

$$UHS_{soil} = UHS_{Standard\ Rock\ (800\ m/s)} * SAPE_{f_o, (V_{S5}, f_o), (V_{S10}, f_o), (V_{S20}, f_o), (V_{30}, f_o)}$$

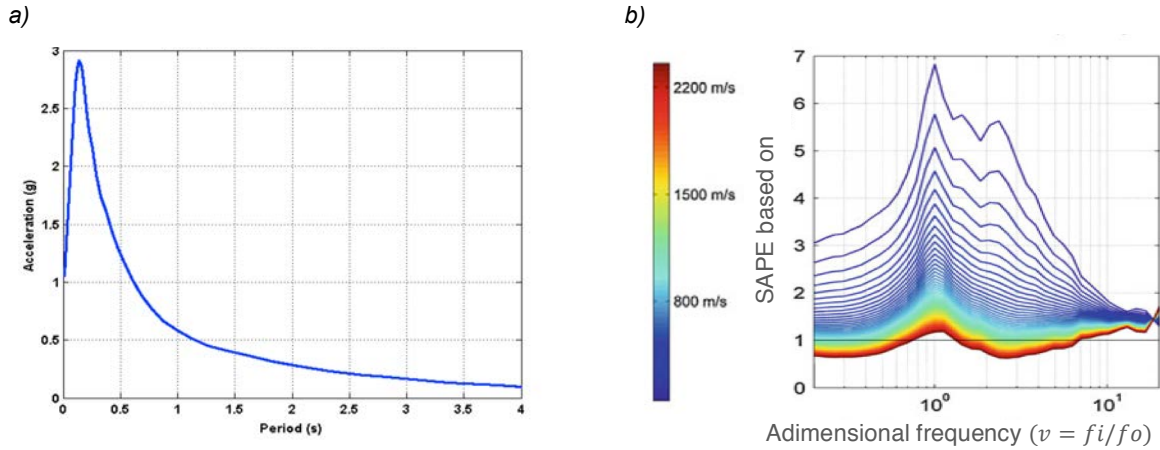


Figure 12. a) Uniform hazard Spectrum at the Euroseistest, for 5000 years return periods on standard rock (800 m/s). b) Response Spectra ratios for couple-parameters ( $V_{s,z}$ ,  $f_0$ ) from Cadet et al. (2011a; 2011b)

The 5000 years return period uniform hazard spectra for standard rock, have been already calculated for the 8 selected ground motion prediction equations using full standard deviation (Figure 11).

On the other hand, the required proxies ( $V_{s,z}$  and  $f_0$ ) needed to apply the SAPE method are derived based on geophysical data (Table 6). The response spectra ratios with the couple-parameters  $V_{s,5}$ ,  $V_{s,10}$ ,  $V_{s,20}$ ,  $V_{s,30}$  and the fundamental frequency are estimated using Cadet et al. approach.

Table 6: Euroseistest average shear wave velocity up to top  $z$  meters and its fundamental frequency.

$V_{s,5}$ (m/s)	$V_{s,10}$ (m/s)	$V_{s,20}$ (m/s)	$V_{s,30}$ (m/s)	$F_0$ (Hz)
144	153	170	186	0.7

The expressions used from Cadet et al. 2011b to derive the response spectra ratios are:

- SAPE (Site Amplification Prediction Equation) based on couple-parameters  $V_{s,z}$  and  $f_0$ :

$$SAPE_{V_{s,z}}(v) = (X_{ref1}/V_{s,z})^\beta(v)$$

- SAPE (Site Amplification Prediction Equation) based only on  $f_0$ :

$$SAPE_{f_0}(v) = (X_{ref1}/f_0)^\beta(v)$$

- With  $v$  being the dimensionless frequency, defined as :

$$v = f/f_0$$

All the coefficients needed in order to calculate the different SAPE for different proxies are indicated in Appendix 4 Cadet et al. (2011b).

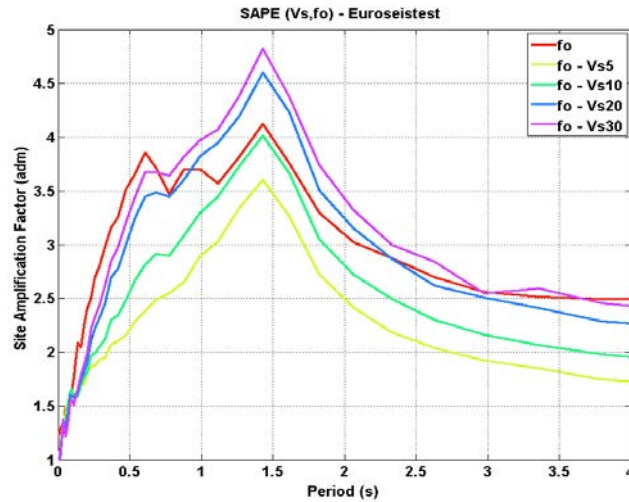


Figure 13. Euroseistest site amplification prediction equations (SAPE) for various proxies based on Cadet et al. (2011b).

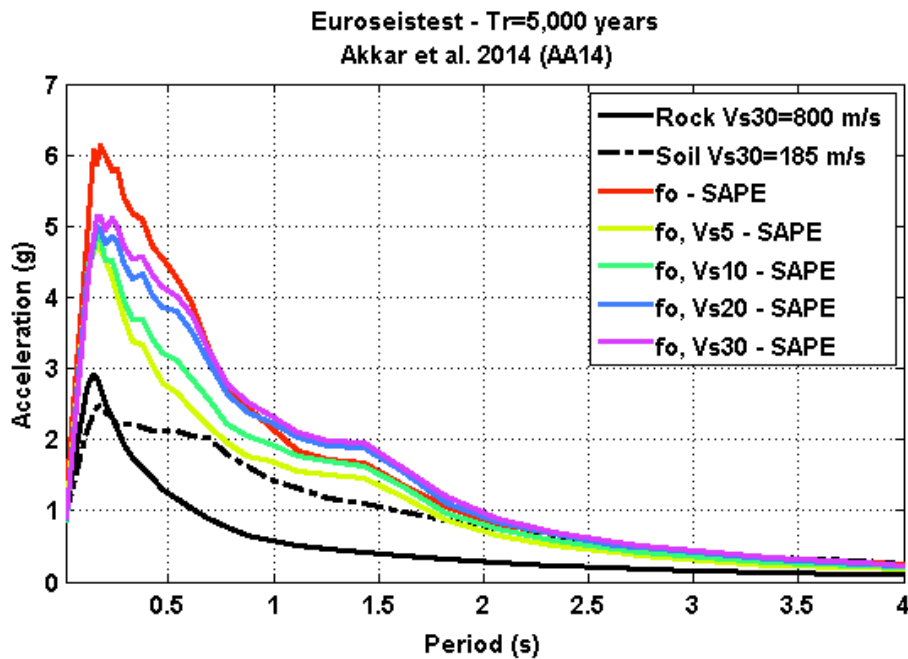


Figure 14. Uniform hazard spectrum at the Euroseistest, for a 5000 years return period, using Akkar et al. 2014 (AA14) GMPE : **Level 0** - standard rock (black dotted line), **Level 0** - Soil  $V_{S30}=186$  m/s (black dash-dotted line), **Level 0.5** – Soil (fo) (red), **Level 0.5** – Soil (fo,  $V_{S5}$ ) (light green), **Level 0.5** – Soil (fo,  $V_{S10}$ ) (green), **Level 0.5** – Soil (fo,  $V_{S20}$ ) (blue), (fo,  $V_{S30}$ ) (magenta).

The SAPE approach predicts larger amplification values than the Level 0 approach using proxies. Based on the SAPE approach (Level 0.5), accelerations predicted on soil can be twice as large as the accelerations relying on level 0 method (proxies), at 5000 yrs return period (Figure 14).

It is important to comment on the linear assumption of the SAPE, which is questionable at very large return periods, of interest for critical facilities. The SAPE considered here, i.e., those proposed by Cadet et al., 2011b, which are the only one available at present, do not take into account nonlinear effects; whereas the recent GMPEs selected take into account these effects through  $V_{S30}$  proxy (e.g. Akkar et al. 2014). As stated in section 2.2.2.3, there

might exist in the near future (for instance Régnier et al., 2016) some new SAPEs that will offer the possibility to consider non-linear effects in a more physical way than what is presently proposed in GMPEs. In any case however, such an approach remains quite simple and generic, and will not, even with new generations of SAPEs, allow to use single station sigma for the rock hazard.

### 3.4 PSHA2 : SITE-SPECIFIC APPROACHES

Site-specific approaches are advocated for those cases in which the complex geometric configuration or the specific material properties of the site require a detailed calculation of the soil response (e.g., including nonlinear site response analysis) in order to provide realistic seismic hazard for the site.

First of all, the selected ground-motion models (host) must be adjusted to our specific target region (target), through “host to target adjustments”.

#### 3.4.1 Host to target adjustments

At Euroseistest, a very high velocity contrast has been observed at the bottom of the basin (196 m depth), with the presence of a very hard rock ( $V_S = 2600$  m/s, see soil profile in Figure 7). This high impedance contrast effect cannot be captured properly by the selected ground-motion models, and in addition, the high rock velocity requires some correction to the rock prior to the introduction of the site-specific amplification, for two reasons: a) the real shear wave velocity of the rock is out of the useable range of all the selected GMPEs and b) the high frequency attenuation factor ( $\kappa$ ) implicitly present in the GMPE models through the original data set they are based on, is not necessary the same as the one of the selected site.

The selection of host models has been well documented first by Cotton et al. 2006, then by demavaud et al., 2012 and Stewart et al., 2014. The basis for host to target corrections, including both velocity / impedance correctios and high-frequency attenuation "κ" correction, are related to the site term of the stochastic model presented in Boore 2003a.

Boore (2003a) expresses the total spectrum of the motion at a site as:

$$Y(M_o, R, f) = E(M_o, f)P(R, f)G(f)I(f)$$

$Y(M_o, R, f)$ : Total spectrum of the motion at a site.

$E(M_o, f)$ : The source term

$P(R, f)$ : The Path term

$G(f)$ : The Site term

$I(f)$ : Type of Ground Motion

Following Boore’s definition, the corrections applied here are related to the site term  $G(f)$ , which in turn is subdivided into and **amplification term**  $A(f)$  and the attenuation or **diminution operator**  $D(f)$

$$G(f) = A(f) D(f)$$

To perform the host-to-target adjustment, corrections on both the amplification and the diminution terms are required, and described in the following.

### 3.4.1.1 Correction 1: Shear Wave Velocity Correction Factor (Amplification term $A(f)$ )

Firstly, the amplification term is given by the square root of the impedance ratio between the source and the surface (Boore 2003a):

$$A(f(z)) = \sqrt{Z_s / \bar{Z}(f)}$$

$$Z_s = \rho_s \beta_s$$

Where  $\rho_s$  and  $\beta_s$  are the density and shear-wave velocity near the source.  $\bar{Z}(f)$  is an average of near-surface seismic impedance. It is a function of frequency because it is a time-weighted average from the surface to a depth equivalent to a quarter wavelength:

$$\bar{Z}(f) = \frac{\int_0^{t(z(f))} \rho(z) \beta(z) dt}{\int_0^{t(z(f))} dt}$$

In which the upper limit of the integral is the time for shear waves to travel from depth  $z(f)$  to the surface. The depth is a function of frequency and is chosen such that  $z$  is a quarter-wavelength for waves traveling at an average velocity given by:

$$\bar{\beta} = \frac{z(f)}{\int_0^{z(f)} \frac{1}{\beta(z)} dz}$$

The condition of a quarter-wavelength,

$$z = \frac{\bar{\beta}}{4f}$$

Then yields the following implicit equation for  $z(f)$ ,

$$z = \frac{1}{4 \int_0^{z(f)} \frac{1}{\beta(z)} dz}$$

In practice, it is easiest to compute  $f$  and  $\bar{Z}$  for a given  $z$ . By changing variables from time to depth, the previous equation becomes:

$$\bar{Z}(f) = \int_0^{t(z(f))} \rho(z) \beta(z) dt / \int_0^{t(z(f))} dt$$

$$(1/4) \bar{\beta} / f$$

$$\bar{Z}(f) = \int_0^{z(f)} \rho(z) dz / \int_0^{z(f)} \frac{1}{\beta_z} dz$$

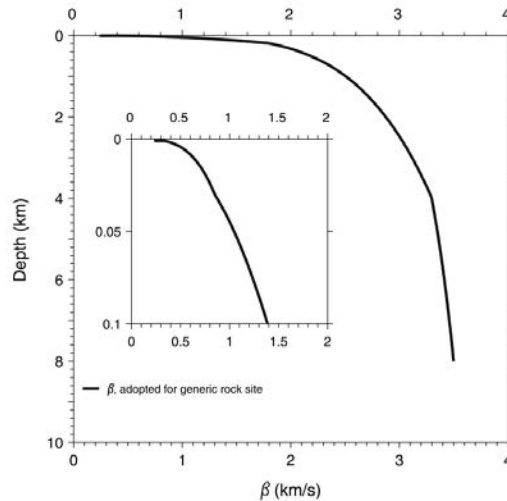


Figure 15. S-wave velocity versus depth used by Boore and Joyner (1997) for computing amplifications on generic “soft” rock sites (adapted from Boore and Joyner, 1997.)

The  $V_S$  correction factors were calculated based on the site amplification function derived by Boore et al. 2003a (Figure 16).

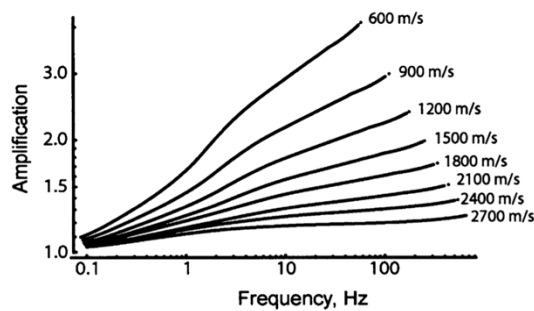


Figure 16. Impedance amplification term for various rock  $V_{S30}$  values (Boore et al 2003a).

Following Boore’s approach, the  $V_S$  site amplification function for a standard rock of 800m/s, as well as the  $V_S$  amplification function for a hard rock with  $V_s=2600$  m/s (bottom of Euroseistest basin) were calculated.

Once the  $V_S$  / impedance amplification functions are derived, the velocity correction factor can be obtained by simply dividing the amplification factor for very hard rock by the amplification factor for standard rock (Figure 17).

$$A(f)_{htt} = \frac{A(f(z))_{v_s=2600 \text{ m/s}}}{A(f(z))_{v_s=800 \text{ m/s}}}$$

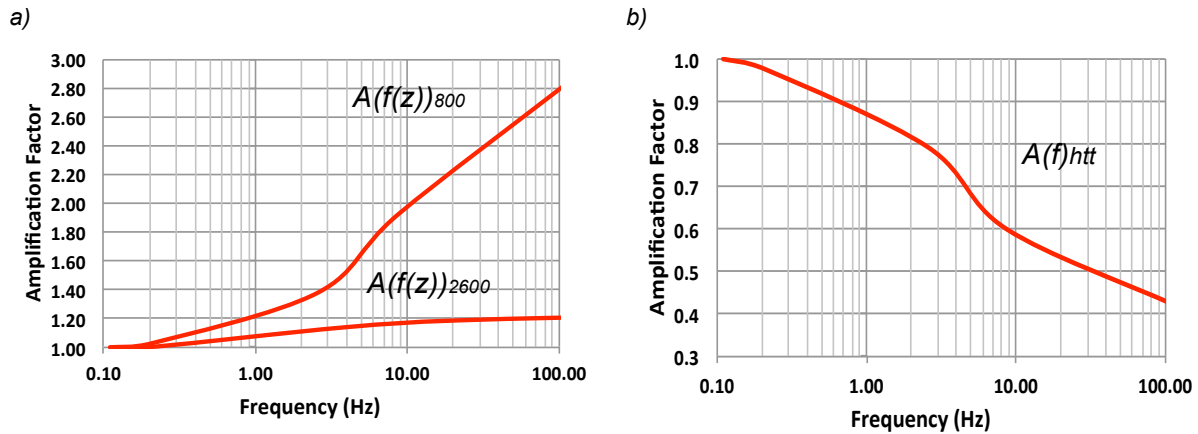


Figure 17. a) Site amplification functions for a standard rock with a  $V_s=800\text{m/s}$  and for a hard rock with a  $V_s=2600\text{ m/s}$ . b)  $V_s$  (impedance) correction factor.

According to the definition of this impedance term, the  $V_s$  correction factors should be applied in the Fourier domain. It is also worth noting that the  $V_s$  correction is GMPE independent, and can be applied directly to the uniform hazard spectra no matter the ground motion prediction used.

### 3.4.1.2 Correction 2: High Attenuation factor “kappa” correction (Diminution function $D(f)$ )

The second correction is related to the high frequency attenuation factor “kappa” (Anderson and Hough, 1984). The correction is performed here according to the most recent methodology, as proposed by Al Atik et al. (2014).

It is important to mention, that several approaches describing how to account for kappa effects are currently available in literature. However, for this study the Al Atik et al. 2014 method is selected for being a recent, simple and widely accepted method that can be applied as an a posteriori correction to the already calculated uniform hazard spectrum.

According to the exposed definition of the kappa corrections, this one should be applied on the Fourier Spectra domain and inverted afterwards, in this case, via random vibration theory to obtain the corrected response spectra.

The decision of whether to apply first the  $V_s$  correction and then the kappa correction or vice versa is not straightforward. However, it was decided to apply first the  $V_s$  correction, which will affect the host kappa definition, and then apply the kappa correction to finally reflect the target kappa. If done in the reverse way, the target kappa would be affected by the  $V_s$  correction and the resulting modified  $\kappa$  value would be different from the wished one.

Another key point to emphasize is the dependency of the kappa correction on ground-motion prediction model, whereas the  $V_s$  / impedance correction is GMPE independent. For the kappa correction, it is necessary to calculate the  $\kappa$ -scaled factors for each GMPE, as each GMPE has its own host kappa.

Having mentioned the most relevant aspects that concern this correction and to get to the point, the high-frequency spectral decay of earthquake spectra has been modeled by Anderson and Hough (1984) as:

$$D(f) = A_0 \exp(-\pi k_o f)$$

Where the high frequency attenuation factor ( $\kappa$ ) is the spectral decay parameter controlling the rate of high frequency amplitude decay (Al Atik et al. 2014) (Figure 18).

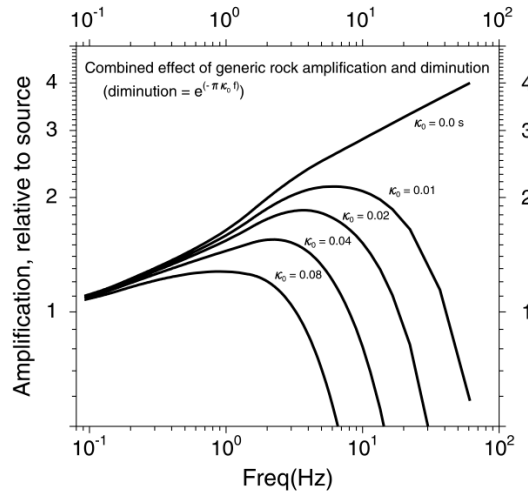


Figure 18. Combined effect of generic rock amplification and diminution terms for a rock with  $V_s=600$  m/s. (Boore 2003a).

### 3.4.1.3 Host to target application

Applying the  $V_s$  correction (Boore, 2003a) and following the Al Atik et al. (2014) method for deriving kappa ( $k$ ) scaling factors to account for site-specific ( $k$ ) estimates, a partially non-ergodic UHS corrected to a very hard rock ( $V_s$ -kappa correction) was finally obtained.

Along all this study, the python open source tool **Strata** (Kottke and Rathje, 2008 a,b) was used to migrate from the response spectra domain to the Fourier spectra domain and vice versa. This open source computational tool allows us to derive Fourier amplitude spectrum (FAS) consistent with the response spectrum from the GMPE. Host-to-target corrections (impedance correction based on rock  $V_{S30}$ , and  $\kappa$  correction) are then applied in the Fourier domain, and the modified Fourier spectra are converted into Response Spectra on target rock surface using the same RVT based tool.

Below, a description on how to apply step by step the host-to-target adjustments is described.

#### 3.4.1.3.1 Step 1: From Disaggregation Select the Mw that contributes more to the hazard.

The hazard disaggregation on standard rock allows to identify the main magnitude and distance scenarios contributing to the hazard.

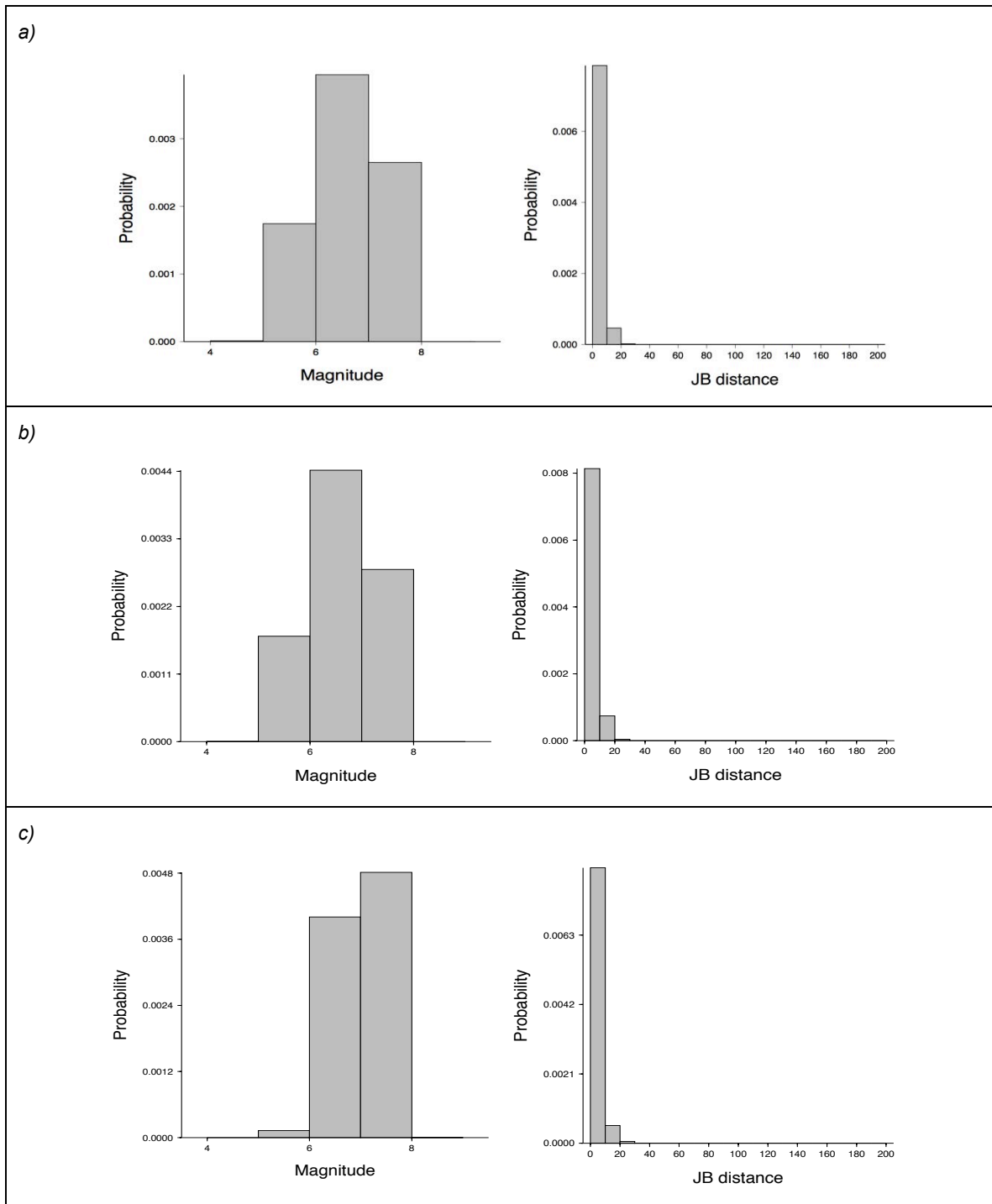


Figure 19. . . Disaggregation in magnitude and distance (GMPE AA14) –  $T_r=5000$  years, for different oscillator periods : a)  $S_a(0\text{ s})=PGA$ , b)  $S_a(0.2\text{ s})$ , c)  $S_a(1.0\text{ s})$ .

Figure 19 shows the disaggregation in magnitude and distance at 5000 yrs, when using the ground-motion equation AA14 for a standard rock (800 m/s), for three representative oscillator periods (0, 0.2 and 1.0 s). In this case, magnitudes 5 to 8, with a predominance of magnitude between 6 and 8, are contributing to the hazard at distances lower or equal to 20 km. The scenario  $M_w=6.5$  at  $D=10$  km, which corresponds satisfactorily to all dominant

scenario whatever the oscillator period, is selected to calculate the response spectra and apply the Vs-k-correction.

Al Atik et al. (2014) propose averaging kappa from different scenarios to obtain the Vs-kappa scaling factors. However, in the present study we have observed that the estimation of kappa following Al Atik method (visual inspection) highly depends on the practitioner, and in fact depends more on the practitioner than on a given magnitude/distance scenario.

#### 3.4.1.3.2 Step 2: Calculate the host GMPE response spectra for the selected Mw, D scenario.

The response spectra are computed for the selected magnitude and at short distances on stiff soil or on rock, for each of selected GMPEs.

Scenarios with short distances are used to minimize the impact of anelastic attenuation (Q) on the high-frequency part of the response spectrum and FAS. Relatively high  $V_{S30}$  values are used to avoid over-whelming the rock  $\kappa$  with soil damping.

To perform the host-to-target adjustments, it is necessary to calculate the response spectra for the Mw=6.5 and D=10 km scenario for the 8 selected GMPEs, since the kappa correction is ground-motion model dependent. For illustration purposes, the methodology is applied using AA14 ground-motion model (Figure 20 to 26).

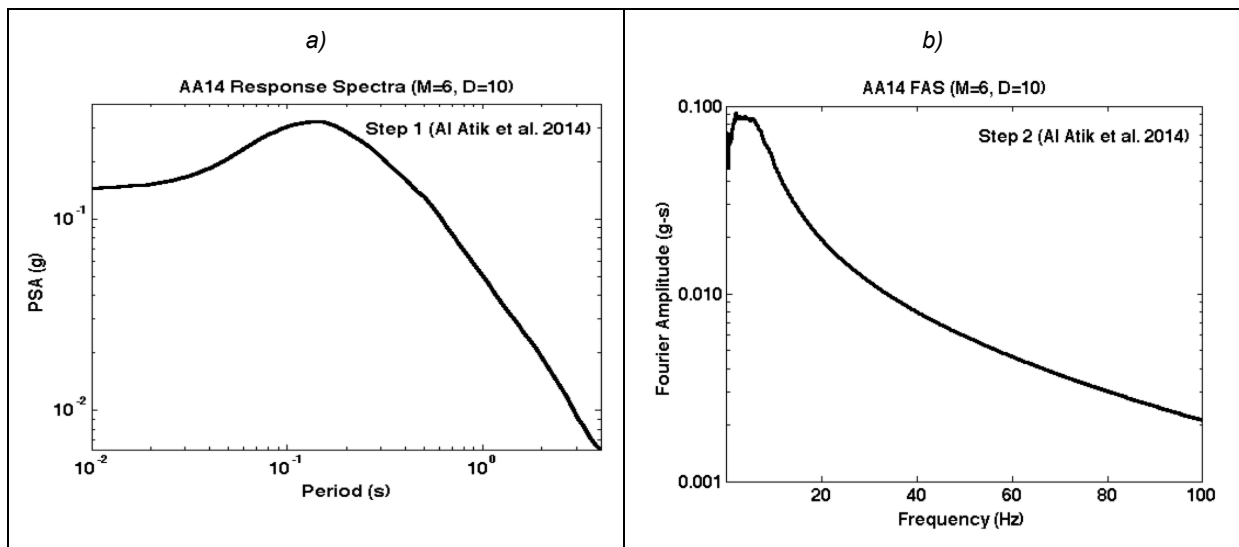


Figure 20. a) Response spectra on standard rock for AA14, Mw=6.5, D=10km and VS30=800 m/s. b) Fourier Amplitude spectra obtained via IRVT (Strata) for AA14 standard rock, Mw=6.5, D=10km and VS30=800 m/s.

#### 3.4.1.3.3 Step 3: Calculate the FAS via IRVT

The Inverse Random Vibration Theory (IRVT) is used as implemented in Strata (Kottke and Rathje, 2008a,b) to invert the host GMPE response spectra to obtain the compatible Fourier Amplitude Spectra (FAS), Figure 21a.

#### 3.4.1.3.4 Step 4: Apply the Vs correction factors

The  $V_S$  correction factors are applied to the compatible Fourier Amplitude Spectra (FAS) obtained in step 3, following Boore 2003a, by multiplying the FAS by the  $V_S$  correction factors (Figure 21b).

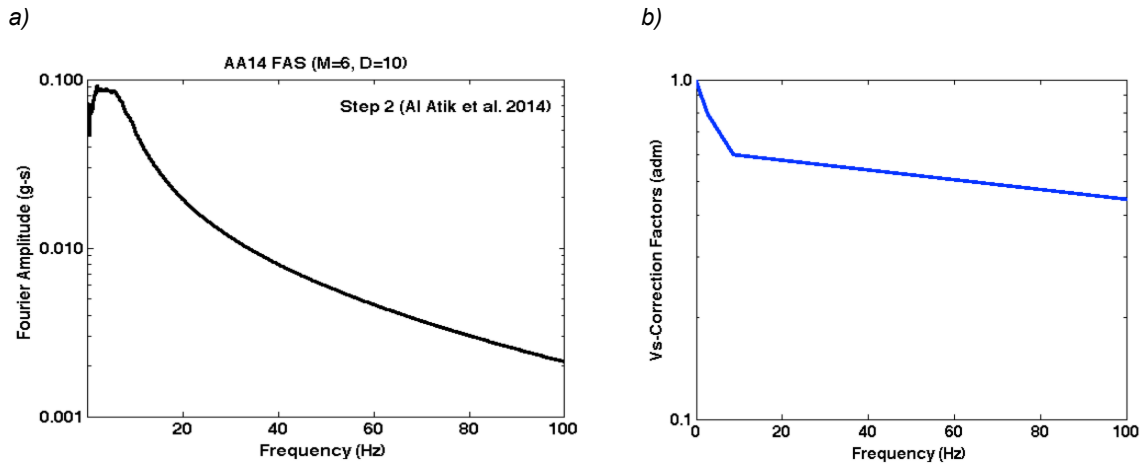


Figure 21. a) Fourier Amplitude spectra for AA14 standard rock,  $M_w=6.5$ ,  $D=10\text{km}$  and  $V_{S30}=800\text{ m/s}$ , b)  $V_S$  correction factors, to move from a standard rock (800m/s) to a very hard rock (2600 m/s).

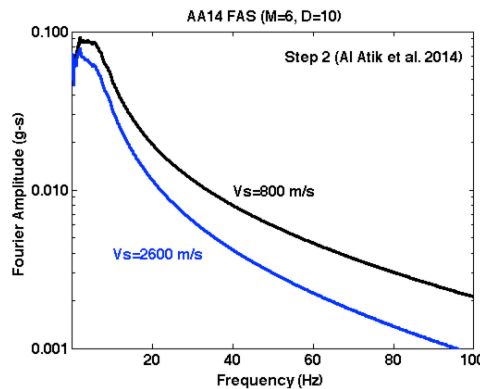


Figure 22. Fourier Amplitude spectra for AA14 standard rock,  $M_w=6.5$ ,  $D=10\text{km}$  and  $V_{S30}=800\text{ m/s}$  (black) and Fourier Amplitude spectra for AA14 standard rock,  $M_w=6.5$ ,  $D=10\text{km}$  and  $V_{S30}=2600\text{ m/s}$  (black).

#### 3.4.1.3.5 Step 5: Calculate kappa host ( $k_h$ ) and kappa target ( $k_t$ )

The host  $k_h$  is estimated on each response spectra-compatible FAS based on the slope in the high-frequency spectra by fitting the Anderson and Hough (1984)  $\kappa$  function,  $A_0 \exp(-\pi\kappa f)$ , to the linear part of  $\ln(a)$  versus  $f$  (Figure 23a). The host kappa for the 8 selected ground motion models are shown in Table 7. Only ground motion models where the within- and between-event aleatory components ( $\phi$ ) and ( $\tau$ ) are clearly separated terms are considered. The "host-kappa" values are found to vary significantly from 0.0312 to 0.0442, which indicates that the  $\kappa$ -adjustment will be more or less significant depending on the GMPE, with a final impact of the hazard estimates depending on the weights of each GMPE. It would be by far simpler, and less subjective, if the  $\kappa$  values to be associated to each GMPE were provided by the GMPE developers (for new GMPEs), or in summary, consensual tables for already existing GMPEs.

Table 7 High frequency attenuation factor ( $k_h$ ) for the selected ground motion models, where ( $\phi$ ) and ( $\tau$ ) were separated terms.

<b>Kappa Host (<math>k_h</math>) – GMPE</b>						
<b>AB10</b>	<b>CY08</b>	<b>ZA06</b>	<b>AA14</b>	<b>CA14</b>	<b>BA14</b>	<b>CY14</b>
0.0366	0.0331	0.0353	0.0395	0.0312	0.0442	0.0321

The target kappa was derived by analysing the slope in the high-frequency spectra from various acceleration records at the Euroseistest. The analysis was originally performed by O.J. Ktenidou within the framework SIGMA project, and the target kappa value was selected on this basis. Since the corrections are made for a very hard rock at depth, the station used to derive this kappa was TST\_196 (Table 8). The value considered here should be considered as an example in order to illustrate the  $\kappa$ -correction procedure.

Table 8. High frequency attenuation factor ( $k_h$ ) at the Euroseistest derived from the analysis of ground motion records at station TST\_196.

<b>Kappa Target (<math>k_t</math>) - Euroseistest</b>
0.024

**3.4.1.3.6 Step 6: Correct kappa host ( $k_h$ ) to kappa target ( $k_t$ ).**

The  $\kappa$  scaling is then applied (Figure 23b) by multiplying the host, VS30 modified FAS by the exponential term:

$$\exp(-\pi f(k_{target} - k_{host}))$$

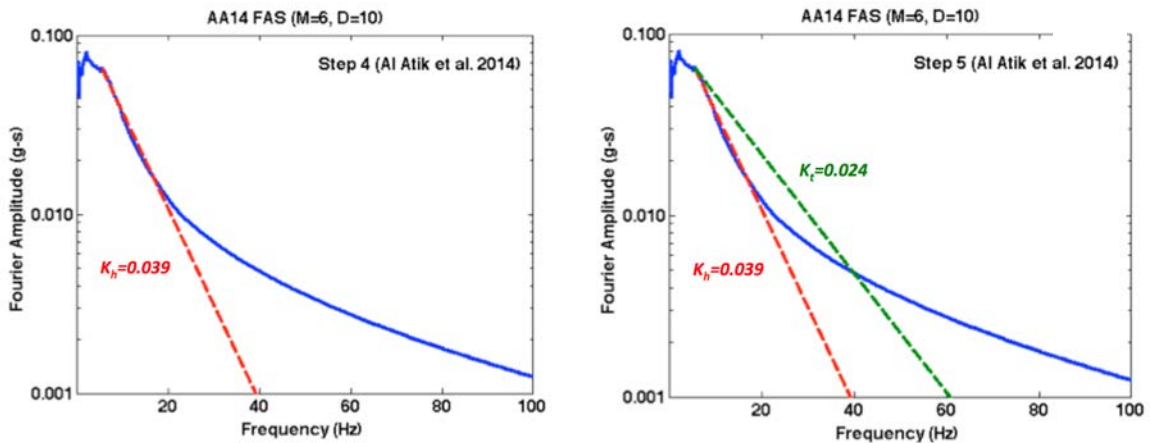


Figure 23. AA14 Fourier Amplitude Spectra for  $M_w=6.5$ ,  $D=10$  and  $V_s=2600$  m/s: a) Kappa host ( $k_h$ ). b) Kappa target ( $k_t$ ).

**3.4.1.3.7 Step 7: Apply IRV to obtain Vs-kappa corrected Response Spectra**

The Vs-kappa corrected FAS are then converted into response spectra with the RVT theory via the *Strata* tool (Figure 24).

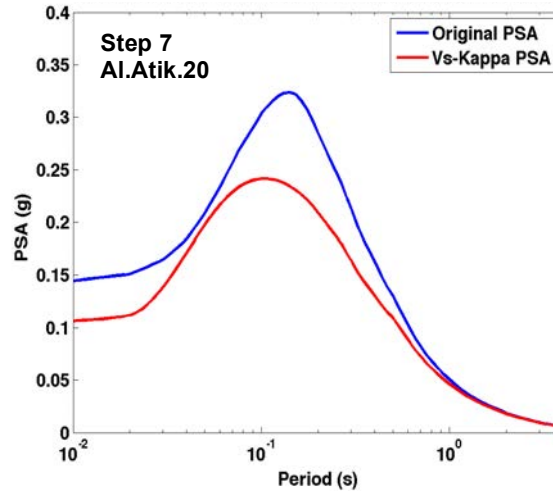


Figure 24. a) Original AA14 response spectra (blue) and Vs-kappa corrected AA14 response spectra (red).

**3.4.1.3.8 Step 8: Vs-k scaling factors**

For checking purposes, the combined (VS,  $\kappa$ ) scaling factors for response spectra and the dominant scenario are obtained by dividing the (VS,  $\kappa$ ) corrected response spectra by the original GMPE response spectra for the same scenario, i.e., Mw=6.5, D=10 km and the "standard rock" Vs=800 m/s, Figure 25.

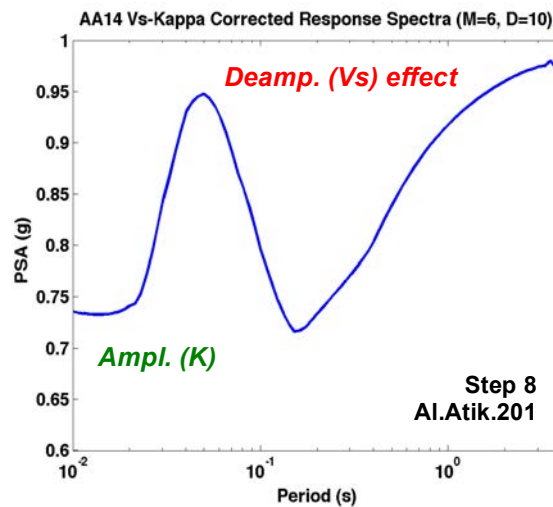


Figure 25. Step 8: Vs – kappa scaling factors for AA14 response spectra.

Finally, it is worth stressing that the Vs adjustments are GMPE independent, while the kappa adjustments are GMPE dependent and should be calculated separately for each ground-motion model. All the mentioned steps are described in the following flux diagram postulated by Al Atik et al. 2014 (Figure 26)

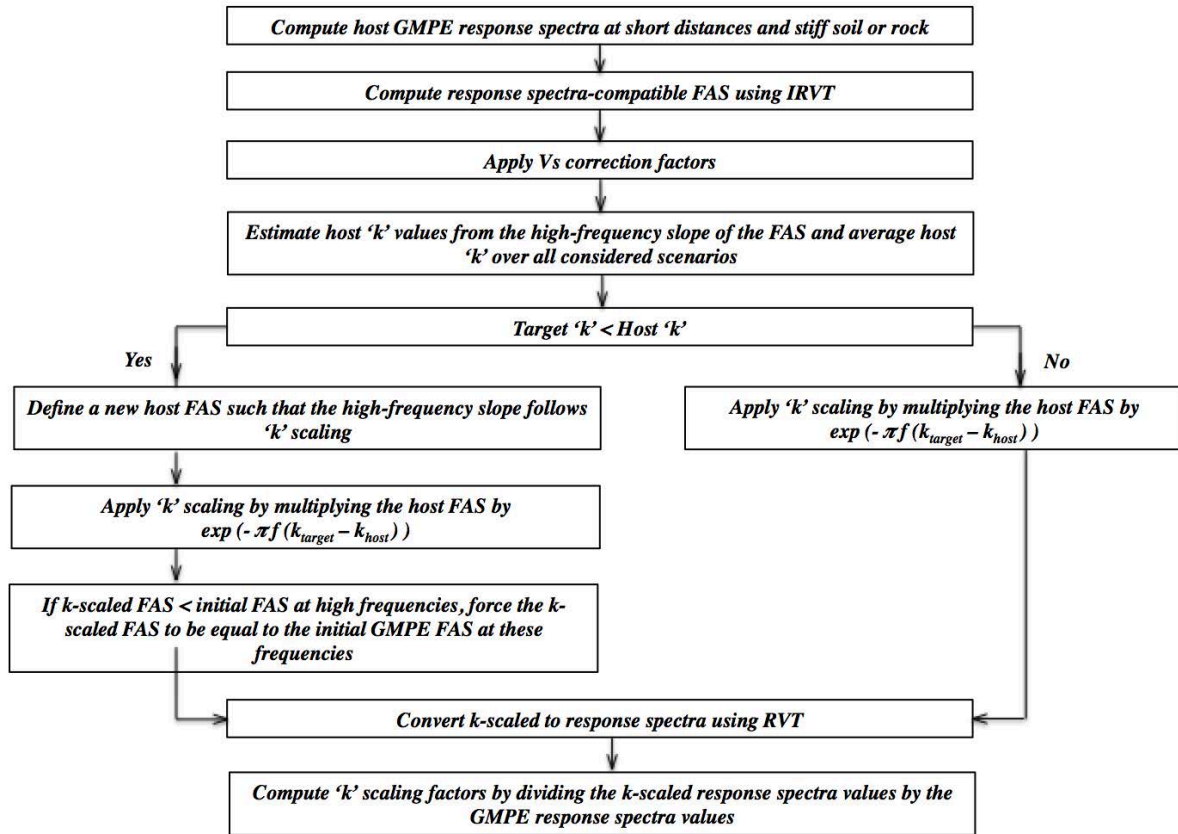


Figure 26. Steps for deriving vs-kappa scaling factors using the IRVT approach. (Modified Flux diagram from Al Atik et al. 2014).

### 3.4.2 Level 1a) Linear Site specific residual ( $\delta S_{2s,s}$ from GMPEs)

Considering multiple recordings of ground motion at a particular site,  $S$ , it is possible to estimate the systematic site effects,  $\delta S_{2s,s}$ , and its standard deviation  $\phi_{ss,s}$ , and removing them from the ground-motion variability.

Firstly, the total within-event residual standard deviation ( $\phi$ ) of the GMPE must be replaced by the single-station within-event variability  $\phi_{ss,s}$  to obtain the "single-station sigma" rock hazard. This adjustment needs to be performed on the open source python codes of Openquake (available in GitHub) for each one of the selected GMPEs. It is important to remark that not all the GMPEs have their standard deviation separated into between-event and within-event. Therefore, some of them cannot be used for this approach unless a separation of its standard deviation is previously done.

Again, the AA14 GMPE is used here for illustration. Its total standard deviation is indeed separated into  $\tau$  and  $\phi$  terms.

Ktenidou et al. (2015) estimated the single-station sigma at the bottom of the Euroseistest basin (TST\_196, Table 8). In the OpenQuake GMPE implementation, the total within-event standard deviation ( $\phi$ ) must be replaced by the single-station within-event standard deviation  $\phi_{ss,s}$ .

Breakdown of residuals from Al Atik et al. 2010:

$$\Delta = \delta W_{es} + \delta B_e$$

<i>Symbol</i>	<i>Residual Component</i>	<i>Standard Deviation</i>
$\Delta$	Total Residuals	$\sigma$ (Aleatoric)
$\delta B_e$	Between event residual	$\tau$ (Aleatoric)
$\delta W_{es}$	Within event residual	$\phi$ (Aleatoric)

Further breakdown:

$$\delta W_{es} = \delta S2S_s + \delta WS_{es}$$

<i>Symbol</i>	<i>Residual Component</i>	<i>Standard Deviation</i>
$\delta S2S_s$	Site term	$\phi_{S2S}$ (Epistemic)
$\delta WS_{es}$	Site and event term	$\phi_{SS}$ (Aleatoric)

$$\sigma = \sqrt{\phi^2 + \tau^2}$$

$$\sigma = \sqrt{\phi_{S2S}^2 + \phi_{SS}^2 + \tau^2}$$

$\phi_{S2S}$ : Site to site variability (**Spatial**).

$\phi_{SS}$ : Single station within event variability (**Temporal**).

**Ergodic Assumption:** Standard deviation across spatial extent  $\phi_{S2S}$  (across sites) is weighted equally to standard deviation across time  $\phi_{SS}$ .

Since the  $\delta S2S_s$  can be defined for a single site (deterministic), then the variability induced by these residuals should also be removed from the calculations:

$$\sigma = \sqrt{\phi_{SS}^2 + \tau^2}$$

Resulting in the single station standard deviation:

$$\sigma_{SS} = \sqrt{\phi_{SS}^2 + \tau^2}$$

$\sigma_{SS}$ : Single station standard deviation.

Then, the single station standard deviation will now be "Partially non ergodic", since ergodic assumption is removed by eliminating the  $\phi_{S2S}^2$  term.

Two different  $\phi_{SS}$  values are considered

- the 0.45 constant value found by Rodriguez-Marek et al. (2013), derived from a large database of ground-motions from multiple regions.

- the  $\phi_{SS,s}$  values determined by Ktenidou et al. at Euroseistest (Table 8).

The first of these 2 options consists in replacing the total within-event component of the GMPE by a constant, "default" value for all spectral periods as explained by Rodriguez et al. 2013, who conclude that a constant value of single station sigma ( $\phi_{SS}$ ) equal to 0.45 (In units) fits well across all oscillator periods.

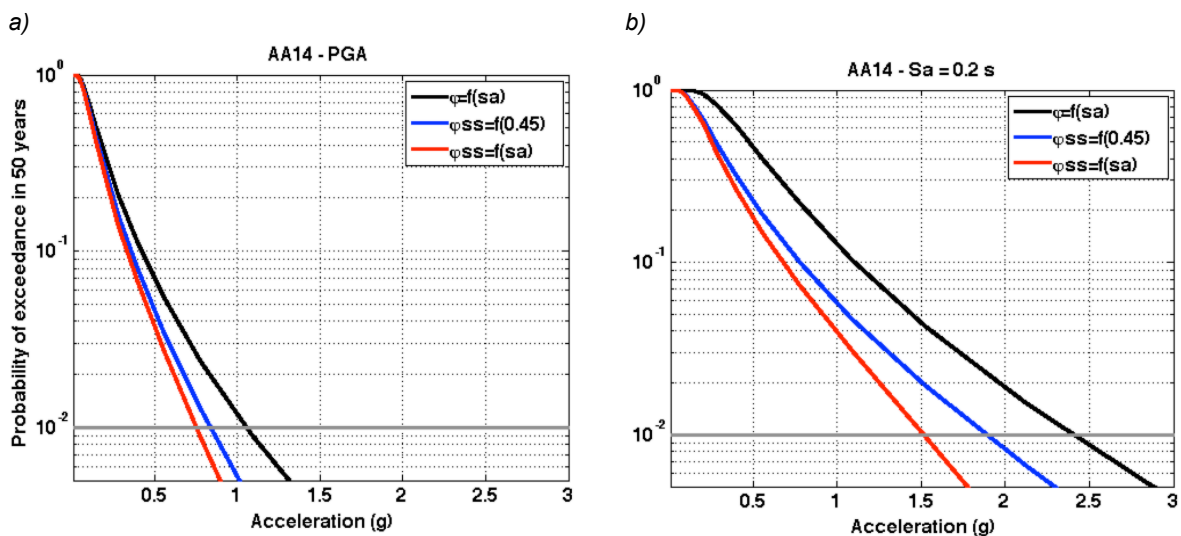
The second option uses a site-specific single station sigma ( $\phi_{ss}$ ), which varies with the spectral period: the values used here are those derived by Ktenidou et al. 2015 at the Euroseistest, which are listed in Table 9, where they are also compared with total within-event variability of the example GMPE AA14.

Table 9: Euroseistest single station sigma (ln scale) calculated at station TST\_196 at depth. (Ktenidou et al. 2015).

Period (s)	$\phi$ (AA14)	$\phi_{ss,s}$	Period	$\phi$ (AA14)	$\phi_{ss,s}$
0.00	0.6201	0.3526	0.20	0.6645	0.2149
0.01	0.6215	0.3764	0.30	0.6599	0.1827
0.02	0.6266	0.3629	0.50	0.6512	0.3201
0.05	0.6622	0.3187	0.65	0.6652	0.2180
0.10	0.6670	0.3676	0.75	0.6744	0.4970
0.13	0.6789	0.2659	1.00	0.6787	0.6025
0.15	0.6796	0.2647	2.00	0.7254	0.5183

The probabilistic seismic hazard is re-calculated using the modified GMPE, the corresponding hazard curves and Uniform Hazard Spectra are displayed in Figure 27.

While modifying the GMPE implementation, linear interpolation was used for the frequencies not reported in Table 9, and a constant single-station sigma ( $\phi$ ) was used for periods from 2 to 4 s due to lack of information. The huge impact of the value of within-event aleatory variability on the hazard curve is obvious, especially at log return periods, at all oscillator periods, which both draws the attention of the usefulness of site monitoring to obtain a site-specific measurement of the within-event variability, and calls for much care in its measurement.



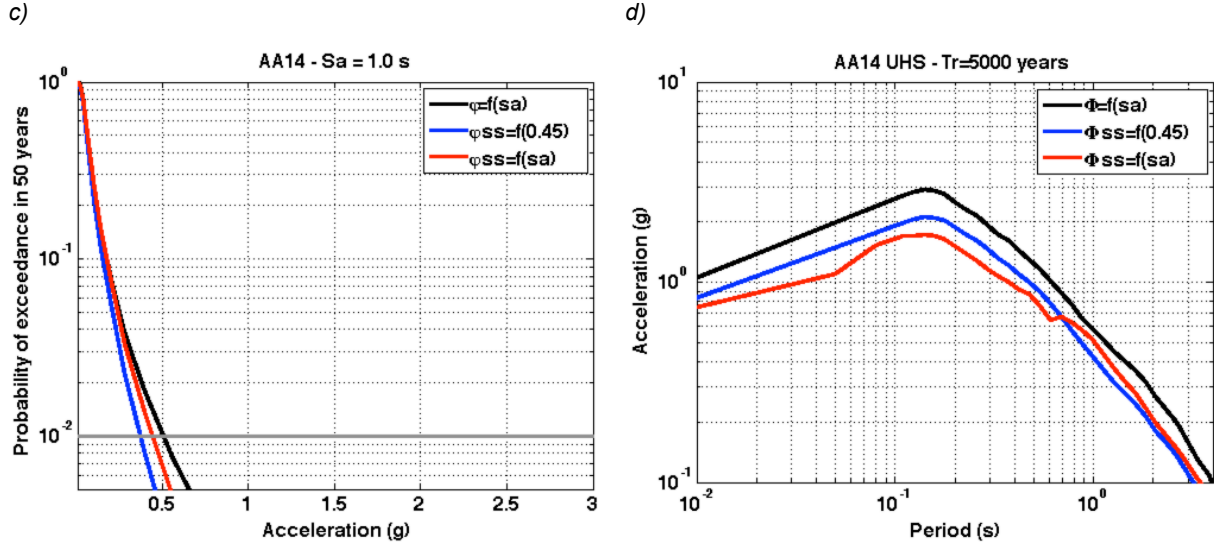


Figure 27. a) hazard curves for PGA spectral ordinate. b) hazard curves for  $Sa=0.2$  s. c) hazard curves for a  $Sa=1.0$  s. d) uniform hazard spectra for a  $Tr=5000$  years. Calculations are performed with GMPE AA14. Total sigma (black),  $\phi$  term replaced by single station sigma  $\phi_{ss,s}(T) = 0.45$  following Rodriguez-Marek et al (blue) and  $\phi$  term replaced by single station sigma  $\phi_{ss,s}(T)$  derived by Ktenidou et al. 2015 (red).

Finally, the systematic deviation of the observed amplification at this site,  $\delta S2S_s$ , which is period-dependent, needs to be "added" to the modified hazard values obtained with the single station standard deviation  $\phi_{ss,s}$ . This should be done by applying the following expression to the recently calculated UHS,  $\mu_{GMPE}(T)$ ,

$$\mu_{corrected}(T) = \mu_{GMPE}(T) \cdot \exp^{\delta S2S_s(T)}$$

with  $\mu_{GMPE}(T)$  being the the Uniform Hazard Spectrum

One must be very careful in the value of  $\delta S2S_s$  to be used for the correction. The default values of  $\delta S2S_s$  estimated from the GMPEs are the residuals with respect to the predictions including the site term S embedded in the GMPE. Therefore, if the  $\delta S2S_s$  terms are used in order the estimate the relative amplification between two different sites (for instance here the surface site TST\_0 and the deep borehole site TST\_196), see section 2.3.3.3 above with the term  $\Delta\delta S2S$ , they should be first corrected to express the residual with respect to exactly similar site conditions (i.e., same  $V_{S30}$ ), which we call the residual "without the site term" and label with the subscript "WOST", in opposition to the default  $\delta S2S_s$  value, which is "with the site term", and is labeled with the subscript "WIST"

For instance, for the example GMPE of Akkar et al. 2014, the site term S is defined by the following equation :

$$\ln(S) = \begin{cases} b_1 \ln(V_{S30}/V_{REF}) + b_2 \ln \left[ \frac{PGA_{REF} + c(V_{S30}/V_{REF})^n}{(PGA_{REF} + c)(V_{S30}/V_{REF})^n} \right] & \text{for } V_{S30} \leq V_{REF} \\ b_1 \ln \left[ \frac{\min(V_{S30}, V_{CON})}{V_{REF}} \right] & \text{for } V_{S30} > V_{REF} \end{cases}$$

With  $V_{REF} = 750$  m/s and  $V_{CON} = 1000$  m/s.

So that the "without site term" residual should be computed as:

$$\ln(\delta S2S_s(T)_{WOST}) = \ln(\delta S2S_s(T)_{WIST}) + \ln(S)$$

WIST: With site term.

WOST: Without site term.

The corresponding original and corrected residuals are listed in Table 10 for the two sites TST\_0 and TST\_196.

Table 10: Euroseistest systematic deviation of the observed amplification,  $\delta S2S_s$ , as estimated by Ktenidou et al. 2015 for the AA14 GMPE (second and third columns), and corrected using Akkar et al. 2014 site term (fourth and fifth columns), and converted into amplification factors (sixth and seventh columns).

Period (T)	With Site term (WIST)		Without Site term (WOST)		Without Site term (WOST)	
	$\ln(\delta S2S_s)$ (TST_0)	$\ln(\delta S2S_s)$ (TST_196)	$\ln(\delta S2S_s)$ (TST_0)	$\ln(\delta S2S_s)$ (TST_196)	( $\delta S2S_s$ ) (TST_0)	( $\delta S2S_s$ ) (TST_196)
0.00	0.285	-0.442	0.8708	-0.5628	2.389	0.5696
0.01	0.231	-0.393	0.8124	-0.5133	2.253	0.5985
0.02	0.199	-0.359	0.7570	-0.4742	2.132	0.6224
0.05	0.510	-0.639	0.8062	-0.6999	2.239	0.4966
0.10	0.412	-0.714	0.7892	-0.7914	2.202	0.4532
0.13	0.262	-0.606	0.8169	-0.7209	2.264	0.4863
0.15	0.146	-0.580	0.8198	-0.7193	2.270	0.4871
0.20	0.088	-0.366	0.9982	-0.5535	2.713	0.5749
0.30	0.081	-0.242	1.2327	-0.4794	3.431	0.6192
0.50	0.006	-0.137	1.3249	-0.4091	3.762	0.6643
0.65	-0.038	-0.250	1.3332	-0.5324	3.793	0.5872
0.75	0.000	-0.166	1.4054	-0.4563	4.077	0.6336
1.00	-0.061	0.057	1.3521	-0.2348	3.865	0.7907
2.00	-0.026	0.110	1.2429	-0.1519	3.466	0.8591
3.00	-0.026	0.110	1.1702	-0.1369	3.223	0.8720
4.00	-0.026	0.110	1.0287	-0.1077	2.798	0.8979

Figure 28a shows the corrected  $\delta S2S_s(T)$  for both stations at depth and at the surface for AA14, while Figure 28b shows the amplification factors  $exp^{\delta S2S_s(T)}$  (columns 6 and 7 in Table 10) needed to correct the uniform hazard spectrum by accounting the systematic deviation of the observed amplification Figure 29.

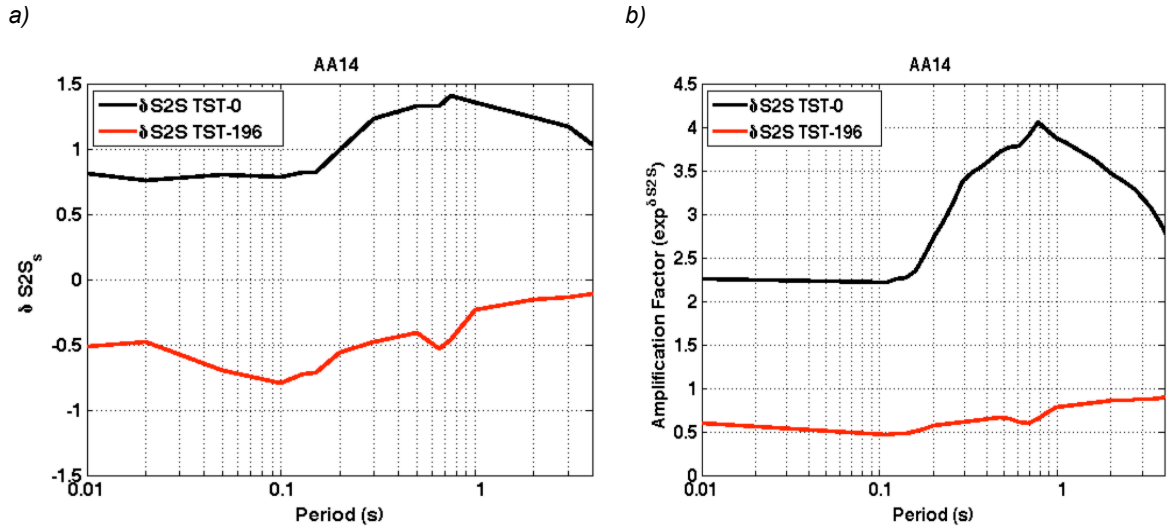


Figure 28. a) AA14 systematic deviation of the observed amplification ( $\delta S2S$  residual) without including the site term as a function of the period, for station TST\_0 (black) at the surface and TST\_196 (red) at depth. b) Corresponding Amplification Factors (AA14) as a function of the period.

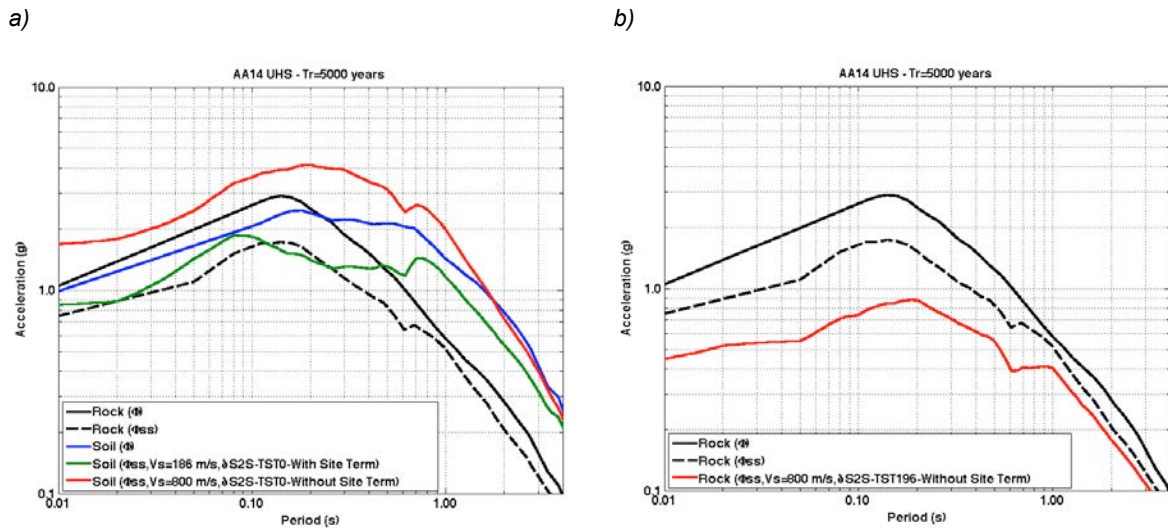


Figure 29. Application of site-specific residual  $\delta S2S_s$  to the AA14 Uniform Hazard Spectrum for 5000 years return period on rock. a) Soil Hazard : Level 1a: single station sigma  $\phi_{ss,s}(T)$  on soil with  $\delta S2S_{TST0} - WIST$  (green), and single station sigma  $\phi_{ss,s}(T)$  on soil with  $\delta S2S_{TST0} - WOST$  (red), to be compared with the "Level0" full sigma  $\phi(T)$  on soil (blue) b) Rock hazard with various assumptions: Full sigma  $\phi(T)$  on standard rock (black), Level 1a: single station sigma  $\phi_{ss,s}(T)$  on standard rock (sahed black), and the single station sigma  $\phi_{ss,s}(T)$  on very hard rock corrected with the site residual  $\delta S2S_{TST196}$  (red), thus corresponding to within motion at depth.

The uniform hazard spectra on soil at the surface (TST\_0) was obtained in two different ways by using site specific residuals:

$$- UHS_{Soil}(T) = UHS_{Rock}(\phi_{ss}, V_s=186 \text{ m/s})(T) \cdot \exp^{\ln(\delta S2S_{TST0}(T) WIST^*)} \quad (\text{Figure 29a, green})$$

$$- UHS_{Soil}(T) = UHS_{Soil}(\phi_{ss}, V_s=800 \text{ m/s})(T) \cdot \exp^{\ln(\delta S2S_{TST0}(T) WOST^*)} \quad (\text{Figure 29a, red})$$

\* See values on Table 10.

Also, the uniform hazard spectra on very hard rock at depth (TST\_196) was obtain using site specific residual as follow:

$$- UHS_{Very\ Hard\ Rock}(T) = UHS_{Rock}(\phi_{ss}, v_s=800\ m/s)(T) \cdot \exp^{\ln(\delta S2S_{TST196}(T)_{WOST*})} \quad (\text{Figure 29b, red})$$

The significant difference between red and green curves on Figure 29a, comes from the type of  $\delta S2S$  correction term, and *in fine* for the accounting or not of a non-linear term:

- The red ( $\delta S2S_{WOST}$ ) applies the  $\delta S2S$  with respect to a GMPE without any site term, i.e., the residual with respect to a standard rock. As the residual is derived from available data, which all correspond to weak to moderate motion ( $pga < 0.05g$ ), it corresponds to the linear amplification of TST\_0 site with respect to a standard rock
- The green curve ( $\delta S2S_{WIST}$ ) applies the  $\delta S2S$  with respect to the full AA14 GMPE, which a non-linear site term. The residual is measured with respect to a soft soil with  $VS30 = 186\ m/s$ , i.e., the  $VS30$  value at TST\_0, and corresponds to the "overamplification" with respect to a generic site, again in the linear domain since it is derived from the same date. This residual is then applied in the same way to the single-station sigma hazard at a site with  $VS30 = 186\ m/s$ , which does include the non-linear effect for such a soft soil

Applying a partially non-ergodic PSHA by using single station sigma and adding the systematic site effects,  $\delta S2S_s$  represents a decrease on the epistemic uncertainty and a significant reduction of the expected hazard with full sigma at the site (a factor of 2 at PGA level) for this particular case.

Nevertheless, this does not mean that every time that a site specific non ergodic PSHA is apply, a lower value of acceleration in comparison with the full sigma model will be obtained, since the systematic site effects,  $\delta S2S_s$ , could induce to hazard values above the median value predicted by the GMPE (full sigma) and also larger values of  $\phi_{ss, s}$  with respect to the full sigma could also happened.

The main shortcoming of this method, is the precondition of availability of enough records to be able to derive the within and between events residuals at the site of interest. Once the data is available, calculating this values does not signify an enormous amount of effort against the big gain in terms of uncertainty reduction.

### 3.4.3 Level 1b) Linear Site response analysis, Instrumental.

The Euroseistest has been instrumented since 1993. Strong motions recorded by the EUROSEIS permanent network (network code: EG) are available on line (<http://euroseisdb.civil.auth.gr>) for visualization and/or downloading through the "Database search" page (in sac, little-endian, or ascii formats ; Pitilakis, et al. 2013). Many site response studies have been led at the site.

Two types of instrumental site response analysis are shown here:

- standard spectral ratios based on accelerogram data set recorded on the Euroseistest array during the period April 1994 to June 1996 (Raptakis et al. 1998).

- amplification function calculated using  $\delta S2S$  approach (Ktenidou et al. 2015).

### 3.4.3.1 Case 1: Standard Spectral Ratios (SSR)

Considering Standard Spectral Ratios based on stations TST\_0 and PRO (Figure 30), the reference rock is similar to standard rock (800 m/s), and no host-to-target adjustment is required. The transfer function can be applied directly.

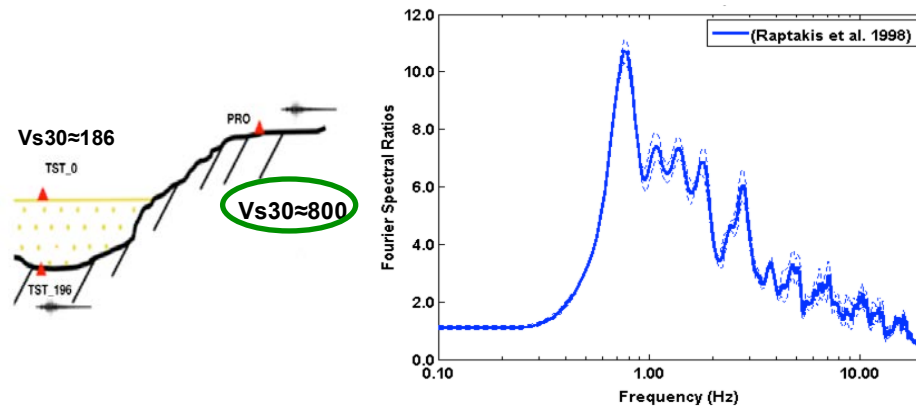


Figure 30. Standard spectral ratios (SSR) derived using information from stations TST\_0 at the surface on soft soil, and PRO station also at surface but on weathered rock with shear wave velocity around 800 m/s Raptakis et al. 1998.

The procedure to calculate the uniform hazard spectra on soil (Figure 30) will require to:

- 1) Calculate the partially non-ergodic uniform hazard spectrum as defined in the previous section using single-station sigma approach.
- 2) Invert the uniform hazard spectrum via inverse random vibration theory (IRVT) to obtain the corresponding Fourier amplitude spectra (FAS). The amplification function has indeed been derived in the Fourier domain.
- 3) Apply the linear transfer function obtained via standard spectral ratios (TST\_0/PRO) by Raptakis et al. 1998 to the Amplitude Fourier spectra.
- 4) Invert again via random vibration theory (RVT) the Fourier amplitude spectra on soil, to obtain its corresponding response spectra on soil.

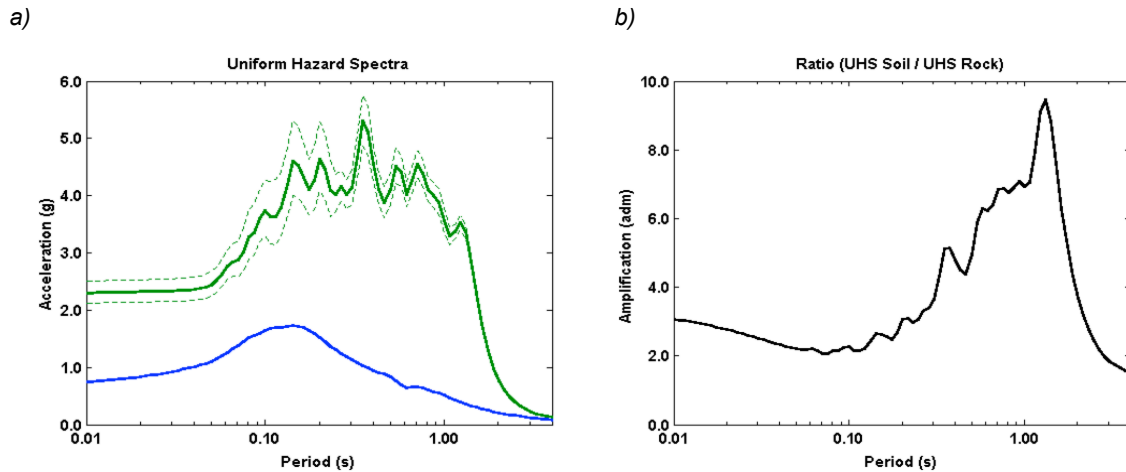


Figure 31. AA14 uniform hazard spectrum for 5000 years return period: **a) Level 1a - Rock:** Single station sigma (blue), **Level 1b – Soil Raptakis:** Single-station sigma, Raptakis et al. 1998 transfer function, (dark green). **b) Ratio (UHS Soil / UHS Rock).**

### 3.4.3.2 Case 2: $\delta S2S$ Approach Amplification Function

The amplification function derived by Ktenidou et al. 2015 following a  $\delta S2S$  approach can be applied to account for site effects. However this time, host-to-target corrections are required, since the reference rock station is TST\_196, a borehole station at the bottom of the basin, on very hard rock ( $V_s = 2600 \text{ m/s}$ ).

The procedure to calculate the uniform hazard spectra on soil is the following:

The procedure to calculate the uniform hazard spectra on soil (Figure 34) will require to:

- 1) Obtain the systematic site effects,  $\delta S2S_s$ , and its standard deviation  $\phi_{SS}$  at station TST\_196.
- 2) Calculate the partially non-ergodic uniform hazard spectrum as defined on the previous section using single station sigma approach.
- 3) Apply the corresponding host to target adjustments as described on the previous section to obtained the  $V_s$ -kappa corrected uniform hazard spectrum on very hard rock.

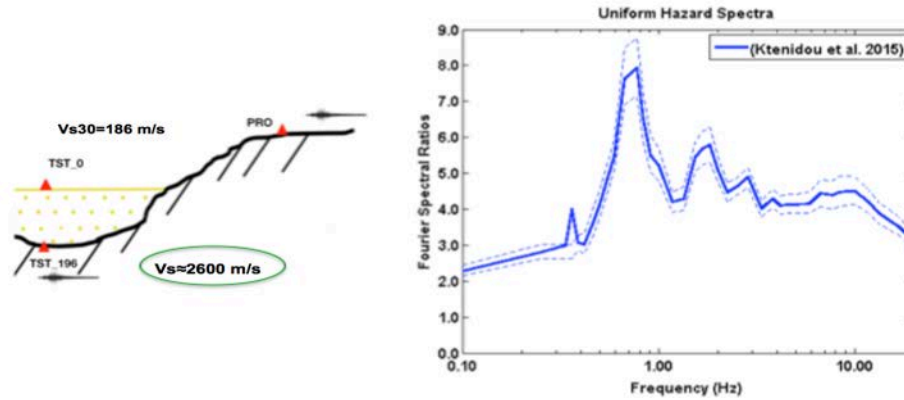


Figure 32. Linear transfer function obtained via  $\delta S2S$  approach by Ktenidou et al. 2015 between station TST\_0 at the surface (soft soil) and station TST\_196 at the bottom of the basin (very hard rock).

- 4) Since the Vs-kappa uniform hazard spectrum after host-to-target corrections still refers to hazard at the surface, a depth correction is required. This correction accounts for the existence at depth of destructive interferences and the absence of free-surface effects in the high-frequency range at station TST\_196 (Cadet et al. 2012a , Figure 33).

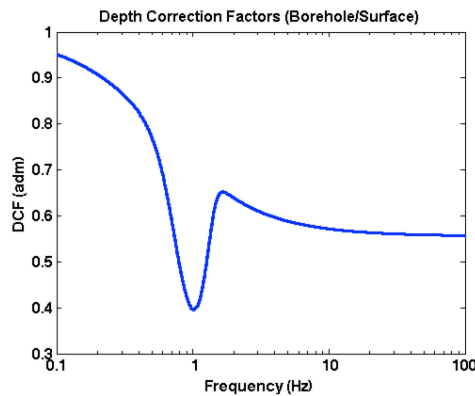


Figure 33. Depth correction factors according to Cadet et al. 2012a (Borehole/Surface), Fourier domain.

- 5) Multiply the Vs-kappa-depth corrected Fourier Amplitude Spectra by the linear transfer function obtained via  $\delta S2S$  approach by Ktenidou et al. 2015 (Figure 32).

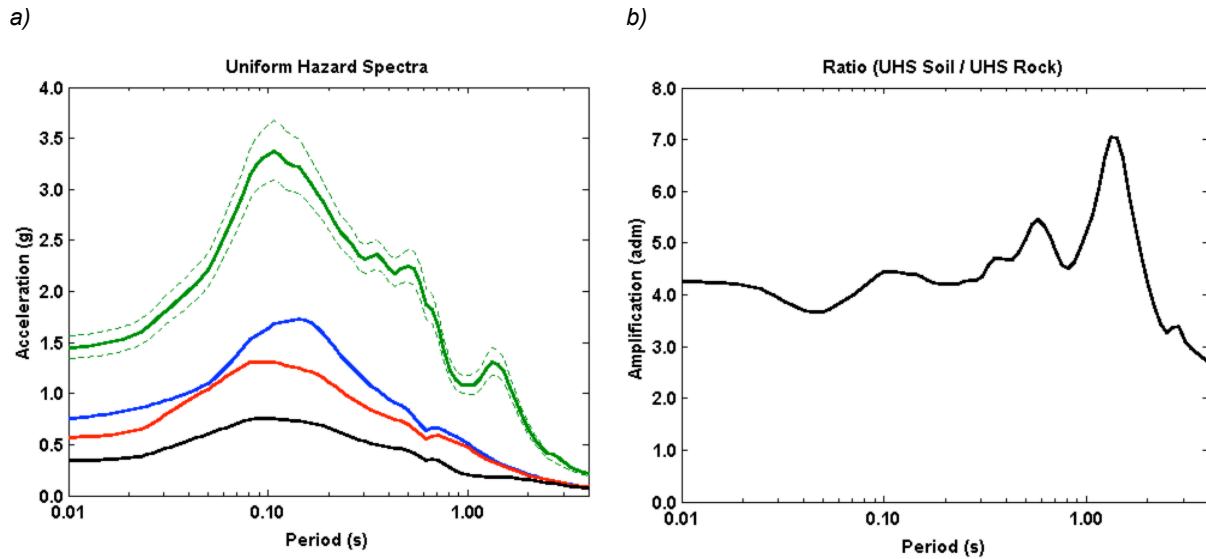


Figure 34. AA14 uniform hazard spectrum for 5000 years return period: **Level 1a - Rock**: Single-station sigma (blue), **Level 1a - Rock**: Single-station sigma, host-to-target adjustments (red), **Level 1a - Rock**: Single station sigma, host-to-target adjustments, depth correction (black), **Level 1b - Soil**: Single-station sigma, host-to-target adjustments, depth correction and Ktenidou et al. 2015 transfer function, (dark green). b) Ratio UHS Soil ( $\phi_{ss} - htt-DCF-Ktenidou$ ) / UHS Rock ( $\phi_{ss-htt-DCF}$ ).

#### 3.4.4 Levels 1c and 2a: Linear and Nonlinear Site response analysis, Numerical.

The main difference with respect to previous approaches is the way the amplification function from rock to soil is calculated. In the previous cases, the amplification function was derived either instrumentally or numerically. The calculations were done in the linear domain, thus the de-amplification of the ground motion due to nonlinear properties of the soil was not captured.

In the instrumental cases, the ground-motion time histories used to derive the linear transfer function were based on low-magnitude or long distance events, with low enough acceleration and strain levels for the soil to remain in the linear behavior domain. In the numerical analysis, larger events can be considered and non linearity needs to be taken into account.

The aim here is to capture the nonlinear behavior of the soil. The Fortran code NOAH (Bonilla et al., 2000) is selected to calculate a nonlinear amplification function. One must remember that NOAH is one of the nonlinear codes available. The choice of the code is non-unique and bears uncertainty.

NOAH is a **NO**nlinear **A**nelastic **H**ysteretic finite differences code, which computes the nonlinear wave propagation in water saturated soil deposits subjected to vertically incident SH ground motion (Bonilla et al., 2000).

Figure 35 describes the degradation curves used to calculate the material resistance parameters for each one of the considered layers. These degradation curves have been proposed specifically for the Euroseistest within the framework of the SIGMA project.

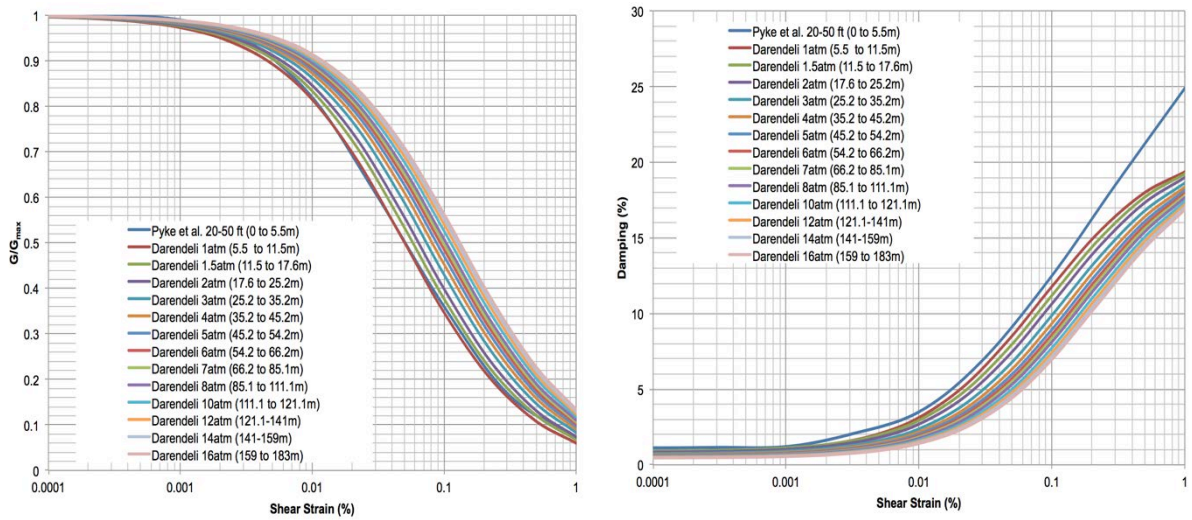


Figure 35. Euroseistest Degradations Curves proposed within the framework of the SIGMA project for the nonlinear site specific model.

Based on the mentioned degradation curves and the geophysical exploration, the soil profile material properties and resistance parameters used in this study are shown in Table 11 and Table 12.

Table 11. Euroseistest material properties model with water table below at 1m depth.

Layer	Thickness (m)	Description	Vs (m/s)	Vp (m/s)	Rho (kg/m3)	Qs (adm)
0 - 5.5	5.50	SiltySand(SM)	144	1524	1077	14.4
5.5 - 17.6	12.10	SiltyClay(CL-ML)	177	1583	1083	17.7
17.6 - 54.2	36.60	LeanClay(CL)	264	1741	1097	26.4
54.2 - 81.2	27.00	FatClay(CH)	388	1952	1117	38.8
81.2 - 131.1	49.90	SiltyClay(CL-ML)	526	2200	1151	52.6
131.1 - 183.0	51.90	SiltyClay(CL-ML)	701	2520	1215	70.1
183.0 - Rock	-	Weatheredrock	2600	-	1446	-

Table 12. Euroseistest material resistance model.

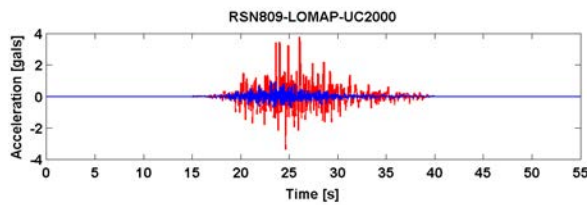
Layer	$\xi$ (%)	$\gamma_{0.5}$ (%)	$\tau$ (kPa)	$\sigma$ (Pa)	$\phi$ (deg)	Ko (adm)
0 - 5.5	0.3	0.050	21398	29060	47	0.26
5.5 - 17.6	0.3	0.063	40799	122377	19	0.67
17.6 - 54.2	0.3	0.085	124058	383629	19	0.68
54.2 - 81.2	0.3	0.105	335024	728493	27	0.54
81.2 - 131.1	0.3	0.130	774534	1158141	42	0.33
131.1 - 183.0	0.3	0.150	1631498	1749120	69	0.07
183.0 - Rock	0.3	-	-	-	-	-

### 3.4.4.1 Sensitivity to acceleration level

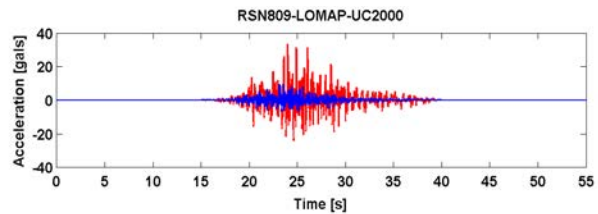
Once described the soil model to be run in the linear and nonlinear calculations with NOAH, a simple case with one accelerogram (RSN809-LOMAP-UC2000) scaled to PGA values of 0.001, 0.01, 0.1, 0.2, 0.5 and 1.0 g was considered. Accelerations on rock (blue) and on soil (red) are shown in Figure 36a to Figure 36f, and the corresponding Fourier Amplitude Spectra on rock and soil are displayed in Figure 37a to Figure 37f.

This first example aims at identifying the relation between nonlinear effects and PGA level. A unique accelerogram is considered, scaled to different values of PGA, some of them remaining on the linear domain, and the others showing features of de-amplification due to soil effects (damping, destructive interference, among others).

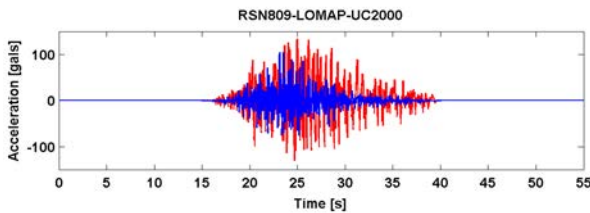
a) PGA values on rock: 0.001 g (1 gals)



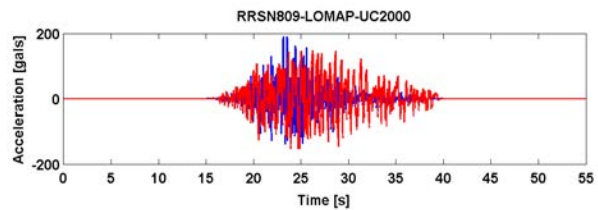
b) PGA values on rock: 0.01 g (10 gals)



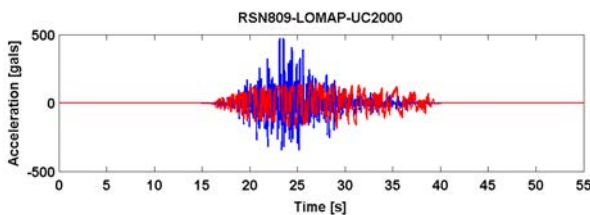
c) PGA values on rock: 0.1 g (100 gals)



d) PGA values on rock: 0.2 g (200 gals)



e) PGA values on rock: 0.5 g (500 gals)



f) PGA values on rock: 1.0 g (1000 gals)

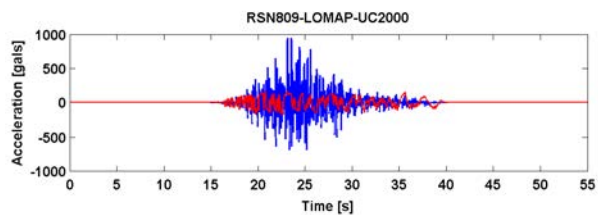
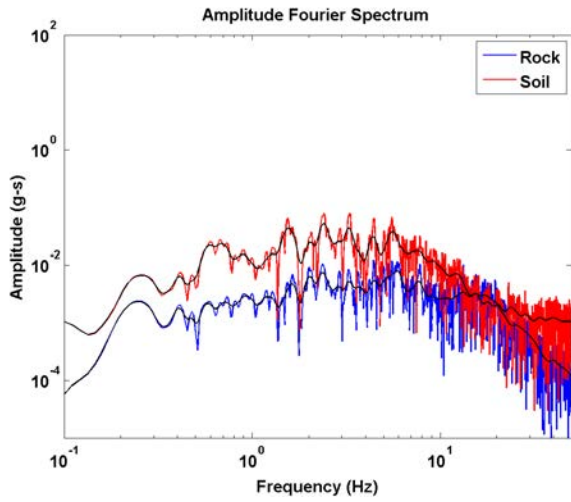
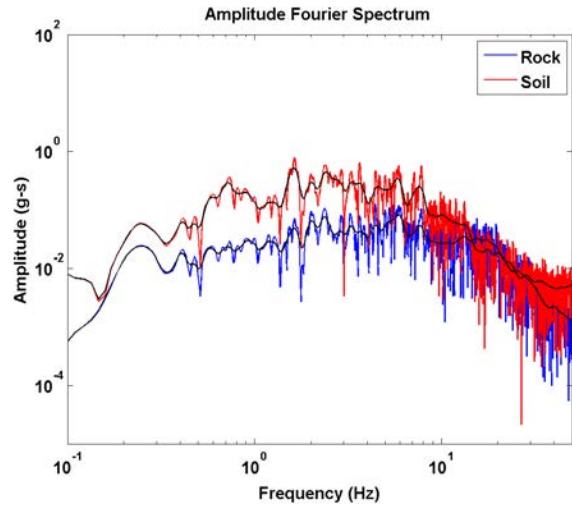


Figure 36. a) RSN809\_LOMAP\_UC2000 Accelerogram scaled to a PGA values on rock: a) 0.001 g, b) 0.01 g, c) 0.1 g, d) 0.2 g, e) 0.5 g, f) 1.0 g, for rock at TST\_196 (blue) and soil (red) cases at station TST\_0 at the surface.

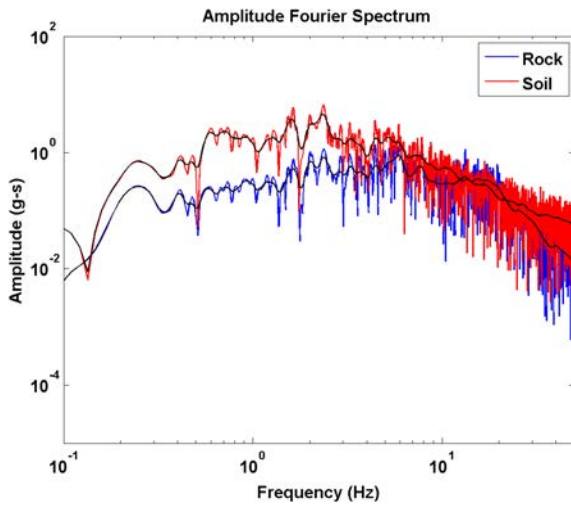
a) PGA values on rock: 0.001 g (1 gals)



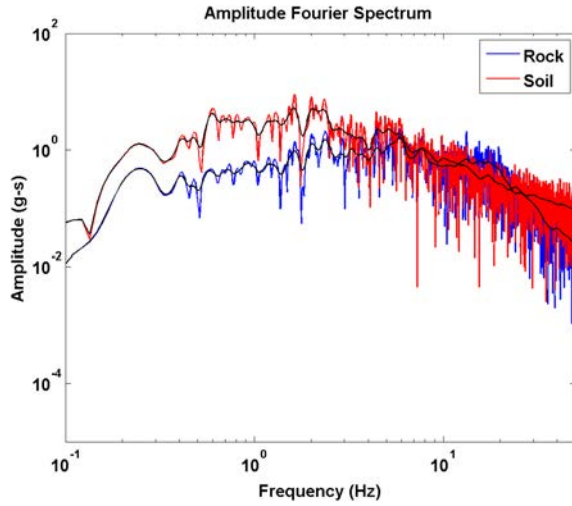
b) PGA values on rock: 0.01 g (10 gals)



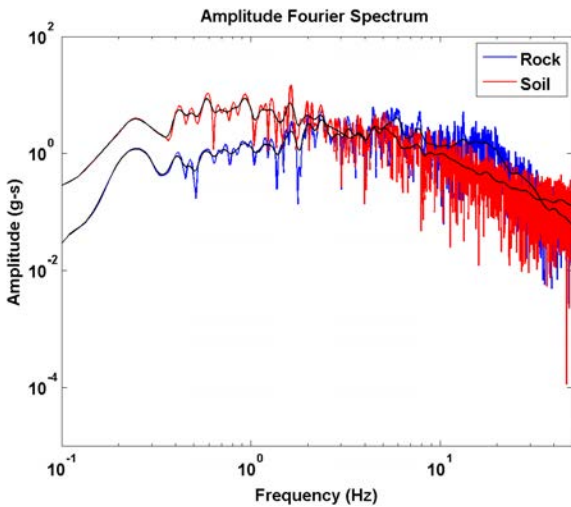
c) PGA values on rock: 0.1 g (100 gals)



d) PGA values on rock: 0.2 g (200 gals)



e) PGA values on rock: 0.5 g (500 gals)



f) PGA values on rock: 1.0 g (1000 gals)

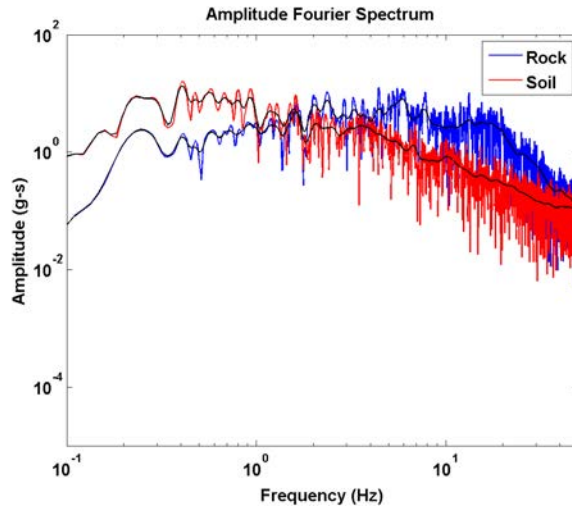


Figure 37. a) RSN809\_LOMAP\_UC2000 Fourier amplitude spectra scaled to a PGA values on rock: a) 0.001 g, b) 0.01 g, c) 0.1 g, d) 0.2 g, e) 0.5 g, f) 1.0 g, for rock at depth at station TST\_196 (blue) and on soil at station TST\_0 at the surface (red).

Konno and Ohmachi (1998) smoothing is applied to the Fourier Spectra and Transfer Functions. The Konno and Ohmachi (1998) smoothing function is defined by the following expression:

$$W_B(f, f_c) = \frac{\sin\left(\left(\log_{10}\left(\frac{f}{f_c}\right)\right)^b\right)}{\left(\left(\log_{10}\left(\frac{f}{f_c}\right)\right)\right)^b},$$

Where,

$f$  is the frequency.

$f_c$  is the central frequency where the smoothing is performed.

$b$  is the bandwidth coefficient.

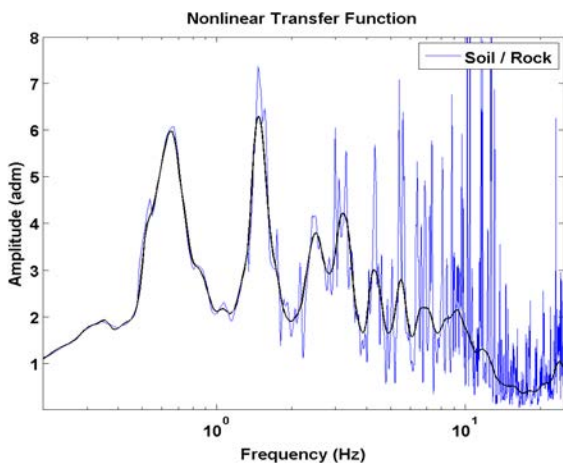
This smoothing function is recommended for analysis in the frequency domain because it ensures a constant number points at low and high frequency.

The bandwidth of the smoothing function is constant in a logarithmic scale. A small value of  $b$  will lead to a strong smoothing, while a large value of  $b$  will lead to a low smoothing of the Fourier spectra.

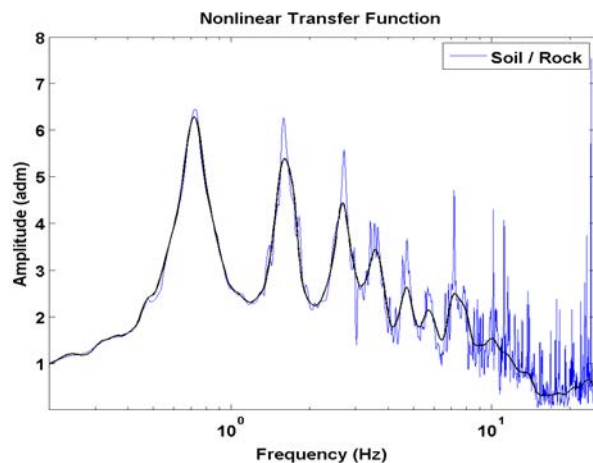
The transfer functions from rock to soil in the Fourier domain correspond to the ratios between the Fourier spectra on soil and the Fourier spectra on rock (Figure 37).

$$TF(f) = |X(f)_{Soil}| / |X(f)_{Rock}|$$

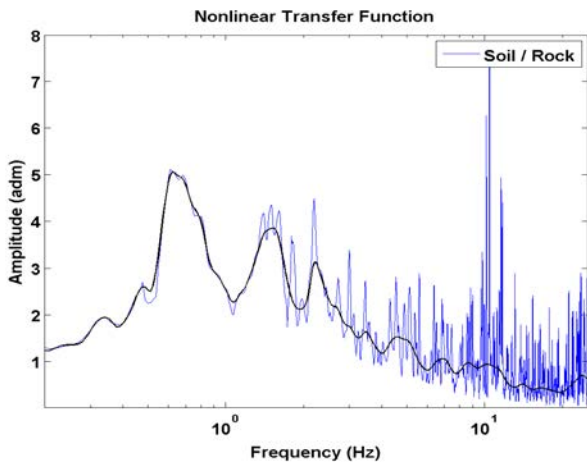
a) PGA values on rock: 0.001 g (1 gals)



b) PGA values on rock: 0.01 g (10 gals)



c) PGA values on rock: 0.1 g (100 gals)



d) PGA values on rock: 0.2 g (200 gals)

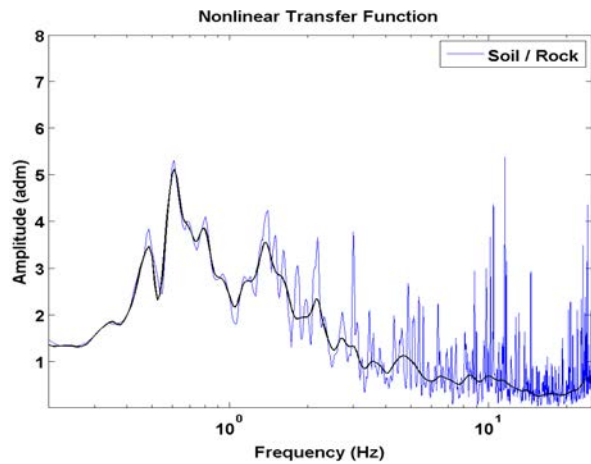
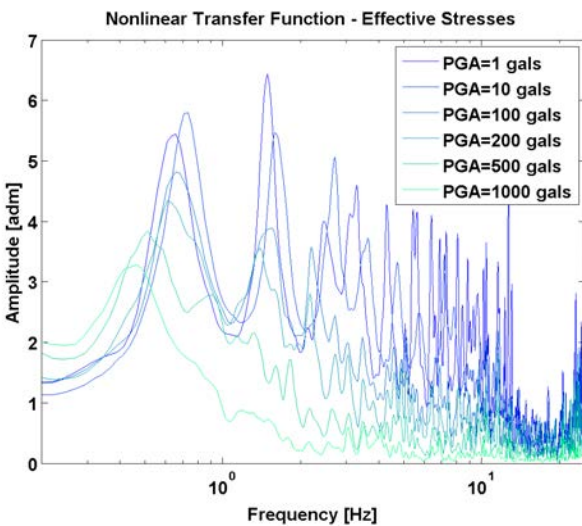


Figure 37 a) RSN809\_LOMAP\_UC2000 Transfer Function for scale records to PGA values on rock: a) 0.001 g, b) 0.01 g, c) 0.1 g, d) 0.2 g, e) 0.5 g, f) 1.0 g. Raw (blue), smooth (black).

The nonlinearity and de-amplification effect of the soil as a function of the acceleration level can be clearly perceived in Figure 38, where the transfer function decreases when larger PGA values are considered. The transfer function is divided by two at the fundamental frequency, considering PGA levels from 0.001 g to 1.0 g.

a)



b)

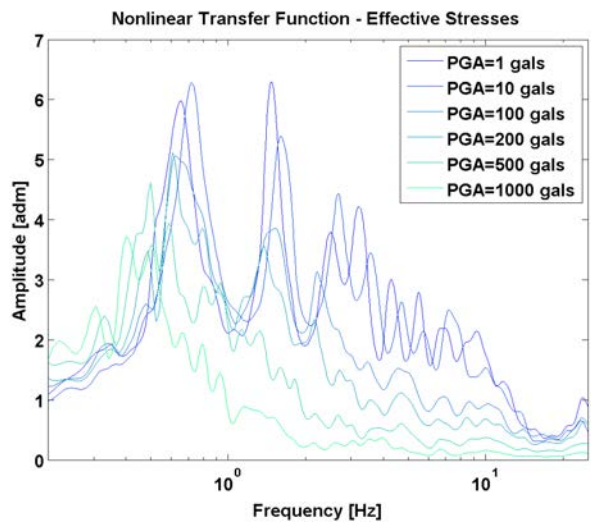


Figure 38. a) Raw Transfer Functions at the Fourier domain, for each of the 6 scaled acceleration records to different acceleration levels b) Smoothed Transfer Functions at the Fourier domain, for each of the 6 scaled acceleration records to different acceleration levels.

Now, accelerograms fitting the 5000 years return period uniform hazard spectrum must be selected to perform the nonlinear site response analysis.

The option to consider several accelerograms fitting the uniform hazard spectrum allows to take into account the record-to-record variability of the non-linear site response, and to compare it with the variability of site response as a function of the site pga: the non-linear

response leads to significantly larger (and systematic) changes compared to the "aleatory" variability of the site amplification factor associated to changes in the input waveforms.

The PEER Strong Motion Database is used to obtain 10 accelerograms fitting the UHS at 5000 years return period (Figure 39). Other databases, as well as other fitting technique, could be used. Both horizontal components are used to define the mean transfer function at the Euroseistest site.

#### **3.4.4.2 Overall methodology**

The overall methodology to obtain surface site-specific spectra with a numerical estimation of the site amplification, is described below, together with a reference to the figures illustrating the example application to Euroseistest, that will be commented in more detail in the next sections.

- 1) Calculate the single-station sigma uniform hazard spectrum for the desired return period and the selected GMPEs, in this case, the 5000 years return period and AA14.
- 2) Apply the  $V_s$ - $k$  scaling factors (Figure 25).
- 3) Select the accelerograms by fitting the 5000 years uniform hazard spectrum including  $v_s$ - $k$  correction and single stations sigma, using an appropriate fitting tool. Here the PEER Strong Motion Database is used to obtain accelerograms with its corresponding scaling factors (Table 13). The average amplification factors are very weakly sensitive to the selection procedure, provided the overall frequency content is correctly matched.
- 4) Adapt the selected accelerograms recorded at the surface to accelerograms at depth, by removing the free field effect. In the present application and with the 1D site response code used, this correction is performed by dividing all the acceleration records by a factor of 2, and setting "elastic" boundary conditions at the base of the soil column. It is recommended NEVER to use deconvolution procedures to impose "within motion" at depth.
- 5) Perform the nonlinear wave propagation for each accelerogram using a linear and nonlinear wave propagation code. Here NOAH is selected (Nonlinear Anelastic Hysteretic finite difference code - L.F. Bonilla).
- 6) Plot the acceleration time series on rock (from the PEER database) and at site surface (output from NOAH after performing wave propagation). Figure 40 shows some acceleration records used to derive the linear transfer function (linear case), while Figure 41 shows acceleration records for the nonlinear case.
- 7) Calculate the Fourier amplitude spectra for each accelerogram on rock at depth and on soil at the surface and apply Konno and Ohmachi 1998 smoothing, for both the linear and nonlinear cases (Figure 42 and Figure 43).
- 8) Compute the linear and nonlinear rock to soil transfer functions for each event, and apply Konno and Ohmachi 1998 smoothing, for both linear and nonlinear cases (Figure 44 and Figure 45).
- 9) In the same graph, plot all raw transfer functions for both, linear and nonlinear cases, Figure 46 and Figure 47. Repeat this step, but with the smoother transfer functions, Figure 48 and Figure 49.
- 10) Obtain the mean and its corresponding standard deviation of all the calculated smoothed transfer functions, for both, linear and nonlinear cases, Figure 48 and Figure 49.

- 11) Invert via random vibration theory using Strata (Kottke and Rathje, 2008a,b) or any other tool, the  $V_s$ -kappa corrected 5000 years uniform hazard spectrum, to obtain the compatible Fourier Amplitude Spectra.
- 12) Multiply the  $V_s$ -kappa corrected 5000 years Fourier Amplitude Spectrum by the mean and the 16% and 84% percentiles Transfer Function, to obtain the Fourier Amplitude on Soil.
- 13) Invert one more time from the Fourier domain to the time domain the soil amplitude Fourier Spectras via Strata (Kottke and Rathje, 2008a,b) to finally obtain the compatible response spectra on soil using a linear and nonlinear transfer function, Figure 50.

### **3.4.4.3 Application to Euroseistest**

#### **3.4.4.3.1 Selection of input accelerograms**

To derive the linear and nonlinear transfer functions numerically using NOAH, the first step consists in the selection of ground-motion records that will be used as incident motions at the bottom of the basin.

The uniform hazard spectrum considered is the UHS for 5000 years return period, calculated with single-station sigma and host-to-target adjustments. Host-to-target adjustments are required since the input motion is placed at TST\_196 at depth (very hard rock,  $V_s = 2600 \text{ m/s}$ ).

Here the effect at depth of destructive interferences is considered inside the 1D wave propagation on the code. The free field effect of the UHS must be removed, by dividing the input acceleration records at depth by a factor of 2.

Figure 39 shows the target uniform hazard spectrum (red) using single-station sigma after applying host-to-target correction, superimposed to the response spectra of the 10 selected acceleration records (light gray), as well as mean  $\pm$  standard deviation (black solid line and dashed lines).

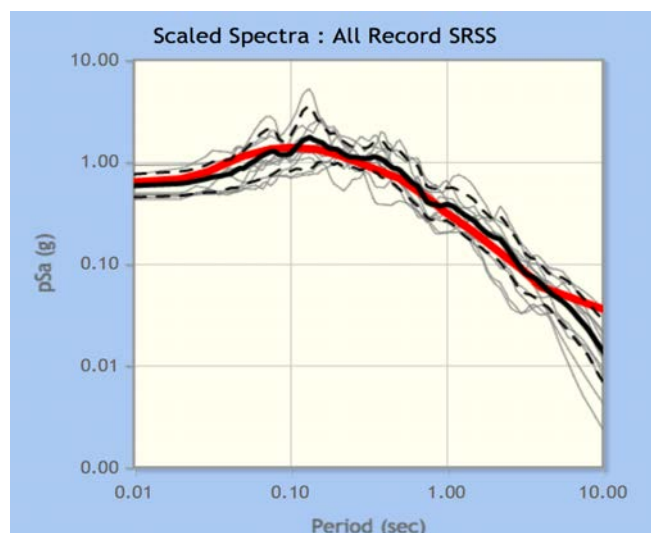


Figure 39. Selected Records fitting the 5000 years return period, uniform hazard spectra using single station sigma and host to target adjustments at the Euroseistest.

Table 13 lists the selected records with some basic information and the corresponding scaling factors

Table 13. Summary of Metadata of Selected Records fitting the 5000 years return period uniform hazard spectra at the Euroseistest (PEEER database).

EQ	SF	D 5-95% (s)	Earthquake Name	Year	Station Name	Magnitude	Rjb (km)	Vs30 (m/s)
1	1.44	9.0	Loma Prieta	1989	UCSC	6.93	12.15	714
2	1.08	9.7	Loma Prieta	1989	UCSC Lick Observatory	6.93	12.04	714
3	2.34	8.3	Northridge-01	1994	Vasquez Rocks Park	6.69	23.10	996
4	0.79	11.3	Chi-Chi Taiwan	1999	TCU045	7.62	26.00	705
5	0.58	29.1	Manjil Iran	1990	Abbar	7.37	12.55	724
6	1.11	11.7	Hector Mine	1999	Hector	7.13	10.35	726
7	2.68	19.6	Tottori Japan	2000	OKYH07	6.61	15.23	940
8	1.75	17.3	Tottori Japan	2000	OKYH14	6.61	26.51	710
9	1.69	12.8	Tottori Japan	2000	SMNH10	6.61	15.58	967
10	1.18	22.6	Iwate Japan	2008	IWT010	6.9	16.26	826

\*EQ (Earthquake number), SF (Scale Factor), D (Duration).

#### 3.4.4.3.2 Non-lienar 1D simulations

The first step consists in calculating the acceleration records at the surface, implying that accelerograms have been scaled, filtered and the free field has been removed.

Figure 40 shows the acceleration records on rock (blue) and on soil (red) for the linear case. The acceleration records used for the linear case are the same as in the nonlinear case, but scaled by a factor of 1/1000 to have small values of acceleration.

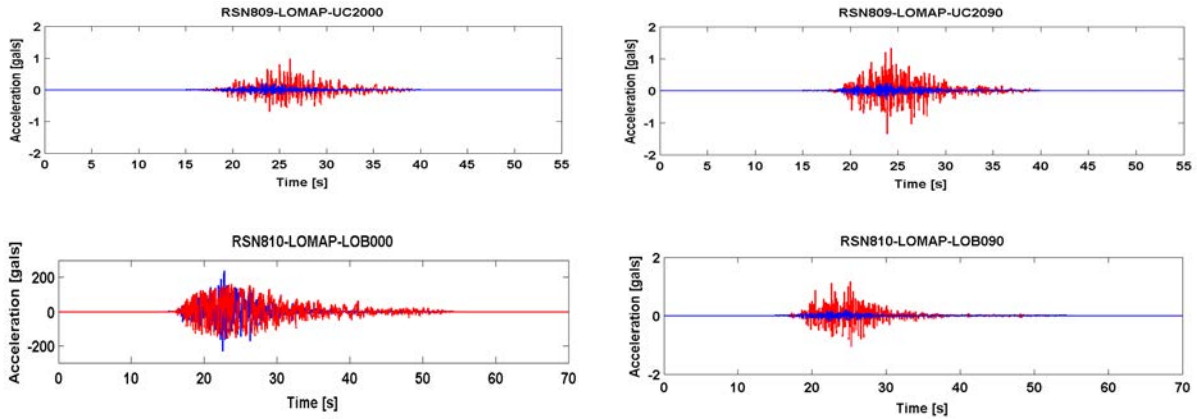


Figure 40. Linear case: Acceleration records on rock from the PEER database (blue) and on soil at the surface obtained after performing wave propagation with NOAH (red). The other accelerograms are displayed in Appendix B

Looking at the graphs on Figure 40 the amplification effect is clear, the peak ground-motion acceleration on soil is much larger than the peak ground acceleration on soil for all cases.

Likewise Figure 41 shows the soil and rock acceleration records, but this time for those fitting the 5000 years return period. In this case, the de-amplification effect of the soil can be observed : the acceleration on soil is not always larger than on rock, and the peak ground motion on rock at depth and on soil at the surface are in many cases very similar.

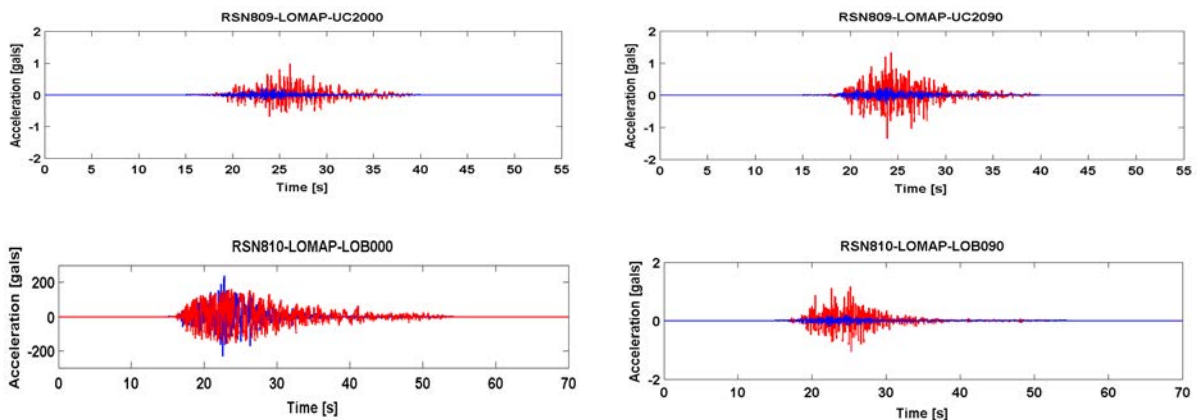


Figure 41. Nonlinear case: Acceleration records on rock from the PEER database (blue) and at the surface obtained after performing wave propagation with NOAH (red). The other accelerograms are displayed in Appendix B.

Once extracted the accelerograms in rock and soil, the next step will be to compute the Fourier Amplitude Spectra for each acceleration record on soil and rock (Figure 42 and Figure 43).

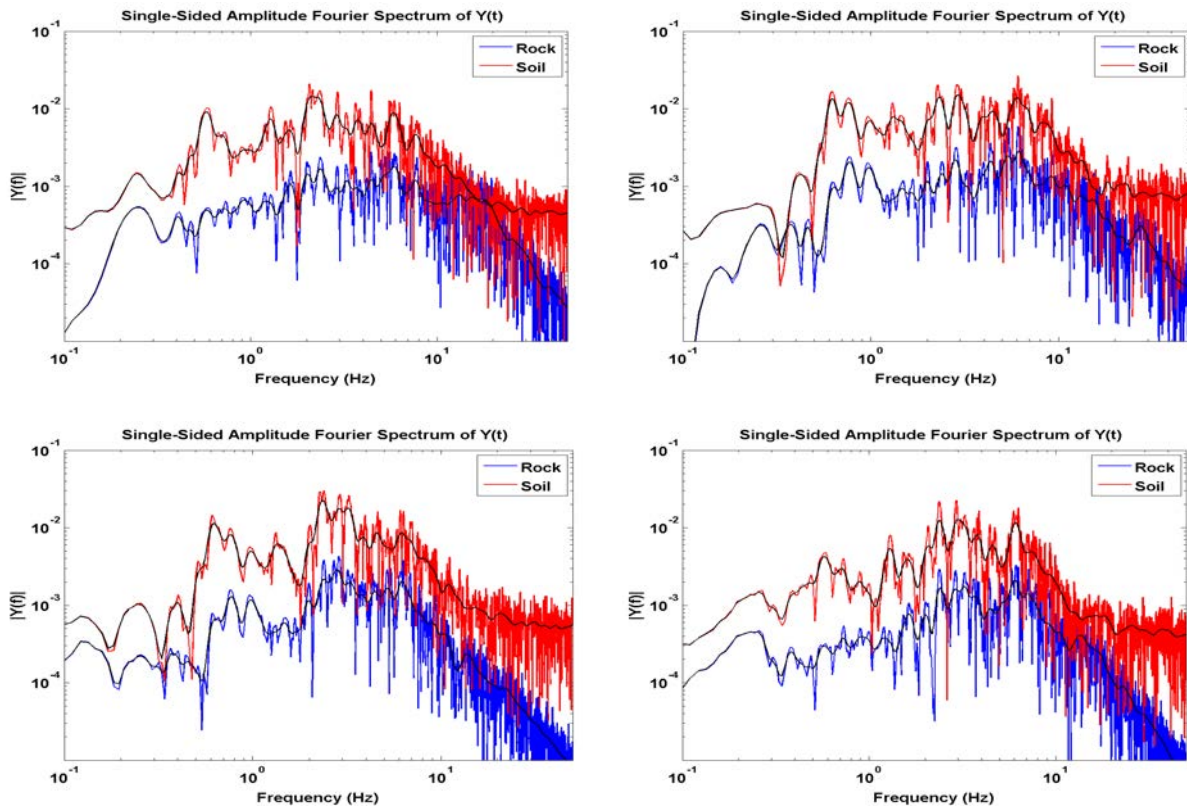
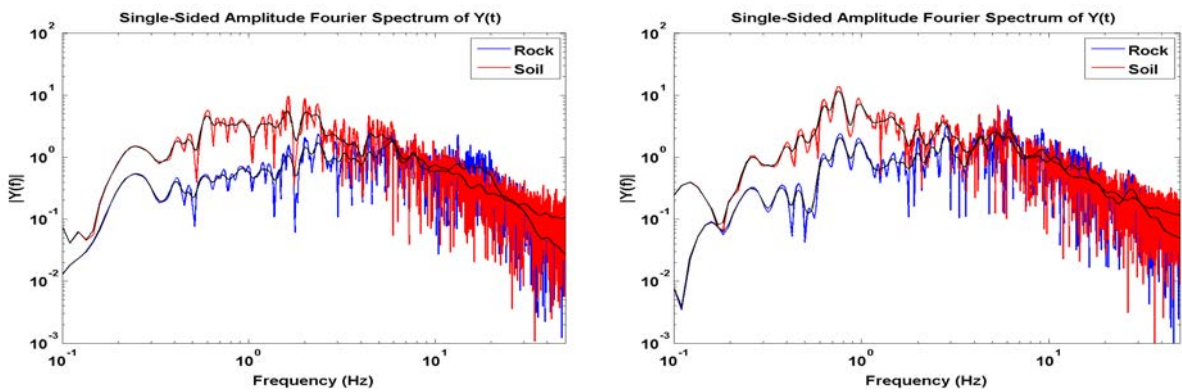


Figure 42. Linear case: Amplitude Fourier Spectras on rock (blue) and at soil (red) for each one of the considered acceleration records. The additional Fourier Amplitude Spectra's corresponding to the ten selected accelerograms and both horizontal components are provided in Appendix B.



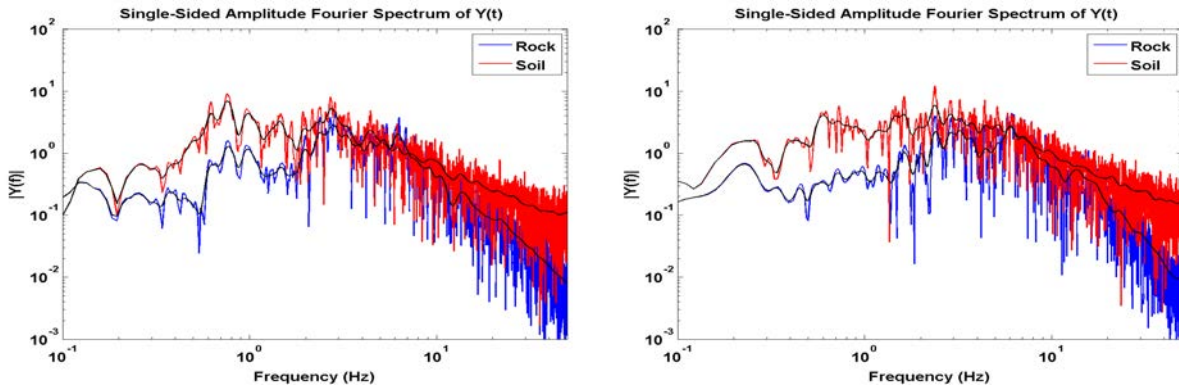


Figure 43. Nonlinear case: Amplitude Fourier Spectras on rock (blue) and at soil (red) for each one of the considered acceleration records. The additional Fourier Amplitude Spectra's corresponding to the ten selected accelerograms and both horizontal components are provided in Appendix B.

### 3.4.4.3.3 Fourier Transfer functions

The following step consists in deriving the transfer functions, by dividing the Fourier Amplitude Spectrum on soil at the surface, by the Fourier Amplitude Spectrum on rock at the bottom of the basin (Figure 44 and Figure 45).

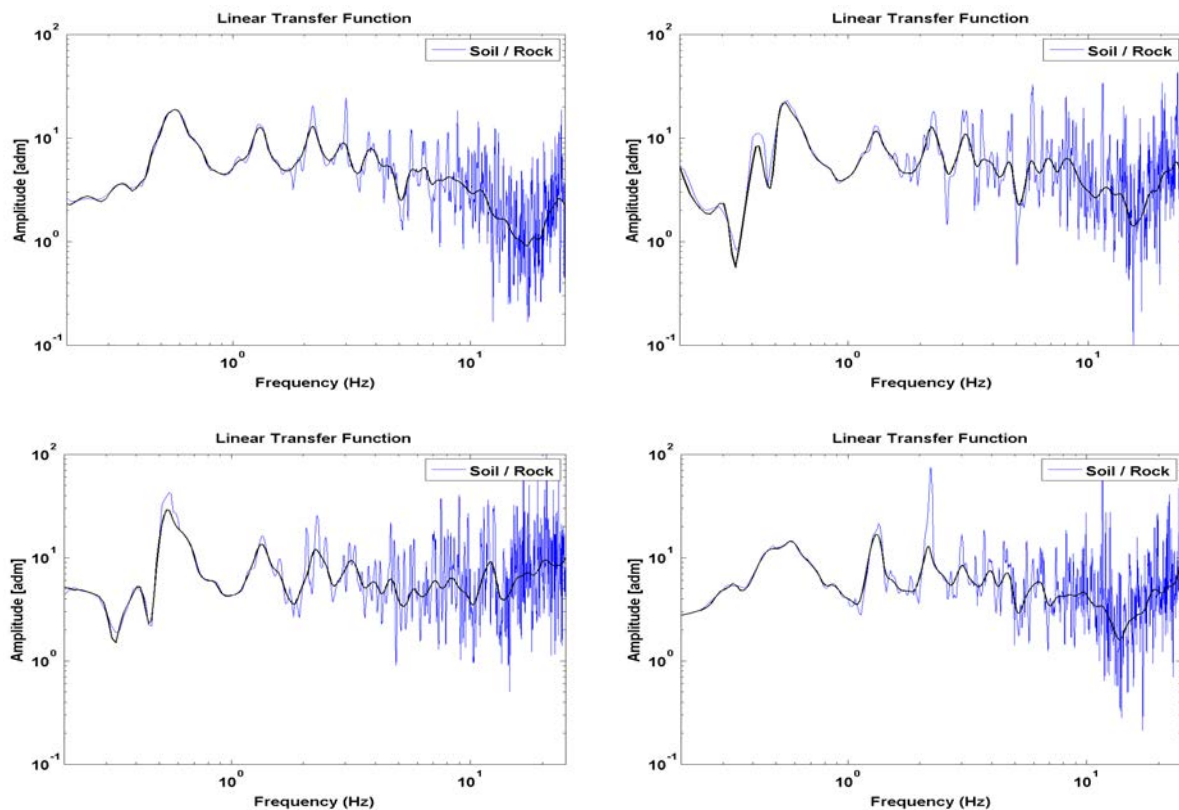


Figure 44. Linear case: Fourier domain transfer functions soil/outcropping rock for the considered acceleration records. Blue lines correspond to raw transfer function, black lines to smoothed one. The other transfer functions are displayed in Appendix B.

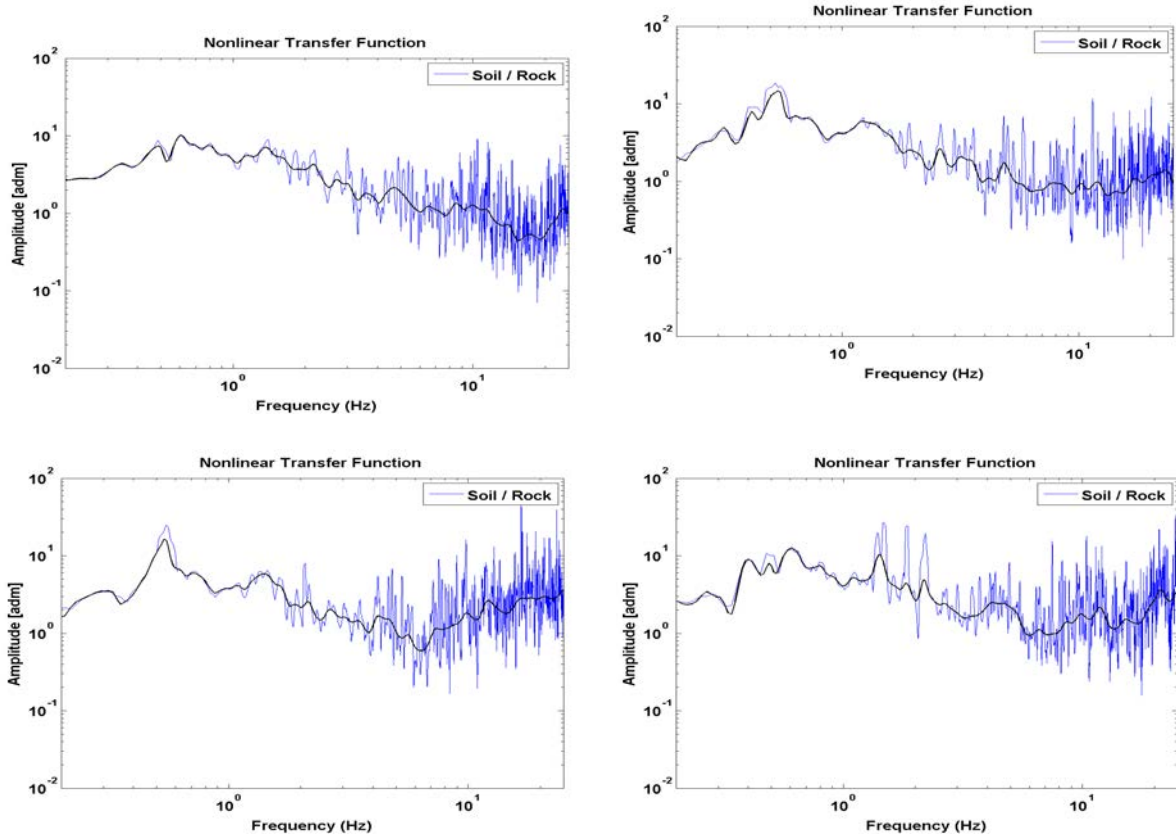


Figure 45. Nonlinear case Fourier domain transfer functions soil/outcropping rock for the considered acceleration records. Blue lines correspond to raw transfer function, black lines to smoothed one. The other transfer functions are displayed in Appendix B.

Figure 46 and Figure 47 show the raw (unsmoothed) transfer functions for the linear and nonlinear cases respectively.

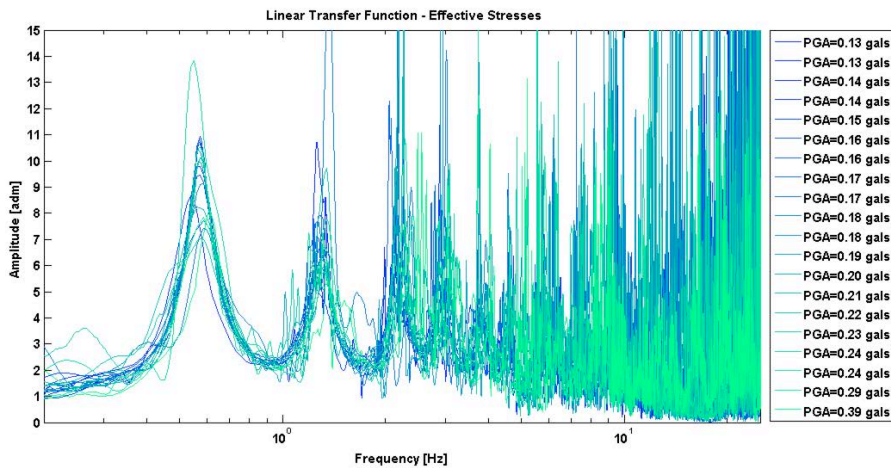


Figure 46. Linear Case: Transfer Functions in the Fourier domain for the 10 selected acceleration records and both horizontal components.

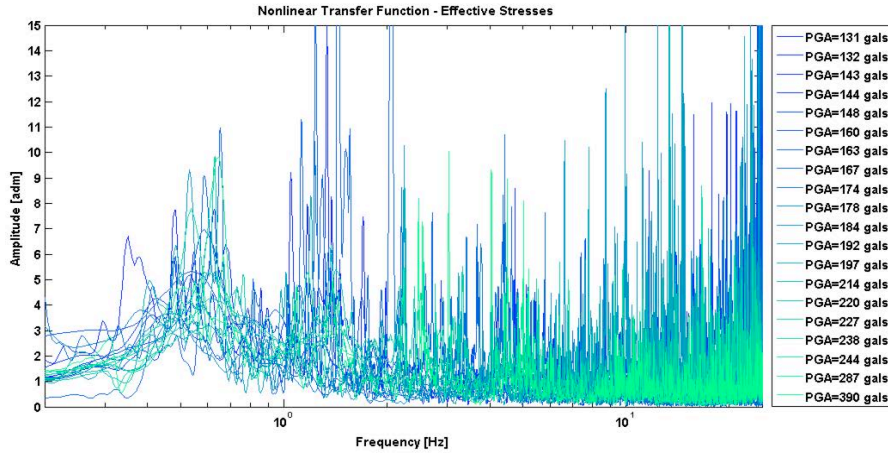


Figure 47. Nonlinear Transfer Functions in the Fourier domain for the 10 selected acceleration records and both horizontal components.

After calculating the transfer functions in the linear (Figure 46) and nonlinear (Figure 47) cases, Konno and Ohmachi 1998 smoothing is applied and the mean and standard deviation of the transfer functions can be calculated.

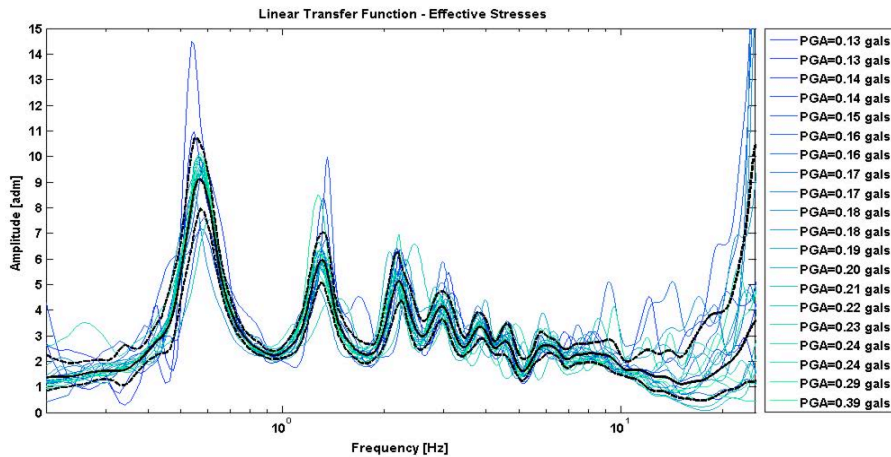


Figure 48. Smoothed Linear Transfer Functions in the Fourier domain for the 10 selected acceleration records and both horizontal components.

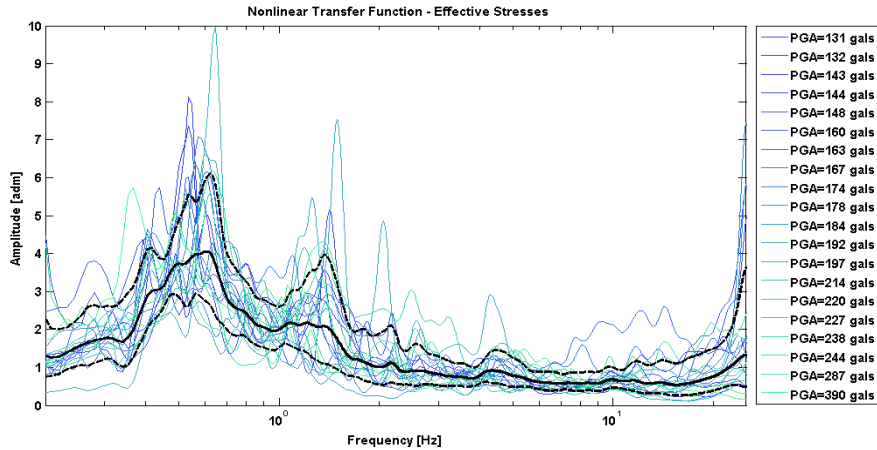


Figure 49. Smoothed Nonlinear Transfer Functions in the Fourier domain for the 10 selected acceleration records and both horizontal components.

The next step consists in applying the linear and nonlinear mean transfer function to the reference rock Fourier spectra (i.e., the Fourier spectra corresponding to single station sigma vs-kappa corrected 5000 years), and then transforming into response spectra via random vibration theory (RVT).

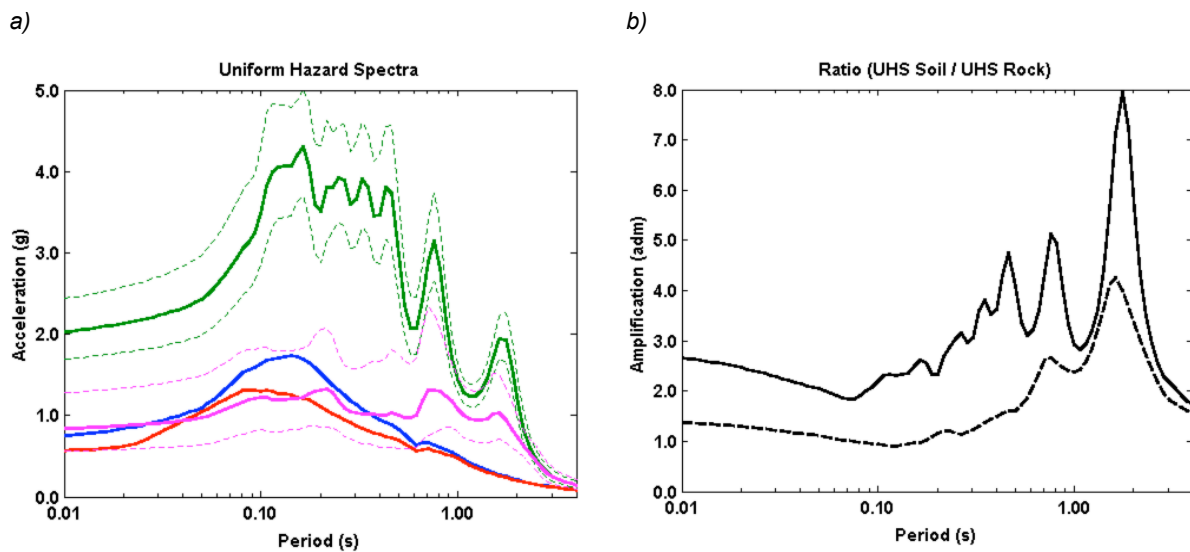


Figure 50. AA14 uniform hazard spectrum for 5000 years return period: **a) Level 1a - Rock:** Single-station sigma (blue), **Level 1b - Rock:** Single-station sigma, host-to-target adjustments, (red), **Level 1c – Soil Linear-htt:** Single-station sigma, host-to-target adjustments, linear transfer function  $\pm$  stdv (dark green), **Level 2a – Soil Nonlinear-htt:** Single-station sigma, host-to-target adjustments, nonlinear transfer function  $\pm$  stdv (magenta). **b)** Ratio between soil and rock UHS spectra in the linear (solid black line, = green PSA / red PSA), and non-linear (dashed line, = magenta PSA / red PSA).

Figure 50a displays the uniform hazard spectra after applying the different linear and nonlinear transfer function. The Vs-Kappa effect (i.e., host-to-target adjustments) is found for this particular case – to have a significantly lower impact than the considered behaviour for the soil, linear or non-linear.

### 3.5 COMPARISON OF ALL APPROACHES, CONCLUSIONS AND RECOMMENDATIONS

#### 3.5.1 Overall comparison

An overview of the results obtained at Euroseistest site with the different methods is presented in Figure 56. The UHS obtained from generic or partially site specific approaches, Level 0 and Level 0.5 are shown, as well as from the site-specific approaches (Level, 1a, 1b, 1c and 2a). Some specific comparisons are detailed in Figures 51 through 55, for an easier understanding.

Figure 51 focuses on the "generic" (levels 0 and 0.5) spectra for "standard" rock and soil, with full aleatory variability sigma. For the particular TST0 site, the consideration of SAPE accounting for both  $f_0$  and  $V_{S30}$ , leads to larger values, especially around the fundamental frequency  $f_0$ , than the consideration of recent GMPEs. The reasons are two-fold: a) the absence of NL behaviour in the considered SAPE, while the GMPE considered here (AA14) does take it into account (this is the main reason for the short period differences) ; b) low  $f_0$  and low  $V_{S30}$  lead, on this specific example, to larger (linear) amplification than simply low  $V_{S30}$  (main reason at longer periods, where NL effects are not expected to be significant)

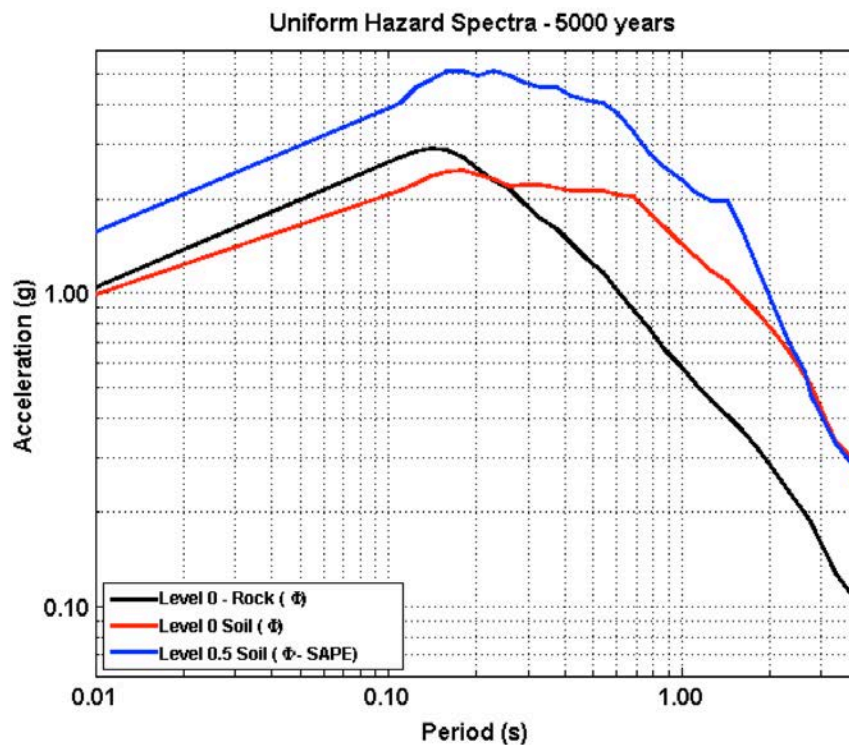


Figure 51. AA14 uniform hazard spectrum for 5000 years return period. Generic or partially site specific Approaches: Level 0 – Standard Rock ( $\phi$ ): Full sigma and  $V_{S30} = 800$  m/s (black), Level 0 – Soil ( $\phi$ ): Full sigma,  $V_{S30} = 186$  m/s (red), Level 0.5 - Soil ( $\phi$ , SAPE): Full sigma, SAPE ( $V_{S30}$ ,  $f_0$ ) (blue).

Figure 52 compares all the rock spectra obtained with different values of the within-event variability (full or single-station sigma), with or without host-to-target adjustments (standard rock or hard, less attenuating rock), with or without depth correction factors (outcropping motion at surface or within motion at depth). At short period, the largest hazard reduction are associated with the reduction of the within-event variability ("single-site-sigma" effect, close to a factor of 2), and to the "within" motion effect (*to be used only when the site-specific amplification is measured or computed with respect to the motion at depth*). The reductions are smaller a longer periods (say,  $T \geq 1$  s), except when considering the within motion and one particular approach (Cadet et al., 2011a) to estimate the depth-correction effect, because of the specificity of the site with a destructive interference effect at 0.7 Hz. Finally, it is also worth mentioning that the "HTT" adjustment has only limited effects despite the large velocity at depth, mainly because of the  $\kappa$  correction which "boosts" the short periods. There are some indications that this peculiar effect is deeply correlated with the current " $V_{S30}$ -  $\kappa$ " HTT approach and the underlying assumptions (stochastic modelling with  $V_s$  effects accounted for through impedance effects only, possible bias in  $\kappa$  measurements), and that other approaches using GMPEs specifically established for hard-rock sites (Laurendeau et al., 2015) would lead to larger reductions, in particular at short periods. The presently used HTT adjustment techniques are likely to be significantly conservative.

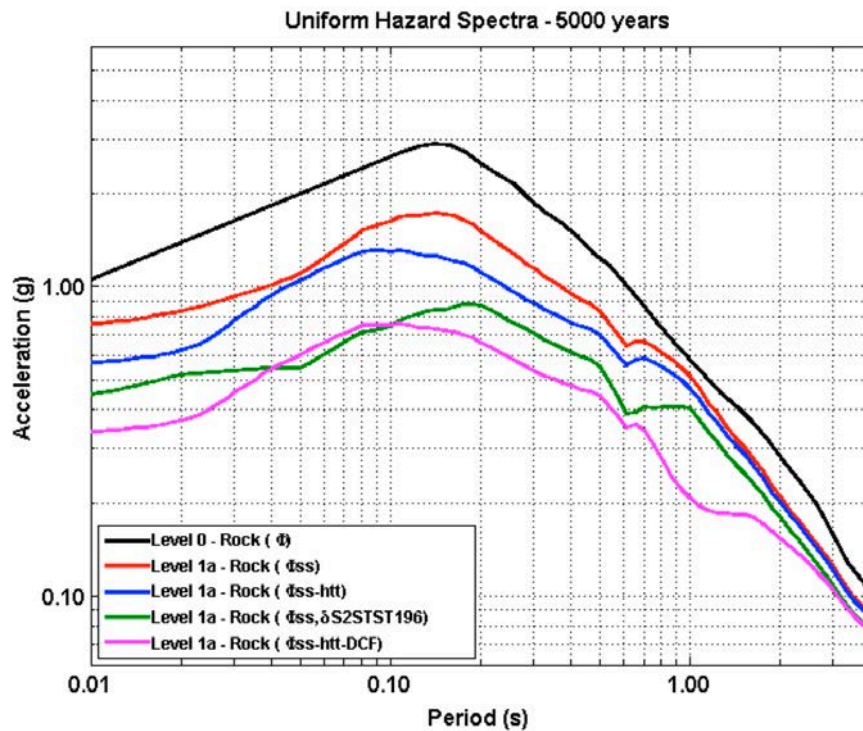


Figure 52. AA14 uniform hazard spectrum for 5000 years return period. Site specific Approaches: Level 0 – Standard Rock ( $\phi$ ): Full sigma and  $V_{S30} = 800$  m/s (black), Level 1a – Rock ( $\phi_{ss}$ ): Single station sigma and  $V_{S30} = 800$  m/s (red), Level 1a – Hard Rock ( $\phi_{ss}, htt$ ): Single station sigma,  $V_{S30} = 800$  m/s, host to target adjustments (blue), Level 1a – Hard Rock ( $\phi_{ss}, \delta S2S TST_{196}$ ): Single station sigma,  $V_{S30} = 800$  m/s,  $\delta S2S TST_{196}$  WOST (dark green), Level 1a – Hard Rock ( $\phi_{ss}, htt, DCF$ ): Single station sigma,  $V_{S30} = 800$  m/s, host to target adjustments, depth correction factors (magenta).

Figure 53 displays all the results obtained with site-specific estimates of the site *linear* response (level 1), together with the corresponding reference rock spectra (single site sigma estimates, with or without HTTA, outcropping or within motion). The variability of the results is quite significant in the short period range (a factor of 3), but is the largest (up to factor of 4) at intermediate periods, especially around and below the site fundamental period (1.5 s). The origin of this intermediate period variability is two-fold: the way the reference motion is defined (with or without HTT, outcropping or within), and the way the linear site amplification is estimated: numerical or instrumental, and for the instrumental estimates, the way it has been derived (SSR with respect to an outcropping "standard" rock, or  $\Delta(\delta S2S_s)$ ). One should also keep in mind that some variability is associated to instrumental or numerical estimates (mainly aleatory in the first case, and mainly epistemic in the second): it was not taken into account here, but the literature shows it corresponds at least to a factor  $\pm 50\%$ .

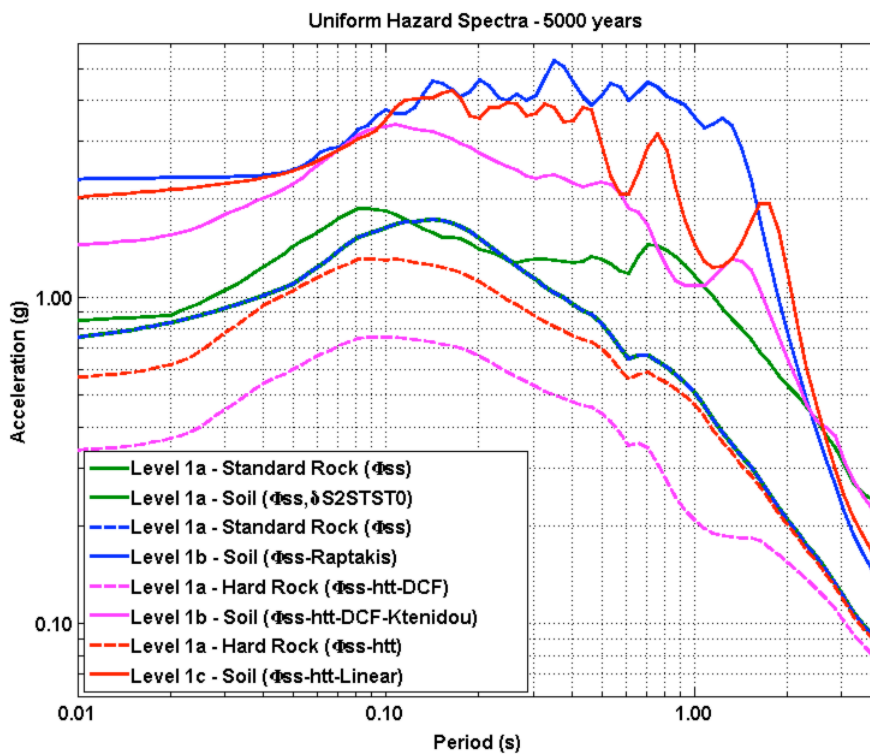


Figure 53. AA14 uniform hazard spectrum for 5000 years return period. Site specific Approaches – Level 1: Level 1a – Standard Rock ( $\phi_{ss}$ ): Single station sigma and  $V_{S30} = 800$  m/s (dark green dashed), Level 1a – Soil ( $\phi_{ss}, \delta S2S TST_0$ ): Single station sigma,  $V_{S30} = 186$  m/s,  $\delta S2S TST_0$  WIST (dark green continuous), Level 1a – Standard Rock ( $\phi_{ss}$ ): Single station sigma and  $V_{S30} = 800$  m/s (blue dashed), Level 1b – Soil ( $\phi_{ss}, Raptakis$ ): Single station sigma,  $V_{S30} = 800$  m/s, Raptakis et al. 1998 transfer function (blue continuous), Level 1a – Hard Rock ( $\phi_{ss}, htt, DCF$ ): Single station sigma,  $V_{S30} = 800$  m/s, host to target adjustments, depth correction factors (DCF), (magenta dashed), Level 1b – Soil ( $\phi_{ss}, htt, DCF, Ktenidou$ ): Single station sigma,  $V_{S30} = 800$  m/s, host to target adjustments, depth correction factors (DCF), Ktenidou et al. 2015 transfer function (magenta continuous), Level 1a – Hard Rock ( $\phi_{ss}, htt$ ): Single station sigma,  $V_{S30} = 800$  m/s, host to target adjustments (red dashed), Level 1c – Soil ( $\phi_{ss}, htt, Linear$ ): Single station sigma,  $V_{S30} = 800$  m/s, host to target adjustments, linear transfer function NOAH (red continuous).

Figure 54 focuses on the results of the level 2 approach (non-linear site response), leading to much lower surface spectra, especially at short periods. This reduction is typically the effect of non-linear site response. As repeatedly shown in the benchmarking exercises of recent years (Stewart et al., 2008; Kwok et al., 2008; Stewart & Kwok, 2009; Régnier et al., 2015a,b; 2016), numerical estimates of non-linear site response are associated with a significant amount of epistemic uncertainty, which increases with the input motion level. The code-to-code variability estimates observed by Régnier et al., 2016b – for similar non-linear parameters – are around 40-50% for input acceleration levels around 0.5 g. Such a variability should be considered in the present estimates (see the discussion below in section 3.5.2).

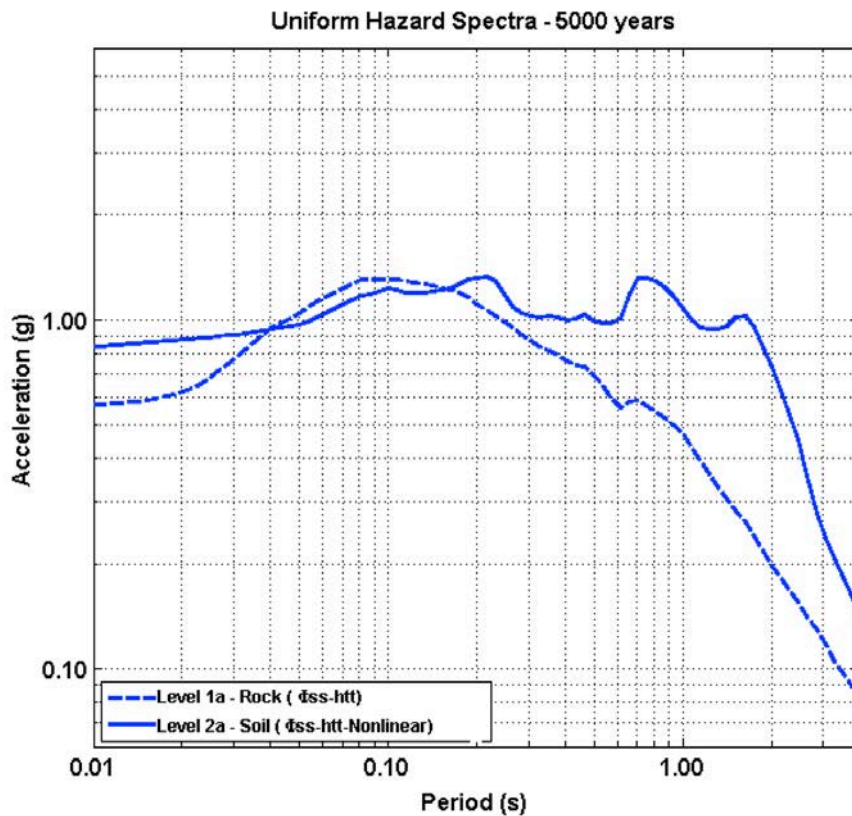


Figure 54. AA14 uniform hazard spectrum for 5000 years return period. Site specific Approaches – Level 2: Level 1a – Rock ( $\phi_{ss}, htt$ ): Single station sigma, host to target adjustments,  $V_{S30} = 2600$  m/s (blue dashed), Level 2a – Soil ( $\phi_{ss}, htt, Nonlinear$ ): Single station sigma, host to target adjustments, nonlinear transfer function NOAH,  $V_{S30} = 186$  m/s (blue continuous).

Figure 55 compares all the results (levels 0, 1 and 2) in terms of soil surface spectra only. Even without taking into account the aleatory or epistemic variabilities associated with the estimation of site-specific site response (i.e., soil profile, degradation curves, damping, pore water effects, etc.), the overall variability of the site spectra reaches extreme values around a factor of 3 at short periods (pga values from 0.8 to 2.4 g), 4 to 5 at intermediate periods, and decrease to a factor of 2 at long periods. In the present case of a rather thick and soft soil deposit, linear, site-specific response estimates lead to larger values than the standard level 0 approaches, despite the consideration of single-site sigma: the site amplification is significantly larger than the average one accounted for in GMPEs using generic proxies.

Only the joint consideration of single-site sigma and non-linear site response leads to a reduced hazard; it should not however be generalized to all possible real situations, as it also results from the fact that the present, example case corresponds to a rather high seismicity area, and thick and soft soils with a prominent reduction effect of non-linear soil behaviour.

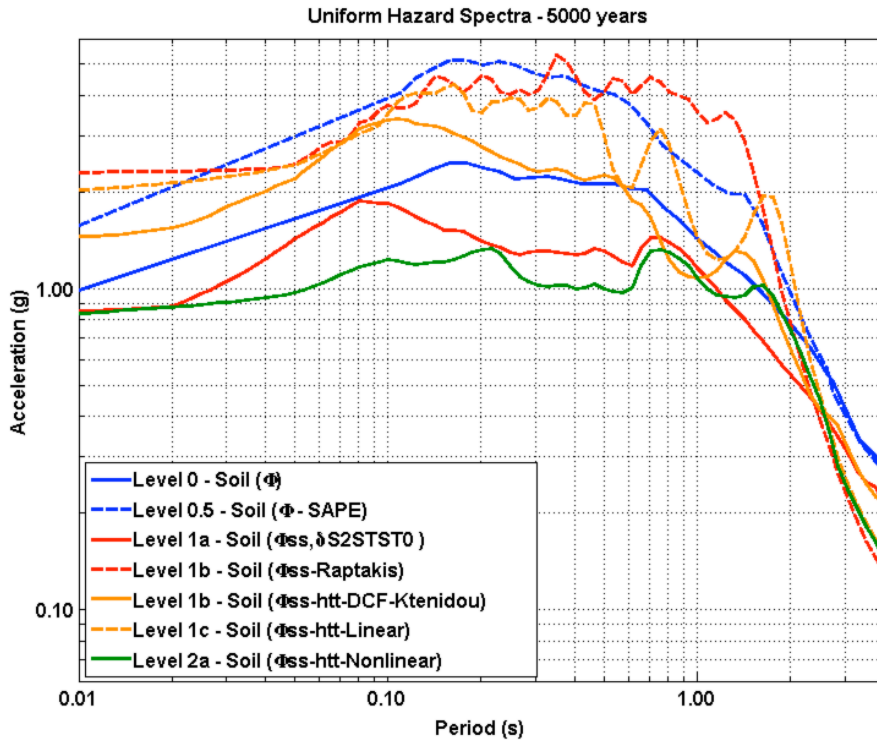


Figure 55. AA14 uniform hazard spectrum for 5000 years return period. All approaches on Soil: Level 0 – Soil ( $\phi$ ): Full sigma,  $V_{S30} = 186$  m/s (blue), Level 0.5 - Soil ( $\phi$ , SAPE): Full sigma, SAPE ( $V_{S30}$ ,  $f_0$ ) (blue dashed), Level 1a – Soil ( $\phi_{SS}$ ,  $\delta S2S$  TST\_0): Single station sigma,  $V_{S30} = 186$  m/s,  $\delta S2S$  TST\_0 WIST, (red), Level 1b – Soil ( $\phi_{SS}$ , Raptakis): Single station sigma,  $V_{S30} = 800$  m/s, Raptakis et al. 1998 transfer function (red dashed), Level 1b – Soil ( $\phi_{SS}$ , htt, DCF, Ktenidou): Single station sigma,  $V_{S30} = 800$  m/s, host to target adjustments, depth correction factors (DCF), Ktenidou et al. 2015 transfer function (yellow), Level 1c – Soil ( $\phi_{SS}$ , htt, Linear): Single station sigma,  $V_{S30} = 800$  m/s, host to target adjustments, NOAH Linear transfer function (yellow dashed), Level 2a – Soil ( $\phi_{SS}$ , htt, Nonlinear): Single station sigma,  $V_{S30} = 800$  m/s, host to target adjustments, NOAH Nonlinear transfer function (dark green)

Figure 56 wraps up all the corresponding rock and soil spectra, again for only one example GMPE, AA14. The rock spectra (black and grey cruves) exhibit a very large variability (up to a factor about 3) especially in the short to intermediate period range ( $T < 1$  s) depending on the value of the aleatory variability (full or single-site sigma), the HHTA correction and the differences between outcropping and within motion. The hazard at soil surface (color curves) exhibits a similar variability (large at short to intermediate periods, i.e., a factor of 3 for periods shorter than the site fundamental period, and reduced below a factor of 2 at longer periods). The larger values correspond to linear amplification, estimated either instrumentally or numerically or with SAPE), while the lowest value corresponds to non-linear simulation on top of (hard-rock,  $V_S$ - $\kappa$  corrected, single-site sigma) hazard. The "Level 0" curve (red) is found to be intermediate between those various values.

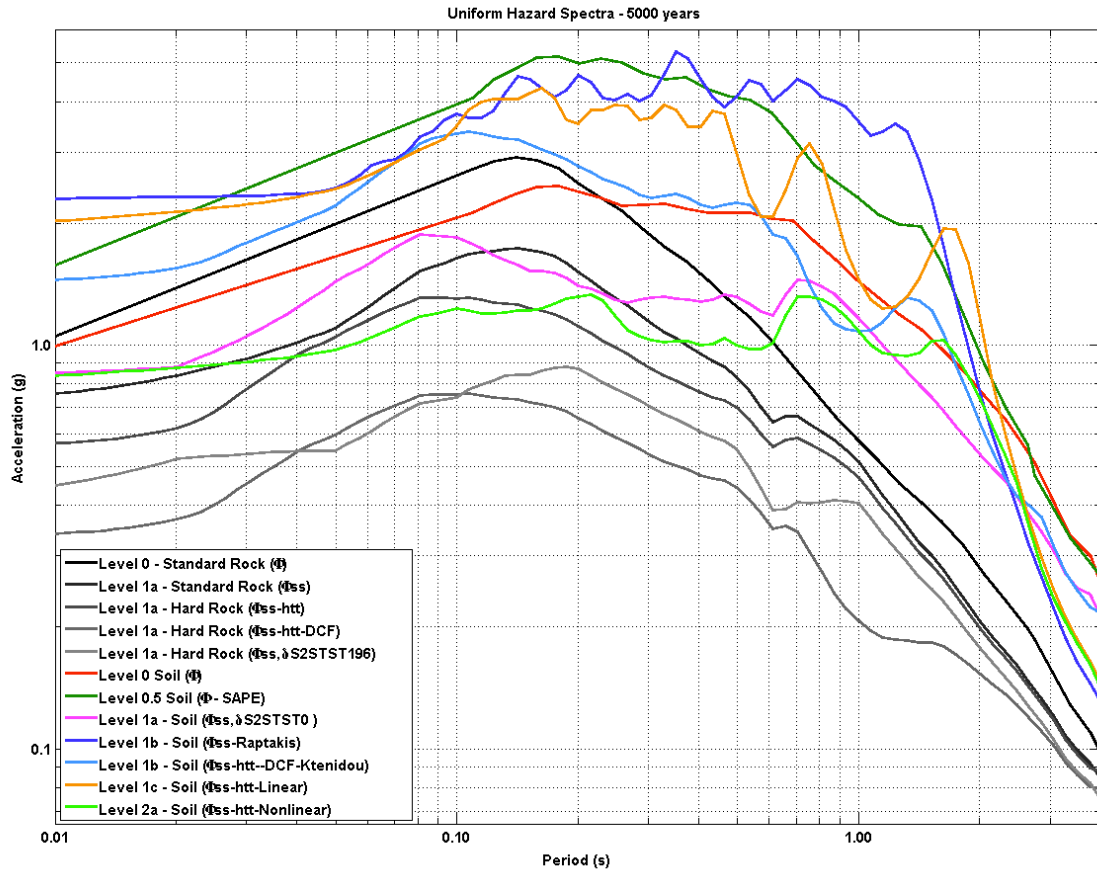


Figure 56. Overall comparison of soil and rock spectra obtained with the various approaches from Level 0 to Level 2a, for the AA14 GMPE and 5000 years return period: Level 0 – Rock ( $\phi$ ): Full sigma and  $V_{S30} = 800$  m/s (black), Level 1a – Rock ( $\phi_{ss}$ ): Single station sigma and  $V_{S30} = 800$  m/s (dark grey), Level 1a – Rock ( $\phi_{ss}, htt$ ): Single station sigma, host to target adjustments,  $V_{S30} = 2600$  m/s (grey), Level 1b – Rock ( $\phi_{ss}, htt, DCF$ ): Single station sigma, htt, DCF,  $V_{S30} = 2600$  m/s (light grey), Level 1b – Rock ( $\phi_{ss}, Raptakis$ ): Single station sigma,  $V_{S30} = 186$  m/s (magenta), Level 0 – Soil ( $\phi$ ): Full sigma,  $V_{S30} = 186$  m/s (red), Level 0.5 - Soil ( $\phi, SAPE$ ): Full sigma, SAPE ( $V_{S30}, f_0$ ), (dark green), Level 1a – Soil ( $\phi_{ss}, \delta S2S TST_0$ ): Single station sigma,  $V_{S30}, \delta S2S TST_0$  (magenta), Level 1b – Soil ( $\phi_{ss}, Raptakis$ ): Single station sigma, Raptakis et al. 1998 transfer function, (dark blue), Level 1b – Soil ( $\phi_{ss}, htt, DCF, Ktenidou$ ): Single station sigma, host to target adjustments, depth correction factors, Ktenidou et al. 2015 transfer function (light blue), Level 1c – Soil ( $\phi_{ss}, htt, Linear TF$ ): Single station sigma, host to target adjustments, linear transfer function NOAH (orange), Level 2a – Soil ( $\phi_{ss}, htt, Nonlinear TF$ ): Single station sigma, host to target adjustments, nonlinear transfer function NOAH (light green).

### 3.5.2 Conclusions and recommendations

Site-specific hazard calculations aim at providing improved hazard estimates at well-characterized sites. Several authors have shown that nonlinearities in site response and the associated uncertainties are important in estimating site-specific hazard (McGuire et al 2001, 2002 and Bazzurro and Cornell, 2004). However, classical PSHA does not capture properly these phenomena, and only the most recent ground-motion prediction equations (such as the NGA-West2) are able to take into account nonlinear behavior, in a very generic and approximate way though.

Several approaches are possible to merge site-specific estimates of site response and rock hazard, corresponding to different sophistication levels and different kinds of epistemic uncertainties. The aim in this first example was to illustrate the application of the various methods listed in section 2, the associated issues, and to compare their results, in order to better appreciate the gains against the required costs and efforts when performing this type of analysis. There are certainly numerous limitations in this single example application, which prevent from drawing too general conclusions and recommendations. We will thus start with listing these limitations and the steps that are still missing and that should be part of a complete application for a critical facility. This limited application proves however helpful and useful in pointing several issues related to the application of the various approaches, and proposing some recommendations for their practical use for real facilities.

#### 3.5.2.1 Euroseistest results : limitations and missing analysis

An exhaustive study for Euroseistest should have also included the following components :

- The repetition of all this work for a collection of acceptable GMPEs (for instance those listed in sections 2.2.1 and 3.3.1) : this does not present technical difficulties, it simply requires a significant time, in particular for HTTA " $V_{S30} - \kappa$ " adjustment procedures which cannot be automatized and require a careful, relatively subjective and time-consuming analysis of host spectra associated to disaggregated scenarios (which are also GMPE dependent, in principle). Also, the selection of accelerograms for NL site response computations should then be GMPE dependent, as the UHS hard-rock spectra are GMPE dependent; however, we do think that the variability of the NL response averaged over 10 input accelerograms remains negligible compared with the GMPE to GMPE variability of rock hazard estimate, and that the recommended practice is to select real accelerograms roughly associated to the dominant scenarios, and to compute once for all the NL site response for this collection of accelerograms scaled to different pga values – following what had been done during the PEGASOS/PRP studies. This latter "belief" still has to be clearly proved, and this is one of the "to-do" things for C. Aristizabal PhD work.
- The consideration of other numerical estimates of the site response. In particular for this site, it has been shown (Maufroy et al., 2015a,b; 2016a,b) that the geometrical effects (2D and 3D) do include significant modifications in the linear site response, which a broader band amplification resulting from a slight increase at the fundamental mode (0.7 Hz) and higher 1D harmonics, and a larger increase in-between in the 1-2 Hz band. These geometrical effects are also associated with a

larger event-to-event variability because of the sensitivity to backazimuth and incident angles, for local events (Maufroy et al., 2015a,b). It does not present major technical difficulties and will be done within the framework of C. Aristizabal's PhD: it should lead to a slight increase of the "Level 1c" results in the period range 0.25 – 1 s, as shown in Figure 8.

- The consideration of epistemic uncertainty on numerical estimates of linear and non-linear site response. This is indeed – in our opinion – the main missing part in this example application, as the consideration of single station sigma should be associated with the accounting of epistemic uncertainty in the site response. The associated uncertainty components are the uncertainty on velocity profiles and damping values (1D linear response, 1DL), complemented with the uncertainty on NL parameters (1D non-linear response, 1DNL), and in case of pronounced 2D or 3D geometry, with the uncertainty on the geometrical characteristics (nDL, nDNL).
  - The site response computations associated with the 1DL case are rather simple and fast, there is basically no code-to-code variability, the main issue is the assessment of the soil profile uncertainties and the generation of the associated profiles. This is commonly done in the US world by generating "randomized profiles" around the "best estimate" profile, through the consideration of vertical correlation lengths and typical standard deviations or coefficient of variations (around 30%) for the velocity estimate at each depth. The tests performed on this approach within the PEGASOS/PRP project showed that many of the so-generated randomized profiles had dispersion curves (DC) well outside the confidence intervals of the dispersion curves measured with MASW (Multichannel Analysis of Surface Waves) or Microtremor array, and that a filter should be applied to keep only those of the randomized profiles corresponding to dispersion curves within the acceptable limits. As another strong criticism to the "randomized profile" US practice is the implicit, and strong, assumption, that the soil is perfectly horizontally layered, and that the random variations are only in the vertical direction, the latter "DC filtering of randomized profiles" is presently the recommended procedure, but it requires the knowledge of such confidence interval for the dispersion curves.
  - The epistemic uncertainty associated to the NL site response (1DNL) includes basically two components. The first one is the code-to-code variability, associated with the variability of NL models and numerical schemes, which has been shown by Régnier et al. (2015a,b and 2016) to reach a factor up to 0.4 (ln scale) for input pga levels around 0.5g. The second one is related to the uncertainties in the measurement of NL parameters. There are only very few, and till now mainly subjective, estimates of such uncertainties, and it is very difficult to give numbers. Several scientists think that the impact of such parameter uncertainties is at least as important as the impact of code-to-code variability. The recommendation is definitely a) to use several codes with different NL constitutive laws and b) to perform a sensitivity analysis around the "best estimate" NL parameters. See item 7 in section 2.3.5 on p. 25.
  - There also exists an epistemic variability associated with the 2D / 3D geometry. This has been thoroughly investigated and quantified on some extensively studied sites such as Euroseistest in the linear case (Maufroy et

al., 2015b, 2016a,b), and never - to our knowledge – in the 2D or 3D NL case. One must be aware that such investigations, to be significant, need to be comprehensive, and require large number of cases and therefore large (or even huge...) high performance computer capacity. This is not affordable for most facilities, especially as it should be associated with detailed geophysical and geotechnical surveys to start constraining the 2D / 3D model. The cost of such sensitivity analysis to fully grasp the actual epistemic uncertainty, exceeds by far the cost of several instruments (probably including vertical arrays) carefully designed to measure directly the site response (see above section 2.3.3).

- Finally, only "mean" site response estimates have been considered in this report, whatever their origin (I;e., instrumental or numerical), while they do exhibit some "aleatory variability". Instrumental (Fourier) SSRs are generally characterized by a standard deviation  $\sigma_{SSR}$  around 0.6 – 0.7 (ln scale), which cumulates the variabilities associated to changes in incident wavefield characteristics (incidence angle, back-azimuth, wavefield composition: body and surface waves, among others); it therefore very probably includes some uncertainties which are considered epistemic in the numerical approach. The origin of aleatory variability in numerical estimates is limited or hidden (for instance 1D site response estimates do not consider obliquely incident waves or surface waves), especially in the linear case and when the site response is defined in the Fourier domain as a transfer function; in the NL case, the phase content of the input waveform induces some variability in the response, which may be considered aleatory. When the site response is defined by amplification factors in the response spectra domain, the phase and frequency contents of the input waveform also generates some "aleatory" variability, that will impact also the linear case. A key question is whether such an aleatory variability is already accounted for in the single-station sigma or not. Our personal answer is YES for all numerical estimates (except may be for strongly NL response), and NO for instrumental site response estimates, which, as already mentioned, combine aleatory and epistemic variabilities. In the latter case, only the epistemic part should be added, but it is extremely difficult in most cases to separate epistemic and aleatory components, because hundreds of recordings are needed to separate correctly (i.e., in a statistically meaningful way) the physical, deterministic effects (back-azimuth for instance) from the completely unpredictable, aleatory ones. One practical suggestions could be to consider that they are comparable, and therefore that the variability  $\sigma_{INSTR,epis}$  to be added to the mean instrumental estimates to account for the epistemic uncertainty, would then be  $\sigma_{INSTR,epis} = \sigma_{SSR} / \sqrt{2}$ . These answers and suggestions are subjective, and should be openly debated in view of reaching some consensus for the recommended practice.

### **3.5.2.2 Conclusions for Euroseistest**

Despite the above mentioned limitations, several relatively robust conclusions can be drawn from the panel of results obtained at Euroseistest.

One of the characteristics of the selected example site is the existence of a **large amplification over a broad frequency range**, due to a combination of several factors (the large velocity contrast at depth, the low velocity at surface, and the graben structure leading to additional "valley effects"), which lead to a site amplification significantly larger than the generic, average amplification accounted for in GMPEs. Basically, site-specific hazard estimates are thus larger than "generic" Level 0 estimates for low acceleration levels / short return periods, and lower at long return periods / large acceleration levels because of the impact of NL effects in thick, soft sediments.

An important general conclusion of this study is related to the **practical complexity of host to target corrections**, to convert a "standard rock" hazard into the corresponding one for the actual, harder rock that is found on the site.

- As discussed before, the  $V_{S30}$  correction is GMPE independent and can be applied to all GMPEs as a preliminary step.
- On the other hand, the kappa correction is GMPE dependent, which means that each GMPE of the logic tree needs to be corrected. The high frequency attenuation factor correction, better known as kappa correction, has proved to be particularly uneasy to perform and highly time consuming. The determination of kappa is difficult to automate; kappa values are obtained by visual inspection, depending more on the practitioner than on a particular magnitude/distance scenario. More research needs to be done on this issue, and one of the most appealing direction is the development of new GMPEs which be valid also for very hard rock.

About **Level 0** approaches, it is important to stress the changes brought by the recent ground motion prediction equations, which now include almost systematically a non-linear component in the site term (as a consequence of improved data and/or extensive NL modeling). When the panel of selected GMPEs includes both linear and non-linear site terms, the epistemic variability of Level 0 hazard estimates on soil sites is significantly larger than the corresponding estimates on rock site. One may also incidentally indicate that recent GMPEs have very complex functional forms, and it is safer to use already written and validated implementation codes (such as Openquake).

With respect to the **Level 0.5 approach**, it has been found for Euroseistest that

- the twin accounting for  $V_{S30}$  and  $f_0$  leads to higher amplification compared to the site term embedded in GMPEs, even when only the linear part of the site term is considered in the latter. This increased amplification is more consistent with the actual observations and measurements for the considered site, for the reasons already mentioned above),
- the limitation of the considered SAPE to the linear domain leads to an overestimation of the site response for large rock hazard levels: critical infrastructures should be designed for large return periods (i.e., 5000 years or more), leading to ground motion levels where nonlinearity is expected.

However, this example SAPE application is mainly intended to provide an illustration of the conceptual framework of this approach, in view of future improved, "plug-in type" SAPE elements that could account independently, on a more physical basis than what is done in GMPEs, for various site effect components: 1D resonance in soft soils, reduction effects on hard-rock, effects of surface or subsurface geometry ("aggravation factors"), NL modulations.

**Site specific approaches (Levels 1 and 2)** present the major advantage of allowing a reduction of the within-event variability, which leads, at long return periods, to a significantly reduced rock hazard. However, it should be very clearly stated that performing a site-specific hazard analysis does not necessarily imply a reduction of the hazard but only of the aleatoric uncertainty: The site response may indeed be significantly different, and thus in some cases larger, than the "average", "generic" effects accounted for in a very simplified and crude way in GMPEs. In addition, if the site-specific knowledge is severely limited, use of single-station sigma should be accompanied with the accounting for a significant epistemic uncertainty (Al Atik et al. 2010), which may partly or totally compensate for the reduction of the aleatory variability (see also above the section 3.5.2.2).

Although they are not mandatory for such site-specific approaches, **in-situ recordings** have multiple interests: they allow to estimate the site response with several approaches (Site to referene spectral ratio SSR, Generalized Inversion, site residuals  $\delta S_2S$ , at least), and they allow to calibrate numerical simulation tools at least in the linear domain, i.e. for low strains / weak motion.

All the **linear** response analysis (Level 0.5 ( $\phi, SAPE$ ), Level 1a ( $\phi_{SS}, \delta S_2S TST\_0WOST$ ), Level 1b ( $\phi_{SS}, Raptakis$ ), Level 1b ( $\phi_{SS}, htt, DCF, Ktenidou$ ), Level 1b ( $\phi_{SS}, htt, Linear NOAH$ )) lead to spectra significantly higher than the Level 0 ( $\phi, Vs_{30}$ ) for this particular example. This illustrates the huge impact of soil non-linearity (included in AA14) compared to linear response, and therefore the practical interest to include soil non-linearity in hazard estimates. However, this should be done very carefully, with the use of several independent GMPEs, or with dedicated SAPEs, to be sure that the linear part of the site response is not severely underestimated by the generic GMPEs – as it is the case for Euroseistest -.

This impact of NL behavior in thick soils is even more emphasized in the "**Level 2**", site-specific nonlinear response analysis (Level 2a ( $\phi_{SS}, htt, Nonlinear NOAH$ )), which cumulates the lowering effects of reduced aleatory variability and non-linear behavior, leading to hazard estimates lower than for the Level 0 ( $\phi, Vs_{30}$ ). One must keep in mind however the large variability in the numerical simulation on non-linear site response, which was not considered in this example and should be for a real case. The Prenolin benchmarking exercise (Régnier et al., 2015a,b, 2016a) organized within the framework of the SIGMA and SINAPS@ French R&D projects, showed that the results do vary between the different codes and teams, and that this epistemic variability increases with the acceleration level, up to 40-50% for input acceleration levels around 0.5 g. The recommendations about the use of NL simulation outlined in section 2.3.5 should be applied to correctly account for the epistemic uncertainty (Bazurro and Cornell. 2004a), which is much larger for the NL case than for the linear case.

### 3.5.2.3 Tentative recommendations

At this stage, here are below some propositions of recommendations which should be discussed in a larger panel, and probably amended, before being recommended as one of the level of the "STREST" project

- 1) Always start with Level 0 approaches, using a variety of recent GMPEs considered valid for the site under study. The Euroseistest example shows that the main drawback of this approach, from a safety concern, is the risk to severely underestimate the specific amplification of the site under study.

- 2) The interest of Level 0.5 approach is very limited right now because of the scarcity of SAPEs. Nevertheless, this situation may rapidly evolve in next years, allowing to counterbalance the above mentioned limitations of Level 0 results, through still simplified, but much more precise estimation of the site term, taking into account a larger number of site parameters than simply  $V_{S30}$  (e.g.: fundamental frequency, velocity profile, soil type: cohesive or cohesionless, geometrical characteristics such valley shape ratio, ...) and a larger number of relevant physical phenomena : NL behaviour, 2D or 3D aggravation factors. The resulting hazard estimates would then be probably on the safe side, due to the consideration of full aleatory variability
- 3) Site specific approaches allowing the use of a reduced aleatory variability imply significant additional costs in terms of geological, geophysical, and geotechnical surveys, careful and redundant numerical simulation and/or in-situ seismological instrumentation. Recommendations about the use of either numerical simulation or in-situ instrumentation are detailed in sections 2.3.4, 2.3.5, and 2.3.3.
- 4) In-situ instrumentation, when properly designed (see section 2.3.3), has multiple advantages, including setting constraints on numerical simulation estimates, and thus limiting the cost of either extensive site surveys to feed the site models for numerical simulation, or of comprehensive sensitivity studies. There is very little experience on the practical interest of such instrumentation of industrial sites given the cultural reluctance of the engineering and industrial communities; however, the few sites where very detailed site-specific hazard assessment have been performed all came to the same conclusion after much spending on surveys and numerical simulations: the ground truth comes from in-situ earthquake recordings... Recommending ad-hoc in-situ instrumentation will, in the long run, provide an invaluable feedback from all instrumented industrial sites, and allow to carefully assess the practical pros and cons, and the cost.
- 5) The main limitation of in-situ instrumentation, especially in low-to-moderate seismicity areas, is the non-access to the NL site response. As a consequence, the surface hazard estimates based on instrumental site response estimates (site-to-reference spectral ratio,  $\delta S2S$ , Generalized Inversion, ...) are biased towards higher values and are on the safe side. One way to correct them could be to use "plug-in" modulations correcting for the differences between non-linear and linear response. Even though such a way has never been used till now, the work presently undertaken within the framework of the SINAPS@ project could provide practical tools in the very near future (see for instance Régnier et al., 2016a). An important question, as such correction factors are more generic than site-specific, is whether their use is consistent with the use of single station sigma. This should be discussed, but our opinion is that it should be possible, since it is presently accepted to combine the use of single station sigma with the the current HTTA practice, which is NOT purely site specific (it is based on the use of "generic" rock profiles, and sometimes fuzzy, non-site-specific  $V_{S30-k}$  correlations). This is in some way analog to what is shown in Figure 29a, with the differences between the red (linear) and green ((with AA14 non-linear term) curves.

- 6) Most site-specific approaches, and in particular those based on numerical simulation, face the need for Host-to-Target adjustment. The present HTTA techniques prove to be very complex and stamped with subjectivity, leading to time-consuming procedures, and rather high epistemic uncertainties. The seismological and engineering communities should find a way to simplify these adjustment techniques. The most appealing direction is to establish GMPEs that be valid also for hard to very hard rock sites, which presently means using either deep downhole recordings, or deconvolution of surface recordings down to hard bedrock using reliable velocity profiles (Laurendeau et al., 2015). Other elements that would help in applying the present HTTA techniques would be to assign to each published GMPE consensual values of  $\kappa$ .
  
- 7) The  $\delta S2S$  approach is thus very appealing, as it becomes the simplest possible site-specific approach: it does not require HTT adjustment if the residual  $\delta S2S$  is measured with respect to standard rock. One must be careful however in the reliability of the measurement of the  $\delta S2S$  residual : it must be done for each considered GMPE, and unfortunately it might be that some of those GMPEs are NOT valid for the magnitude and distance range of the available site recordings, especially in low to moderate seismicity countries. The measurement of  $\delta S2S$  for each considered GMPE should therefore be carefully documented.

## **4 REGIONAL AND SITE-SPECIFIC TSUNAMI HAZARD ASSESSMENT FOR STREST TEST SITES**

A site-specific Probabilistic Tsunami Hazard Analysis (PTHA) involves the production of a full source-to-site numerical tsunami simulation on a high-resolution digital elevation model for each and every potential source scenario considered. In the case of Seismic PTHA (SPTHA), both local and distant sources, as well as the full aleatory variability of the seismic source, particularly in the near-field, must be taken into account. Moreover, the entire set of numerical simulations needs to be repeated for each alternative branch of fundamental assumptions when exploring epistemic uncertainty (see D3.1).

As a result, the computational coast of site-specific SPTHA would be generally almost unaffordable in practice. Hence, specific strategies are being developed for reducing the computational burden (Geist and Lynett, 2014). These strategies are typically based on crude approximation methods extrapolating inland the offshore wave heights (e.g. UNISDR 2015), and/or performing an oversimplification of the seismic source variability and applying cruder selection of the relevant seismic sources (e.g. Thio et al., 2010). These procedures are thus necessarily characterized by very large epistemic uncertainties.

A novel methodology to reduce the computational cost associated to a site-specific scale tsunami hazard assessment for earthquake-induced tsunamis has been recently introduced by Lorito et al., 2015 (hereinafter, L15), who have shown demonstrative applications to several test sites along the Eastern Sicily and Crete coasts. Such methodology has been developed within the Italian Flagship Project RITMARE funded by the Italian Ministry of Education, University and Research, and the EC FP7 project ASTARTE. This methodology allows a significant and consistent reduction of the epistemic uncertainty associated to probabilistic inundation maps, as it balances between the completeness of the earthquake model and the computational feasibility. It allows in fact performing high-resolution inundation simulations on realistic topo-bathymetry only for the relevant seismic sources.

For the applications in STREST, we plan to use such a methodology, or a refined version of it. In particular, we will use the more complete Event Tree developed in (Selva et al., submitted, hereinafter, S15), including a separate treatment of subduction and background (crustal) earthquakes, which allows for a more focused use of available information and for avoiding significant biases. Moreover, the L15 method is included into an ensemble modelling approach (Marzocchi et al., 2015, D3.1), allowing a full quantification of epistemic uncertainty. The full details of this refined approach will be given in deliverable D3.7, when the results of the applications at the test sites will be presented.

Here, we extract and just briefly describe an example from L15, in order to provide the reader with its main concepts, and to highlight the basic elements that are needed to perform a similar analysis for reducing the epistemic uncertainty in site-specific assessments. The full details of the method and its sample application can be found in L15. In particular, we here focus on the technique introduced for the computational cost reduction, which allows quantifying PTHA based on inundation modelling. The method is focused on PTHA of seismic origin (SPTHA), but it is absolutely general and can be used also when dealing with

other types of tsunami sources (landslides, volcanoes, etc.) as well as when dealing with alternative models and epistemic uncertainty assessment. Further than illustrating the methodology, in the following session we also report on the progresses made within STREST concerning the developments required to the application of the presented method to the test sites of Thessaloniki (GR) and Milazzo (I), which will allow a significant reduction of epistemic uncertainty on the PTHA that will be reported in deliverable D3.7.

#### **4.1 A METHODOLOGY FOR A FEASIBLE SITE-SPECIFIC SPTHA, FROM LORITO ET AL., 2015**

In order to reduce the number of numerical simulations really needed for SPTHA, in L15, we (i) introduce a (here simplified with respect to S15) event tree to achieve an effective and consistent exploration of the seismic source parameter space and assess the relative probability of occurrence; (ii) use the computationally inexpensive linear approximation for tsunami propagation to construct a preliminary SPTHA that calculates the probability of maximum offshore tsunami wave height (HMax) at a given target site; (iii) apply a two-stage filtering procedure to these 'linear' SPTHA results, for selecting a reduced set of sources that can represent the whole set of sources, and (iv) calculate 'non-linear' probabilistic inundation maps at the target site, using only the selected sources.

##### **4.1.1 The simplified Event Tree for seismic source aleatory variability analysis**

An Event Tree (ET) is a branching graph representation of events in which individual branches are alternative steps from a general prior event, state, or condition, and which evolve into increasingly specific subsequent events. ET analysis is then a logical inductive process used to determine the path from an initiating event to the various consequences and the expected frequency of each consequence, and it has found application in many fields of science (e.g. Clifton and Ericson 2005), including geophysics (e.g. Newhall and Hoblitt 2002). Its different branches represent different possibilities, not alternative models as in logic trees (e.g. Bommer and Scherbaum 2008).

Here, the ET provides a controlled discretisation of earthquake parameter space, in order to (i) define the set of source scenarios and (ii) assess the probability of occurrence for each scenario. For illustrative purposes, the ET we introduced, fully explores only magnitudes and positions of earthquakes occurring on a subduction interface. All the details of this ET implementation and the resulting probabilities can be found in L15. The more detailed ET designed for real applications is being now prepared (S15) and it will be used, for example, for the creation of the Italian national PTHA in the framework of the agreement between INGV and the Italian Department of Civil Protection (DPC).

In PTHA, and often also in PSHA, analytic probability models are usually developed for the uncertainty, and their probability density function (PDF) is integrated into the rate (frequency) term. We here introduce a different discretised form for the hazard integral, with corresponding discretised probability distributions. The main purposes of the controlled discretisation introduced in L15 are to avoid oversimplifications in the treatment of source parameters, and to cover their entire range without ending up with huge synthetic catalogues that may arise when representing low probability events is needed, e.g. when considering great or mega earthquakes with very long Average Return Periods (ARPs). Conversely, with

the ET approach, the tails of the assumed PDF can be efficiently explored. This is important because the parameters (e.g. size, peak slip) of ‘extreme’ tsunamigenic events, such as Sumatra-Andaman 2004 or Tohoku 2011, are likely falling in these tails and, if so, one may think of them as responsible for quite heavy tails of tsunami hazard and risk distributions. The ET nodes may be also variously explored, for example depending on the ARP of interest for a specific application, by adjusting the ranges and the sampling steps as needed. Also a hierarchization of the source parameters with respect to their influence on the hazard intensity would help optimize the sampling scheme, and a finer sampling could be adopted when hazard sensitivity is higher.

#### 4.1.2 Definition of the optimal subset of sources for site-specific PTHA (probabilistic inundation maps)

The optimal subset of sources that are actually needed for a site-specific assessment can be chosen among all sources explored by the ET for the regional assessment, by means of a two-step filtering procedure based on the analysis of the results offshore.

Therefore, the regional tsunami hazard is first assessed using as intensity measure the HMax offshore (at 50 m depth), which can be calculated using the inexpensive linear long wave approximation on a relatively coarse calculation grid.

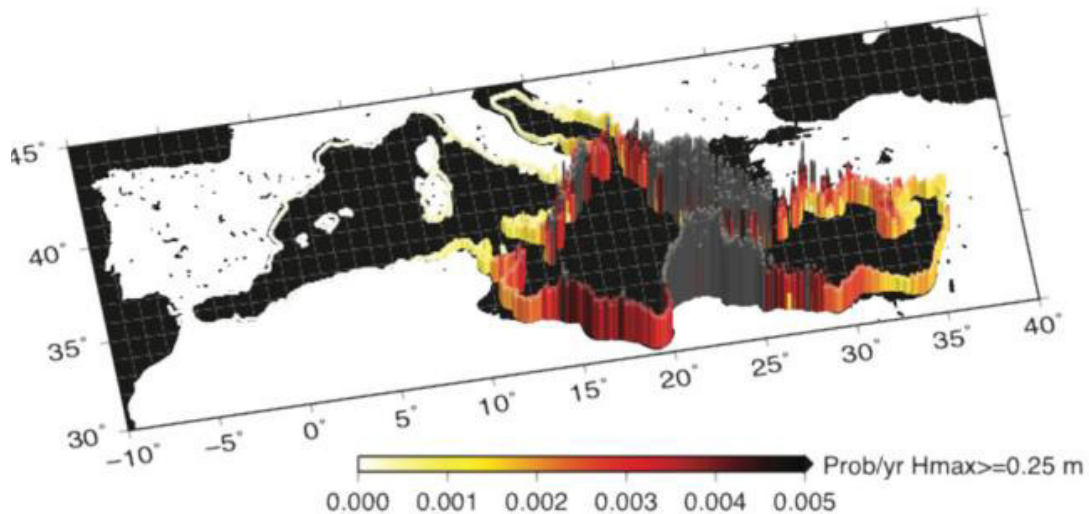


Figure 57 : Example of annual probability of exceedance of 1m tsunami wave height at the 50 m isobaths around the Mediterranean Sea due to subduction earthquakes on the Hellenic Arc

In Figure 57, for example, the annual probability of 1 m HMax exceedance due to subduction earthquakes along a portion of the Hellenic Arc, is shown. At each offshore point of interest the full hazard curve is obtained. Each scenario prescribed by the ET contributes to the hazard curve if its ensuing tsunami hazard intensity (HMax) exceeds prescribed thresholds. The results are combined according to the frequency of the causative earthquake.

Before moving to site-specific analysis, a ‘control profile’ is defined in front of the site for which the inundation maps are needed (Figure 58), that is a set of offshore points where regional hazard curves have been calculated. The Figure also shows the nested grids of

progressively increasing spatial resolution used around the test sites for numerical simulations of tsunami inundation. The length of the profile needs to be tuned in order to be representative of the typical wavelengths involved at the specific site (see details in L15).

Only those scenarios that contribute significantly (Filter 1), and that, as a result of a hierarchical cluster analysis (Filter 2), may be representative in terms of tsunami impact at the site of a class of seismic sources, are then retained for more expensive inundation calculations on a high-resolution topo-bathymetric model (Figure 59).

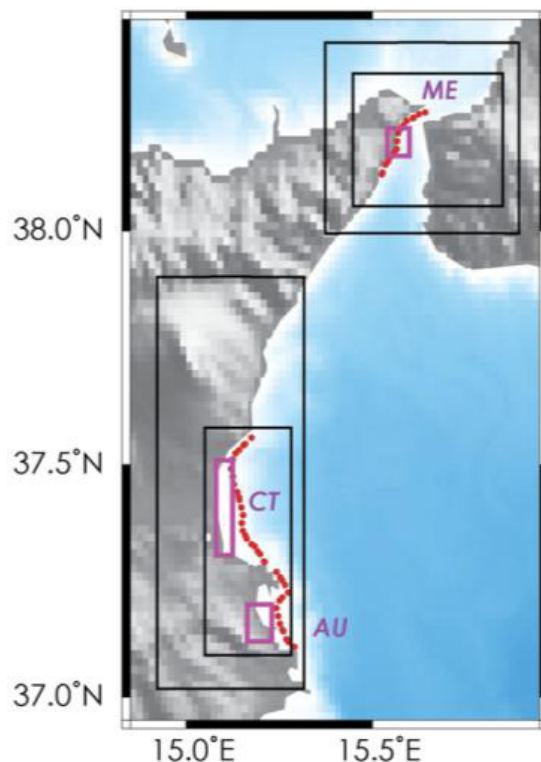


Figure 58. Examples of target sites used in L15 and control profiles (red dots) used for the filtering (selection of the sources relevant for inundation calculations)

To each 'representative scenario' is assigned the probability of the entire cluster of sources it represents, and thus probabilistic inundation maps can be prepared. Figure 59 also shows the correspondence between the offshore hazard curves calculated with the full set of scenarios and those (in red) prepared with only the selected representative scenarios. Figure 60 shows the inundation maps obtained for the flow depth at Messina harbour due to subduction earthquakes on the Hellenic Arc. They show the height exceeded on each point of the map with the probability corresponding to the ARPs of 500 and 5000 yrs. The differences between the map obtained with the selected sources and that obtained with the full set of sources are also analysed.

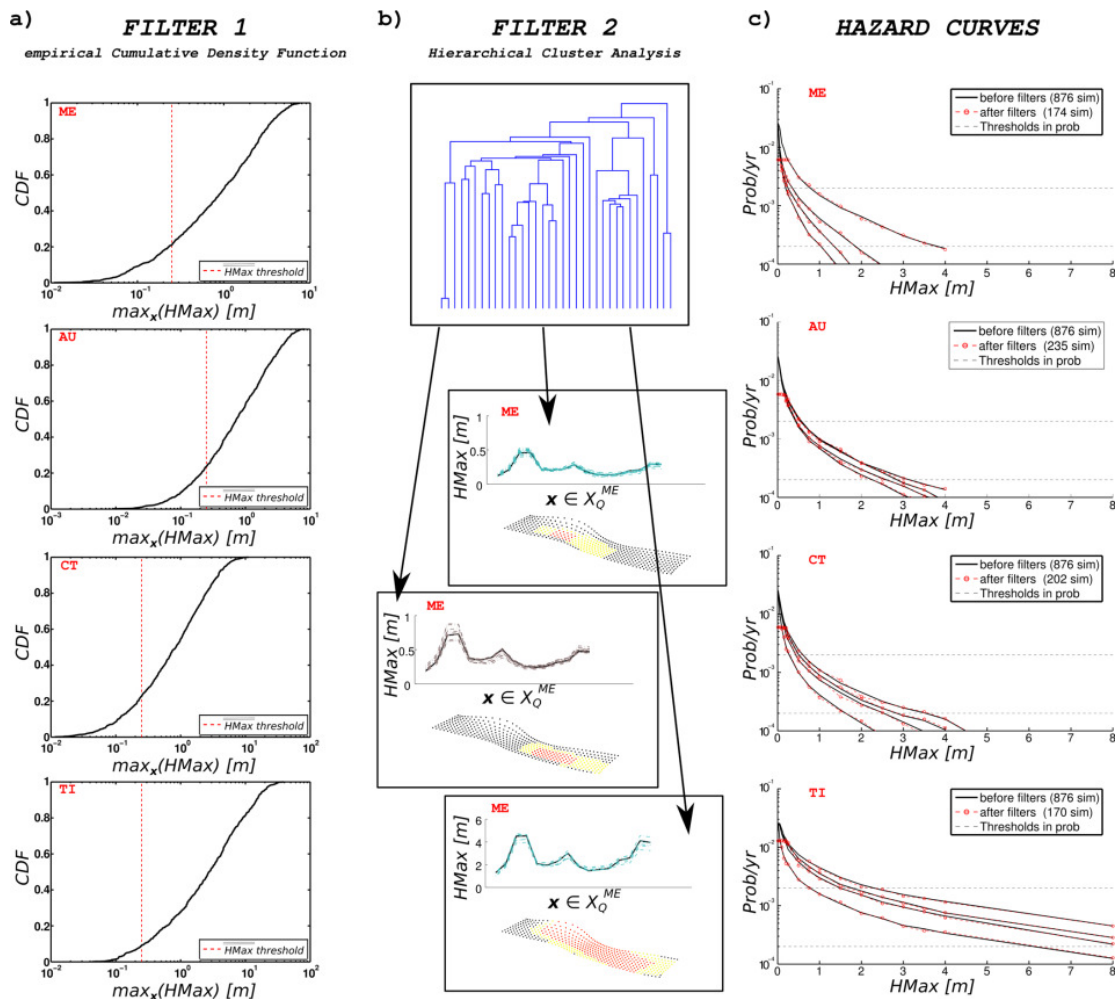


Figure 3

Figure 59 : Illustration of the two-step filtering procedure. Filter 1 selects only those seismic sources that generate a tsunami over the ‘noise threshold’; Filter 2 finds clusters of sources producing comparable effects. To the right, the hazard curves obtained only with selected sources are compared to those obtained with the full set

The main features of the inundation maps are preserved. Further examples, for different target sites and also for the volume flux (speed times flow depth), can be found in L15. We find that the selection of the important sources needed for approximating probabilistic inundation maps can be obtained based on the offshore  $HMax$  values only. The filtering procedure is semi-automatic and can be easily repeated for any target sites.

The comparison between the filtered SPTHA results and those obtained for the full set of sources indicates that our approach allows for a 75–80 per cent reduction of the number of the numerical simulations needed, while preserving the accuracy of probabilistic inundation maps to a reasonable degree. As a result, this approach allow a significant and controlled reduction of the epistemic uncertainty with respect to commonly used cruder approximations.

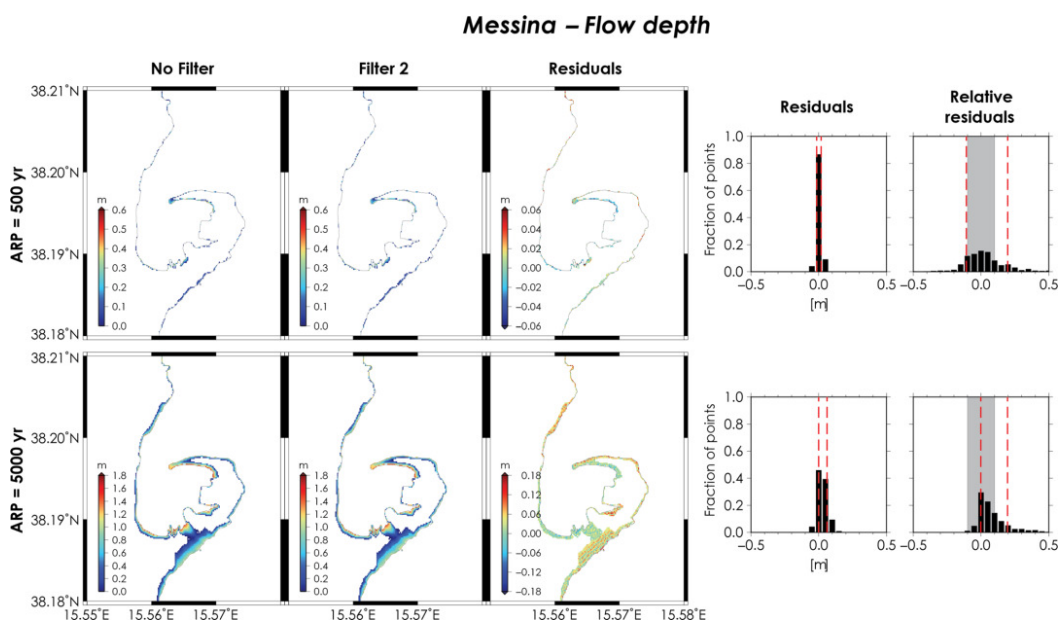


Figure 60 : Comparison of inundation maps obtained with the selected sources to those obtained with the full set

#### 4.1.3 preparation of site-specific analysis for stress test sites

We here report on some progresses made towards site-specific assessment in STREST test sites.

INGV organized a meeting in the premises of its headquarters in Rome on 23/05/2014, attended by the responsible of Thessaloniki (AUTH) and Milazzo (AMRA) test sites. One of the main focuses of the meeting was on the appropriate intensity measures. After the meeting, the STREST WP4 “Vulnerability Fact Sheet” was modified accordingly. Moreover, the formats of the outputs of the PTHA have been agreed. In fact, they will need to be used as input for tsunami risk calculations by the partners. Main points have been agreed also regarding the input data to be provided for the analysis, in particular: the seismic sources (INGV), the topo-bathymetry models (AUTH and AMRA with INGV assistance for the elaboration) with sufficient (metric) resolution within, for example, the harbours, the definition of the target zones and hazard intensities to be considered (AUTH and AMRA). In addition, the need of coherency between seismic and tsunami hazard analyses need to be granted as well as much as possible, through the coherency between the seismic source databases used. While this is desirable for all the assessments, it is fundamental for multi-hazard analyses. It has also been agreed that instead of aggregated hazard results, full outputs from selected tsunami scenarios will be provided for a subsequent systemic risk analysis. This can allow selecting the appropriate simulation for any given seismic source, allowing to link potential Monte Carlo multi-hazard analyses (e.g., Mignan et al. 2014) with PTHA results.

Subsequently, INGV has been working on the preparation of the pre-calculated scenario database for the regional analysis around the sites of interest, aimed at providing offshore SPTHA. This analysis has been completed and presented in several deliverables. This is in fact an input agreed from the beginning to be dependent on the interaction between ASTARTE and STREST.

Regarding the Thessaloniki bay area test site, an intense collaboration was established between INGV and AUTH. A DEM including both detailed bathymetry and topography was prepared as a result of this collaboration (see Figure 61). This grid contains a high definition bathymetry specifically digitized for this case study, merged with a topographic model that includes the built environment in the proximity of the coast. Preliminary simulations of the tsunami inundation have been performed to test the coupling of inundation model and topobathymetric data. One example of such simulations is reported in Figure 62.

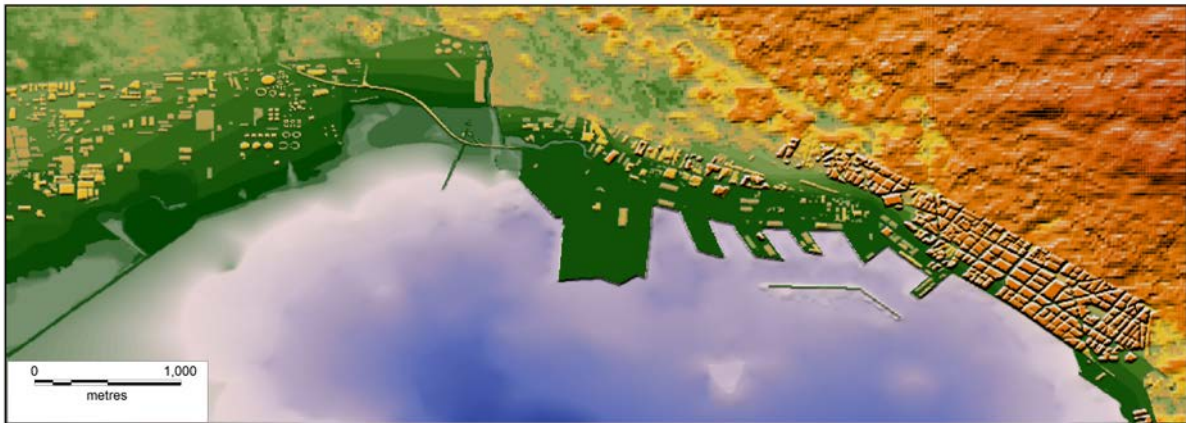


Figure 61 : Snapshot of the high resolution grid (10 m) of the Thessaloniki bay area. This grid will be used to perform simulations of inundation.



Figure 62 :Example of tsunami inundation modelling results on a high resolution grid

For the Thessaloniki area, full simulations have been conducted at the regional scale using the full approach (e.g. the complete event tree) of S15; the control profiles for the two-step filtering procedure have been defined and the preliminary results of the cluster analysis for source selection are being obtained.

At the moment, the topo-bathymetric data for Milazzo test site are still missing and data availability for this test site still need to be assessed.

## 5 References

- Abrahamson N. , W. J. Silva, and R. Kamai (2014). Summary of the ASK14 Ground-Motion Relation for Active Crustal Regions. *Earthquake Spectra*, (in press).
- Abrahamson N. and Silva W. (2008). Summary of the Abrahamson & Silva NGA ground-motion relations, *Earthquake Spectra* 24, 67-97.
- Abrahamson, N.A. 1992. Non-stationary spectral matching, *Seismological Research Letters*, 63(1), p. 30
- Akaike, H., 1973, Information theory as an extension of the maximum likelihood principle: 2nd International Symposium on Information Theory, eds., B. N. Petrov, and F. Csaki, p. 267–281.
- Aki, K., 1957, Space and time spectra of stationary stochastic waves, with special reference to microtremors, *Bull. Earth. Res. Inst. Tokyo Univ.* 25, p. 415-457.
- Akkar S., M.A. Sandıkkaya, And J.J. Bommer (2014). Empirical Ground-Motion Models for Point- and Extended-Source Crustal Earthquake Scenarios in Europe and the Middle East. *Bulletin of Earthquake Engineering*, 12, 1, pp 359-387
- Akkar, S. And Bommer, J.J. (2010). "Empirical equations for the prediction of pga, pgv and spectral accelerations in europe, the mediterranean region and the middle east," *seismological research letters*, 81, 2, 195-206.
- Akkar, S. and Bommer, J.J. 2010. Empirical equations for the prediction of PGA, PGV, and spectral accelerations in Europe, the Mediterranean Region, and the Middle East, *Seismological Research Letters*, 81(2):195–206.
- Akkar, S., And J. J. Bommer (2007). Prediction of elastic displacement response spectra in Europe and the Middle East. *Earthquake Engineering & Structural Dynamics* 36 (10), 1,275–1,301.
- Al Atik L., Kottke A., Abrahamson N., And J. Hollenback (2014), Kappa ( $\kappa$ ) Scaling of Ground-Motion Prediction Equations Using an Inverse Random Vibration Theory Approach, *Bulletin of the Seismological Society of America*, Vol. 104, No. 1.
- Al Atik, L., N. Abrahamson, F. Cotton, F. Scherbaum, J. Bommer, And N. Kuehn (2010). The variability of ground-motion prediction models and its components, *Seismol. Res. Lett.* 81, 794–801.
- Albarello, D. and G. Gargani, 2010. Providing NEHRP Soil Classification from the Direct Interpretation of Effective Rayleigh-Wave Dispersion Curves, *Bulletin of the Seismological Society of America*, Vol. 100, No. 6, pp. 3284–3294, December 2010, doi: 10.1785/0120100052.
- Ambraseys Nn, Douglas J, Sarma Sk, Smit Pm (2005) Equation for the estimation of strong ground motions from shallow crustal earthquakes using data from Europe and the Middle East: horizontal peak ground acceleration and spectral acceleration. *Bull EarthquakeEng* 3:1–53
- Ameri, G. (2013). Preliminary GMPEs based on RESORCE-2013: effect on data selection and metadata uncertainties. Deliverable D2-92. SIGMA Project.
- Ameri, G., F. Hollender, D. Sicilia, P.-Y. Bard and many others, 2015. Operational guide to account for site effects: revised, non-final version. Sigma deliverable D3-152, October 2015, 64 pages.
- Ameri, G., Gallovič, F. and Pacor, F. 2012 Complexity of the Mw 6.3 2009 L'Aquila (central Italy) earthquake: 2. Broadband strong-motion modeling, *Journal of Geophysical Research*, 117(B04308), doi: 10.1029/2011JB008729
- Ameri, G., Pacor, F., Cultrera, G. and Franceschina, G. 2008 Deterministic ground-motion scenarios for engineering applications: the case of Thessaloniki, Greece, *Bulletin of the Seismological Society of America*, 98(3): 1289-1303.
- Anastasiadis, A., Raptakis, D. and Pitilakis, K. 2001. Thessaloniki's detailed microzoning: subsurface structure as basis for site response analysis, *Pure and Applied Geophysics*, 158: 2597-2633
- Anderson, J., And S. Hough (1984). A model for the shape of the Fourier amplitude spectrum of

- acceleration at high frequencies, *Bull. Seismol. Soc. Am.* 74, no. 5, 1969–1993.
- Andrus, R.D., 2003. Guidelines for evaluating liquefaction resistance using shear wave velocity measurement and simplified procedures. US Department of Commerce, Technology Administration, National Institute of Standards and Technology, 2003.
- Antonietti, P.F., Mazzieri, I., Quarteroni, A. and Rapetti, F. 2012. Non-conforming high order approximations of the elastodynamics equation, *Computer Methods in Applied Mechanics and Engineering*, 209–212: 212–238.
- Apostolidis, P., Raptakis, D., Roumelioti, Z. and Pitilakis, K. 2004. Determination of S-wave velocity structure using microtremors and spac method applied in Thessaloniki (Greece), *Soil Dynamics and Earthquake Engineering*, 24: 49-67.
- Assimaki D., Kausel E. and Whittle A.J. (2000). A model for dynamic shear modulus and damping for granular soils, *Journal of Geotechnical and Geoenvironmental Engineering*, ASCE, 126(10), 859-869
- Assimaki, D., and W. Li, 2012. Site and ground motion-dependent nonlinear effects in seismological model predictions. *Soil Dyn. Earthq. Eng.* 143–151.
- Atkinson, G. M. 2006 Single-station sigma, *Bulletin of the Seismological Society of America*, 96 (2): 446–455.
- Baker, J.W. and Cornell, C.A. 2005. A vector valued ground motion intensity measure consisting of spectral acceleration and epsilon. *Earthquake Engineering and Structural Dynamics* 34:1193-1217.
- Bard, P. Y., G. Cultrera, N. Theodoulidis, K. Pitilakis, D. Faeh, S. Parolai, P. Moczo, C. Cornou, E. Chaljub, A. Imtiaz, A. Rovelli, P. Bordonni, F. Cara, G. Digiulio, G. Milana, V. Pessina, M. Piscitutta, A. Savvaïdis, K. Makra, E. Riga, F. Gelagoti, J. Burjanek, C. Cauzzi, T. Boxberger, J. Kristek, F. Hollender, C. Guyonnet-Benaïze, A. Stambouli, D. Zendagui and B. Derras, 2015b. Effects of surface and underground topography on ground motion : An overview of some recent European collaborative results, Invited Talk, SSA2015, April 21-23, 2015, Pasadena, SRL 86:2B, p. 703.
- Bard, P. Y., H. Cadet, B. Endrun, M. Hobiger, F. Renalier, M. Theodoulidis, D. Ohrnberger, F. Fäh, F. Sabetta, and P. Teves-Costa, 2010, From non-invasive site characterization to site amplification: Recent advances in the use of ambient vibration measurements, *Earthquake Engineering in Europe*, 17, Part 2, p. 105–123.
- Bard, P.-Y., E. Chaljub, J. Kristek, P. Moczo, C. Durand and A. Stambouli, 2015a. A numerical analysis of aggravation factors in two-dimensional alluvial valleys. NMEM2015 (International Workshop on Numerical Modeling of Earthquake Ground Motions: waves and ruptures, July 6-8, 2015, Smolenice (Slovakia).
- Bard, P.-Y., G. Cultrera, N. Theodoulidis, K. Pitilakis, D. Fäh, S. Parolai, P. Moczo and the whole NERA WP11 team (2014). Waveform modelling and site coefficients for basin response and topography: main results from NERA WP11. *Second European Conference on Earthquake Engineering and Seismology (2ECEES), Istanbul, Turkey, August 24-29, Paper #2351, 3 pages*
- Bard, P.-Y., A. Imtiaz, C. Cornou, E. Chaljub, G. Cultrera, A. Rovelli, P. Bordonni, F. Cara, G. Di Giulio, G. Milana, V. Pessina, M. Piscitutta, M. Vassallo, G. Calderoni, N. Theodoulidis, A. Savvaïdis, K. Makra, D. Kementzetzidou, K. Pitilakis, E. Riga, F. Gelagoti, D. Fäh, J. Burjánek, S. Parolai, T. Boxberger, P. Moczo, J. Kristek, F. Hollender, C. Guyonnet-Benaïze and M. Cushing, 2015. *Implementation plan: report on final propositions for building codes*, NERA deliverable D11.7, EC FP7 project 262330, 69 pages.
- Bardet, J. P., Ichii, K. and Lin, C.H. 2000, *EERA A Computer Program for Equivalent-linear Earthquake site Response Analyses of Layered Soil Deposits*. University of Southern California, Department of Civil Engineering.
- Bazzurro, P. And Cornell, C. A. (2004). Nonlinear soil-site effects in probabilistic seismic-hazard analysis. *Bulletin of the Seismological Society of America*, 94(6), 2110-2123.
- Bazzurro, P., and Cornell, C. A. (2004a). "Ground-Motion Amplification in Nonlinear Soil Sites with Uncertain Properties." *Bulletin of the Seismological Society of America*, 94(6), 2090-2109.
- Berge-Thierry, C., Cotton, F., Scotti, O., Griot-Pommer, D.A. And Fukushima, Y. (2003). New empirical response spectral attenuation laws for moderate European earthquakes, *J. Earthquake Eng.* 7, 193–222.

- Bindi D., Massa M., Luzi L., Ameri G., Pacor F., Puglia R. And P. Augliera (2014) Pan-European Ground-Motion Prediction Equations for the Average Horizontal Component of PGA, PGV, and 5%-Damped PSA at Spectral Periods up to 3.0 s using the RESORCE dataset. *Bulletin of Earthquake Engineering*, 12, 1, pp 391-430
- Bindi D., Pacor F., Luzi L., Puglia R., Massa M., Ameri G., Paolucci R. (2011). Ground motion prediction equations derived from the Italian strong motion data base. *Bull Earth Eng.*, 9, 6, 1899-1920.
- Biro, Y., And P. Renault (2012). Importance and impact of host-to-target conversions for ground motion prediction equations in PSHA, in Proc. of the 15th World Conference on Earthquake Engineering, 1855, Lisbon, Portugal.
- Bolisetti, C., Whittaker, A. S., Mason, H. B., Almufti, I., Willford, M., 2014. Equivalent linear and nonlinear site response analysis for design and risk assessment of safety-related nuclear structures. *Nuclear Engineering and Design*, 275, 107-121.
- Bommer, J. J. and F. Scherbaum. 2008. The use and misuse of logic trees in probabilistic seismic hazard analysis, *Earthq. Spectra*, 24(4): 997– 1009.
- Bonilla, L.F [2000]. NOAH: Users Manual, Institute for Crustal Studies, University of California, Santa Barbara.
- Boore D.M. And Atkinson G.M. (2008). Ground-motion prediction equations for the average horizontal component of PGA, PGV, and 5%-damped PSA at spectral periods between 0.01 and 10s. *Earthquake Spectra*, Vol. 24, n° 1, p. 67-97.
- Boore, D. M. (2003). Simulation of ground motion using the stochastic method, *Pure Appl. Geophys.* 160, 635–676.
- Boore, D.M., J.P. Stewart, E. Seyhan, And G.M. Atkinson (2014). NGA-West 2 equations for predicting PGA, PGV, and 5%-damped PSA for shallow crustal earthquakes, *Earthquake Spectra*, (in press).
- Boore, D.M., J.P. Stewart, E. Seyhan, And G.M. Atkinson (2014). NGA-West 2 equations for predicting PGA, PGV, and 5%-damped PSA for shallow crustal earthquakes, *Earthquake Spectra*, (in press).
- Bora, S.S, Scherbaum, F., Kuehn, N., And P. Stafford (2014). Fourier spectral- and duration models for the generation of response spectra adjustable to different source-, propagation-, and site conditions. *Bulletin of Earthquake Engineering*, 12, 1, pp 467-493
- Bora, S.S, Scherbaum, F., Kuehn, N., And P. Stafford (2014). Fourier spectral- and duration models for the generation of response spectra adjustable to different source-, propagation-, and site conditions. *Bulletin of Earthquake Engineering*, 12, 1, pp 467-493
- Bray, J. D., Sancio, R. B., Durgunoglu, T., Onalp, A., Youd, T. L., Stewart, J. P., Seed, R. , Cetin, O. K., Bol, E., Baturay, M. B., Christensen, C., and Karadayilar, T. (2004b). Subsurface characterization at ground failure sites in Adapazari, Turkey. *J. Geotechnical and Geoenvironmental Engineering*, ASCE, 130(7): 673-685.
- Burjanek, J., D. Föh, M. Piscuitta, P.-Y. Bard and the NERA-JRA1 team, 2016. Seismic hazard at sites with pronounced topography: overview of observed site effects & recommendations, in preparation for SRL, March 2016.
- Cadet H., Bard, P-Y. And A. Rodriguez-Marek (2012a) Site effect assessment using KiK-net data: Part 1. A simple correction procedure for surface/downhole spectral ratios , *Bulletin of Earthquake Engineering*, 10, 2, pp 421-448
- Cadet H., Bard, P-Y., Duval, A-M. And E. Bertrand (2012b) Site effect assessment using KiK-net data: part 2—site amplification prediction equation based on  $f_0$  and  $V_{sz}$ , *Bulletin of Earthquake Engineering* 10, 2, pp 451-489
- Cadet, H., and A. Savvaidis, 2011, Comparative application of dispersion curve inversion strategies. Case study of noise arrays in the Euroseistest site, Greece, *Near Surface Geophysics*, 9, p. 571–583.
- Cadet, H., and P.-Y. Bard, 2011, Estimer  $V_{S30}$  à partir de la courbe de dispersion, Actes du 8ème colloque national de l'Association Française du Génie Parasismique, Vers une maîtrise durable du risque sismique, Ecole des Ponts ParisTech, Champs-sur-Marne, 6-8 septembre 2011, papier n° 22 Capon, J., 1969, High-resolution frequency–wavenumber spectrum analysis, *Proc. IEEE* 57:8, p.1408–1418.

- Campbell K. W. And Y. Bozorgnia. (2014). NGA-West2 Ground Motion Model for the Average Horizontal Components of PGA, PGV, and 5%-Damped Linear Acceleration Response Spectra *Earthquake Spectra*, (in press)
- Campbell, K. W. (2003). Prediction of strong ground motion using the hybrid empirical method and its use in the development of ground-motion (attenuation) relations in eastern North America, *Bull. Seismol. Soc. Am.* 93, 1012–1033.
- Campbell, K.W. & Y. Bozorgnia (2008). NGA ground motion model for the geometric mean horizontal component of PGA, PGV, PGD and 5%-damped linear elastic response spectra at periods ranging from 0.1 s to 10.0 s. *Earthquake Spectra* 24(1), 139-171.
- Caputo, R., Chatzipetros, A., Pavlides, S., and Sboras, S. 2012. The Greek Database of Seismogenic Sources (GreDaSS): state-of-the-art for norther Greece, *Annals of Geophysics*, 55(5): 859-894
- Cauzzi C. And Faccioli E. (2008). Broadband (0.05 to 20 s) prediction of displacement response spectra based on worldwide digital records. *Journal of Seismology*, Vol. 12, n° 4, p. 453-475.
- Chaljub, E., Moczo, P., Tsuno, S., Bard, P.Y., Kristek, J., Kaser, M., Stupazzini, M., and Kristekova, M. 2010. Quantitative comparison of four numerical predictions of 3D ground motion in the Grenoble valley, France. *Bulletin of the Seismological Society of America*, 100: 1427-1455.
- Chaljub, E., E. Maufroy, P. Moczo, J. Kristek, F. Hollender, P.-Y. Bard, E. Priolo, P. Klin, F. de Martin. Z. Zhang, W. Zhang, X. Chen, 2015. 3-D numerical simulations of earthquake ground motion in sedimentary basins: testing accuracy through stringent models, *Geophysical Journal International* 2015 201 (1): 90-111 doi: 10.1093/gji/ggu472
- Chen, L. and E. Faccioli (2013). Single-station standard deviation analysis of 2010–2012 strong-motion data from the Canterbury region, New Zealand, *Bull. Earthq. Eng.* 11, 1617–1632.
- Chiou B. S.J. And R. R. Youngs (2014) Update of the Chiou and Youngs NGA Ground Motion Model for Average Horizontal Component of Peak Ground Motion and Response Spectra. *Earthquake Spectra*, (in press)
- Chiou, B. S-J., and Youngs, R. R., 2008. An NGA model for the average horizontal component of peak ground motion and response spectra, *Earthquake Spectra* 24, 173–215.
- Cirella, A., Piatanesi, A., Tinti, E., Chini, M. and Cocco, M. 2012. Complexity of the rupture process during the 2009 L'Aquila, Italy, earthquake, *Geophysical Journal International*, 190: 607–621.
- Clifton, A. and I. I. Ericson. 2005. *Hazard Analysis Techniques for System Safety*, John Wiley & Sons, Inc., 528 pp.
- Cocco, M. and Pacor., F. 1993. The rupture process of the 1980 Irpinia, Italy, earthquake from the inversion of strong motion waveforms, *Tectonophys*, 218: 157-177.
- Comina C., Foti S., Boiero D. and Socco, L.V., 2011. Reliability of  $V_{S30}$  evaluation from surface waves tests, *Journal of Geotechn. and Geoenviron. Eng.*, ASCE (June 2011).
- Cornou C., M. Ohrnberger, D. Boore, K. Kudo and P.-Y. Bard, 2009, Derivation of structural models from ambient vibration array recordings: Results from an international blind test, *ESG2006*, Vol.2, p.1127-1219.
- Cotton, F., F. Scherbaum, J. J. Bommer, And H. Bungum (2006). Criteria for selecting and adjusting ground-motion models for specific target regions: Application to central Europe and rock sites, *Journal of Seismology* 10, doi 10.1007/s10950-005-9006-7.
- Dagna. P. 2013. *Enabling SPEED for near Real-time Earthquake Simulations*, PRACE Report.
- Darendeli, B.S. (2001). "Development of a New Family of Normalized Modulus Reduction and Material Damping Curves". PhD Dissertation, The University of Texas at Austin, UMI Number:3025211.
- Day, S.M. and Bradley, C.R. 2001. Memory-efficient simulation of anelastic wave propagation, *Bulletin of the Seismological Society of America*, 91(3): 520–531.
- Deepsoil V5.1 (2012), "User Manual and Tutorial" Youssef M. A. Hashash, Department of Civil and Environmental Engineering, University of Illinois at Urbana-Champaign
- Derras, B., P.-Y. Bard, F. Cotton, 2016. Site-conditions proxies, ground-motion variability and data-driven GMPEs. Insights from NGA-West 2 and RESORCE datasets. *Earthquake Spectra*, accepted, in press.

- Di Alessandro, C., L. F. Bonilla, D. M. Boore, A. Rovelli, And O. Scotti (2012). Predominant-period site classification for response spectra prediction equations in Italy, *Bull. Seismol. Soc. Am.* 102, 680-695.
- Douglas, J., H. Bungum, And F. Scherbaum (2006). Ground-motion prediction equations for southern Spain and southern Norway obtained using the composite hybrid model perspective, *J. Earthq. Eng.* 10, 33–72.
- Drouet, S., S. Chevrot, F. Cotton and A. Souriau, 2008. Simultaneous Inversion of Source Spectra, Attenuation Parameters, and Site Responses: Application to the Data of the French Accelerometric Network, *Bulletin of the Seismological Society of America*, Vol. 98, No. 1, pp. 198–219, February 2008, doi: 10.1785/0120060215
- Elgamal, A., Yang, Z., and Lu, J. 2010. *Cyclic1D Seismic Ground Response Version 1.2, User's Manual*, University of California, San Diego, Department of Structural Engineering.
- Faccioli E, Bianchini A, Villani M (2010) New ground motion prediction equations for  $t > 1$  s and their influence on seismic hazard assessment. In: Proceedings of the University of Tokyo Symposium on Long- Period Ground Motion and Urban Disaster Mitigation, March 17–18, Tokyo, Japan
- Faccioli E, Bianchini A, Villani M (2010) New ground motion prediction equations for  $t > 1$  s and their influence on seismic hazard assessment. In: Proceedings of the University of Tokyo Symposium on Long- Period Ground Motion and Urban Disaster Mitigation, March 17–18, Tokyo, Japan
- Faccioli, E., Vanini, M., and R. Paolucci (2013), Site-specific probabilistic study for the Po Plain area, SIGMA Deliverable D4-94.
- Fondasol Geotechnique (2013), "Grenoble (38)-RealisationRéalisation d'un sondage carotte et deux sondages destructifs. Investigations géotechniques", Institut Max Von Laue, CGR13.0078-Piece n°001-Indice B
- Foti S., Comina C., Boiero D. and Socco L.V., 2009, Non uniqueness in surface wave inversion and consequences on seismic site response analyses, *Soil Dynamics and Earthquake Engineering*, Vol. 29 (6), p.982-993
- Foti, S., Parolai, S., Albarello, D., Picozzi, M., 2011, Application of Surface-Wave Methods for Seismic Site Characterization, *Surveys in Geophysics*, 32, 6, 777-825.
- Garofalo, F., S. Foti, F. Hollender, P.Y. Bard, C. Cornou, B.R. Cox, M. Ohrnberger, D. Sicilia, M. Asten, G. Di Giulio, T. Forbriger, B. Guillier, K. Hayashi, A. Martin, S. Matsushima, D. Mercerat, V. Poggi and H. Yamanaka, 2016. InterPACIFIC project: comparison of invasive and non-invasive methods for seismic site characterization. Part I: Intra-comparison of surface wave methods. SDEE, in press, <http://dx.doi.org/10.1016/j.soildyn.2015.12.010>
- Garofalo, F., S. Foti, F. Hollender, P.-Y. Bard, C. Cornou, B.R. Cox, A. Dechamp, M. Ohrnberger, D. Sicilia and C. Vergnault, 2016. Interpacific project : comparison of invasive and non-invasive methods for seismic site characterization. Part II : intercomparison between surface-wave and borehole methods. SDEE, in press, <http://dx.doi.org/10.1016/j.soildyn.2015.12.009>.
- Geist, E. L., and P. J. Lynett. 2014. Source processes for the probabilistic assessment of tsunami hazards. *Oceanography* 27(2):86–93. doi:10.5670/oceanog.2014.43.
- Grant, D.N. and Diaferia, R. 2012. Assessing adequacy of spectrum-matched ground motions for response history analysis. *Earthquake Engineering and Structural Dynamics* 42(9): 1265-1280.
- Guillier B., C. Cornou, J. Kristek, P. Moczo, S. Bonnefoy-Claudet, P.-Y. Bard, D. Fäh, 2006, Simulation of seismic ambient vibrations: does the H/V provide quantitative information in 2D-3D structures? Third International Symposium on the Effects of Surface Geology on Seismic Motion, Grenoble, France, 30 August - 1 September 2006, Paper Number: 185.
- Hancock, J., Watson-Lamprey, J., Abrahamson, N.A., Bommer, J.J., Markatis, A., McCoy, E. and Mendis R. 2006. An improved method of matching response spectra of recorded earthquake ground motion using wavelets. *Journal of Earthquake Engineering*(10): 67–89.
- Hernandez, B., Cocco, M., Cotton, F., Stramondo, S., Scotti, O., Courboux, F., and Campillo, M. 2004. Rupture history of the 1997 Umbria-Marche (central Italy) main shocks from the inversion of GPS, DInSAR and near field strong motion data, *Annals of Geophysics*, 47(4): 1355-1376.
- Herrero, A. and Bernard, P. 1994. A kinematic self-similar rupture process for earthquakes, *Bulletin of the Seismological Society of America*, 84(4): 1216–1228.

- Hobiger, M., P. Y. Bard, C. Cornou, and N. Le Bihan, 2009, Single station determination of Rayleigh wave ellipticity by using the random decrement technique (RayDec), *Geophysical Research Letters*, 36, L14303.
- Hollender F., André M., Guyonnet-Benaize C., Cornou C., Caillot V and Bard P.-Y., 2011a, *Can high daily-variation of noise level alter results of ambient vibration H/V technique?*, 4<sup>th</sup> IASPEI/IAEE International Symposium: Effects of Surface Geology on Seismic Motion, August 23-26, 2011.
- Iervolino, I., Galasso, C., Cosenza, E. 2010. REXEL: Computer aided record selection for code-based seismic structural analysis. *Bulletin of Earthquake Engineering* 8:339-362.
- Jayaram, N. and Baker, J.W. 2009. Correlation model of spatially distributed ground motion intensities, *Earthquake Engineering and Structural Dynamics*, 38: 1687–1708.
- Jerram, J. (2007). “Seismic Liquefaction Prediction and Nonlinear Response in Soils: Application to the Grenoble Region”. PhD Dissertation, Université de Grenoble.
- Jongmans, D., K. Pitilakis, D. Demanet, D. Raptakis, J. Riepl, C. Horrent, G. Tsokas, K. Lontzetidis and P.-Y. Bard, 1998. EURO-SEISTEST: Determination of the geological structure of the Volvi basin and validation of the basin response, *Bull. seism. Soc. Am.*, **88-2**, 473-487.
- Kaneko, F., Kanemori, T., and Tonouchi, K., 1990, Low Frequency Shear Wave Logging in Unconsolidated Formations for Geotechnical Applications: Geophysical Applications for Geotechnical Investigations, Frederick L. Paillet and Wayne R. Saunders, Editors, 79-98
- Kaklamanos, J., Baise, L.G., Thompson, E.M., Dorfmann, L., 2015. Comparison of 1D linear, equivalent-linear, and nonlinear site response models at six KiK-net validation sites. *Soil Dyn. Earthq. Eng.* 69, 207–219.
- Kaklamanos, J., Bradley, B.A., Thompson, E.M., Baise, L.G., 2013. Critical Parameters Affecting Bias and Variability in Site-Response Analyses Using KiK-net Downhole Array Data. *Bull. Seismol. Soc. Am.* 103, 1733–1749.
- Kaklamanos, J., and B.A. Bradley, 2015. Evaluation of 1D nonlinear total-stress site response model performance at 114 KiK-net downhole array sites. 6th International Conference on Earthquake Geotechnical Engineering 1-4 November 2015 Christchurch, New Zealand.
- Kim, B., Hashash, Y.M., 2013. Site response analysis using downhole array recordings during the March 2011 Tohoku-Oki earthquake and the effect of long-duration ground motions. *Earthq. Spectra* 29, S37–S54.
- Kottke, Albert R., and Rathje, Ellen M. (2008) Technical Manual for Strata. PEER Report 2008/10. University of California, Berkeley, California.
- Kristek, J., P. Moczo, P.-Y. Bard, F. Hollender, S. Stripajová and Z. Margočová, 2015. Numerical study of site effects in a class of local sedimentary structures. NMEM2015 (International Workshop on Numerical Modeling of Earthquake Ground Motions: waves and ruptures, July 6-8, 2015, Smolenice (Slovakia).
- Kristek, J., P. Moczo, P.-Y. Bard, F. Hollender, S. Stripajová, Z. Margočová, E. Chaljub et C. Durand, 2015. Identification of key site features for site effect evaluation: extensive numerical sensitivity studies of sedimentary basin structures. Sigma deliverable D3-151, Mai 2015, 217 pages.
- Ktenidou O. et al. (2014) Ground motion uncertainty and variability in Euroseistest, Greece. SIGMA Deliverable D2-132.
- Ktenidou O.-J., Z. Rouselioti, N. Abrahamson, F. Cotton, K. Pitilakis, F. Hollender (2015). ‘Site effects and ground motion variability: traditional spectral ratios vs. GMPE residuals’, SSA Annual Meeting, Pasadena, 21-23 April
- Ktenidou, O.-J., F. Cotton, N. Abrahamson, And J. Anderson (2014). Taxonomy of kappa: A review of definitions and estimation approaches targeted to applications, *Seismol. Res. Lett.* 85, no. 1
- Ktenidou, O.-J., S. Drouet, F. Cotton, N. Abrahamson (2014). ‘Physics of kappa: insights from Euroseistest data’. Invited presentation at the 2nd European Conference on Earthquake Engineering & Seismology, Istanbul, 24-29 August, 2014.
- Kwok, A.O., Stewart, J.P., Hashash, Y.M., 2008. Nonlinear ground-response analysis of Turkey Flat shallow stiff-soil site to strong ground motion. *Bull. Seismol. Soc. Am.* 98, 331–343
- Lacoss, R.T., Kelly, E.J. and Toksöz, M.N., 1969, Estimation of seismic noise structure using arrays. *Geophysics* 34, 21–38.

- Laurendeau, A., F. Cotton, O. -J. Ktenidou, L -F. Bonilla, And F. Hollender (2013). Rock and stiff-soil site amplification: Dependencies on  $V_{S30}$  and kappa ( $\kappa_0$ ), *Bull. Seismol. Soc. Am.* 103, no. 6.
- Laurendeau, A., L. Foundotos, F. Hollender, et P.-Y. Bard, 2015. Correction of surface records of their site effect before developing GMPE: an alternative approach to get reference incident ground motion (application to KiK-net data). *Sigma / SINAPS@ deliverable SINAPS@-2015-V1-A1-T3-1*, 74 pages.
- Li, W. and D. Assimaki (2010). Site- and motion-dependent parametric uncertainty of site-response analyses in earthquake simulations. *Bulletin of the Seismological Society of America*, Vol. 100, 3, pp. 954-968
- Lin, P.-S., Chiou, B., Abrahamson, N., Walling, M., Lee, C.-T., and Cheng, C.-T. 2011. Repeatable Source, Site, and Path Effects on the Standard Deviation for Empirical Ground-Motion Prediction Models, *Bulletin of the Seismological Society of America*, 101(5): 2281–2295.
- Lorito, S., J. Selva, R. Basili, F. Romano, M.M. Tiberti, and A. Piatanesi. 2015. Probabilistic hazard for seismically induced tsunamis: accuracy and feasibility of inundation maps, *Geophys. J. Int.* 200 (1): 574-588. doi:10.1093/gji/ggu408
- Luzi, L., R. Puglia, F. Pacor, M. R. Gallipoli, D. Bindi, M. Mucciarelli (2011). Proposal for a soil classification based on parameters alternative or complementary to  $V_{s,30}$ . *Bulletin of Earthquake Engineering*, 9, 6, pp 1877-1898
- Mai, P.M., Spudich, P. and Boatwright, J. 2005. Hypocenter locations in finite-source rupture models, *Bulletin of the Seismological Society of America*, 95(3): 965–980.
- Manakou M., Raptakis D., Apostolodis P., Chavez Garcia F.J., Pitilakis K., 2007. The 3D geological structure of the Mygdonian sedimentary basin (Greece). *Procc. in 4<sup>th</sup> International Conference on Earthquake Geotechnical Engineering*, Paper No. 1686
- Manighetti, I., Campillo, M., Sammis, C., Mai, P.M. and King, G. 2005. Evidence for self-similar, triangular slip distributions on earthquakes: implications for earthquake and fault mechanics, *Journal of Geophysical Research*, 110(B05302): 1–25.
- Marzocchi W, Taroni M, Selva J (2015), Accounting for Epistemic Uncertainty in PSHA: Logic Tree and Ensemble Modeling, *Bulletin of the Seismological Society of America*, 105 (4), doi: 10.1785/0120140131
- Mazzieri, I., Stupazzini, M., Guidotti, R. and Smerzini, C. 2013. SPEED: Spectral elements in elastodynamics with Discontinuous Galerkin: a non-conforming approach for 3D multi-scale problems, *International Journal for Numerical Methods in Engineering*, 95(12): 991–1010.
- Mendoza, C. and Hartzell, S. H. 1988. Inversion for slip distribution using teleseismic P waveforms; North Palm Springs, Borah Peak, and Michoacan earthquakes, *Bulletin of the Seismological Society of America*, 78(3): 1092-1111.
- Maufroy E., Cruz-Atienza V.M., and Gaffet S. ( 2012). A robust method for assessing 3-D topographic site effects: a case study at the LSBB Underground Laboratory, France, *Earthquake Spectra* 28.3 1097-1115. doi:10.1193/1.4000050
- Maufroy E., Cruz-Atienza V.M., Cotton F., and Gaffet S. ( 2014b). Frequency-scaled curvature as a proxy for topographic site effect amplification and ground-motion variability, *Bull. Seism. Soc. Am.* 105.1 354-367. doi:10.1785/0120140089
- Maufroy, E., E. Chaljub, F. Hollender, J. Kristek, P. Moczo, P. Klin, E. Priolo, A. Iwaki, T. Iwata, V. Etienne, F. De Martin, N. Theodoulidis, M. Manakou, C. Guyonnet-Benaize, K. Pitilakis, and P.-Y. Bard, 2015a. Earthquake ground motion in the Mygdonian basin, Greece: the E2VP verification and validation of 3D numerical simulation up to 4 Hz, *Bull. seism. Soc. Am.*, v. 105, p. 1398-1418, doi:10.1785/0120140228.
- Maufroy, E. Chaljub, F. Hollender, P.-Y. Bard, J. Kristek, P. Moczo, F. De Martin, N. Theodoulidis, M. Manakou, C. Guyonnet-Benaize, K. Pitilakis and N. Hollard, 2015b. Validating the numerical simulation approach for ground motion prediction: General framework and latest lessons from the E2VP project. Invited theme lecture, 6ICEGE (6th International Conference on Earthquake Geotechnical Engineering) Christchurch, New-Zealand, November 1-4, 2015.
- Maufroy, E., E. Chaljub, F. Hollender, P.-Y. Bard, J. Kristek, P. Moczo, F. De Martin, N. Theodoulidis, M. Manakou, C. Guyonnet-Benaize, N. Hollard and K. Pitilakis, 2016. Numerical simulation AND ground motion prediction: Verification, validation and beyond - lessons from the E2VP project, submitted to *Soil Dynamics and Earthquake Engineering* (special 6ICEGE issue), February 2016.

- McGuire RK, WJ Silva, and CJ Costantino. 2001. Technical Basis for Revision of Regulatory Guidance on Design Ground Motions: Hazard-and Risk-Consistent Ground Motion Spectra Guidelines. NUREG/CR-6728, U.S. Nuclear Regulatory Commission, Washington, D.C
- McGuire RK, WJ Silva, and CJ Costantino. 2002. Technical Basis for Revision of Regulatory Guidance on Design Ground Motions: Development of Hazard-and Risk-consistent Seismic Spectra for Two Sites. NUREG/CR-6769, U.S. Nuclear Regulatory Commission, Washington, D.C.
- Menq, F.Y. (2003). "Dynamic Properties of Sandy and Gravelly Soils". PhD Dissertation, The University of Texas at Austin.
- Mignan, A., Wiemer S. and Giardini D. (2014), The Quantification of Low-Probability–High-Consequences Events: Part I. A Generic Multi-Risk Approach, *Natural Hazards*, 73, 1999-2022, doi: 10.1007/s11069-014-1178-4
- Morikawa, N., Kanno, T., Narita, A., Fujiwara, H., Okumura, T., Fukushima, Y., and Guerpinar, A. 2008. Strong motion uncertainty determined from observed records by dense network in Japan, *Journal of Seismology*, 12(4): 529–546.
- Mozco, P., Kristek, J. and Galis, M. 2014. *The Finite-Difference modelling of earthquake motions: waves and ruptures*, Cambridge University Press.
- Nakamura Y., 1989, A method for dynamic characteristics estimation of subsurface using microtremor on the ground surface, *Quarterly Report Railway Tech. Res. Inst.*, 30-1, 25-33.
- Newhall, C.G. and R. P. Hoblitt. 2002. Constructing event trees for volcanic crises, *Bull. Volcanol.*, 64, 3–20.
- Paolucci, R., Mazzieri, I., Smerzini, C. and Stupazzini, M. 2014. Physics-based earthquake ground shaking in large urban areas, in *Perspectives on European Earthquake Engineering and Seismology, Second European Conference on Earthquake Engineering and Seismology*, Istanbul, 24-29 August 2014.
- Papazachos B. C., Mountrakis D., Psilovolikos A., and Leventakis G., 1979. Surface Fault Traces and Fault Plane Solutions of the May-June 1978 Major Shocks in the Thessaloniki Area, Greece, *Tectonophysics* 53, 171-183.
- Papazachos, B. C., Papaioannou, C., Papazachos, C. B. and Savvaidis, A. S. 1997. *Atlas of isoseismal maps for strong shallow earthquakes in Greece and surrounding area (426BC - 1995)*, Ziti Publications, Thessaloniki, pp 192.
- Papazachos, B.C., Comninakis, P.E., Karakaisis, G.F., Karakostas, B.G., Papaioannou, C., Papazachos, C.B. and Scordilis, E.M. 2000. *A catalogue of earthquakes in Greece and surrounding area for the period 550BC-1999*, Publ. Geophys. Laboratory, University of Thessaloniki, 1, 333pp.
- Papazachos, B.C., Comninakis, P.E., Scordilis, E.M., Karakaisis, G.F. and Papazachos, C.B. 2010. *A catalogue of earthquakes in the Mediterranean and surrounding area for the period 1901 – 2010*, Publ. Geophys. Laboratory, University of Thessaloniki.
- Papazachos, C.B. and Nolet, G. 1997. P and S deep velocity structure of the Hellenic area obtained by robust nonlinear inversion of travel times, *Journal of Geophysical Research*, 102: 8349–8367
- Parolai, S., 2013. CHAPTER 14: Investigation of Site Response in Urban Areas by using Earthquake Data and Seismic Noise (S. Parolai) in **New Manual of Seismological Observatory Practice (NMSOP-2) (nmsop.gfz-potsdam.de)** PDF. - DOI:10.2312/GFZ.NMSOP-2\_ch14
- Parra, E. 1996. *Numerical Modeling of Liquefaction and lateral Ground Deformation including Cyclic Mobility and Dilative Behavior in Soil Systems*. PhD Dissertation, Department of Civil Engineering, Rensselaer polytechnic Institute, Try, NY.
- Perron, V., F. Hollender, P.-Y. Bard, C. Gélis et C. Guyonnet-Benaize, 2015. Utilité de l'instrumentation in situ : recommandations et exemples d'application pour l'évaluation des effets de site dans un contexte de sismicité faible à modérée, Actes du 9<sup>ème</sup> colloque national AFPS2015, 30 Novembre – 2 Décembre 2015, Paris-Marne-la-Vallée, 11 pages.
- Pitilakis, K., and Anastasiadis, A., 1998. Soil and site characterization for seismic response analysis, *Proceeding of the XI ECEE*, Paris 6-11 Sept. 1998, *Inv.Lectures*, pp.65-90.
- Pitilakis, K., Franchin, P., Khazai, B., Wenzel, H. (eds) 2014a. *SYNER-G: Systemic Seismic Vulnerability and Risk Assessment of Complex Urban, Utility, Lifeline Systems and Critical*

*Facilities, Methodology and Applications, Geotechnical, geological and earthquake engineering*, vol 31. Springer, Dordrecht. ISBN 978-94-017-8834-2

- Pitilakis, K., Riga, E. and Anastasiadis, A. 2015. New design spectra in Eurocode 8 and preliminary application to the seismic risk of Thessaloniki, Greece, In: Ansal A., Sakr M. (eds.), *Perspectives on Earthquake Geotechnical Engineering, Series: Geotechnical, Geological and Earthquake Engineering*, Vol. 37, Springer Netherlands, pp 45-91.
- Pitilakis, K., Riga, E., Makra, K., Gelagoti, F., Ktenidou, O-J., Anastasiadis, A., Pitilakis, D., and Izquierdo Flores C.A. 2014b. *Deliverable D11.5 Code cross-check, computed models and list of available results - AUTH contribution*, Network of European Research Infrastructures for Earthquake Risk Assessment and Mitigation (NERA), Seventh Framework Programme, EC project number: 262330
- Pitilakis, K., Z. Roumelioti, D. Raptakis, M. Manakou, K. Liakakis, A. Anastasiadis and D. Pitilakis (2013). The EUROSEISTEST strong ground motion database and web portal, *Seism. Res. Lett.* 84(5), 796-804.
- Prevost, J.-H. 1985. A Simple Plasticity Theory for Frictional Cohesionless Soils. *Soil Dynamics and Earthquake Engineering* 4(1): 9-17.
- Raptakis, D., Theodulidis N., and Pitilakis K. (1998) Data Analysis of the Euroseistest Strong Motion Array in Volvi (Greece): Standard and Horizontal-to-Vertical Spectral Ratio Techniques. *Earthquake Spectra*: February 1998, Vol. 14, No. 1, pp. 203-224.
- Régnier, J., L.F. Bonilla, P.Y. Bard, H. Kawase, E. Bertrand, F. Hollender, M. Marot and D. Sicilia (2015a). PRENOLIN Project: a benchmark on numerical simulation of 1D non-linear site effect. 1 – verification phase based on canonical cases. 6ICEGE ((6th International Conference on Earthquake Geotechnical Engineering) Christchurch, New-Zealand, November 1-4, 2015.
- Régnier, J., L.F. Bonilla, P.Y. Bard, H. Kawase, E. Bertrand, F. Hollender, M. Marot, D. Sicilia and A. Nozu (2015b). PRENOLIN Project: a benchmark on numerical simulation of 1D non-linear site effect. 2 – Results of the validation phase. 6ICEGE (6th International Conference on Earthquake Geotechnical Engineering) Christchurch, New-Zealand, November 21-4, 2015.
- Régnier, J., H. Cadet and P.-Y. Bard, 2016a. Empirical quantification of the impact of non-linear soil behavior on site response. *Bull. Seism. Soc. Am.*, under revision, March 2016.
- Régnier, J., L.F. Bonilla, P.-Y. Bard, E. Bertrand, F. Hollender, H. Kawase, D. Sicilia, M. Marot, D. Assimaki, A. Amorosi, D. Boldini, A. Chiaradonna, F. Demartin, M. Ebrille, G. Falcone, E. Foerster, S. Foti, C. Gélis, G. Gazetas, J. Gincery, N. Glinsky, J. Harmon, Y. Hashash, S. Iai, B. Jeremic, S. Kramer, S. Kontoe, J. Kristek, G. Ianzo, A. di Lernia, F. Lopez-Caballero, E.D. Mercerat, P. Moczo, S. Montoya-Noguera, M. Musgrove, A. Nieto-Ferro, A. Pagliaroli, F. Pisano, A. Richterova, S. Sajana, M.P. Santisi d'Avila, J. Shi, F. Silvestri, G. Tropeano, L. Vernucci, K. Wanabe, L. Chen, A. Ghofrani and G. McAllister, 2016b. International benchmark on numerical simulations for 1D, non-linear site response (PRENOLIN): verification phase based on canonical cases. *Bull. seism. Sc. Am.*, accepted with minor revision.
- Renalier F. and Endrun B., (2009), Comparative analysis of classical measurements and newly developed methods, NERIES program. JRA4, Task C, Deliverable D6.
- Renalier, F., (2010), Caractérisation sismique de sites hétérogènes à partir de méthodes actives et passives: variations latérales et temporelles, Ph.D. Thesis, Joseph Fourier University, Grenoble, 224 pages.
- Roble, C.J., W.J. Silva, G.R. Toro, And N. Abrahamson (1996). Variability in Site-Specific Seismic Ground-Motion Predictions. Uncertainty in the Geologic Environment: From Theory to Practice, Proceedings of "Uncertainty '96" ASCE Specialty Conference, Edited by C.D. Shackelford, P.P. Nelson, and M.J.S. Roth, Madison, WI, Aug. 1-3, pp. 1113-1133.
- Roble, C., & Chiou, B. (2004, March). A proposed Geindex model for design selection of non-linear properties for site response analysis. In International workshop on uncertainties in nonlinear soil properties and their impact on modeling dynamic soil response. PEER Headquarters, UC Berkeley (pp. 18-19).
- Rodriguez-Marek A., F. Cotton, N. A. Abrahamson, S. Akkar, L. Al Atik, B. Edwards, G. A. Montalva, And H. M. Dawood (2013) A Model for Single-Station Standard Deviation Using Data from Various Tectonic Regions, *Bulletin of the Seismological Society of America*, Vol. 103, No. 6, pp. 3149-3163.

- Roumelioti, Z., Theodulidis, N. and Kiratzi, A. 2007. The 20 June 1978 Thessaloniki (Northern Greece) earthquake revisited: slip distribution and forward modelling of geodetic and seismological observations, *4<sup>th</sup> International Conference on Earthquake Geotechnical Engineering*, June 25-28, Paper no. 1594.
- Rubinstein, J. L., 2011. Nonlinear site response in medium magnitude earthquakes near Parkfield, California. *Bulletin of the Seismological Society of America*, 101(1), 275-286.
- Sandikkaya, M.A, Akkar, S. And P-Y Bard (2013). A Nonlinear Site-Amplification Model for the Next Pan-European Ground-Motion Prediction Equations. *Bull Seismol Soc Am* 103, No. 1, pp. 19–32.
- Schnabel, P.B., Lysmer, J., Seed, H.B., 1972. SHAKE : a computer program for earthquake response analysis of horizontally layered sites (report). Earthquake Engineering Research Centre, Berkeley, California.
- Sèbe, O., P.-Y. Bard, et J. Guilbert, 2003. Estimation des effets de site par déconvolution aveugle multicanaux, application aux données accélérométriques en forage de Garner Valley. *VI<sup>ème</sup> Colloque National de l'AFPS, Ecole Polytechnique, 1-3 Juillet 2003, Vol. I, 157-164.*
- Sèbe, O., P.-Y. Bard and J. Guilbert, 2005. Single station estimation of seismic source time function from coda waves: the Kursk's disaster, *Geophys. Res. Lett.*, Vol. 32, No. 14, L14308, doi:10.1029/2005GL022799, 2005.
- Seed, H.B. and I.M. Idriss, 1969. Influence of soil conditions on ground motions during earthquakes, *J. Soil Mech. and Found. Div.*, ASCE, 95 (SM1)
- Seed H.B., Idriss I.M., 1970. Soil Moduli and Damping Factors for Dynamic Response Analyses, Report N°. EERC 70.10, Earthquake Engineering Research Center, University of California, Berkeley, December, 61p.
- Seed, R. B., Cetin, K. O., Moss, R. E. S., Kammerer, A., Wu, J., Pestana, J., Riemer, M., Sancio, R. B., Bray, J. D., Kayen, R. E., and Faris, A. 2003. *Recent advances in soil liquefaction engineering: A unified and consistent framework*. Keynote presentation, 26<sup>th</sup> Annual ASCE Los Angeles Geotechnical Spring Seminar, Long Beach, CA.
- Selva, J., R. Tonini, I. Molinari, M. M. Tiberti, F. Romano, A. Grezio, D. Melini, A. Piatanesi, R. Basili, S. Lorito, 2015. Quantification of source uncertainties in Seismic Probabilistic Tsunami Hazard Analysis (SPTHA). *Submitted to Geophysical Journal International*.
- SESAME European research project WP12, Guidelines for the implementation of the H/V spectral ratio technique on ambient vibrations –measurements, processing and interpretation– Deliverable D23.12. December 2004.
- Seyhan, E. And J. P. Stewart (2014) Semi-Empirical Nonlinear Site Amplification from NGA-West 2 Data and Simulations. *Earthquake Spectra* (in press)
- Smerzini, C. and Villani, M. 2012. Broadband numerical simulations in complex near field geological configurations: the case of the MW 6.3 2009 L'Aquila earthquake, *Bulletin of the Seismological Society of America*, 102 (6): 2436–2451
- SRM-LIFE Research project, Deliverable 4, 2004. *Geotechnical maps of the area. Geotechnical classification*. (in Greek) Collaboration of the Laboratory of Soil Mechanics, Foundation and Geotechnical Earthquake Engineering of AUTH and the Institute of Engineering Seismology and Earthquake Engineering
- SRM-LIFE Research project, Deliverable 5, 2005. *Technical report presenting 1D and 2D seismic response analyses*. (in Greek) Collaboration of the Laboratory of Soil Mechanics, Foundation and Geotechnical Earthquake Engineering of AUTH and the Institute of Engineering Seismology and Earthquake Engineering
- Stacey, R. 1988. Improved transparent boundary formulations for the elastic-wave equation, *Bulletin of the Seismological Society of America*, 78(6): 2089–2097.
- Stewart, J., Kwok, A., 2009. Nonlinear Seismic Ground Response Analysis: Protocols and Verification Against Array Data. PEER Annu. Meet. San Franc.-Present. 84.
- Stewart, J. P., J. Douglas, M. Javanbarg, Y. Bozorgnia, N. A. Abrahamson, D. M. Boore, K. W. Campbell, E. Delavaud, M. Erdik, And P. J. Stafford (2014). Selection of ground motion prediction equations for the global earthquake model, *Earthquake Spectra* (in press).

- Stewart, J.P., A.O-L Kwok, Y.M.A. Hashash, N. Matasovic, R. Pyke, Z. Wang and Z. Yang, 2008. Benchmarking of Nonlinear Geotechnical Ground Response Analysis Procedures, Pacific Earthquake Engineering Research Center. *University of California, Berkeley*.
- Stokoe K.H. II, Wright S.G., J.A. Bay and J.M. Roesset., (1994). Characterization of geotechnical sites by SASW method, *Geophysical Characterization of Sites*, R.D. Woods Ed.: 15-25.
- Stupazzini, M., Paolucci, R. and Igel, H. 2009. Near-fault earthquake ground-motion simulation in Grenoble Valley by high-performance spectral element code, *Bulletin of the Seismological Society of America*, 99(1): 286–301.
- Thio, H.K., P. Somerville, and J. Polet. 2010. *Probabilistic tsunami hazard in California*. Pacific Earthquake Engineering Research Center, PEER Report 2010/108, University of California, Berkeley.
- Toro, G. R. (1995) Probabilistic models of site velocity profiles for generic and site-specific ground-motion amplification studies. Technical Rep. No.779574, Brookhaven National Laboratory, Upton, N.Y.
- UNISDR, 2015. *Making Development Sustainable: The Future of Disaster Risk Management*. Global Assessment Report on Disaster Risk Reduction. Geneva, Switzerland: United Nations Office for Disaster Risk Reduction (UNISDR).
- US NUCLEAR REGULATORY COMMISSION. (2001). Technical basis for revision of regulatory guidance on design ground motions: hazard-and risk-consistent ground motion spectra guidelines. Report NUREG/CR-6728.
- US NUCLEAR REGULATORY COMMISSION. (2002). Technical basis for revision of regulatory guidance on design ground motions: Development of hazard- and risk-consistent seismic spectra for two sites, NUREG/CR-6769.
- Van Houtte, C., S. Drouet, And F. Cotton (2011). Analysis of the origins of  $\kappa$  (Kappa) to compute hard rock to rock adjustment factors for GMPEs, *Bull. Seismol. Soc. Am.* 101, no. 6, 2926–2941.
- Vucetic, M., and R. Dobry, 1991. Effect of soil plasticity on cyclic response, *ASC Journal of Geotechnical Engineering*, 117(1), p. 89-109, 1991.
- Walling, M., Silva, W., & Abrahamson, N. (2008). Nonlinear site amplification factors for constraining the NGA models. *Earthquake Spectra*, 24(1), 243-255.
- Wathelet, M., (2008). An improved neighborhood algorithm: parameter conditions and dynamic scaling, *Geophysical Research Letters*, 35.
- Weatherill, G., Esposito, S., Iervolino, I., Franchin, P. and Cavalieri, F. 2014. *Framework for seismic hazard analysis of spatially distributed systems*, In SYNER-G: Systemic Seismic Vulnerability and Risk Assessment of Complex Urban, Utility, Lifeline Systems and Critical Facilities, Methodology and Applications, Chapter: 3, Publisher: Springer Netherlands, Editors: K. Pitilakis, P. Franchin, B. Khazai, H. Wenzel, pp.57-88
- Wells, D. L. and Coppersmith, K. J. 1994. New empirical relationships among magnitude, rupture length, rupture width, rupture area, and surface displacement, *Bulletin of the Seismological Society of America*, 84(4): 974-1002.
- Woods R. D. and K.H. Stokoe (1985). Shallow Seismic Exploration in Soil Dynamics. Richart Commemorative Lectures, ASCE, Detroit Michigan, R. D. Woods, Ed. 1985, pp. 120-156.
- Yang, Z. 2000. *Numerical Modeling of Earthquake Site Response Including Dilation and Liquefaction*. Ph.D. Dissertation, Dept. of Civil Engineering and Engineering Mechanics, Columbia University, New York, NY.
- Yee, E., Stewart, J.P., Tokimatsu, K., 2013. Elastic and large-strain nonlinear seismic site response from analysis of vertical array recordings. *J. Geotech. Geoenvironmental Eng.* 139, 1789–1801.
- Zalachoris, G., Rathje, E.M., 2015. Evaluation of One-Dimensional Site Response Techniques Using Borehole Arrays. *J. Geotech. Geoenvironmental Eng.* 04015053.
- Zhao J.X., Zhang J., Asano A., Ohno Y., Oouchi T., Takahashi T., Ogawa H., Irikura K., Thio H.K., Somerville P.G., Fukushima Y. and Fukushima Y. (2006). Attenuation relations of strong ground motion in japan using site classification based on predominant period. *Bulletin of the Seismological Society of America*, vol. 96, n° 3, p. 898-913.

Zhang, J., Andrus, R., and Juang, C. (2005). "Normalized Shear Modulus and Material Damping Ratio Relationships." *J. Geotech. Geoenviron. Eng.*, 10.1061/(ASCE)1090-0241(2005)131:4(453), 453-464.

## 6 Appendix A - Overview of in-situ site characterization surveys (from Ameri et al., 2015)

This section will discuss about the need of site geological, geophysical and geotechnical characterization and site seismological instrumentation. Of course, the level of complexity of characterization/instrumentation depends on the choice of site effect evaluation method, but characterization/instrumentation is also mandatory to get the minimum information to help on the choice of site evaluation method itself, the whole process is therefore iterative.

The minimum level of site characterization is surely the determination of the  $V_{S30}$  value beneath the site. Then, the determination of the fundamental frequency of the site,  $f_0$ , usually easily archived, is useful. Then, increasing in the level of complexity in the used method, the whole **1D  $V_S$  profile** (and associated parameters<sup>3</sup>) down to the bedrock including the evaluation of  **$V_S$  within the bedrock**, is mandatory. Then, depending 1/ on the probability of occurrence of non-linearity for strong motion (which depends on the overall considered seismic hazard and – as a preliminary proxy – the minimum  $V_S$  value within the  $V_S$  profile) and 2/ the possible aggravation of site effect caused by 2D or 3D geometry, both or either **non-linear properties** of soil and whole **2D/3D  $V_S$  distribution** (and associated parameters) should be achieved. In parallel, as far the chosen site effect evaluation method implies a computation of the amplification of the site effect by numerical simulations, evaluation of **empirical amplification** obtained by seismological instrumentation (through SSR measurements) is mandatory if we want to reduce uncertainties associated to site  $V_S$  distribution evaluation. Finally, if the chosen method implies the use of host-to-target adjustment, then the evaluation of **kappa** value of bedrock, also achievable by seismological instrumentation, is highly recommended in order to reduce uncertainty.

Hence, whatever approach (detailed in the previous chapter) is chosen for the consideration of site effects, site characterization is a crucial early stage to get the necessary information. The implementation of a geological model is often an important step to feed numerical models; it will typically be conducted based on the knowledge of the site at a scale depending on the size of considered basin from 1 km<sup>2</sup> to few tens of km<sup>2</sup>. Site investigations may be complemented using in-situ and laboratory testing. Do we deal with a homogeneous or a heterogeneous site is maybe one of the fundamental issues to be addressed before performing specific investigations.

The aim of investigation of site effect is to find answers to such questions as what is the geometry of the site, does the site present non-linear soil behavior, what is the spatial

---

<sup>3</sup> Actually, we generally need 5 profiles to perform a simulation:  $V_S$ ,  $V_P$ , density,  $Q_S$  and  $Q_P$ , nevertheless, the  $V_S$  profile is the one that have the major impact on the results of simulation.  $Q$  factors are very difficult to measure (if not impossible with the current characterization methods) and we usually use scaling relation deriving  $Q_S$  and  $Q_P$  from  $V_S$  and  $V_P$  and the corresponding uncertainty impact should be assess by simulation sensitivity studies. Basically,  $V_P$  profile accuracy will predominately have an impact on vertical amplification and should also be carefully determine as far this issue is important for the corresponding study.

variability of the different characteristics of the soil, etc. In order to obtain answers, different investigation techniques (in situ and in laboratory) exist, depending on what it is desired to investigate.

In any case, it is however important to emphasize that from the proper implementation of these investigations will depend the reliability of the site response calculation, and by extension the reduction of uncertainties.

The following paragraphs provide an overview of different techniques of investigations.

## **6.1 GEOLOGICAL, GEOPHYSICAL AND GEOTECHNICAL CHARACTERIZATION**

We will not review here all the possible methods that can help in the site characterization, we will focus on the ones that are particularly associated to the site effect phenomenology and the ones for which special enhancement efforts were done within the SIGMA and CASHIMA program.

### **6.1.1 Basic preliminary studies**

Of course, the first step of any site effect study should be a synthesis of all previous available “material”. That starts from studying existing geological map at regional and local scale, the existing borehole information (through [infoterre.brgm.fr](http://infoterre.brgm.fr) in France for example), the possible existing reflection seismic profiles (lot of profiles were done in France in 70th and 80th and raw data are in public domain after 10 years), etc.

Very often in France, site effect studies have to be done on site where facilities already exist and previous local geotechnical studies are available, so, the preliminary study could be done at two scales; local and near-regional one.

The main objective of this study is to get an idea of the overall quality of geological formation beneath the site (are we on rock or soil?) and the overall geometry of geological formation (are the different geological formation arranged in horizontal strata or does exist any suspicion on more complex geometry, as synclinal, graben-like basin, old valley or canyon that were filled with soft material<sup>4</sup>?).

Cross-hole measurements may have already been done on sites and reports could be available. Nevertheless, our own experience showed that some of this test can be completely wrong (with sometimes more than a 2 factor of error) and unless some strong reliability proofs exist, we strongly recommend not using it as a reliable material.

### **6.1.2 H/V method**

Regardless of the site effect evaluation method, we strongly recommend the implementation of “Ambient Vibration H/V measurements”. This method is rather easy and cheap to implement and can provide information of the site effect fundamental frequency values, and also provide information about the site geometry.

---

<sup>4</sup> This configuration is frequent in South-East of France due to the numerous “incisions events” that occurred during the Miocene period, as the “Messinian salinity crisis”.

This method consists in measuring the ambient noise in continuous mode with velocimeters (never accelerometers!) and then computing the ratio between the horizontal and vertical frequency content (Nakamura, 1989). In late 90<sup>th</sup> and early 2000<sup>th</sup>, this method was often used without care and erroneous interpretations were often produced. Thanks to the SESAME effort (SESAME 2004), guidelines were produced and now this technique is reliably and robust.

We obviously recommend following the SESAME guidelines, but we wish to add other few recommendations based on our own experience of H/V implementation on French nuclear site contexts. Indeed, the surveys made within the SESAME program and on which the associated recommendations were based, were mainly done in urban context. The overall ambient vibration on industrial site, often built far from large cities, may be quite different.

1. Before implementing large number of measuring points, start to perform a measurement on whole 24 hour period. Then check if there are differences on the H/V curve between night and day. In some (rare but possible) cases, the response may be different (Hollender et al. 2011). In those cases, choose the best time period to implement measurement.
2. When possible (that is to say in any case except in case of concrete or pavement), bury the sensor for the measurement.
3. Perform measurement on longer periods than the ones proposed in Sesame Guidelines, especially on “low frequency” sites ( $f_0 < 1$  Hz), at least one hour, two if possible.
4. Use large time-windows in the signal processing that the one proposed in Sesame Guidelines (example: 180 to 240 second time windows for low frequency” sites allow to decrease standard deviation at low frequency and enhance the peak resolution).

H/V measurement can provide the fundamental frequency of site effect on the studied site (but never its amplitude) but can also be used to assess the depth of bedrock and its possible variation when the technique is implemented along profile. In this case, do not make over-interpretation concerning H/V frequency in the border of basins: H/V measurement interpretation is based on a 1D physics and when the bedrock slope is too high, the measured  $f_0$  may be lower than what the actual bedrock depth is. Guillier et al. 2006 demonstrated this feature with simulation and we already encounter this situation with real data.

### **6.1.3 Soil class, $V_{s30}$ and velocity profile determination**

In seismic site response analysis, a key role is played by the shear-wave velocity model of the site since shear wave propagation controls ground motion amplification phenomenon. From the simplest site effect evaluation methods (that need a soil class or  $V_{s30}$  value) to the most elaborated ones (that need a whole 3D  $V_s$  distribution) a  $V_s$  measurement is mandatory.

The shear wave velocity distribution can be retrieved either with **invasive tests**, such as the cross-hole test or the down-hole test, or **non-invasive methods**. Invasive methods are usually considered more reliable than the non-invasive ones because they are based on the interpretation of local measurements of shear wave traveltimes. They also provide a good resolution. However these methods require the drilling of at least one borehole making them quite expensive. Hence, they are usually adopted in projects of relevant importance.

Nevertheless, the real reliability of these methods could also sometimes be over-estimate. Non-invasive techniques provide cost efficient alternatives. Specifically, in the last decades the methods based on the analysis of surface wave propagation are getting more and more established (Foti et al., 2011). These methods can be implemented with a low budget without impacting the site. However, they need a processing and inversion of the experimental data that are much more time and computational consuming and should be carried out carefully. The surface wave inversion problem is indeed non-linear, mixed determined and it is affected by solution non-uniqueness. These factors could induce interpretation ambiguities of the final shear-wave velocity model (Foti et al., 2009). In the literature different techniques for both the processing (McMechan and Yedlin, 1981; Park et al., 1999, Nolet and Panza, 1976) and the inversion (Lai, 1998; Socco and Boiero, 2008; Socco et al., 2009; Xia et al., 1999) of the experimental data have been proposed. These techniques can be considered reliable if expert users apply them. However, because of the cost and time effectiveness of surface wave methods and the availability of “black-box” software, surface wave methods are being increasingly adopted also by inexpert users. This leads often to strongly erroneous results that corollary induces a general lack of confidence in non-invasive methods in a part of the earthquake engineering community.

The SIGMA and CASHIMA programs pay a particular attention to these issues through the InterPACIFIC (Intercomparison of methods for site parameter and velocity profile characterization) subproject that is aiming at the comparison of the main techniques for surface wave methods (intra-methods comparison) as well as the comparison between such non-invasive techniques and the invasive ones (inter-methods comparison) in order to evaluate the reliability of the results obtained with such different techniques. These comparisons help us to improve the understanding on those theoretical and practical issues whose differences in the implementation could impact the results. As a consequence, the suggestion of guidelines for a good practice for non-expert users is another challenging task of the InterPACIFIC project.

More details on invasive and non-invasive technics are given in Appendix B.

[In the final version of the present report, the conclusion and main points of the ongoing InterPacific project will be included, we mention here in the current version the main trends].

#### **6.1.3.1 Invasive methods**

These methods are usually considered as reliable methods. Nevertheless, we showed within the InterPacific project (Garofalo et al., 2016a,b), where several different invasive technics were implemented by several different companies in three different sites, that the standard deviation between whole measurements is clearly higher than expected. Some other recent works that aimed to produce a synthesis of previous geotechnical test on industrial sites showed that sometime, results are not only imperfect but completely incoherent (with more than a 2 factor between the produced value and the real value). Even within the InterPacific project, we also noted completely incoherent results (downhole tests made by one company) that we considered as outliers and that we did not include in statistics (see Figure 63).

Our recommendation is to use results of invasive methods with care, being conscious about the associated errors bars, not as perfect and definitive results.

In order to qualify tools or companies before making a measurement on a new site, the InterPacific project let the possibility to perform testing measurement on 2 sites (hard rock and stiff soil) which are now widely documented.

We also mention the existence of “PSSL method” that produced robust results (within the errors bars of usual cross-hole and down-hole measurements). PSSL is widely used in USA and Japan, but not yet in France. It allows in-situ measurement within a single hole to rather high depth (several hundreds of meters) where cross-hole or down-hole measurement are no more efficient (respectively due to hole trajectory uncertainties or energy losses) (see more details en Appendix B). In order to perform good PSSL, care should be taken for the casing grouting.

### **6.1.3.2 Non-invasive methods**

The recommendation for non-invasive method implementation will be a stand-alone outcome of the SIGMA program.

The blind-test step of InterPacific project showed that when the provided velocity profiles are considered within a realistic depth ranges (that is to say that are coherent with maximum wavelength available with the uses acquisition geometry), the results are more satisfactory than initially expected. Standard deviation of  $V_S$  value, when considered at a given depth, is still higher than for invasive technics. But paradoxically and surprisingly, non-invasive technics provided  $V_{S30}$  value with a comparable standard deviation than invasive technics (and even lower for one site).

### **6.1.3.3 Invasive vs. non-invasive methods**

Of course, we will not recommend choosing either invasive either non-invasive methods: both are complementary. Non-invasive methods have a low vertical resolution. For example, they are not able to identify with a sufficient vertical resolution some feature like the low velocity layer on the Grenoble test-site (that is so important for non-linear simulation of this site). Nevertheless, for more global parameter (like  $V_{S30}$ ) or even for 1D transfer function estimation based on computed velocity profiles, they provide robust and reliable results.

On a given site, we recommend to perform both technics. At least one borehole triplet can be made to perform reliable cross-hole measurements down to 30 or 50 m. One borehole can be prolonged to higher depth (if possible down to bedrock) and be used for PSSL measurement. In addition, one or several profiles (if 2D or 3D model are needed) based on non-invasive methods can be implemented for a better uncertainty evaluation and lateral variation estimation. Invasive methods do not have real penetration depth limitation if the chosen arrays are large enough. Hence, they can be a mandatory complement for site where the bedrock depth is too large to allow invasive measurements down to the bedrock with reasonable costs.

In any case, it is worth to complete “invasive geophysical methods” like cross-hole measurements and “non-invasive” methods by geotechnical boreholes for soil identification (grain size distribution, Atterberg limits, moisture content...), or even simple sample lithological description in order to control the verisimilitude of results.

Note also that the velocity of bedrock is an important parameter for site response estimation. If this velocity is not measurable beneath the site, complementary measurement should be conducted where the bedrock is outcropping in the side of the basin, taking into account in the whole interpretation that the bedrock may be weather near the surface and that the velocity may increase with depth.

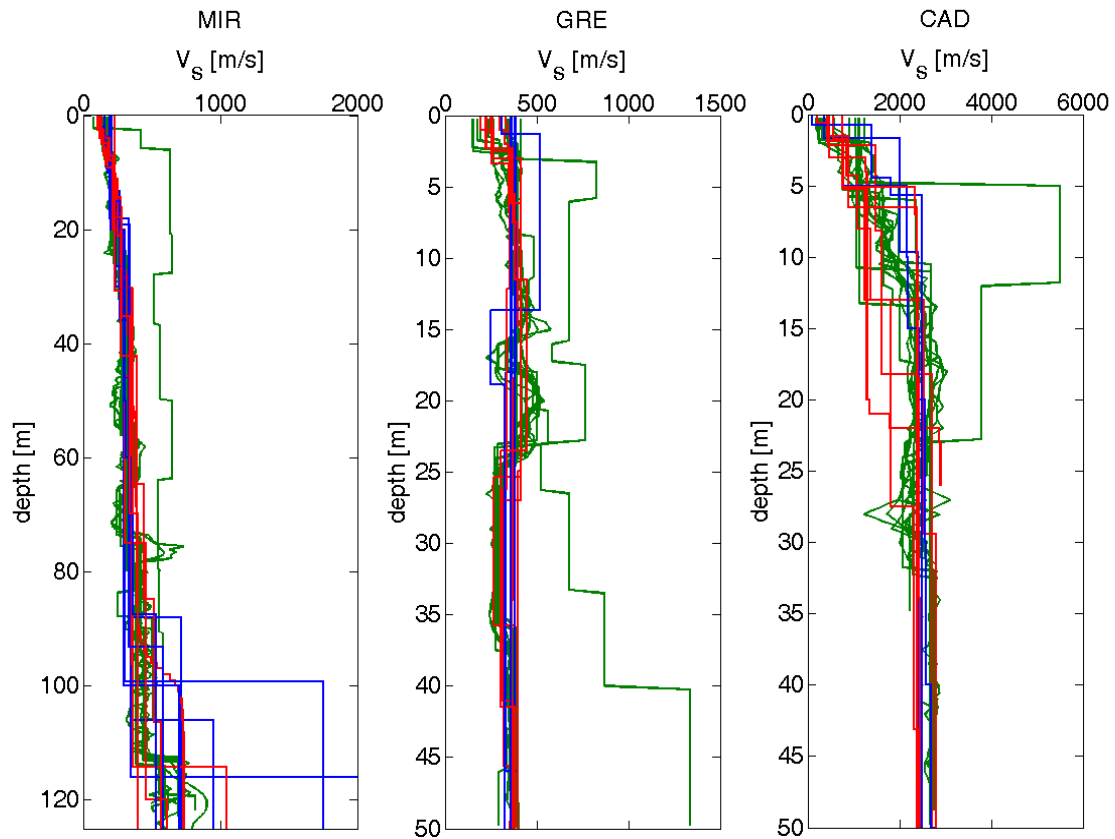


Figure 63: Main results of InterPacific project (Garofalo et al., 2016a,b): Comparison among the  $V_s$  profiles obtained with invasive methods (in green) and non-invasive methods, distinguishing between those profiles related to the analysis of active and passive seismic data (in red) and only passive seismic data (in blue). The comparison is performed for each site: Mirandola (MIR, in the left panel), Grenoble (GRE, in the central panel) and Cadarache (CAD, in the right panel).

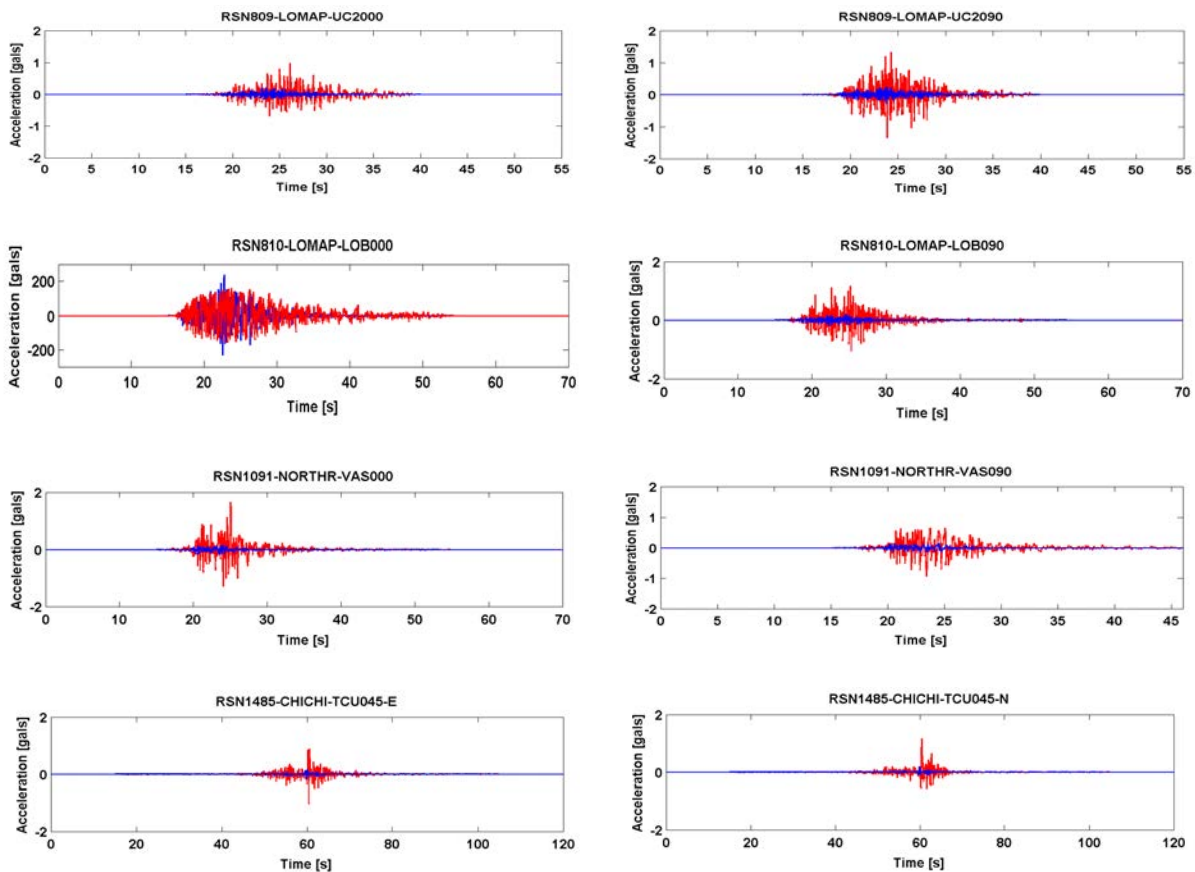
## 7 Appendix B: Ground motion records, Amplitude Fourier Spectra and Transfer Functions used on numerical approaches.

This appendix presents the different acceleration records on rock and soil fitted to the 5000 years return period at the Euroseistest for the ten selected earthquakes, both horizontal components and for the linear and nonlinear cases after wave propagation via NOAH.

Also, the Fourier Amplitude Spectra and the Fourier Transfer Function for each acceleration record are shown below, and based on them, the mean transfer function for the linear and nonlinear cases were derived and used on this study to obtain the uniform hazard spectra on soil for the linear and nonlinear case using numerical approaches (Level 1c and Level 2a).

### 7.1 LINEAR CASE (LEVEL 1C)

#### 7.1.1 Acceleration records.



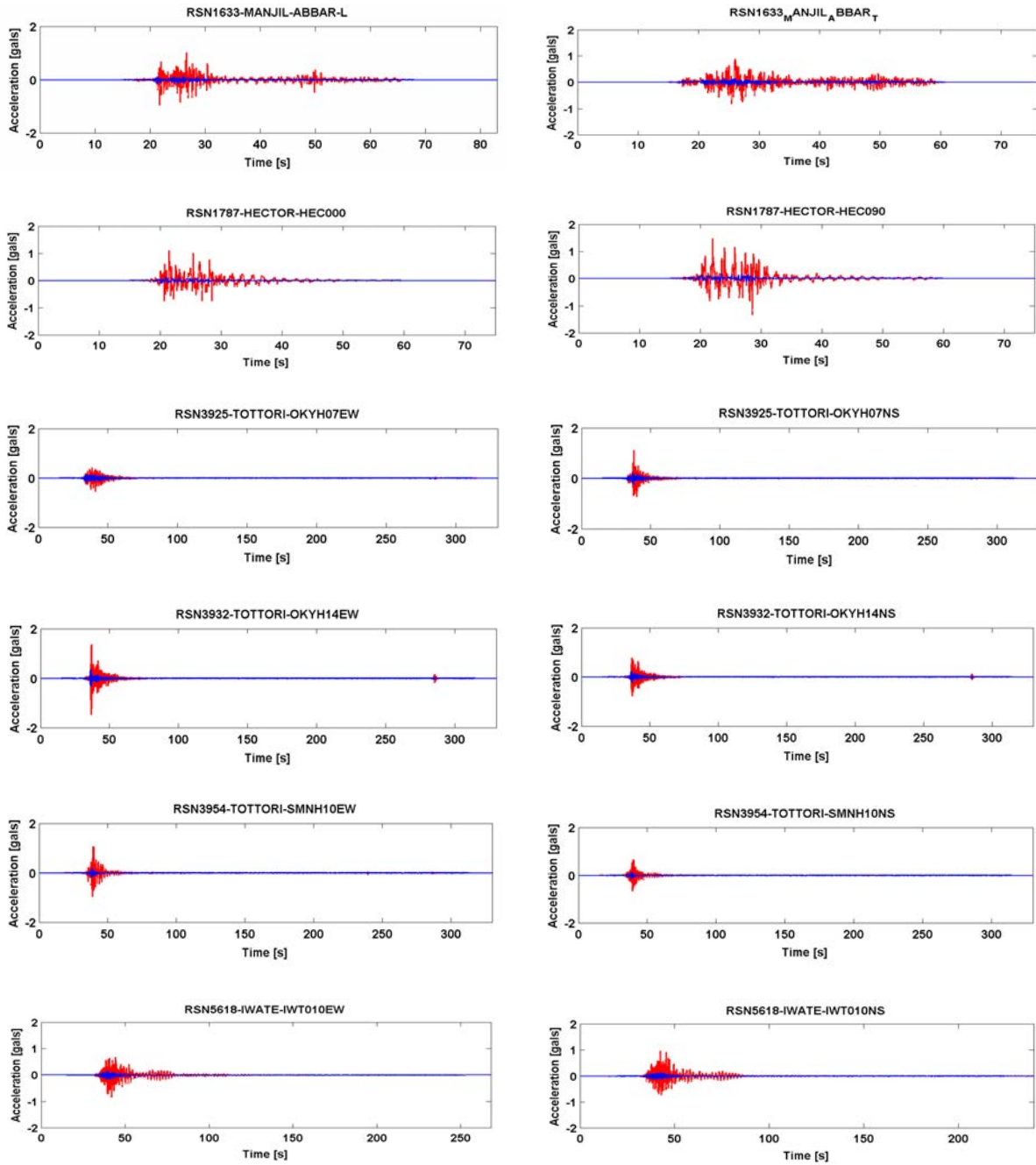
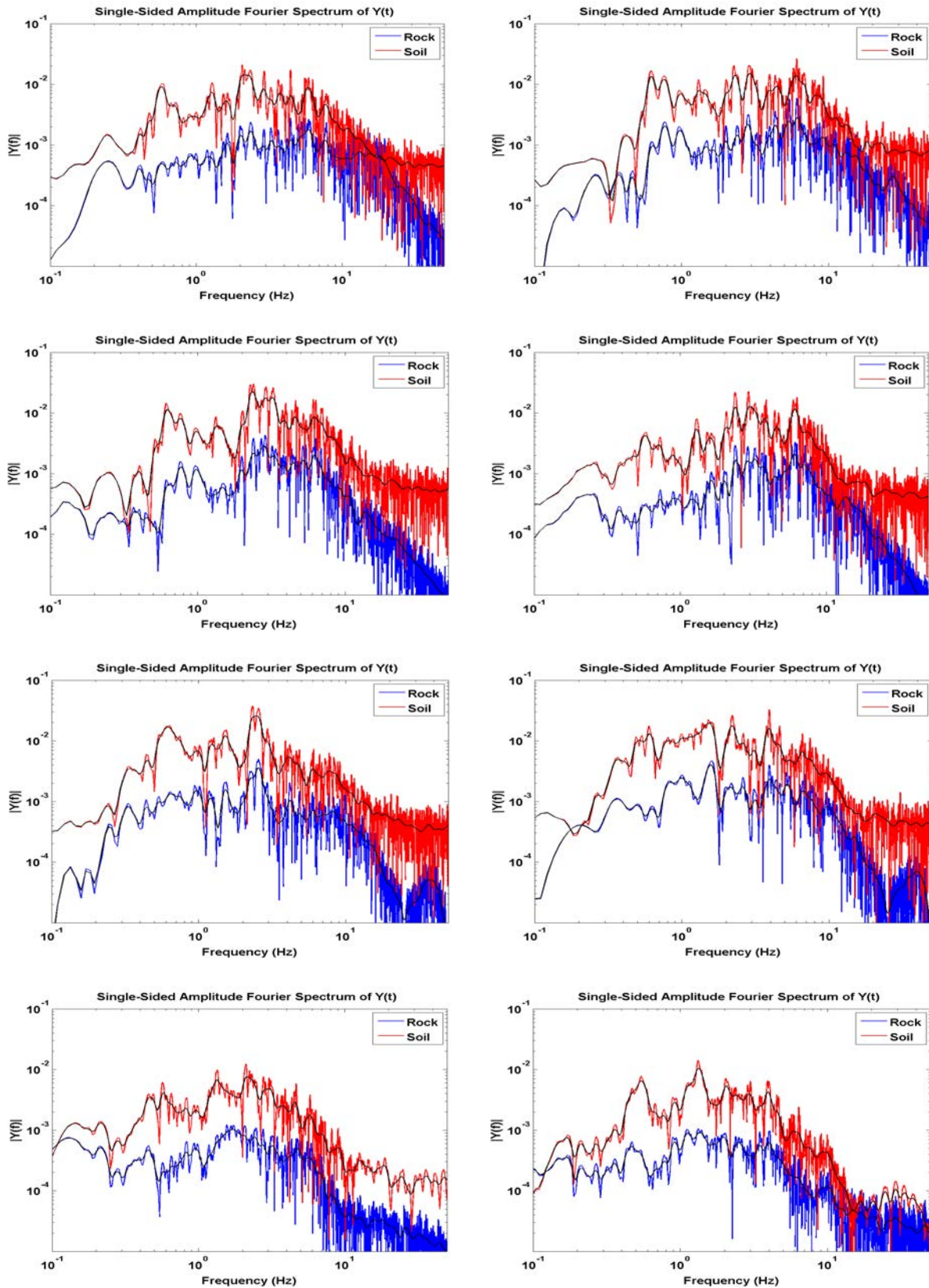
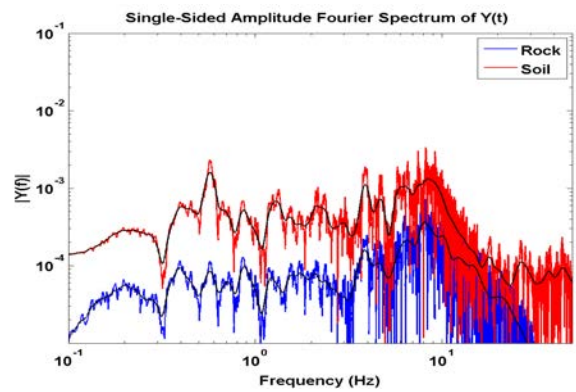
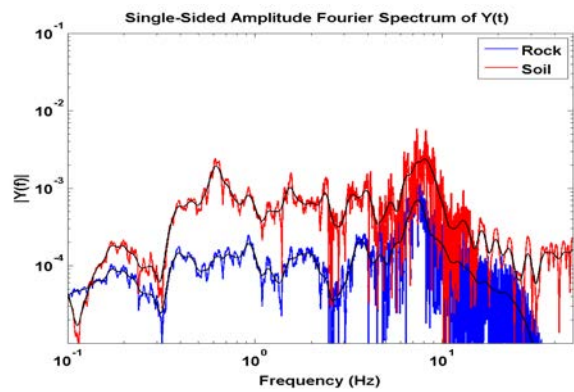
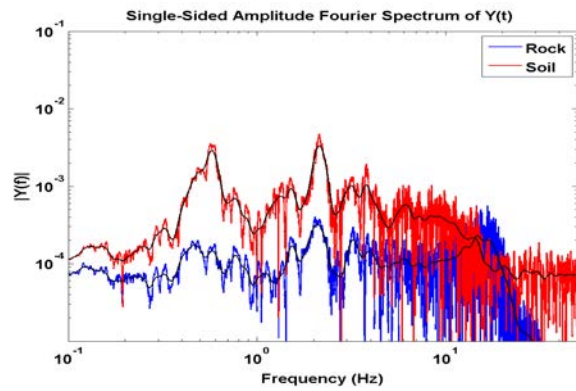
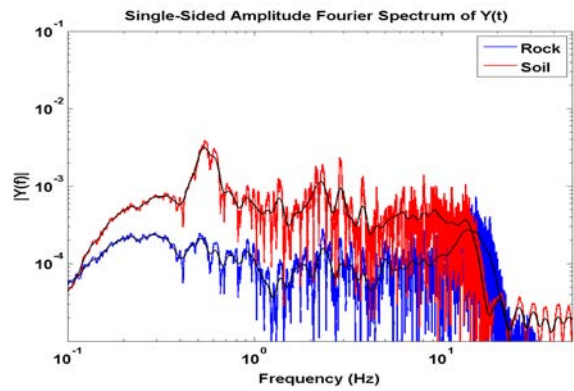
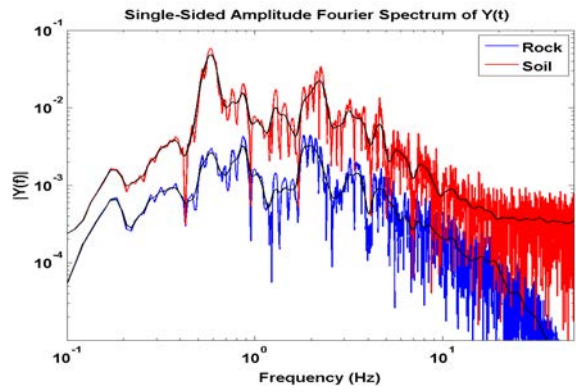
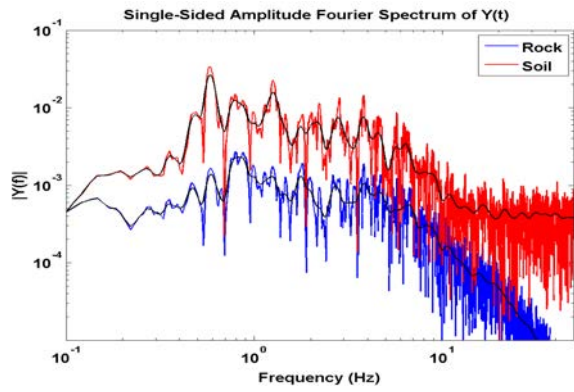
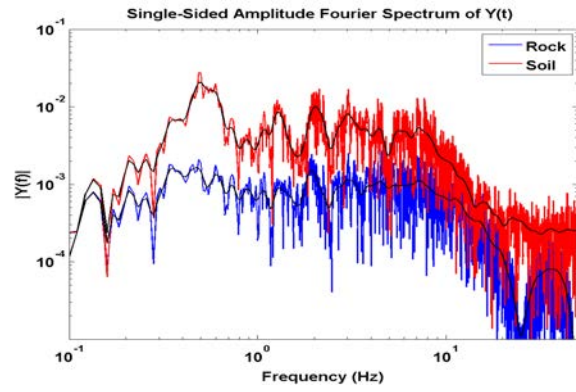
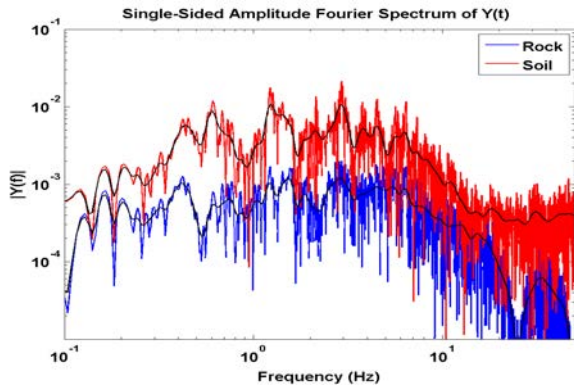


Figure 64. Linear case: Acceleration records on rock from the PEER database (blue) and at the surface obtained after performing wave propagation with NOAH (red).

### 7.1.2 Amplitude Fourier Spectra





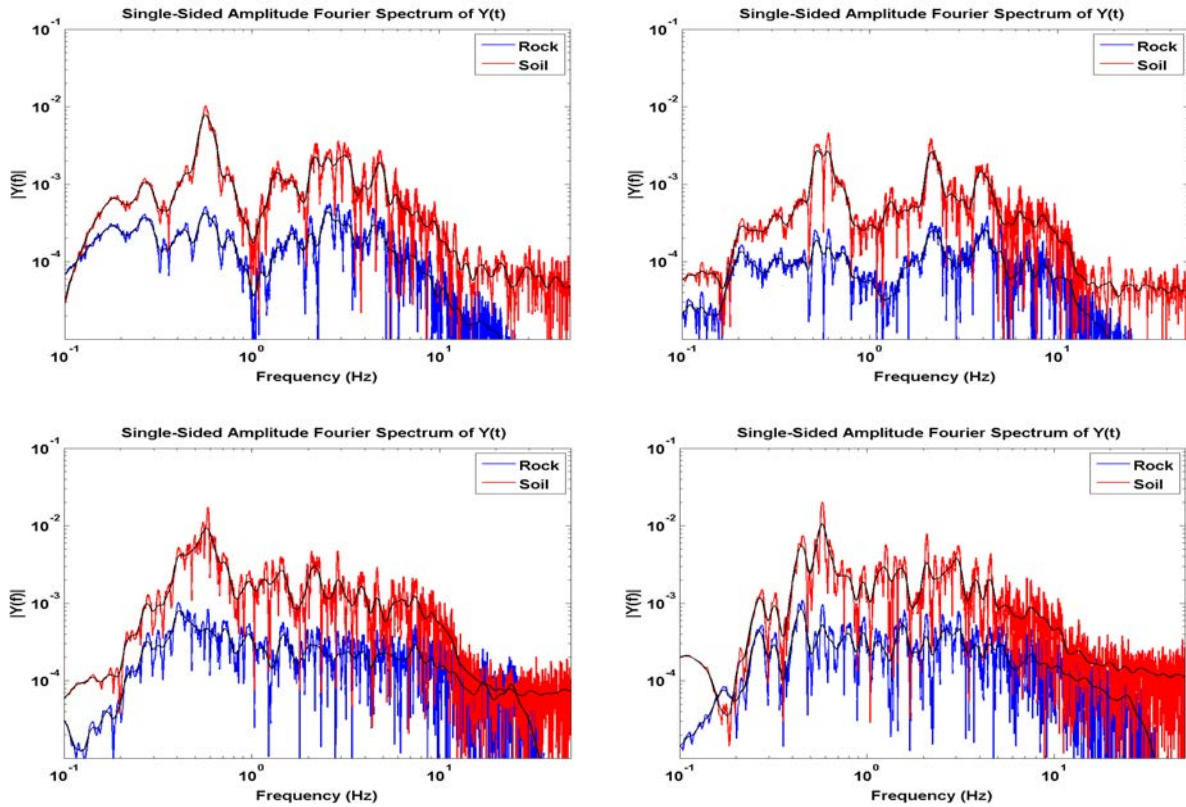
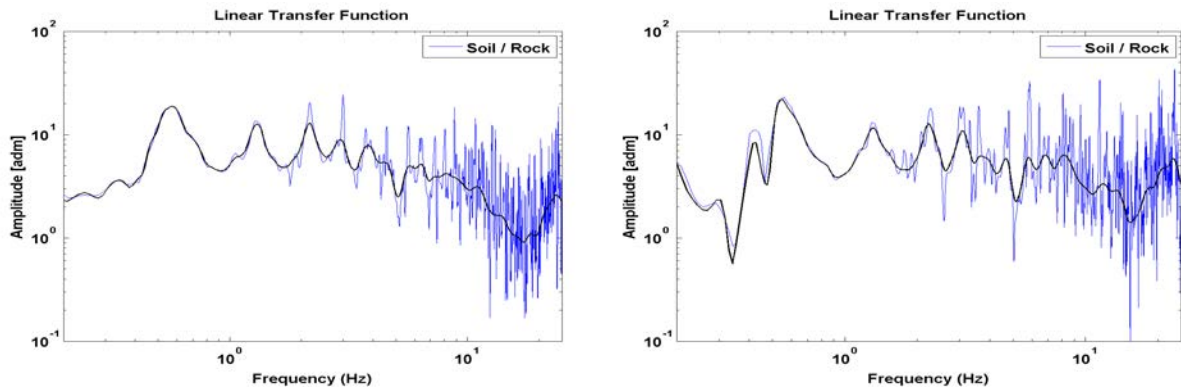
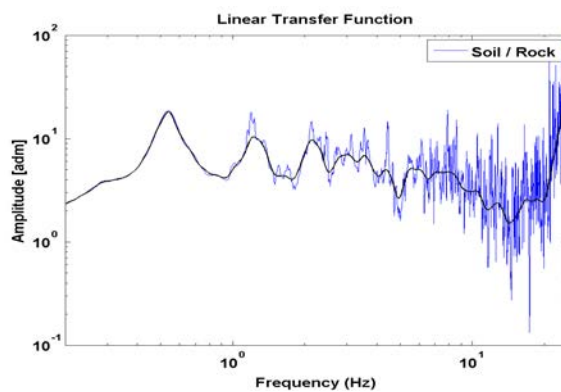
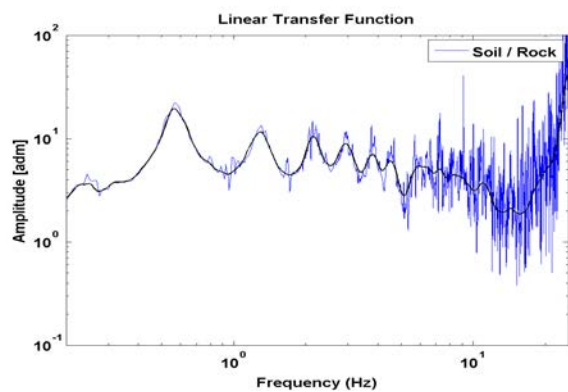
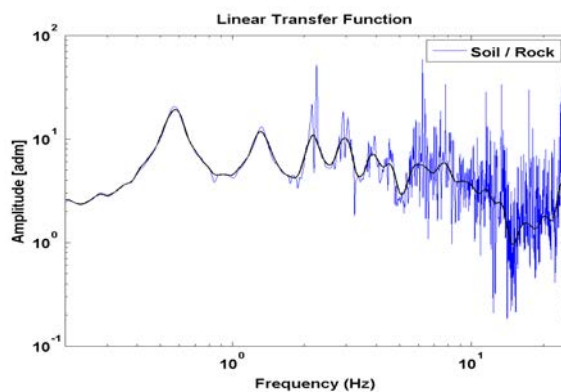
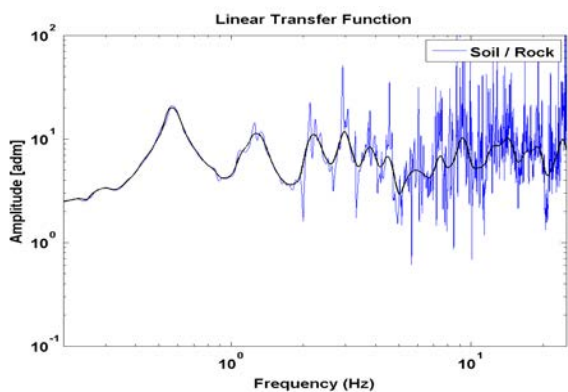
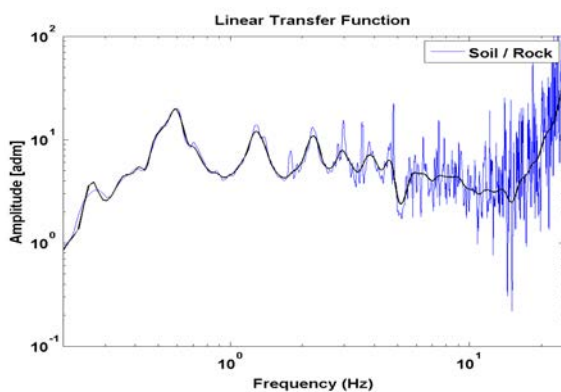
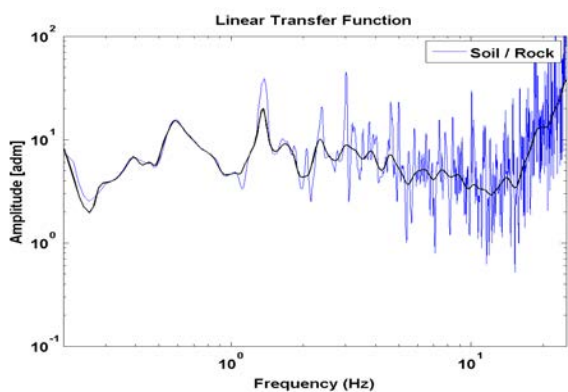
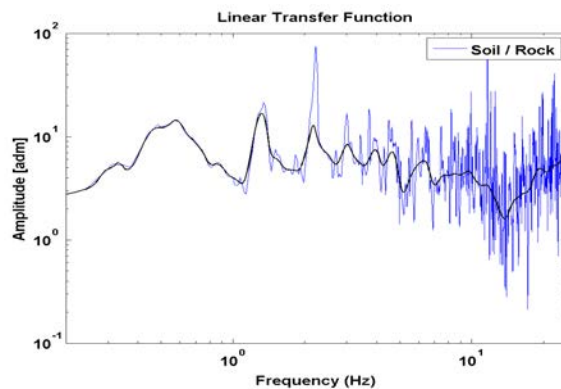
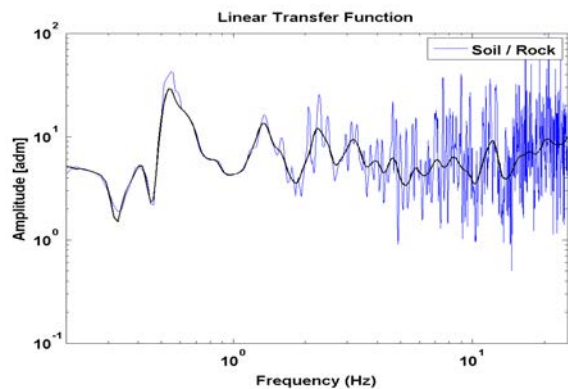
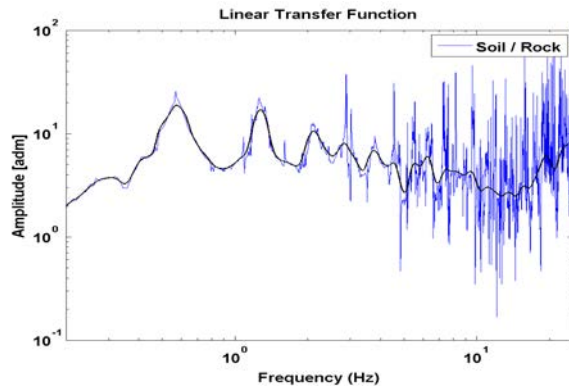
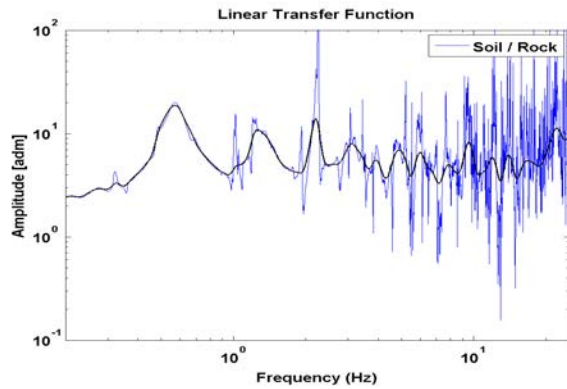
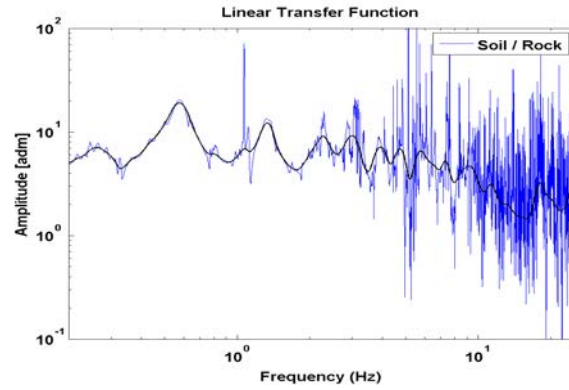
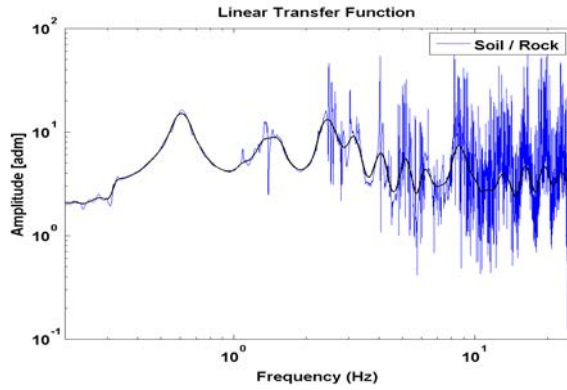
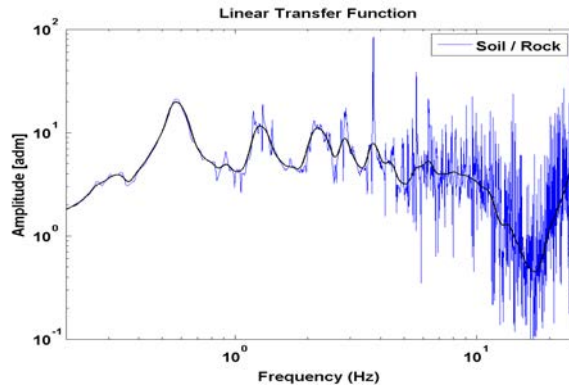
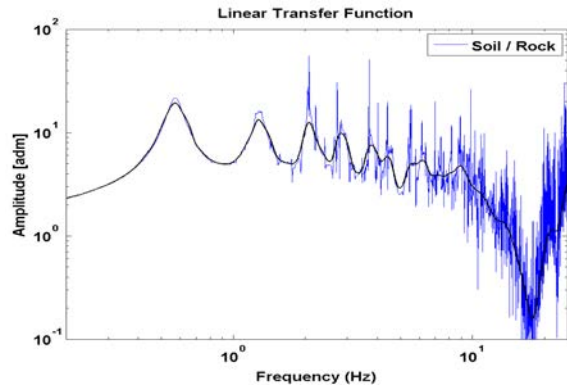
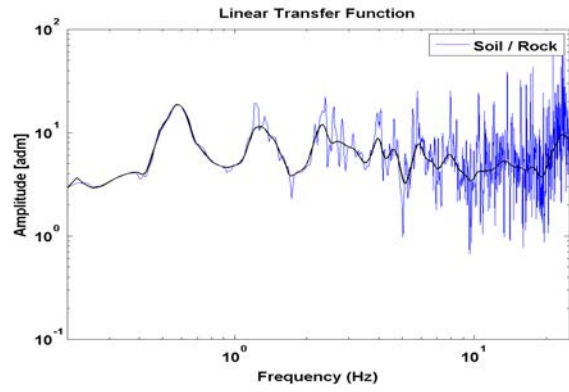
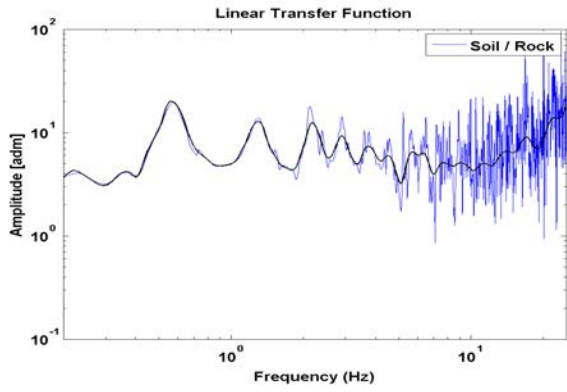


Figure 65. Linear case: Amplitude Fourier Spectra on rock (blue) and at soil (red) for each one of the considered acceleration records.

### 7.1.3 Transfer Functions







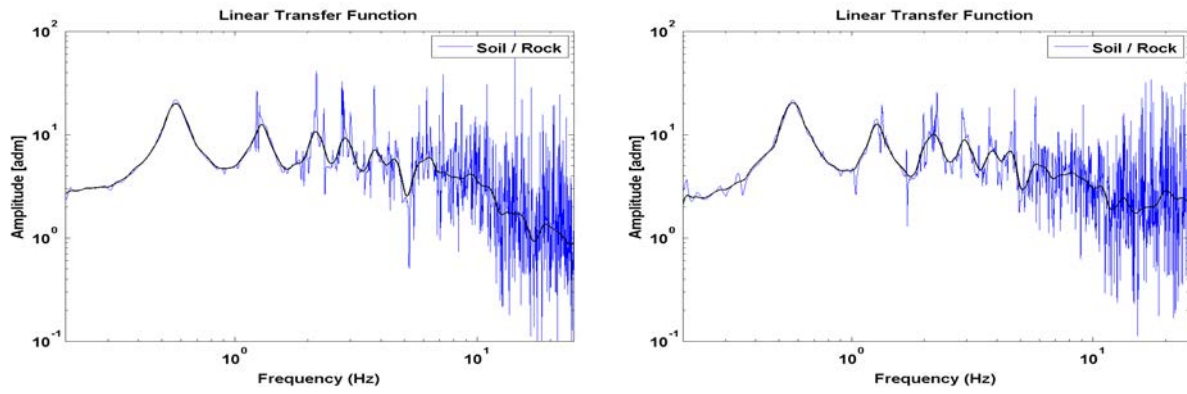
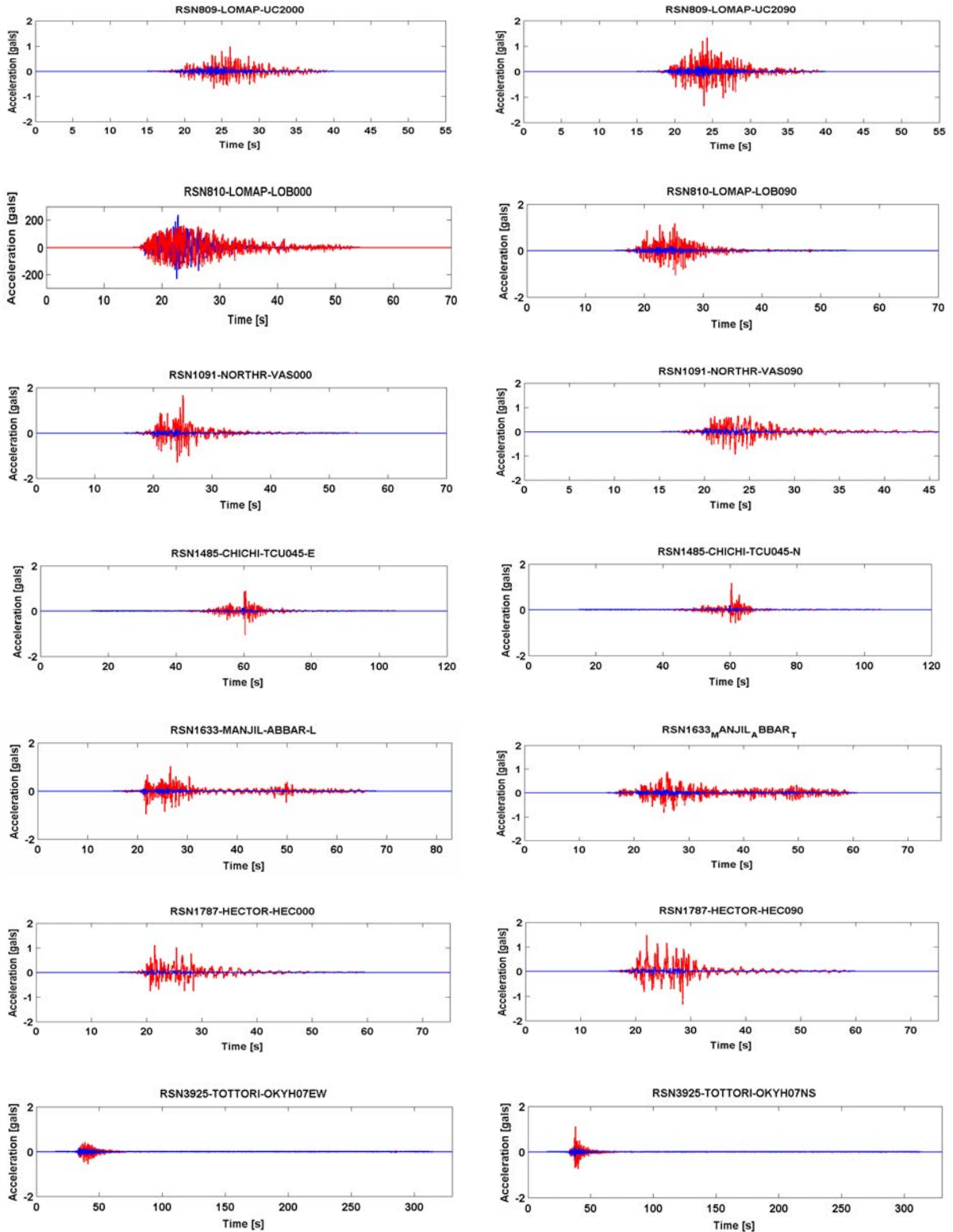


Figure 66. Linear case: Transfer Function on rock (blue) and at soil (red) at the Fourier domain for each one of the considered acceleration records.

## 7.2 NON-LINEAR CASE (LEVEL 2A)

### 7.2.1 Acceleration records.



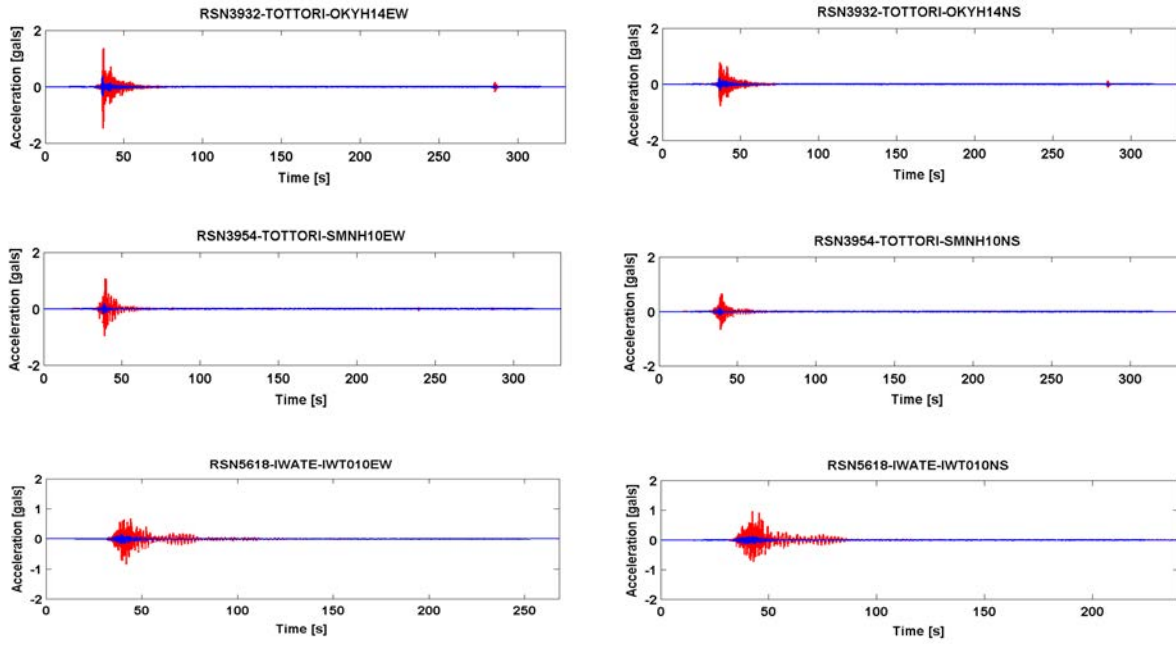
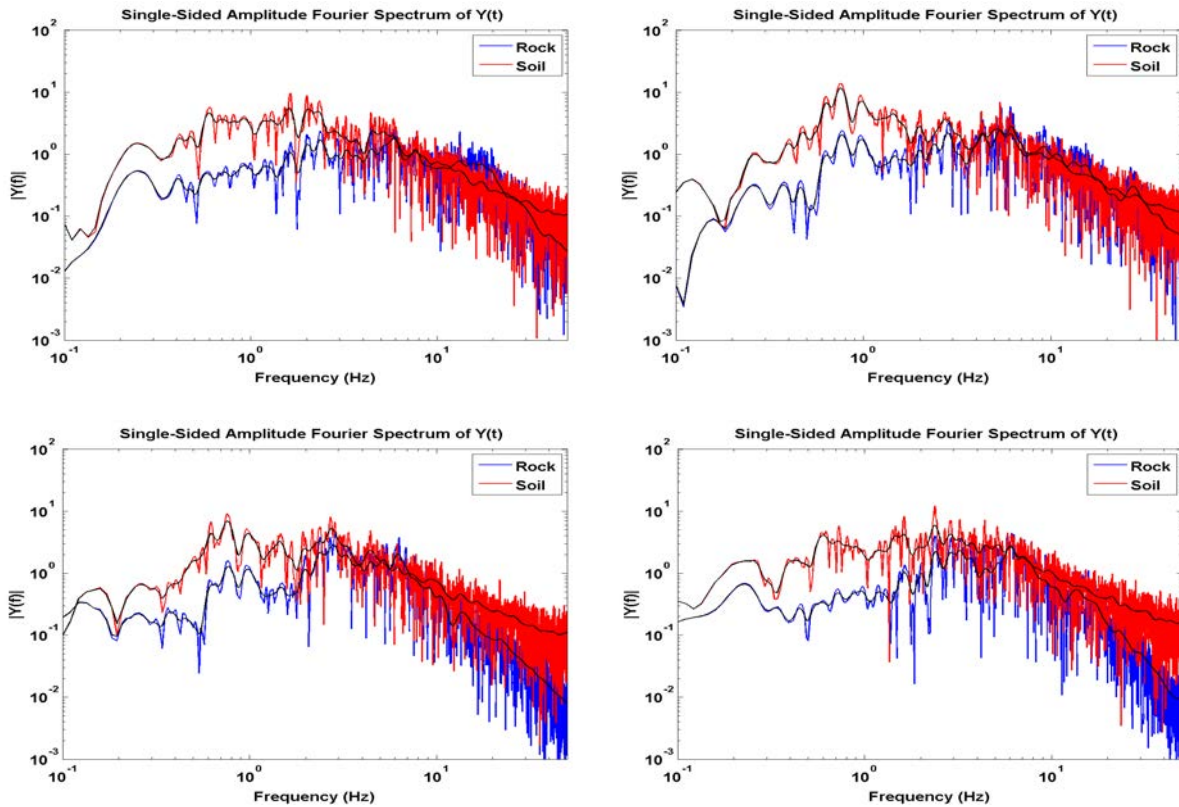
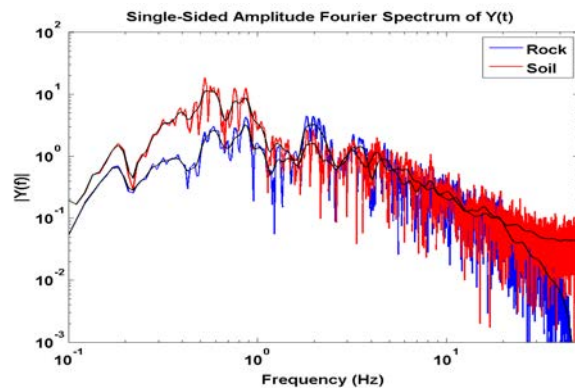
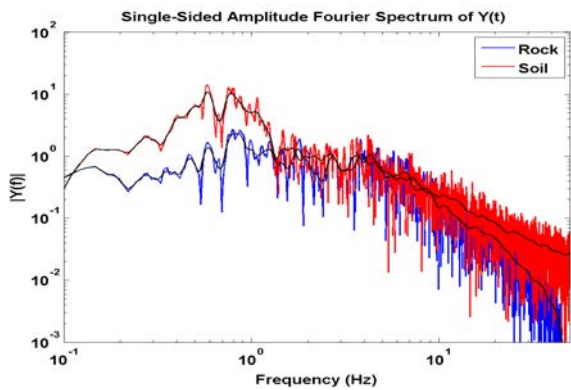
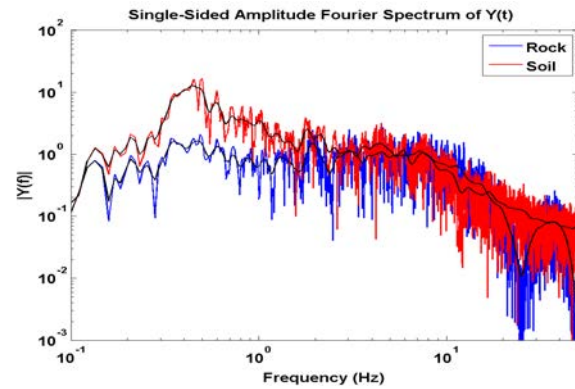
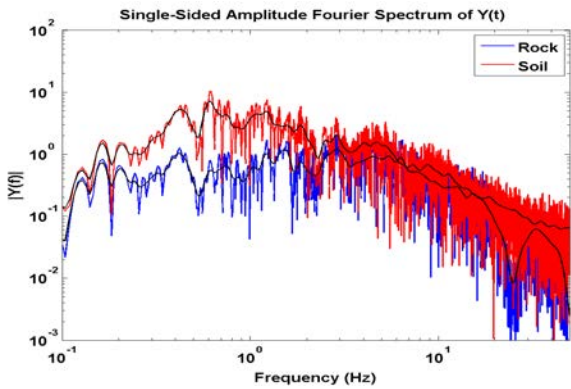
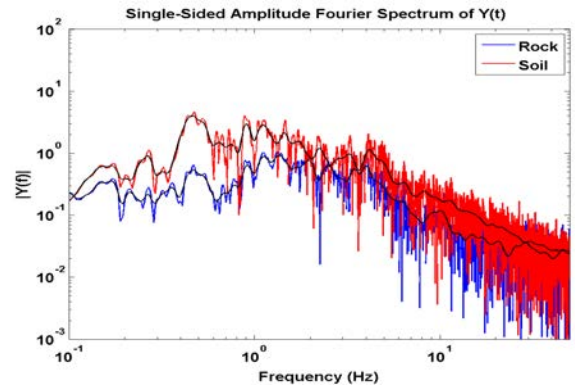
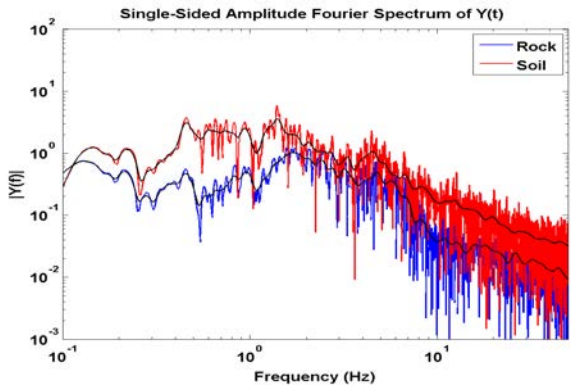
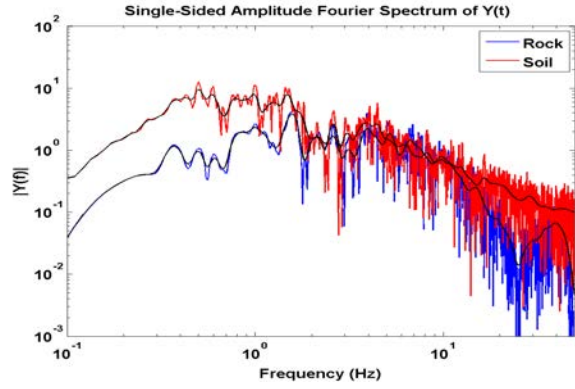
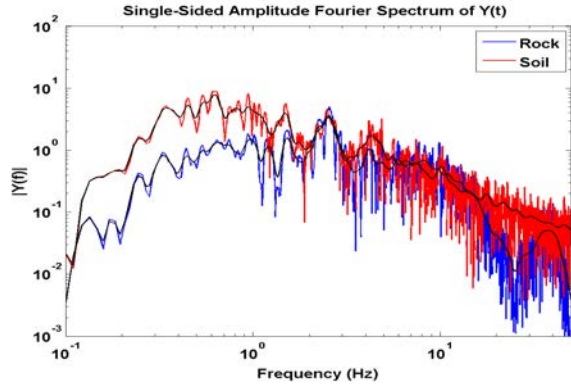


Figure 67. Nonlinear case: Acceleration records on rock from the PEER database (blue) and at the surface obtained after performing wave propagation with NOAH (red).

## 7.2.2 Amplitude Fourier Spectra





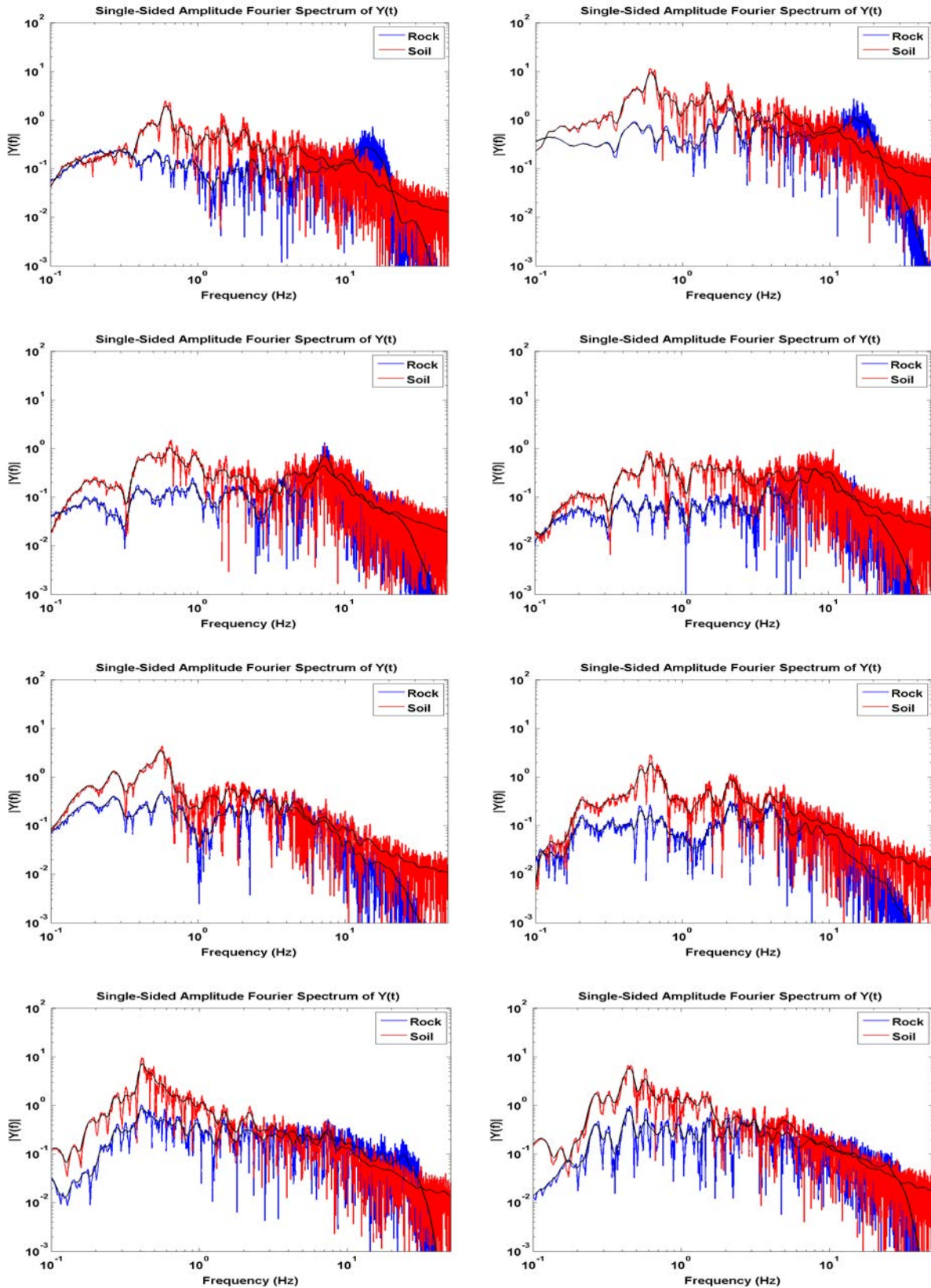
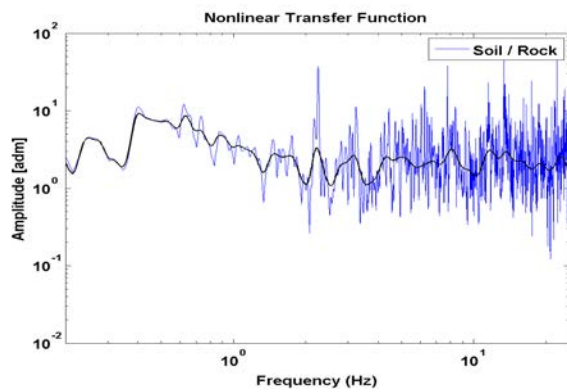
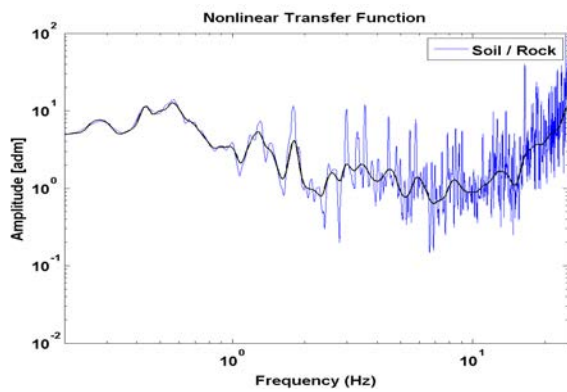
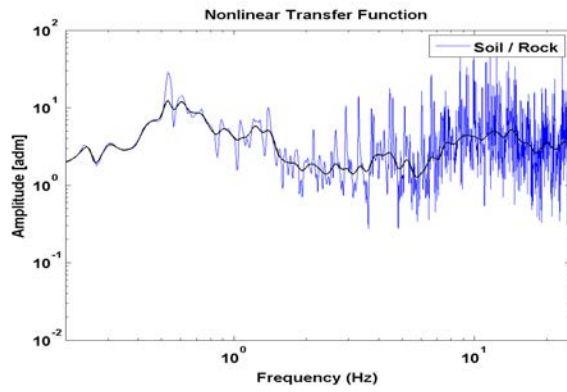
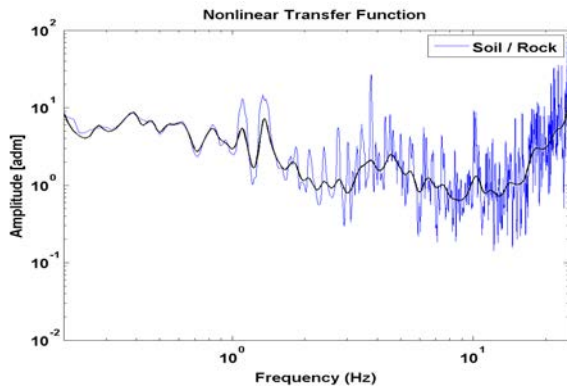
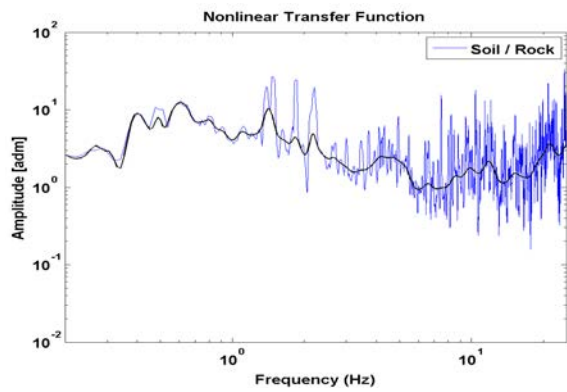
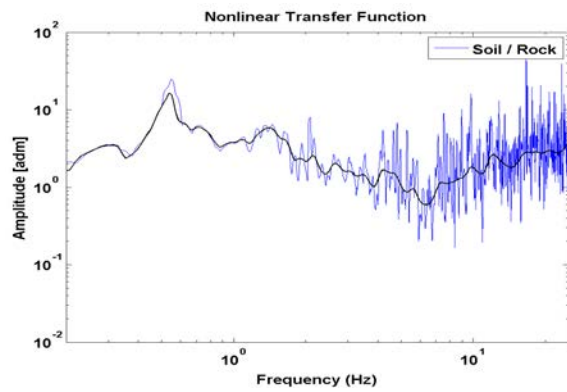
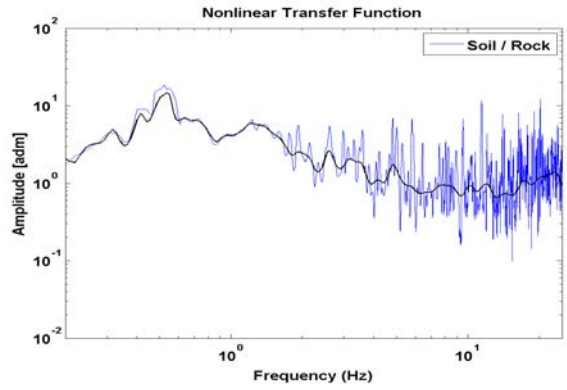
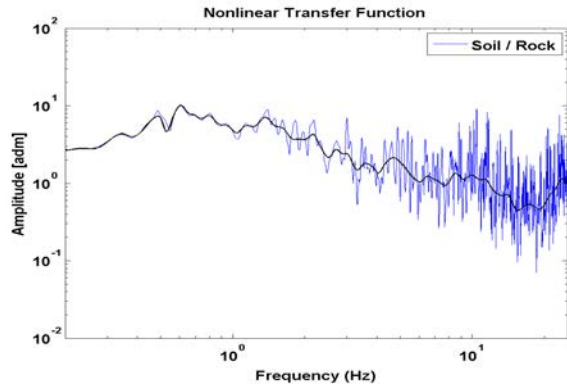


Figure 68. Nonlinear case: Amplitude Fourier Spectras on rock (blue) and at soil (red) for each one of the considered acceleration records.

### 7.2.3 Transfer Functions





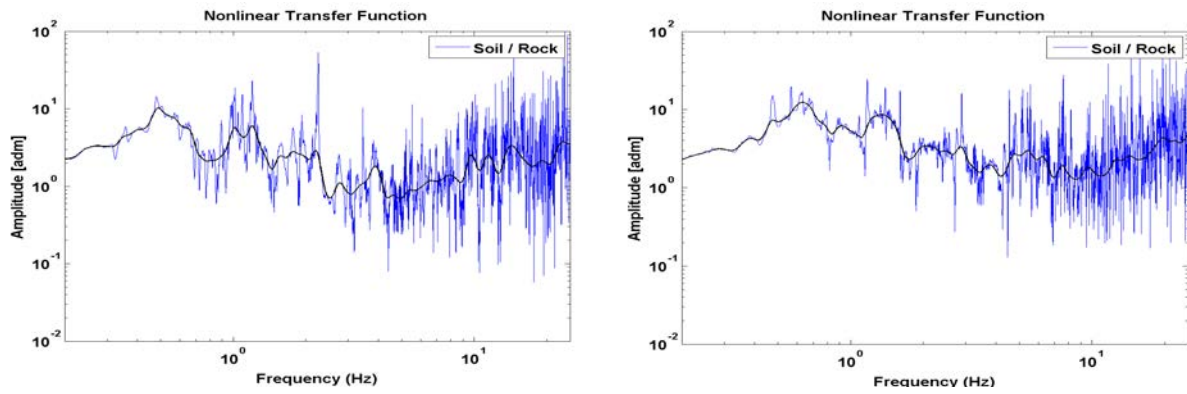


Figure 69. Nonlinear case: Transfer Function on rock (blue) and at soil (red) at the Fourier domain for each one of the considered acceleration records.